ANALYSIS OF THE REPERTOIRE OF INSULIN-REACTIVE $CD8^+$ T CELLS

PhD

2014

JAMES ALEXANDER PEARSON

DECLARATION

This work has not been submitted in substance for any other degree or award at this or any other university or place of learning, nor is being submitted concurrently in candidature for any degree or other award.

Signed ……J Pearson…… Date ……14/10/2014……

STATEMENT 1

This thesis is being submitted in partial fulfillment of the requirements for the degree of PhD.

Signed ……J Pearson…..…… Date ……14/10/2014……

STATEMENT 2

This thesis is the result of my own independent work/investigation, except where otherwise stated.

Other sources are acknowledged by explicit references. The views expressed are my own.

Signed ……J Pearson…… Date ……14/10/2014……

STATEMENT 3

I hereby give consent for my thesis, if accepted, to be available for photocopying and for inter-library loan, and for the title and summary to be made available to outside organisations.

Signed ……J Pearson…… Date ……14/10/2014……

STATEMENT 4: PREVIOUSLY APPROVED BAR ON ACCESS

I hereby give consent for my thesis, if accepted, to be available for photocopying and for inter-library loans **after expiry of a bar on access previously approved by the Academic Standards & Quality Committee.**

Signed ……J Pearson…… Date ……14/10/2014……

ABSTRACT

Proinsulin is an auto-antigen in type 1 diabetes in the Non-obese Diabetic (NOD) mouse. The $CD8^+$ T cell clone, G9C8, which utilises a T cell receptor (TCR) comprising TRAV8-1*01TRAJ9 and TRBV19*01TRBD1TRBJ2-3, recognises insulin B15-23 presented by $H\text{-}2K^d$, escapes negative selection and rapidly causes diabetes upon adoptive transfer into immunocompromised NODscid mice.

To understand how these insulin B15-23 reactive $CD8^+$ T cells develop, G9C8-derived single TCR TRAV8-1*01TRAJ9 chain transgenic NOD mice were generated. These mice were bred with different proinsulin-expressing NOD mice to generate proinsulin1 deficient, proinsulin2 deficient, proinsulin2 over-expressing and proinsulin1 and 2 deficient mice with a mutated proinsulin transgene, preventing G9C8 antigen recognition.

Although proinsulin-specific $CD8^+$ TCR repertoire changes in TRBV19 were seen in these mice, the proportion of insulin B15-23 reactive $CD8^+$ T cells was unaffected by proinsulin expression. Interestingly, TCR clonotyping of these insulin B15-23 reactive T cells revealed minimal shared sequences between the strains, with mice exhibiting individual clonal expansions. However, by isolating TRBV19-expressing insulin B15-23-responsive T cells, shared sequences across the different proinsulin-expressing mice were identified, with a requirement of TRBJ2-3 for insulin recognition (used by the original G9C8 T cell clone).

Furthermore, male proinsulin2 deficient TRAV8-1*01TRAJ9 mice developed diabetes, with a higher incidence seen upon antibiotic administration. Although the TCR repertoire was unaffected by antibiotics, the gut microbial diversity was greatly reduced in all the mice with age, independent of antibiotic use, with firmicutes bacteria comprising 90-97% of the microbiota.

In summary, proinsulin expression and antibiotics modify diabetes susceptibility; however, insulin B15-23 reactive T cells develop independently of antigen expression and are not directly affected by antibiotics. This data suggests that

non-antigen dependent mechanisms exist in controlling the development of auto-reactive T cells, but T cell activation and pathogenicity is influenced indirectly by a combination of antigen expression and gut microbiota.

PRESENTATION OF THIS WORK

ORAL PRESENTATION OF THIS WORK

CONFERENCE NAME	MEETING DATES	LOCATION
Diabetes UK Vale of Glamorgan Voluntary Group	17th June 2014	Vale of Glamorgan, UK
Institute of Infection and Immunity Seminar Series	20th January 2014	Cardiff, UK
28th Annual Life Sciences Postgraduate Research Day	15th November 2013	Cardiff, UK
Institute of Infection and Immunity Annual Meeting	26th September 2013	Bridgend, UK

POSTER PRESENTATION OF THIS WORK

CONFERENCE NAME	MEETING DATES	LOCATION
British Society for Immunology Annual Congress	1-4th December 2014	Brighton, UK
Institute of Infection and Immunity Annual Meeting	20th November 2014	Cardiff, UK
Diabetes UK Annual Professional Conference	5-7th March 2014	Liverpool, UK
13th International Congress of the Immunology of Diabetes Society	7-11th December 2013	Lorne, Australia
Diabetes UK Annual Professional Conference	13-15th March 2013	Manchester, UK
Diabetes UK 6th Annual Networking Day for Students	28th November 2012	London, UK
27th Annual Life Sciences Postgraduate Research Day	16th November 2012	Cardiff, UK
Immune Tolerance and Autoimmune Disease	26-27th April 2012	Cambridge, UK

ACKNOWLEDGEMENTS

There are many people who need to be thanked for all their help and hard work in producing this thesis. Firstly, I would like to thank everyone in the Diabetes Research Group for all their hard work and support in helping this work come to fruition. In particular, I would like to thank Dr Terri Thayer for teaching me all the technical skills required for this work, as well as providing great insight into the project and offering many constructive suggestions. I would also like to thank her for all the long hours and days we spent optimising and conducting the experiments. I would also like to thank Dr Evy DeLeenheer and Mrs Joanne Davies for their incredible support in managing the mouse colony as well as their mentoring and teaching, which has greatly helped the success of this work. I would also like to thank Miss Larissa Camargo da Rosa, Mrs Xin Zhao, Dr Mark Lewis, Dr Stephanie Hanna, Dr Claire Hocter and Miss Amy Phillips for all their help with experiments and the extra-curricular support they have provided. Most importantly, this work could not have been done without my supervisor's help. I would like to thank Professor Susan Wong who has been influential in helping me develop as a researcher over the past 3 years and who has continued to inspire me. There are so many things I am grateful to her for, including; the long weekly meetings discussing all of this work, her guidance in developing this work and especially, her belief in me and allowing me to pursue other research avenues in conjunction with my main work. Without Professor Wong's help, I would not have been able to do this PhD. I should also add that she has been incredibly influential in helping with all of my diabetes awareness events and because of her I look forward to starting my first post-doctoral research position at Yale University as a Fulbright-Diabetes UK Research Scholar.

This work could not have been completed without the help of other research and technical staff including Dr James McLaren, Dr Kelly Miners, Dr Kristin Ladell and Professor David Price, without whom, the clonotyping work could not have been done. In addition, I would like to thank all the staff in the animal facility for their continued help as well as Mrs Catherine Naseriyan for keeping the flow cytometer working. Furthermore, I would like to thank the autoantibody

laboratory at Bristol University for allowing me to conduct the insulin autoantibody experiments, and Dr Li Wen and her colleagues at Yale for not only providing a great amount of data looking at the gut microbiota but also for their hard work and help in shaping this novel research area in our group. I would also like to thank Diabetes UK for funding this work and providing numerous opportunities to discuss the work with patients and carers for those with diabetes.

Additionally, special thanks should be given to my family. Both my mum and stepdad have been a huge support during my entire time at university and I thank them for always believing in me. I am very lucky to have two parents who are kind, caring, devoted and happy to give up their time supporting my ventures. Furthermore, I would also like to thank my step sister, brother, their partners and my new baby niece for providing me with many opportunities to relax outside of the lab. I would like to thank my partner Chris, and his family for allowing me to stay with them while writing up my thesis. By helping create a work environment, providing much needed tea and cake breaks and many other social activities, I have been able to finish writing this work, which I am entirely grateful for. Finally, I would like to further thank Chris, my confidant and the love of my life for providing me with much needed support, even when things have been hard. He has been my rock and has been incredibly understanding of all the long hours and weekends spent working so I owe him a big thank you for all of his support. Therefore, it is to him, his family and all of my family that I dedicate this work. Thanks for always being there!

CONTENTS

THESIS FIGURES

THESIS TABLES

ABBREVIATIONS

APC	Allophycocyanin
APCs	Antigen presenting cells
APC Cy7	Allophycocyanin Cyano dye Cy7
APCs	Antigen presenting cells
bp	Base Pair
BSA	Bovine Serum Albumin
BV421	Brilliant Violet 421
CD	Cluster of Differentiation
cDNA	Complementary DNA
CDR	Complementarity determining region
CFA	Complete Freund's adjuvant
CLP	Common Lymphoid Progenitor
COS	Cells of CV-1 origin carrying SV40 genetic material
cpm	Counts per minute
Dβ	T cell Receptor Diversity β chain gene
DC(s)	Dendritic cells
DN	Double Negative
DNA	Deoxyribonucleic acid
dNTPs	Deoxynucleotide triphosphates
DP	Double Positive
EAE	Experimental autoimmune encephalomyelitis
ELISA	Enzyme-linked immunosorbent assay
ER	Endoplasmic Reticulum
ETP	Early thymus progenitor
FBS	Fetal bovine serum
FITC	Fluorescein isothiocyanate

g	Gravity
HRP	Horse radish peroxidase
HSC	Haematopoietic Stem Cell
^{125}I	Iodine 125
IAA	Insulin Autoantibody
IFA	Incomplete Freund's adjuvant
IFN-γ	Interferon gamma
IGRP	Islet Glucose-6-Phosphatase related subunit protein
IL	Interleukin
ITAMs	Immunoreceptor tyrosine-based activation motifs
Jα	T cell Receptor Joining α chain gene
Jβ	T cell Receptor Joining β chain gene
MHC	Major Histocompatibility Complex
MHCI	Major Histocompatibility Complex Class I
MHCII	Major Histocompatibility Complex Class II
MIP-1β	Macrophage Inflammatory Protein 1β
MLN	Mesenteric lymph node
mRNA	Messenger Ribonucleic Acid
rRNA	Ribosomal Ribonucleic Acid
NFAT	Nuclear Factor of Activated T cells
NIH	National Institute of Health
nm	Nanometer
NOD	Non-Obese Diabetic Mouse
OD	Optical Density
p#	position (# = any number)
p:MHC	Peptide: MHC Complex
PBS	Phosphate Buffered Saline

PD-1	Programmed Death 1
PD-L1	Programmed Death Ligand 1
PD-L2	Programmed Death Ligand 2
PE	Phycoerythrin
PE-Cy7	Phycoerythrin Cyano dye Cy7
PerCpCy5.5	Peridinin Chlorophyll A Protein Cy5.5
PGS	Protein G Sepharose
PI1$^{-/-}$	Proinsulin 1 knock out
PI2$^{-/-}$	Proinsulin 2 knockout
PLN	Pancreatic lymph node
PP	Peyer's patches
RAG	Recombination Activating Genes
RIP	Rat Insulin Promoter
RNA	Ribonucleic acid
RPM	Rotations per minute
RSS	Recombination Signal Sequences
SCID	Severely Compromised Immunodeficient mice
SP	Single positive
T1D	Type 1 Diabetes
TAE	Tris Acetate-Ethylenediaminetetraacetic acid
TAP	Transporter Associated with Antigen Processing
TCR	T cell Receptor
TCRα	T cell Receptor α chain
TCRβ	T cell Receptor β chain
TCRCα$^{-/-}$	T cell Receptor α chain Constant region knock out
TCRVα	T cell Receptor Variable α chain gene
TCRVβ	T cell Receptor Variable β chain gene

TILs	Tumour-infiltrating lymphocytes
TLR	Toll-like Receptor
TNF-α	Tumour Necrosis Factor α
TNF-β	Tumour Necrosis Factor β
TRAs	Tissue-restricted antigens
TRAV	T cell Receptor Variable α chain gene
TRBC	T cell Receptor Constant β chain gene
TRBD	T cell Receptor Diversity β chain gene
TRBJ	T cell Receptor Joining β chain gene
TRBV	T cell Receptor Variable β chain gene
TSP	Thymus-seeding progenitor
Vα	T cell Receptor Variable α chain gene
Vβ	T cell Receptor Variable β chain gene
X-GAL	5-bromo-4-chloro-indolyl-β-D-galactopyranoside

CHAPTER 1: INTRODUCTION

1.1 T CELL DEVELOPMENT

1.1.1 EARLY T CELL PROGENITOR DEVELOPMENT IN THE BONE MARROW

Lymphocyte development initiates from haematopoietic stem cells (HSC) within the bone marrow. Notch1 signalling, either dependently or independently of ligands, promotes HSC self-renewal maintaining a pool of lymphocyte progenitors (Stier et al., 2002). Upon receiving differentiation signals, these HSC differentiate into common lymphoid progenitors (CLPs), which are phenotypically characterised by $Lin^{-}IL\text{-}7R^{+}Thy\text{-}1^{-}Sca\text{-}1^{lo}c\text{-}Kit^{lo}$ (Kondo et al., 1997). These progenitors further differentiate to form progenitors of two distinct lymphocyte lineages – T cells and B cells.

Differentiation factors influencing CLPs to differentiate into B Cells include the proto-oncogene LRF, encoded by *Zbtb7a* (Maeda et al., 2007) and Pax5 in B lymphopoeisis, which represses Notch1 activation (Horcher et al., 2001, Souabni et al., 2002). T cell lineage commitment requires Notch-dependent signalling (Radtke et al., 1999, Han et al., 2002, Sambandam et al., 2005) and Hedgehog receptor signalling (El Andaloussi et al., 2006) to ensure T cell survival, proliferation and differentiation.

Upon receiving T cell differentiation signals, these T cell progenitors are recruited to the thymus. This recruitment involves migration and cell adhesion molecules including P-selectin/P-selectin glycoprotein ligand 1, vascular cell adhesion molecule 1, CD44, intercellular adhesion molecule 1 and chemokine receptors, such as CCR9 (Scimone et al., 2006, Rajasagi et al., 2009).

1.1.2 THYMIC T CELL DEVELOPMENT

Early thymus progenitors (ETPs) are the earliest detectable population in the thymus, which differentiate into T cells (Allman et al., 2003), with similar cells identified in the adult blood, possibly acting as an extra-thymic reservoir of progenitors (Schwarz and Bhandoola, 2004). Recently, progenitors which give rise

to ETPs, lose megakaryocyte-erythroid potential but still retain T cell, B cell and granulocyte-megakaryocyte potential as they enter the thymus (Luc et al., 2012). The formation of single positive T cells is dependent on a number of developmental stages mediated by CD25 (IL-2 Receptor α chain) and CD44 (adhesion molecule) expression (Godfrey et al., 1993), as shown in FIGURE 1. Briefly, the Pro-T Cell (Double negative 1; DN1) expresses CD44 and Kit (Stem Cell Factor Receptor), with CD25 expression upregulated as the cell develops into the Double negative 2 (DN2) stage. In DN2, the T cell receptor β (TCRβ) chain rearrangement begins (as do the T cell receptor γ genes (Livák et al., 1999)), downregulating CD44, characterising cells in double negative stage 3 (DN3). Once the TCRβ chain is fully formed, it pairs with a pre-T cell receptor α (TCRα) chain, forming a pre-TCR complex in the double negative 4 (DN4) stage (Saint-Ruf et al., 1994), and is expressed at the cell surface, driving T cell proliferation and expansion. DN4 T Cells, post-proliferation, shrink in size and activate RAG-1 and 2 gene transcription to allow TCRα chain rearrangement. CD4 and CD8 co-receptors are expressed forming Double Positive T Cells (DP), involving both Notch signalling and CXCL2, while IL-7 inhibits DP T cell generation (Yasuda et al., 2002, Schmitt et al., 2004, Tussiwand et al., 2011). Interestingly, the TCRβ chain rearrangement is vital for DN T cells to become DP T cells (Mombaerts et al., 1992a). Further T cell differentiation occurs at the DP stage involving commitment to either the αβ or γδ T cell lineage (Petrie et al., 1992). Finally, single positive (SP) T cells are formed, expressing either CD4 or CD8 co-receptors, regulated by transcription factors e.g. T-helper-inducing POZ/Kruppel-like factor (Th-POK) (He et al., 2005). In addition, while co-receptor signalling strength does not determine which SP T cell develops (Bosselut et al., 2001), the duration of the TCR signalling can dictate which co-receptor is expressed on the T cell (Yasutomo et al., 2000).

FIGURE 1: T CELL DEVELOPMENT IN THE THYMUS

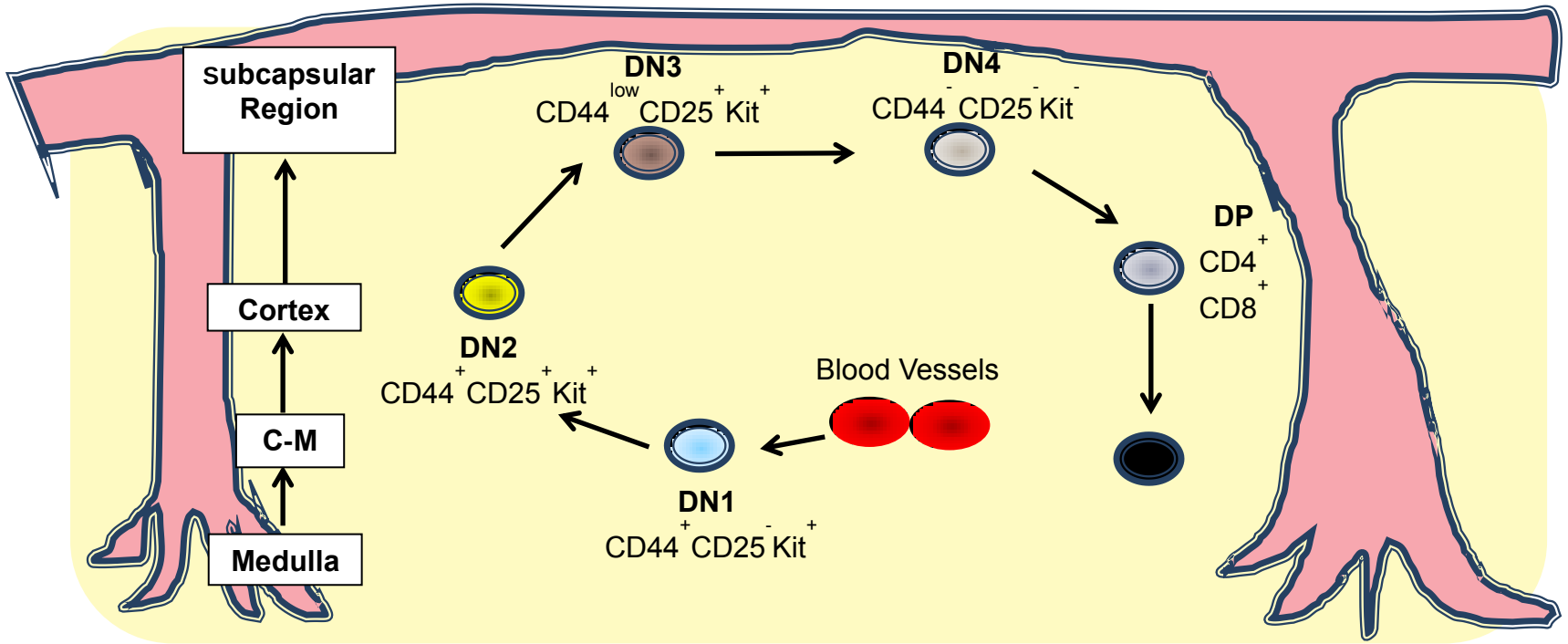

FIGURE 1: DN1 T cell progenitors initially express CD44 and Kit (Stem Cell Factor Receptor) with the T cell Receptor (TCR) DNA in the native germline state. As cells move through the thymic cortex, CD25 becomes expressed (DN2) and the TRBV chain DNA begins recombination. Reduction in CD44 and Kit expression allows the TRBV chain DNA to completely rearrange and pair with a pre-TCRα chain (DN3). Cell surface expression of the pre-TCR results in a loss of CD25, CD44 and Kit expression, allowing the T cell to undergo proliferation. Adapted from (Godfrey et al., 1993).

FIGURE 2: Chromatin packaging of DNA enables vast numbers of genes to be encoded in a spatially restricted manner. *tcra* and *tcrb* loci undergo rearrangement catalysed by the RAG-1 and RAG-2 proteins through recognition of recombination signal sequences (RSS) located at the ends of each V, D and J segment (Schatz et al., 1989, Oettinger et al., 1990). The RAG protein forms a synaptic complex enabling 2 RSS to be brought into proximity to create a double-stranded DNA break (excising the DNA located between the 2 RSS sites). This break creates a 3'OH that attacks a phosphodiester bond in the opposite DNA strand, which forms a 5' phosphate and hairpin DNA structure (McBlane et al., 1995, van Gent et al., 1996). This cleavage works best when the sequence has a 23 base pair spacer that is brought together with a 12 base pair spacer, known as the 12/23 rule (van Gent et al., 1996). Recruitment of proteins such as Artemis with DNA-dependent protein kinases enable the hairpin DNA structure to be opened up and form 5' and 3' overhanging regions allowing non-homologous DNA joining (Ma et al., 2002). RAG expression occurs solely in DN and DP thymocytes ensuring no other rearrangements can occur (Wilson et al., 1994).

FIGURE 2: RAG-DEPENDENT RECOMBINATION OF THE T CELL RECEPTOR β CHAIN LOCUS

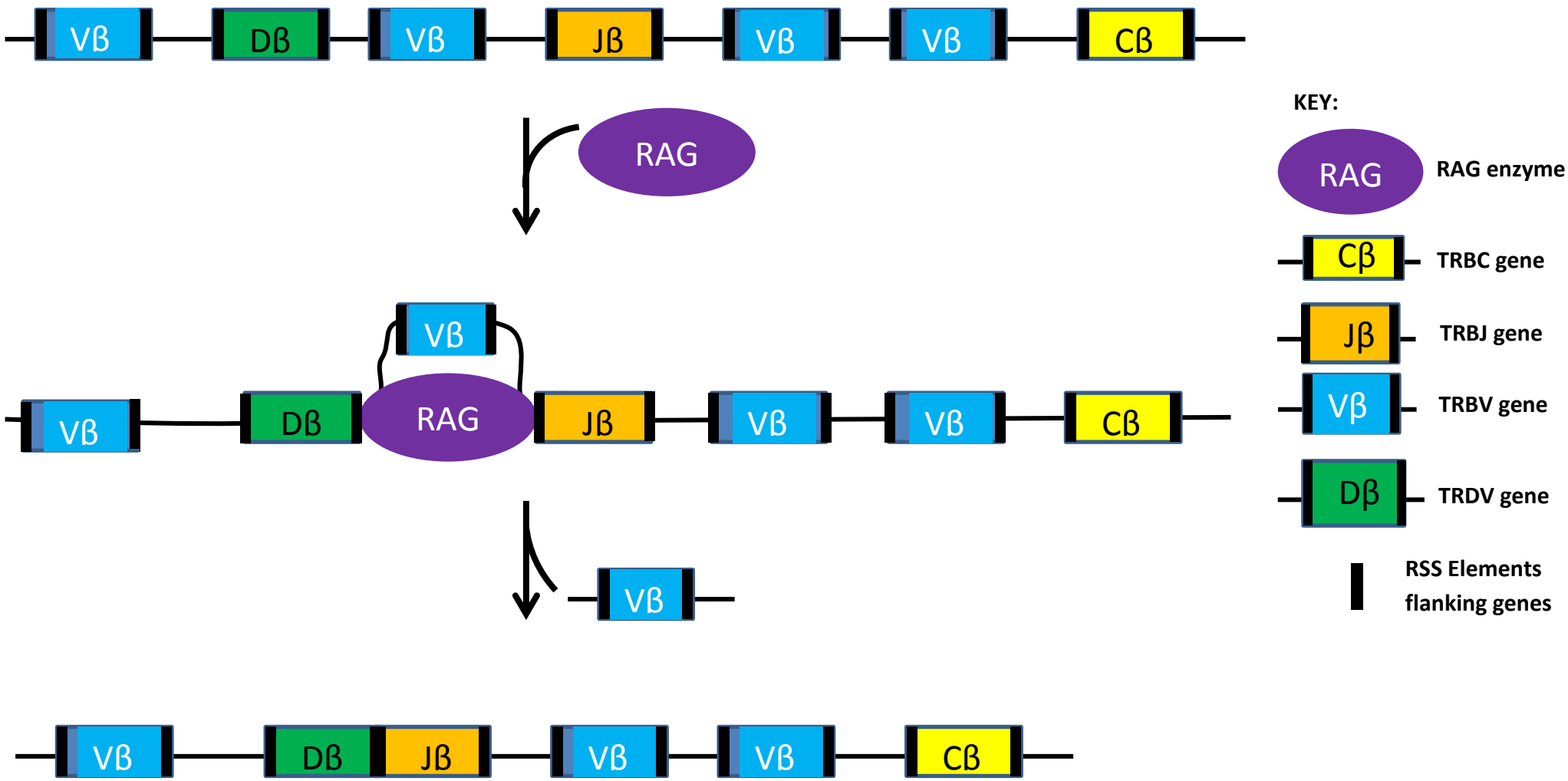

1.1.3 T CELL RECEPTOR

1.1.3.1 TCR GENE REARRANGEMENT

Recombination-activating gene (RAG) enzymes are upregulated in T cells and B cells to enable TCR or Immunoglobulin (Ig) rearrangement. If either RAG-1 or RAG-2 enzymes are deficient, T cell and B cell development is blocked early into the TCR or IG rearrangements, preventing the development of mature lymphocytes (Mombaerts et al., 1992b, Shinkai et al., 1992). RAG expression during T cell development occurs at 2 time points, the DN2 and the DP stages coinciding with TCR gene rearrangements (Wilson et al., 1994, Monroe et al., 1999). In DN2, the TCRβ chain locus (*tcrb* loci) undergoes recombination (FIGURE 2) (Godfrey et al., 1994). Briefly, this involves RAG enzymes which cleave the DNA to join a Diversity (D) and Joining (J) gene together and subsequently recombine the DJ gene segment with a Variable (V) gene segment in DN3 (Schatz et al., 1989, Oettinger et al., 1990, Schatz et al., 1992). In DN4, the rearranged TCRβ chain recombines with an invariant TCRα chain, forming the pre-TCR complex, inhibiting RAG expression and thus further rearrangement (Wilson et al., 1994, Saint-Ruf et al., 1994). Upregulation of CD4 and CD8 (DP) re-stimulates RAG expression and *tcra* loci rearrangement to form a VJ segment (Wilson et al., 1994). Once the final rearranged TCR is expressed, RAG gene expression is repressed. This repression may occur through through erk and abl kinases (Roose et al., 2003) or through NFATc1 directly binding to the RAG locus (Patra et al., 2006).

Unlike the TCRβ chain, the TCRα chain can undergo multiple rearrangements prior to formation of the final expressed TCR, ensuring successful T cell development (Petrie et al., 1993, Wang et al., 1998).

1.1.3.2 TCR DIVERSITY

During recombination, a large TCR diversity is generated. This occurs through combinatorial diversity whereby the RAG enzymes select a single V, D and/or J gene segment from a number of possible candidates (TABLE 1). Additionally, the recombination event lacks proof-reading capabilities and thus nucleotides may be

lost or added through terminal deoxynucleotidyl transferases (Cabaniols et al., 2001). These processes ensure the developing T lymphocytes exhibit a broad TCR repertoire (Robins et al., 2009, Genolet et al., 2012), ensuring reactivity to potential foreign antigens, while in some cases predisposing to autoimmunity.

TABLE 1: THE TOTAL NUMBER OF FUNCTIONAL T CELL RECEPTOR GENES FOR TCRαβ T CELLS

TCR GENE	NUMBER OF GENES
TRAV	112
TRAJ	51
TRAC	1
TRBV	23
TRBD	2
TRBJ	13
TRBC	2

TABLE 1: Data obtained from the IMGT website whereby pseudogenes were excluded from the data while genes containing coding regions with an open reading frame present were included.

1.1.3.3 αβTCR STRUCTURE & SIGNALLING

T cell Receptors (TCRs) comprise an alpha and a beta chain (40-45kDa glycoproteins), each encoded by a series of genes that have undergone rearrangement, as discussed previously, linked by disulphide bonds (Minami et al., 1987b). CD3 molecules also associate with the TCR structure as shown in FIGURE 3. These CD3 molecules include CD3ζ homodimers (16kDa each) linked together by disulphide bonds, while the CD3γε and CD3δε heterodimers are non-covalently linked (Minami et al., 1987b). This association with TCR and CD3 occurs intracellularly prior to cell surface expression (Koning et al., 1988) with TCRαβ heterodimer formation required for CD3 molecule association, cell surface expression and functional competence (Saito et al., 1987, Sussman et al., 1988, Sancho et al., 1989). These CD3 molecules are joined specifically to the TCR

whereby CD3δε localise to a transmembrane 8 amino acid motif within the TCRα chain, and CD3δ with the TCRβ chain (Manolios et al., 1994). However the CD3ε molecule interacts with the extracellular region of the TCRβ chain, while CD3ζ does not interact with the TCRβ chain (Manolios et al., 1994).

Upon antigen binding to the TCR complex, the immunoreceptor tyrosine-based activation motifs (ITAMS) are phosphorylated by tyrosine kinases; Lck (Abraham et al., 1991, van Oers et al., 1996), which interacts with the co-receptors (CD4 or CD8 (Veillette et al., 1988, Rudd et al., 1988)) and Fyn, which associates with the TCR CD3 complex (Samelson et al., 1990). Upon ITAM phosphorylation, ZAP-70 is recruited to the phosphorylated tyrosine sequence and becomes activated (Chan et al., 1991, Straus and Weiss, 1993, van Oers et al., 1996), phosphorylating LAT and SLP-76, which bind and activate phospholipase C-γ (PLC-γ) (Bubeck Wardenburg et al., 1996, Zhang et al., 1998, Yablonski et al., 2001). PLC-γ then cleaves phosphatidylinositol bisphosphate producing diacylglycerol and inositol trisphosphate, which activate other protein kinases and increase intracellular calcium concentration (Truneh et al., 1985, Pantaleo et al., 1987, Granja et al., 1991, Chakrabarti and Kumar, 2000, Zhong et al., 2003). This subsequently leads to transcription factor activation including NF-κB, NFAT and AP-1 which transcribe genes responsible for cell proliferation and differentiation, enabling cells to respond to their stimulus (Sen and Baltimore, 1986, Shaw et al., 1988, Shibuya and Taniguchi, 1989, Rincón and Flavell, 1994). TCR signalling is dependent on ITAM phosphorylation and PLC activation (Mustelin et al., 1990, June et al., 1990) and antigen-dependent TCR signalling is sensitive to cyclic AMP (cAMP) regulation (Klausner et al., 1987) and can be recycled from the cell surface (Minami et al., 1987a).

The tyrosine phosphatase CD45 receptor is one of the critical factors in T cell receptor signalling and due to the presence of splice variants, controlled through hetereogeneous nuclear riboprotein L (hnRNP L) (Gaudreau et al., 2012), 8 CD45 isoforms exist. CD45 is important in TCR signalling through interacting with the CD4 and CD8 co-receptor-associated Lck kinase and activating TCR signalling (Leitenberg et al., 1996, Dornan et al., 2002, McNeill et al., 2007). In addition,

CD8 co-receptor interaction with p:MHC also triggers TCR signalling through phosphorylation of the TCRζ chain (Purbhoo et al., 2001). The CD8 co-receptor can also interact with p:MHC and activate T cells without p:MHC:TCR interactions (Wooldridge et al., 2010a, Clement et al., 2011). CD8:pMHC:TCR interactions are important for controlling T cell responses to altered peptide ligands (Yachi et al., 2006) and cross-reactivity (Wooldridge et al., 2010b, Wooldridge et al., 2012).

1.1.3.4 COMPLEMENTARITY DETERMINING REGIONS

The TCRα and β chains each encode 3 complementarity determining regions (CDR) each and dictate the peptide:MHC specificity. CDR1 and CDR2 regions are encoded within the germline variable gene chosen during V(D)J recombination, whereas the third CDR is encoded by the region spanning the V(D)J gene segments and thus tends to be the most diverse due to imprecise gene segment joining. While the CDR3 is the most diverse, enabling recognition and maximum contact with the peptide(s), the CDR1 and CDR2 residues are also involved in interacting with the MHC ((Danska et al., 1990, Rubtsova et al., 2009, Nakayama et al., 2012) and reviewed by (Goldrath and Bevan, 1999)). In addition, non-CDR3 regions can also provide important peptide interactions allowing the TCR to recognise different peptides (Garcia et al., 1998, Maynard et al., 2005). These CDR regions in both the TCRα and β chains show amino acid sequence bias providing peptide-specific recognition (Prochnicka-Chalufour et al., 1991) and they can also be used to identify the clonality or immunodominance of an immune response (Luciani et al., 2013). In addition, the size of these hypervariable CDR regions can vary, altering the recognition of peptides by the TCR, however the CDR3 loops of most TCRαβ chains are constrained in size and unaffected during the thymic T cell selection process (Rock et al., 1994, Hughes et al., 2003).

FIGURE 3: THE STRUCTURE OF THE αβ T CELL RECEPTOR AND CD3 COMPLEX

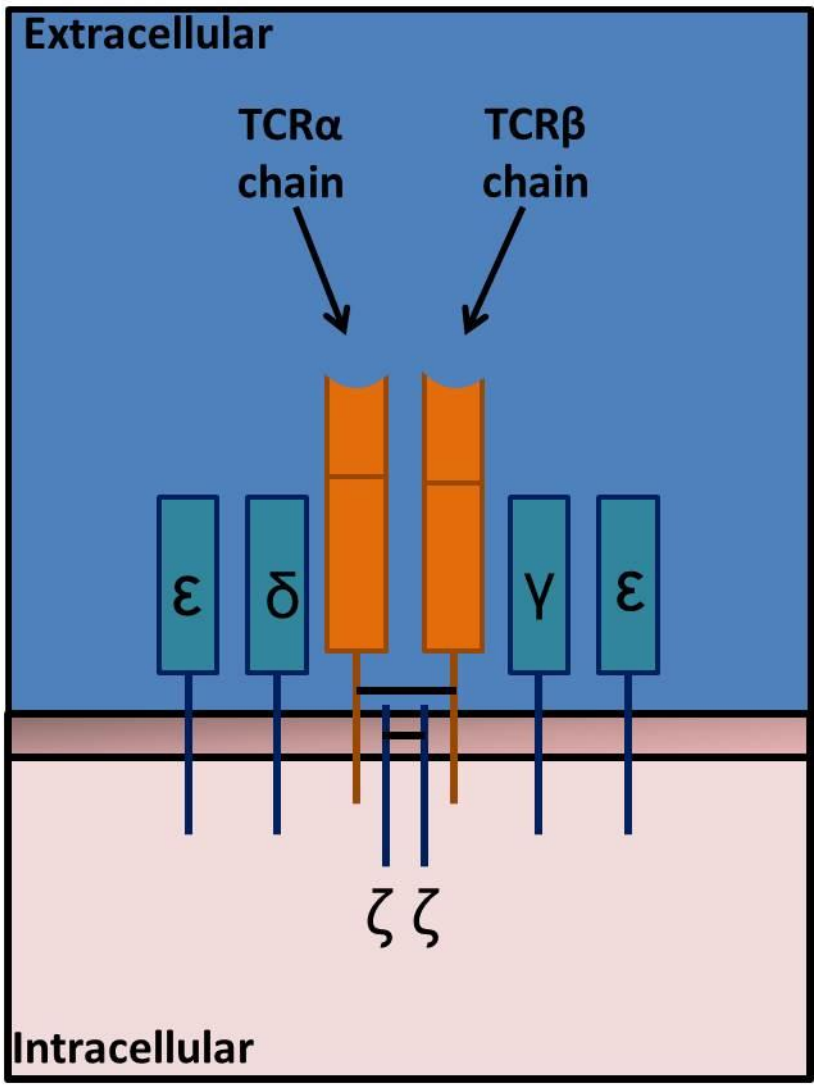

FIGURE 3: The T cell receptor (TCR) comprises variable, joining and diversity regions, which interact extracellularly with peptide presented by MHC complexes. Upon antigen recognition, the TCR signals intracellularly through the CD3 complex (comprising ε,γ,δ and ζ subunits).

1.1.3.5 NON-PEPTIDE:MHC-DEPENDENT T CELL ACTIVATION SIGNALS

In order for T cells to fully become activated they require 2 further signals in addition to the TCR:p:MHC interaction – costimulatory signals and cytokines/chemokine secretion. A number of these T cell:APC interactions are shown in FIGURE 4. Costimulatory activation signals are received through CD28, on the T cell, and B7.1/B7.2 (CD80/86) on the APC. When B7 molecules were over-expressed, providing T cell activation signals, disease could be accelerated (Wong et al., 1998). In addition, T cells receive activation signals from multiple signalling molecules including the 4-1BB receptor interacting with its ligand, 4-1BBL (Hurtado et al., 1995), ICOS interacting with its ligand ICOSL (B7H/B7RP-1) (Dong et al., 2001), CD2 signalling (Hünig et al., 1987, Bachmann et al., 1999), ICAM-3 interacting with DC-SIGN (CD209) (Geijtenbeek et al., 2000) and LFA-1 interacting with ICAM-1/2 (Marlin and Springer, 1987, Staunton et al., 1989). Upon activation, T cells quickly upregulate CTLA-4 (Cytotoxic T Lymphocyte Antigen 4) where it outcompetes CD28, due to higher binding affinity, for binding to CD80/CD86 on the APC, preventing further TCR signalling (Chikuma et al., 2003). Both CTLA-4 and PD-1 (Programmed death 1), on the T cell, inhibit T cell activation and promote tolerance (Walunas et al., 1994, Fife et al., 2009). Regulation of T cell activation is needed to terminate an immune response to protect the host from further immune-mediated damage. In addition, CTLA-4 expression with the B7-independent isoform (li-CTLA-4), also reduce effector T cell cytokine production and the ability to cause disease (Stumpf et al., 2013). B7x delays the onset of disease and protect against disease when B7x is over-expressed (Lee et al., 2012b). However, the role of B7x was only investigated in the context of transgenic mice and therefore it may play an alternate role for other T cell specificities. In addition, T cells can also interact with each other T cells through trogocytosis, where the p:MHCII complexes from APCs can be transferred to $CD8^+$ T cells to promote $CD4^+$ T cell activation (Romagnoli et al., 2013).

Finally, T cell activation also relies upon the production and signalling mediated by cytokines and chemokines and their receptors. When the T cell is activated

through the TCR and costimulatory molecules, the cell rapidly proliferates, mediated by IL-2 acting autologously through the IL-2 receptor. Depending on the cytokines and chemokines present, the T cell can differentiate into a number of different subtypes (FIGURE 5).

$CD8^+$ T cells, once they have become activated and differentiated into effector T cells, can secrete perforin and granzymes (regulated by IL-2 (Janas et al., 2005)), which form pores in the membrane and activate apoptosis of the target cell (reviewed in (Trapani and Smyth, 2002).

1.1.4 ANTIGEN PRESENTATION WITHIN THE THYMUS

1.1.4.1 CELLS PRESENT IN THE THYMUS

In addition to T cells, other cells are present to aid successful T cell development. These include, cortical and medullary thymic epithelial cells, B cells, bone-marrow derived dendritic cells and macrophages (Pearse, 2006). They all express peptide presented by Major Histocompatibility Complex class I (MHCI) or class II (MHCII) molecules to T cells. These molecules were originally identified due to tissue graft rejection experiments (Barth et al., 1956) and were later shown to control the T cell antigen-directed immune response (Benacerraf and McDevitt, 1972). These MHC molecules present antigen to the developing thymocytes (Boyd et al., 1993, Douek and Altmann, 2000), which aid positive and negative selection (central tolerance), ensuring that the TCR is functional and that the developing T cell is not too easily activated or capable of recognising self-antigens as discussed later. They are also vitally important in antigen presentation to T cells in the periphery.

FIGURE 4: T CELL COSTIMULATION ACTIVATORY AND INHIBITORY MOLECULE INTERACTIONS

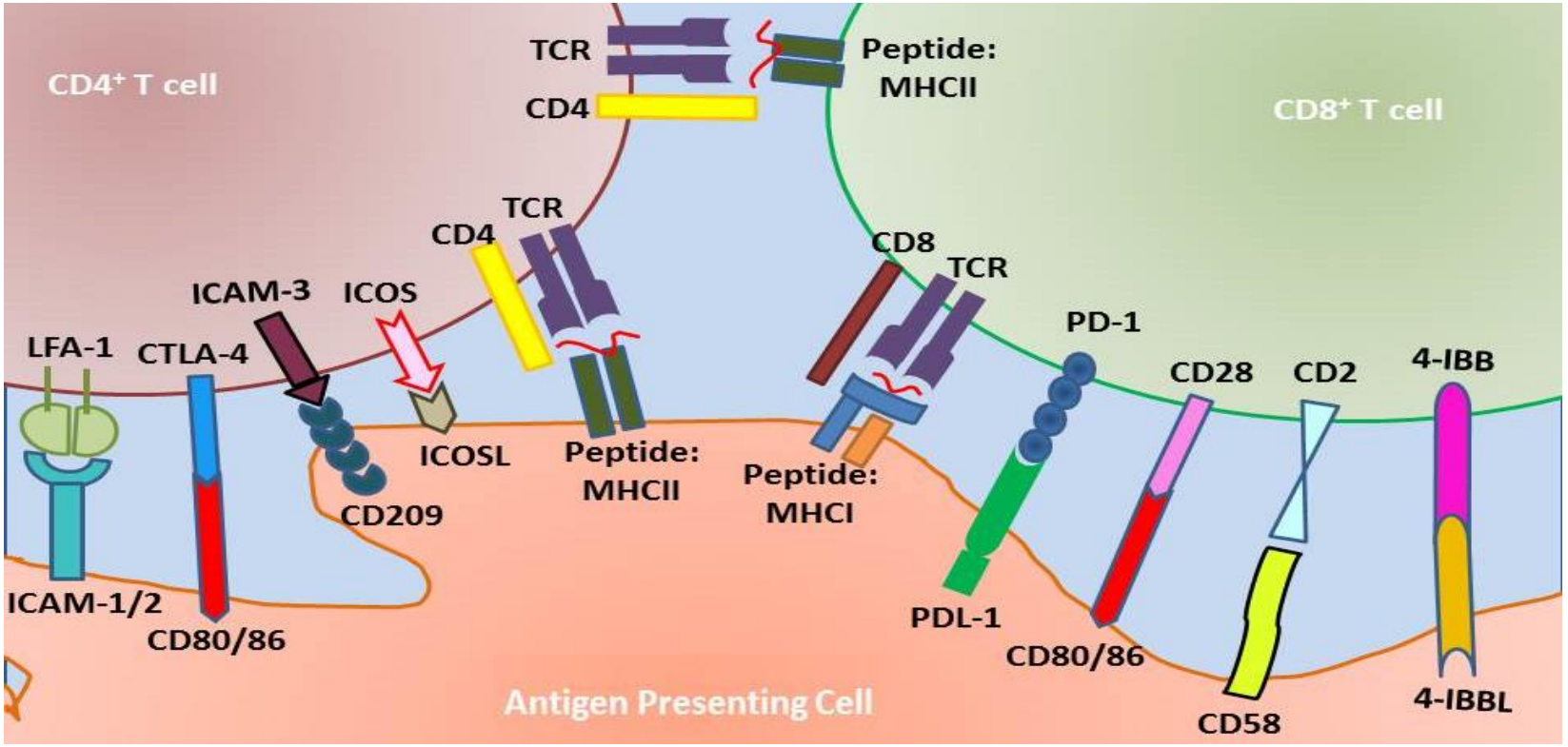

FIGURE 4: T cell interactions with antigen presenting cells (APCs) are needed to provide additional support to T cells. This support can enable T cell activation by signalling through many molecules including CD2, CD28, ICOS, 4-IBB, ICAM-3 and LFA-1 or regulation and inhibition of T cell activation by signalling through CTLA-4 and PD-1. In addition, while $CD8^+$ T cells do not express p:MHCII molecules, through trogocytosis, they are capable of expressing p:MHCII and presenting antigens to $CD4^+$ T cells.

FIGURE 5: CYTOKINE-MEDIATED T CELL DIFFERENTIATED SUBSETS

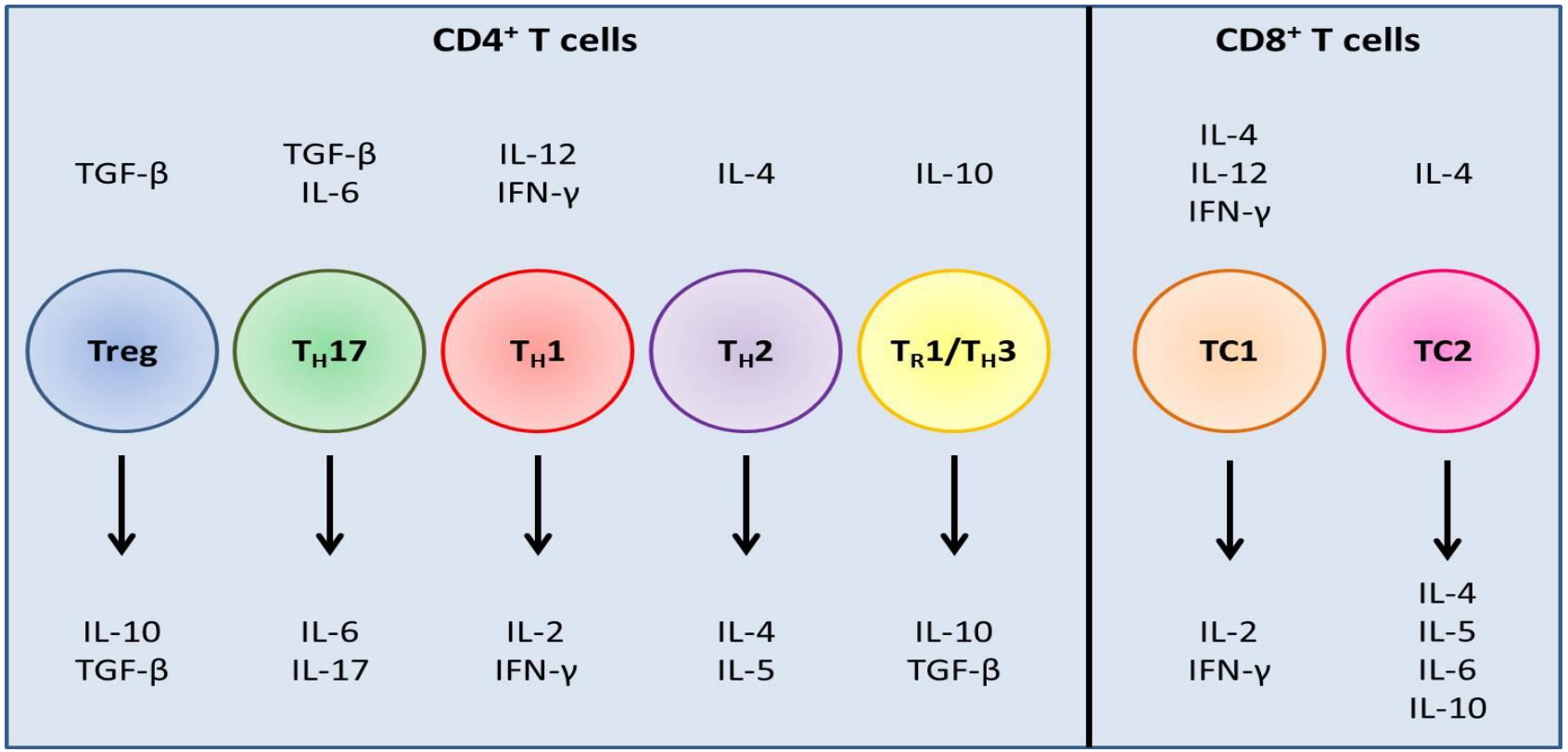

FIGURE 5: For T cell activation, survival and differentiation, the cytokine environment is very important. The presence of cytokines, as well as TCR signalling and costimulation, enables T cells to develop into a variety of T cell subsets, some of which are shown. While there are many cytokines known to impact T cell differentiation and function, only a few are shown. Data extracted from (Sad et al., 1995, Luckheeram et al., 2012).

1.1.4.2 MAJOR HISTOCOMPATIBILITY COMPLEX (MHC) MOLECULES PRESENT PEPTIDES TO T CELLS

MHC molecules present peptide to developing thymocytes and cells in the periphery. MHCI and MHCII present peptides to $CD8^+$ T cells and $CD4^+$ T cells respectively via their TCR molecules. For MHCI peptide presentation, the single chain of MHCI (α chain) is transported into the endoplasmic reticulum where chaperone proteins enable β2 microglobulin association and allow antigenic peptides to bind within the MHC groove prior to cell surface expression (Moore et al., 1988, Degen et al., 1992), as shown in FIGURE 6. For MHCII peptide presentation, antigens are taken up into endocytic vesicles and transported to the endosomes and lysosomes, where the extracellular proteins are degraded by proteases to produce peptides capable of binding to the MHCII molecules (Dunn et al., 1989, Dunn and Maxfield, 1992). However, both endogenous and exogenous peptide-processing pathways can be used by both MHCI and MHCII molecules to bind peptide (Carbone and Bevan, 1990, Dani et al., 2004).

These peptides are produced by proteases degrading the proteins intracellularly. However, the function and availability of specific proteases can change the peptide repertoire, both centrally and peripherally and therefore, depending on the peptide presented, the TCR repertoire can be modified, influencing disease susceptibility (Murata et al., 2007, Nitta et al., 2010, Viret et al., 2011a, Viret et al., 2011b, Zanker et al., 2013). In addition, for longer peptides (i.e. MHCII peptides), the peptide may be able to bind in a different register(s), known as register shifting, once again modifying disease susceptibility (Scott et al., 1998, He et al., 2002, Mohan et al., 2011).

FIGURE 6: PEPTIDE ASSOCIATION WITH MHCI

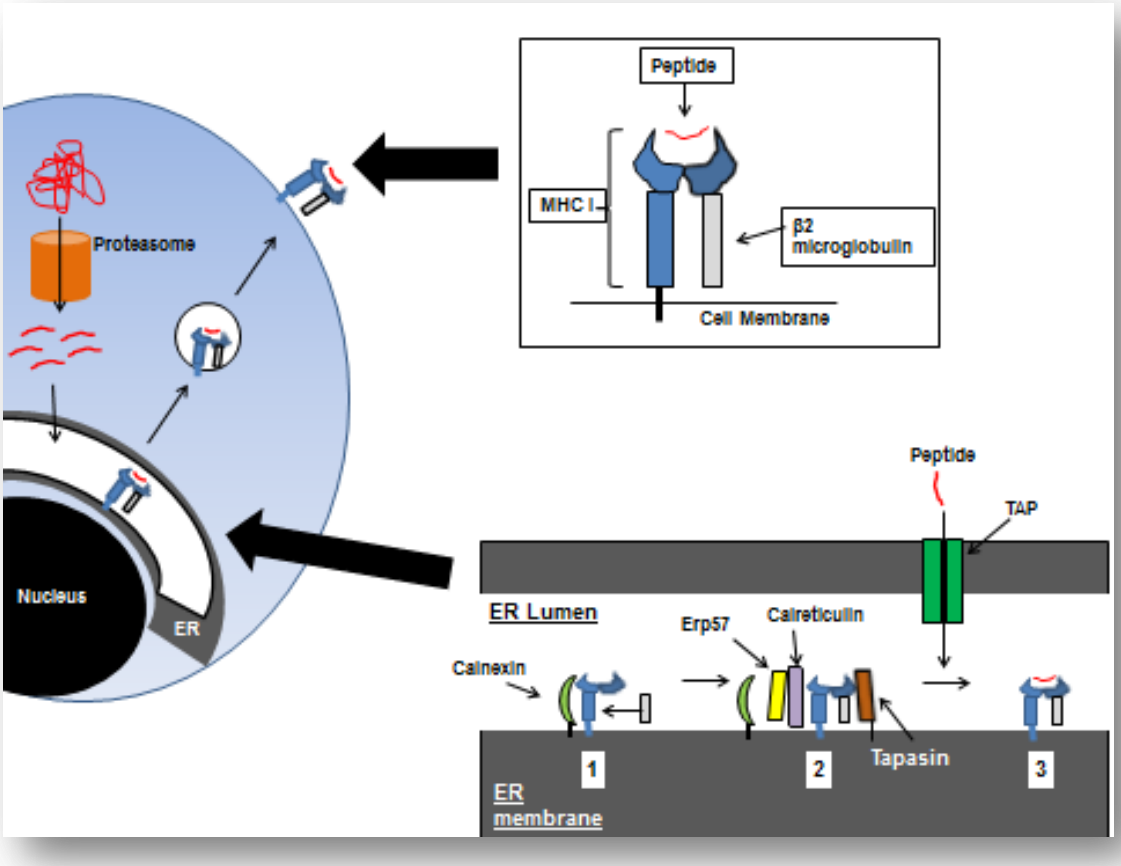

FIGURE 6: MHCI α chain is translocated into the ER lumen where calnexin stabilises the molecule prior to β2 microglobulin binding. Upon binding, calnexin is released and other chaperone proteins are recruited (Erp57, Calreticulin, Tapasin), further stabilising the complex until peptide binds. Peptide is derived from intracellularly-degraded cytosolic proteins by proteasomes, where the peptide products traffic into the ER lumen via TAP proteins. Once the peptide has bound, the pMHC complex buds from the ER to the cell surface via vesicle trafficking. Upon arrival at the cell surface the pMHC complex awaits interactions with the TCR of $CD8^+$ T cells (reviewed by (Germain, 1994)).

1.1.4.3 ANTIGEN EXPRESSION IN THE THYMUS

During T cell development in the thymus, tissue restricted self-antigens are expressed under a transcription factor called the autoimmune regulator (AIRE), predominantly in medullary thymic epithelial cells (Zuklys et al., 2000, Derbinski et al., 2001). AIRE was identified in 1997 with mutations in the *Aire* gene found in patients with autoimmune polyendocrinopathy-candidiasis-ectodermaldystrophy (APECED) (Nagamine et al., 1997). When *Aire* is not expressed APECED develops, characterised by a number of different clinical manifestations including oral candidiasis, hypoparathyroidism, vitiligo and leading to multi-organ autoimmune disease (Ahonen et al., 1990). AIRE is a master regulator ensuring tissue-restricted antigens (TRAs), such as those targeted in APECED e.g. insulin, salivary proteins etc (Anderson et al., 2002). *Aire* is also highly conserved between humans and mice (Blechschmidt et al., 1999) and is responsible for the expression of between ~100-300 different genes. In addition, AIRE expression was shown to be increased in an allele dose-dependent manner with each AIRE encoding allele expressed corresponding to increased TRA (tissue restricted antigen) expression in the thymus (Liston et al., 2004). However, TRA expression in the periphery was unaffected suggesting the thymic microenvironment played an important role in modulating AIRE (Liston et al., 2004, Kont et al., 2008).

Aire expression enables developing T cells to encounter TRAs, ensuring any T cells that recognise these antigens strongly are deleted by negative selection, preventing autoimmunity (Liston et al., 2003). Without AIRE, auto-reactive T cells escape and cause autoimmune disease seen in APECED. Additionally, in autoimmune-disease prone NOD mice, thymic AIRE positive cells were shown to have abnormal morphology indicating the importance of normal morphology in antigen presentation and development of a healthy immune system (Heino et al., 2000). Furthermore, autoreactive T cells may escape due to differences in antigen presentation as insulin, a TRA, has been shown to be post-translationally modified within the periphery, by the formation of a disulphide bond, enabling autoreactive T cells, which escape selection, to become activated within the periphery (Mannering et al., 2005). Other post-translational modifications of

antigens include transglutamination, citrullination, phosphorylation and ubiquitination (reviewed in (Doyle and Mamula, 2012, Dunne et al., 2012)).

1.1.4.4 T CELL SELECTION IN THE THYMUS

As alluded to previously, T cell development requires the formation of a functional TCR that can recognise peptide presented in the thymus and relies on the central tolerance processes known as positive and negative selection. In order to assess if the T cell is functional, positive selection occurs whereby, developing T cells are stimulated for further development if they are able to recognise peptide presented in the context of MHC (Ashton-Rickardt et al., 1993, Ashton-Rickardt et al., 1994, Hogquist et al., 1994, Sebzda et al., 1994). No positive selection can occur when tyrosine kinases (Lck or Zap70) or the tyrosine phosphatase, CD45, are inactivated (Negishi et al., 1995, Byth et al., 1996, Hashimoto et al., 1996). When there is defective positive selection, T cell lymphopenia, correlated with fewer single positive thymocytes, as well as increased autoimmunity, occurs (Fischer et al., 1995, Trop et al., 2000, Zou et al., 2008, Wang et al., 2012a). In addition, T cells that have a high affinity TCR to self-antigens (i.e. a TCR that recognises p:MHC strongly) enable positive selection and the development of $CD4^+$ Tregs (Lee et al., 2012a). In addition, any T cell that is unable to interact with p:MHC complexes dies by apoptosis referred to as "death by neglect" in the thymic cortex (Surh and Sprent, 1994).

Positively selected T cells may also be negatively selected whereby T cells expressing TCRs that recognise p:MHC strongly are deleted, by apoptosis, to prevent the development of autoimmunity. This process only occurs within the thymic medulla (Douek and Altmann, 2000). Depending on the concentration of antigen, either FAS-mediated (Kishimoto and Sprent, 2001) or FAS-independent apoptosis is stimulated (Kishimoto and Sprent, 2000). However, strong TCR signalling can increase cFLIP (caspase-8-homologous FAS-associated death-domain-like interleukin 1β-converting enzyme-inhibitory protein) and thus semi-mature auto-reactive thymocytes can escape from negative selection (Kishimoto and Sprent, 2001). In addition, low affinity interactions enable auto-reactive T cells to escape central tolerance (Zehn and Bevan, 2006, Yin et al., 2011, Enouz et

al., 2012). The presence of antigen is very important and, in some cases, susceptible mice/individuals fail to express enough e.g. in EAE (Klein et al., 2000) and T1D (Bennett et al., 1995), allowing auto-reactive T cells to escape negative selection. Once the thymocytes have migrated out of the thymus, they continue their maturation in the periphery (Boursalian et al., 2004).

1.1.5 PERIPHERAL T CELL ACTIVATION AND REGULATION

While mTECs present antigen to developing T cells in the thymus; peripheral antigen can be expressed by many cell types including APCs i.e. dendritic cells (DCs) and stromal cells. Peripheral antigen expression enables T cells to become activated, tolerised, anergic (become unresponsive) or even deleted (Hawiger et al., 2001, Fife et al., 2006, Lee et al., 2007, Fletcher et al., 2010, Lukacs-Kornek et al., 2011). In addition, MHC expression (Tsai et al., 2013a, Tsai et al., 2013b), lack of costimulation (Chang et al., 1999, Girvin et al., 2000) and the presence of tolerogenic cytokines e.g. IL-10 or TGF-β (Horwitz et al., 2003) can all enable T cell suppressive effects.

Regulatory T cells (expressing $CD25^{+}FoxP3^{+}$) can exert suppressive effects on pathogenic T cells, such as islet-reactive T cells (Martinez et al., 2005). Tregs can be classified into natural Tregs and induced Tregs (converted T cells that have switched to become Tregs) and have many roles including preventing autoimmunity, inducing tolerance to dietary antigens, fetal antigens during pregnancy and commensal bacterial antigens, while also suppressing allergic responses and pathogen-mediated pathology (reviewed in (Corthay, 2009)). While some studies have shown that conventional $CD4^{+}$ T cells do not convert into Tregs (Wong et al., 2007a, Hindley et al., 2011, Relland et al., 2012), others have shown that they are capable of conversion (Fousteri et al., 2012). When $CD4^{+}CD25^{+}$ T cells were depleted, various autoimmune diseases were seen (Sakaguchi et al., 1995). Furthermore, Tregs have been shown to induce self-tolerance to many auto-antigens, preventing autoimmune diseases such as experimental autoimmune encephalomyelitis (McGeachy et al., 2005), rheumatoid arthritis (Ehrenstein et al., 2004) and autoimmune diabetes (Tang et al., 2004, Montane et al., 2011). Interestingly, in the non-obese diabetic (NOD)

mouse model, infection with parasitic *Schistosoma mansoni* soluble egg antigen (SEA; containing the glycoprotein ω-1) prevents diabetes through inducing Tregs, which upregulate FoxP3 in a TGF-β-dependent manner with TGF-β responses increased through Toll-like receptor 2 (TLR-2; a cell surface receptor aiding in pathogen recognition) stimulation (Cooke et al., 1999, Zaccone et al., 2009, Burton et al., 2010, Zaccone et al., 2011).

In addition to the classic $CD4^+CD25^+FoxP3^+$ T cells, other subsets of regulatory cells have been identified, including $CD8\alpha\alpha^+TCR\alpha\beta^+$ T cells (Lu et al., 2008, Kim et al., 2010), $CD8^+CD122^+$ T cells (Rifa'i et al., 2004, Lee et al., 2008) and Tr1 cells (Apetoh et al., 2010), all of which mediate immune regulation.

For naïve auto-reactive $CD8^+$ T cells, they can be peripherally deleted by "suicidal emperipolesis", whereby auto-reactive $CD8^+$ T cells actively invade the hepatocytes and are rapidly degraded in lysosomes (Benseler et al., 2011), or destroyed after an immune response in the liver (John and Crispe, 2004). However, not all auto-reactive T cells can be tolerised effectively and therefore T cells become activated and cause disease.

As mentioned, it is the TCR which dictates the antigen specificity of the T cell and therefore understanding how the T cell, expressing a specific TCR, is able to escape tolerance and cause disease, is important. By following the development of T cells i.e. through using antibodies to the TCRVα and/or TCRVβ chains, the selection of specific TCR chains could be investigated. This enabled researchers to investigate the TCR repertoire to identify if there was any TCR chain bias associated with T cells escaping tolerance and causing disease.

1.1.6 T CELL RECEPTOR REPERTOIRE IN DISEASE

1.1.6.1 TCR REPERTOIRE ANALYSIS METHODS

Investigation of the T cell receptor repertoire enables identification of the TCR chains used by antigen-specific populations of T cells. There are currently 2 main ways of identifying the TCR repertoire. These include using an antibody-based flow cytometry method and using a gene-based approach. In addition, for a more

detailed repertoire study, sequencing the complementarity determining region 3 (CDR3) will identify the portion of the TCR that determines antigen specificity. This effectively identifies the clonotype of a T cell, providing information on the V-(D)-J rearrangement and can provide clearer insight into how the TCR engages with peptide:MHC complexes.

1.1.6.1.1 FLOW CYTOMETRIC METHODS

Assessing TCR repertoire by flow cytometry provides a protein-based approach and enables not only the TCR variable alpha/beta chain to be studied but also other cellular markers e.g. activation markers. In addition, this also allows identification of specific TCR-expressing T cells within a heterogeneous population of cells. The number of cellular markers to be investigated depends on the flow cytometer available. This information provides both qualitative and quantitative information about the variable region of the TCR which can be useful in assessing cell populations with age or treatment. Prior to new advancements in technology, this method was the only way to quantitatively assess the TCR repertoire. Unfortunately, there are also limitations including the lack of availability of antibodies specific to the TCR variable chains e.g. for murine TRBV chains there are currently 14 antibodies available; however for the TRAV chains there are only 4. In addition, this provides a very limited approach with respect to assessing junctional diversity as well as the inability to identify polymorphisms within the TCR repertoire.

1.1.6.1.2 GENE-BASED APPROACHES

Gene-based approaches such as the use of PCR can identify the TCR chain usage. This is invaluable when developing transgenic mouse models i.e. genotyping but may also be used to follow the TCR repertoire diversity following therapy (Douek et al., 1998). Initial genetic approaches to TCR repertoire involved individual specific primers for each chain, identifying if the chain was present or not. The development of quantitative real-time PCR strategies further advanced the field whereby specific primers can be used for the variable and junctional regions (Wettstein et al., 2008) or may be bound to the constant region of the TCR. This provides the ability to study the TCR repertoire diversity in great detail, as it not

only identifies the variable chain but also the diversity and junctional regions too. CDR3 spectratyping is also a powerful technique for investigating the CDR3 region length, shown by peaks, which can change following immunisation (Cochet et al., 1992). These techniques provide greater insight into the TCR repertoire, including how the T cells recognise antigen, and prove very important when antibodies are not available. However, while initially this technique was semi-quantitative, it has become much more quantitative providing clonal frequencies, but no other cellular information on the cells, unlike the data obtained by flow cytometry. In addition, depending on the technique used, individual T cell clones may not be identified at the nucleotide level. Microarray techniques have also been pursued at the single cell level though this relies on data from previous spectratyping experiments (Bonarius et al., 2006).

1.1.6.1.3 NEXT GENERATION SEQUENCING AND CLONOTYPING

Coupling flow cytometry-based cell sorting on a specific population of cells with gene-based approaches can provide numerous advantages while reducing the limitations discussed. In order to get the best nucleotide sequence and therefore the best resolution of the TCR repertoire diversity, Sanger sequencing techniques can be used following PCR amplification of the cDNA and bacterial cloning (although cloning into TCR negative cell lines also works too and may help identify rare antigen-specific clones (Kobayashi et al., 2013)). This specifically enables information to be gathered on the TCR diversity and how it may be modified (Weinstein et al., 2009), providing very detailed information about the repertoire including the identification of shared TCRs (public TCRs) and private TCRs (individual-specific TCRs). This information provides the TCR clonotype, which refers to a “unique nucleotide sequence that arises during the gene rearrangement process for that receptor” (Yassai et al., 2009). However, these techniques have disadvantages including time (although new techniques suggest it can take as little as 10 days (Kobayashi et al., 2013)) and also cost, although costs are reduced as higher-throughput sequencers are developed.

1.1.6.2 TCR REPERTOIRE IN DISEASE

TCR repertoire is important as specific TCR chains/clonotypes may be influential in driving, or protecting mice or individuals, from disease. It has also been acknowledged that TCR repertoire diversity is advantageous to health, with public TCRs providing targets for vaccination and immunotherapy. In addition, as healthy individual's age, there is a reduction in the diversity of the TCR repertoire. While some studies have suggested this does not occur before 75 years of age (Naylor et al., 2005, Pfister et al., 2006), more advanced deep TRBV sequencing has shown a significant reduction present by 40 years of age (Britanova et al., 2014). Analysing the TRBV repertoires and clonotypes in the study by Britanova and colleagues also revealed a reduction in the most abundant public TCRs with age, an important finding for future work on vaccinations in the elderly.

1.1.6.2.1 TCR REPERTOIRE IN INFECTION

Anti-viral $CD8^+$ TCR repertoire is dependent on the recognition of specific antigenic peptides, whereby a single MHC type is capable of presenting different peptides of the same virus and super-imposed epitopes enabling the recruitment of cells with different TCRs (Koning et al., 2013, Sun et al., 2014). In addition, polymorphisms within the MHC can alter antigen presentation, which can affect the TCR repertoire diversity and avidity of $CD8^+$ T cells resulting in either a protective or a pathogenic response (Messaoudi et al., 2002, Gras et al., 2009). It is this avidity for antigen, which in turn selects the $CD8^+$ T cell clone which dominates the immune response (Price et al., 2005).

In human CMV infections, Smith and colleagues showed that exposure to genetic variants of the virus enabled strain-specific T cells to expand prior to the subsequent influx of cross-reactive T cells for CMV peptides (Smith et al., 2014). Interestingly, the initial strain-specific T cells were shown to be unique, with an oligoclonal repertoire within individuals. However, the cross-reactive $CD8^+$ T cells were shown to express a public TCR repertoire that was highly conserved due to the flexibility of the TCR to recognise peptide variants. In addition, a cross-reactive CMV-specific $CD8^+$ T cell had been identified which recognised peptides presented by HLA-A*02:01 and alleles of HLA-B27 (Nguyen et al., 2014).

TRAV3TRAJ31 and TRBV12-4TRBJ1-1 chains formed this TCR with these specific T cells becoming immunodominant following a bilateral lung transplant in the CMV seropositive recipient prior to CMV reactivation. Therefore, this suggested that TCR monitoring in patients may identify clinically relevant changes and provide targets for therapy.

In C57BL/6 mice, a HSV-1 epitope was used to investigate the HSV-1 specific $CD8^+$ T cell repertoire. This showed a TCRVβ10 (TRBV4) bias dominating the response and TCRVβ8 (TRBV13) being sub-dominant (Cose et al., 1995). In a subsequent study, age was shown to increase TCRVβ10^+ (TRBV4^+) HSV-1 specific $CD8^+$ T cells while reducing TCRVβ8 (TRBV13) (Rudd et al., 2011). Specific investigation of these TCRVβ10^+ (TRBV4^+) T cells revealed retention of the identified WG motif within the CDR3β sequence at all ages, although the CDR3β length was shown to be shorter in neonatal mice than adult mice. While identifying this bias, they reported shared clonotypes between the mice but within individual mice they did not find the same dominant clonotype.

There are also TCR repertoire biases within $CD4^+$ T cells in relation to viral infection. This can be seen in mice infected with the Friend virus (a retrovirus) whereby virus-specific $CD8^+$ T cells enable a specific expansion of $CD4^+$ Tregs expressing TCRVβ5 (TRBV12), which reduce the acute response but allow a chronic infection to be established (Myers et al., 2013).

1.1.6.2.2 TCR REPERTOIRE IN CANCER

In cancer, there is an increased presence of Tregs, which enable the survival of the carcinoma. In mouse carcinogen-induced tumour models there is an increased presence of TGF-β and Tregs. Through investigation of the TCR repertoire, Tregs and conventional $CD4^+$ T cells were compared. This revealed distinct TCR repertoires between the subsets. This lack of TCR repertoire sharing indicated that the two populations of T cells had arisen independently and, there was no conversion from conventional T cells into Tregs (Hindley et al., 2011). This has also been shown in relation to foreign antigens (Relland et al., 2012). In a mouse tumour cell injection model, the $CD4^+$FoxP3^+ T cells showed TCRVβ8.1

(TRBV13-3) and TCRVβV6 (TRBV19) were found to be elevated intra-tumorally compared to non-tumour tissue but also that the CDR3 sequences used were biased towards public sequences (Sainz-Perez et al., 2012), suggesting these could be targeted therapeutically.

In human ovarian cancer, freshly isolated tumour-infiltrating T cells (TILs) were shown to have a heterogeneous TRVB repertoire; however, following *in vitro* expansion of $CD8^+$ T cells, a bias was identified with a predominance of Vβ2 and 6 (Peoples et al., 1993). When targeted by TCRVβ monoclonal antibodies, both TCRVβ populations were unable to cause tumour cytotoxicity, highlighting the importance of these TILs and their repertoire bias in targeting cancer. Culturing TILs from renal and ovarian carcinoma in IL-2 also revealed a preferential expansion of T cells utilising Vβ5 and 6 (Halapi et al., 1993). Subsequent high-throughput sequencing of TCRs in ovarian cancer revealed a homogeneous TRBV repertoire intra-tumorally that was distinct from peripheral blood (Emerson et al., 2013). There were also repertoire differences noted between TIL in hepatocellular carcinoma and PBMCs (Weidmann et al., 1992). However, in colorectal tumours, this trend was reversed with a greater diversity intra-tumorally than in adjacent mucosal tissue (Sherwood et al., 2013). In breast cancer there were no reported TRBV repertoire changes (Mathoulin et al., 1993). Identifying bias within the TCR repertoire provides information on how these cells develop and if they clonally expand in response to a specific tumour antigen.

TCR repertoire can also be important clinically, as reduced TCR repertoire diversity with lymphopenia indicates poor survival following chemotherapy for metastatic breast cancer (Manuel et al., 2012). Furthermore, through TRBV CDR3 spectratyping, murine $TCRV\beta1^+$, $TCRV\beta6^+$ and $TCRV\beta13^+$ ($TRBV5^+$, $TRBV19^+$ and $TRBV14^+$) $CD8^+$ T cells were identified as having a response to a tumour antigen (MMC6) without any Graft vs Host disease (GVHD) (Fanning et al., 2013). As $TCRV\beta13^+$ ($TRBV14^+$) expressing $CD8^+$ T cells were able to recognise the antigen using 3 different CDR3 sized-lengths, they showed through pre-exposing these T cells to MMC6, they induced a beneficial graft vs leukaemia effect with minimal GVHD, highlighting the importance of the immune repertoire in cancer therapy.

1.1.6.2.3 TCR REPERTOIRE IN AUTOIMMUNE DISEASE

As discussed in relation to cancer and virus infection, TCR repertoire studies have shown little or no bias towards specific TRAV or TRBV segments in some cases but in others, have revealed important information on cell development with the potential for use in therapy. This is also the case with regard to autoimmune disease.

In rheumatoid arthritis the TRAV and TRBV repertoire has been investigated in the synovia of patients (Olive et al., 1991, Sioud et al., 1992), showing populations of polyclonal T cells with little or no bias. However, in early stages of rheumatoid arthritis there was preferential Vα17 gene usage (Fischer et al., 1996) but this TCR repertoire bias was lost in cases with juvenile (Sioud et al., 1992) and adult (Olive et al., 1991) rheumatoid arthritis. This suggested recruitment of other T cells with disease progression, as also seen in a mouse model of Sjogren's disease (Hayashi et al., 1995). In the collagen-induced mouse model of arthritis, type II collagen is administered intradermally with CFA (complete Freund's adjuvant), which activates antigen-specific T cells causing autoimmune arthritis. These type II collagen-specific T cells were fused with hybridoma partners (lacking a TCR) to investigate the TCR repertoire. Both the TCRα and TCRβ chains exhibited a restricted TCR repertoire including Vα8, 11 or 22 with Jα24, 32, 37 or 42 while the TCRVβ was limited to TCRVβ1, TCRVβ6 and TCRVβ8 (TRBV5, TRBV13 and TRBV19). This TCR restriction provided a target for antibody immunotherapy; upon anti-TCRVβ8.2 (TRBV13-2) antibody administration, the incidence of arthritis was reduced by 60% (Osman et al., 1993). However, studies investigating the repertoire of total T cells, which may respond to many different antigens or peptides, may not provide the most accurate results and therefore antigen-specific repertoire studies may provide greater evidence of a TCR repertoire bias. As for the $CD4^+$ Treg population in rheumatoid arthritits, transfer of polyclonal Tregs induced disease prevention. However, using Tregs expressing a clonotypic TCR for hemagglutinin expressed as an auto-antigen, only prevented antigen-specific pathogenic T cells for the same hemagglutinin antigen and was unable to stop the Th17 T cell accumulation and disease (Oh et al., 2012).

In a limited TCR repertoire mouse model of arthritis, Wong and colleagues investigated how the TCR repertoire was altered in response to self-antigen expression within the CD4 compartment (Wong et al., 2007b). They showed that $CD4^+$ T cells had a fixed TCRVβ5 (TRBV12) chain and a TCRα chain minilocus encoding TCRVα2.3 and either Jα2 or 26. Interestingly, differences within the TCRα chain CDR3 region were observed whereby Tregs tended to have a higher positive charge than conventional $CD4^+$ T cells. This CDR3α chain difference was dependent on self-peptide presentation, as when H2-DM was mutated, fewer peptides were presented. The CDR3 repertoires were much more similar but also shorter, indicating a need for peptide presentation to ensure TCR repertoire diversity and effective Treg repertoire development.

In addition to $CD4^+$ Tregs, $CD8^+CD122^+$ IL10-producing Tregs, important in inflammatory bowel disease and experimental autoimmune encephalitis (EAE), have also been shown to preferentially use TCRVβ13 (TRBV14) to mediate their suppressive activity (Okuno et al., 2013). These T cells also exhibited the most common CDR3 sequence (ASSYRGAEQF) suggesting preferential expansion of these cells.

Additionally, in experimental autoimmune encephalomyelitis (EAE), a mouse model for multiple sclerosis, those mice that were susceptible to disease lacked a splice variant of the proteolipid protein (found in the myelin sheath) within the thymus, leading to a lack of tolerance and thus an auto-reactive TCR repertoire escaped (Klein et al., 2000). This auto-reactive repertoire showed a $CD4^+$ T cell bias for TCRVβ8.2 (TRBV13-2), TCRVβ13 (TRBV14), TCRα2.3 and 4.3 (Urban et al., 1988) and enabled immunotherapy using anti-TCR antibodies to treat the murine disease (Zaller et al., 1990). $CD4^+$TCRVβ8^+ (TRBV13^+) TCR repertoire bias, and to a lesser extent TCRVβ6 (TRBV19), has also been reported in the MRL/lpr model of Sjogren's disease (Hayashi et al., 1995).

In autoimmune thyroid diseases there have been reports showing skewing of the TRAV repertoire in thyroid infiltrating T cells, where only 2-6 TRAV chains were detected in each patient, with each patient expressing an individual dominant

TRAV chain (Davies et al., 1991). Investigation of the TRBV repertoire revealed greater diversity with no apparent skewing (Davies et al., 1992). However, with the advancement of technology, in particular CDR3 spectratyping, a significantly higher skewing within the $CD8^+$ TCRβ CDR3 region was identified in the peripheral blood of patients with Hashimoto's thyroiditis but not in patients with Graves' disease or healthy controls (Okajima et al., 2009). While no specific TRBV bias was noted for any particular chain, it illustrated that some TCRβ chains had a CDR3 of a specific length, especially in patients with disease longer than 5 years and receiving hormone replacement therapy. Disease duration can also influence the TCR repertoire, as seen in patients with early-stage Graves' disease in whom a preference for specific TRBV repertoire (TCRVβ3, 5 and 8) was seen in thyroid-infiltrating T cells (Zhang et al., 2006).

1.1.6.2.4 TCR REPERTOIRE IN TYPE 1 DIABETES

TCR repertoire has been investigated in type 1 diabetes in a variety of models, including the Non-Obese Diabetic (NOD) mouse, which develops spontaneous autoimmune disease similarly to humans (see section 1.2). Expressing protective transgenes for I-E and $I\text{-}A^{g7}$ protected NOD mice from diabetes but failed to alter the level of $CD4^+$ or $CD8^+$ TCRVβ5 (TRBV12), TCRVβ6 (TRBV19), TCRVβ8 (TRBV13) and TCRVβ11 (TRBV16) expressing T cells (Lund et al., 1990). NOD mice and NOD I-E expressing mice were also screened for 14 TRBV chains to see if any differences were responsible for the protective effect, although none were found (Parish et al., 1993). In addition, even NOD mice, which were engineered to genetically lack TCRVβ5, 8, 9, 11, 12 and 13 (TRBV12, 13, 17, 16, 15 and TRBV14), still developed spontaneous autoimmune disease (Shizuru et al., 1991). However, through advancements in technology, with studies designed to specifically follow a given treatment or antigen-specific T cells, TCR repertoire changes have been identified.

Polyclonal B cell reconstitutions in NOD.Igμnull mice, which lack B cells, show a pancreas-specific TRBV expansion that becomes more diverse with age (Vong et al., 2011). In addition after the B cell reconstitution, if the mice were treated with cyclophosphamide, the TRBV repertoire showed a reduction within the pancreas

of TCRVβ1-, 8- and 11- (TRBV5, TRBV13 and TRBV16) expressing T cells but an increase in others e.g. TCRVβ4, 5.2, 9, 16, 17, 18, 19 and 20 (TRBV2, TRBV12-1, TRBV17, TRBV3, TRBV24, TRBV30, TRBV21 and TRBV23).

Investigation of islet-reactive $CD8^+$ T cells from infiltrated islets of young 5-6 week old NOD mice were isolated and examined for any TCR repertoire bias (DiLorenzo et al., 1998). TCRVβ8 (TRBV13) was found to be predominant, having been identified in 5 T cell lines (AI11.B2, AI12.B1p, AI15.A3, AI15.A10 and AI15.F5) but the TRBV repertoire was quite diverse. More noticeable was the prevalence of TCRVα17 members and TCRJα42 which resulted in similar CDR3α loop size and this was suggested to be important for antigen recognition.

Another study, in NOD female islets at 7 weeks, showed a bias in TCRVβ3 and TCRVβ7 (TRBV26 and TRBV29) (Galley and Danska, 1995), despite the presence of the mouse mammary tumour virus which deletes T cells expressing TCRVβ3 (TRBV26) (Fairchild et al., 1991). However, this TCRVβ3 deletional effect is only mediated when NOD mice express I-E (Parish et al., 1993), which normal NOD mice lack.

In islet-infiltrating T cells, TCRVβ5 and TCRVβ8 (TRBV12 and TRBV13) were shown to be preferentially used in pre-diabetic NOD male and female mice, although these T cells were not clonal and varied in CDR3 length (Berschick et al., 1993). Interestingly, the $TCRV\beta5^+$ ($TRBV12^+$) T cells had a preference for associating with TCRJβ2.6 (TRBJ2-6; 30-40%) and lacked any association with TCRJβ1.6 (TRBJ1-6); however these preferences were shared with non-islet tissues including spleen and lymph nodes. As for $TCRV\beta8^+$ ($TRBV13^+$) T cells, there was no selective pressure on the TRBJ chains although, in male NOD islet-infiltrating T cells, there was an increased association of TCRJβ1.1 (TRBJ1-1; 23% vs 5% in females). However, these T cells encompassed both $CD4^+$ and $CD8^+$ T cells and were of unknown antigen specificity, which may suggest reasons why no clonal expansions were identified.

Investigation of antigen-specific TCR repertoire showed a greater TCR α/β chain bias. One antigen, recognised by both humans and mice, is GAD65 (Kaufman et

al., 1993, Endl et al., 1997). In NOD mice, there are two GAD65 epitopes recognised by auto-reactive $CD4^+$ T cells; these are amino acids 530-543 and 524-538, which provide dominant GAD65 reactivity in naïve young NOD mice or immunised NOD mice respectively. Adaptations in TRBV repertoire are responsible for this change in peptide dominance, whereby $TCRV\beta4^+$ ($TRBV2^+$) T cells are preferentially expanded in naive young NOD mice, whereas upon immunisation, $TCRV\beta12^+$ ($TRBV15^+$) $CD4^+$ T cells are preferentially found (Quinn et al., 2001a). In addition, this repertoire change also corresponds to a functional difference resulting in a shift from effector T cells to regulatory T cells.

By generating a single chain TCRβ transgenic mouse expressing TCRVβ8.1, used by the β cell cytotoxic NY8.3 $CD8^+$ T cell clone in NOD mice (Nagata et al., 1994a), Verdaguer and colleagues were able to identify the role of an antigen-specific $CD8^+$ T cell in disease but also determine which TCRα chains pair to enable islet antigen recognition (Verdaguer et al., 1996). Interestingly, in these single chain transgenic mice, they showed specific increased $CD8^+$ T cell pancreatic infilitration, resulting in greater β cell destruction and accelerated diabetes (from 8 weeks) compared to non-transgenic mice and NOD controls, while $CD4^+$ T cells were unaffected. By using this TCRβ chain they showed, in 4/5 oligoclonal lines, a preferential selection of the TCRα chain used by the NY8.3 T cell clone. This T cell clone was later shown to recognise a peptide of IGRP (Lieberman et al., 2003), however, it does demonstrate the bias in TCR repertoire for recognising β cell antigens.

Insulin B9-23-reactive $CD4^+$ T cells show a TCRα chain bias in inducing anti-insulin autoimmunity. *TCRCα*$^{-/-}$ single chain transgenic mice for TRAV5D-4*04TRAJ53, the TCRα chain of the insulin-reactive BDC12.4.1 clone, were shown to dictate insulin auto-reactivity as mice transgenic for TCRVβ2 (TRBV1; the TCRβ chain of the BDC12.4.1 T cell) failed to develop insulin auto-reactivity (Kobayashi et al., 2008). In addition, mice expressing TRAV5D-4*04 but with variable CDR3α regions were shown to induce insulin auto-antibodies, insulitis and respond to peptide *in vitro* (Nakayama et al., 2012). However, insulin auto-reactivity was abrogated when mutating an amino acid in each of the CDR1 (asparagine at position 5) and CDR2

(arginine at position 2) sequences encoded by the TRAV5D-4*04 chain, suggesting other interactions are important in stimulating an antigen-specific response.

Interestingly, islet-reactive TCRs, when sequenced, showed a surprising similarity to the insulin receptor and glucagon receptor, in both humans and NOD mice, as well as to each other (Root-Bernstein, 2009). Therefore, developing novel therapeutics focussing on the interactions between TCRs and their target will have to be very specific to prevent any unwanted effects on the Insulin or glucagon receptor.

TCR repertoire changes can be targeted for use in therapy. For example, in the bio-breeding diabetes prone (BBDP) rats and LEW.1WR1 rats, diabetes could be prevented or reduced through administering an anti-TCRVβ13 (TRBV14) monoclonal antibody treatment, depleting TCRVβ13^{+} T cells (Liu et al., 2012). In addition, when diabetic NOD splenocytes were depleted of each of TCRVβ5, 6, 8 and 11 (TRBV12, TRBV19, TRBV13 or TRBV11) and transferred into young NOD recipients, only the TCRVβ6 (TRBV19) depletion reduced the transfer of diabetes (Edouard et al., 1993). Therefore the TCR repertoire has an important function in aiding the progression of disease. However, further antigen-specific data for CD4 and CD8 T cells are required, together with the TCR repertoire, in order to further understand how antigen expression can shape that specific auto-reactive repertoire, prior to the recruitment of more heterogeneous T cells (Candéias et al., 1991b). One such study investigated the development of IGRP$_{206\text{-}214}$ reactive CD8^{+} T cells in the NY8.3 TCR transgenic NOD mouse. Here, Han and colleagues demonstrated that, in the early stages of disease, low avidity T cells accumulate in the islets causing inflammation (Han et al., 2005). However, this inflammatory environment preferentially expands higher avidity diabetogenic T cells (and outcompetes lower avidity T cells), through avidity maturation, enabling these T cells to contribute to the progression of disease. Therefore, when antigens are released in an inflammatory setting (e.g. β cell destruction), the immune response selects for better responding T cells; thus, while these T cells utilise the

same TCR, the avidity for their antigen changes. However, it is unknown if avidity maturation is also seen in $CD8^+$ T cells that recognise other auto-antigens.

1.2 TYPE 1 DIABETES

1.2.1 HUMAN TYPE 1 DIABETES

Type 1 diabetes is characterised by a loss of insulin production mediated by pancreatic infiltration of auto-reactive T cells causing concomitant destruction of the insulin-producing β cells. This autoimmune disease is increasing in incidence, particularly in children (Gillespie et al., 2004, Bessaoud et al., 2006, Harjutsalo et al., 2008a, Evertsen et al., 2009), with both genetic and environmental factors influencing disease progression, some of which are discussed in relation to the NOD mouse model of type 1 diabetes.

1.2.2 NON-OBESE DIABETIC MOUSE MODEL

1.2.2.1 ANIMAL MODELS

There are two main rodent models of autoimmune diabetes; one is the non-obese diabetic (NOD) mouse model developed by Makino et al (Makino et al., 1980) and the other is the Bio-breeding (BB) rat (Nakhooda et al., 1977). While both models develop spontaneous autoimmune diabetes similarly to humans, only the NOD mouse model will be discussed in further detail.

1.2.2.2 NATURAL HISTORY OF DIABETES IN THE NOD MOUSE

Initially, the pancreatic islets of NOD mice are free from cellular infiltration; however, as the disease progresses the islets become infiltrated by a variety of cells including antigen presenting cells and lymphocytes.

From 4-5 weeks of age, macrophages, neutrophils and dendritic cells (DCs) are seen infiltrating the pancreas of NOD mice (Jansen et al., 1994, Diana et al., 2013). From 7 weeks, macrophages and DCs begin to surround the islets with aid from increased chemokines (CCL19 and CCL21) and enhanced adhesion to fibronectin (Bouma et al., 2005). However, these macrophages are defective at clearing apoptotic debris (O'Brien et al., 2006) and when selectively depleted, through silica injections, prevent insulitis and diabetes (Lee et al., 1988). This

indicates that macrophages are likely to play a role. Importantly, communication between innate and adaptive immune cells is vital for the initiation and progression of type 1 diabetes (Diana et al., 2013).

During the pathogenesis of type 1 diabetes, B lymphocytes also play a critical role. They are found within the islets and can recognise antigens including GAD (De Aizpurua et al., 1994) and insulin (Pontesilli et al., 1987, Michel et al., 1989), to produce auto-antibodies. These auto-antibodies develop from 3 weeks and can help identify potential diabetes risk (Ziegler et al., 1989), as they are associated with islet inflammation but not necessarily diabetes progression (Robles et al., 2003). In addition, NOD B-1a cells ($CD5^+CD19^+CD1d^{med}$) are capable of producing anti-nuclear IgG antibodies during diabetes pathogenesis (Humphreys-Beher et al., 1993) and may activate DCs during the initiation process (Diana et al., 2013). Furthermore, B cell deficient NOD mice, in general, do not develop diabetes (Serreze et al., 1996, Wong et al., 1998) although a few can develop disease (Yang et al., 1997). This relationship is complex however, as B cells alone are unable to induce diabetes in B cell deficient mice, but can do so when repopulated with syngeneic bone marrow (Serreze et al., 1998).

Between 4-6 weeks $CD4^+$ and $CD8^+$ T lymphocytes are detectable within the pancreas, with increasing age associated with severe infiltration of the islets (Miyazaki et al., 1985). Both $CD4^+$ and $CD8^+$ T cells are required for diabetes. This has been shown through genetic mutations in NOD mice (Serreze et al., 1994, Wicker et al., 1994a), in vivo transfers into nude athymic mice (Yagi et al., 1992, Matsumoto et al., 1993) or NODscid mice (Christianson et al., 1993), through antibody immunotherapy to CD8 (Wang et al., 1996), MHC I or II (Boitard et al., 1988, Taki et al., 1991, Nagata et al., 1994a), CD4 (Charlton and Mandel, 1989) or CD3 (Chatenoud et al., 1992). The recruitment of $CD4^+$ and $CD8^+$ T cells enables destruction of the insulin-producing β cells leading to a lack of insulin and the onset of diabetes. While both are important, $CD8^+$ T cells, have shown they can cause β cell-specific lysis in NOD mice (Nagata et al., 1989, Hayakawa et al., 1991) and can recognise islet antigens in the context of $H\text{-}2k^d$ (Nagata et al., 1989) and inhibit islet-derived insulin release (Timsit et al., 1988). In addition to these αβ T

cells, there are also γδ T cells, of which $CD27^{-}CD44^{hi}$ γδ T cells have also been implicated as effectors of type 1 diabetes through IL-17 secretion (Markle et al., 2013b). The αβ T cells target many pancreatic antigens, leading to activation and destruction of the β cells, as will be discussed later.

Approximately 70% of female and 20% of male NOD mice develop diabetes by 35 weeks, but this varies in different colonies around the world (Pozzilli et al., 1993). Interestingly, sexual dimorphism can be altered by castration, whereby male NOD mice become more susceptible to diabetes development and female castration reduced the diabetes incidence (Makino et al., 1981, Hawkins et al., 1993). In addition, testosterone treatment of female NOD mice was shown to reduce diabetes incidence and protect from the development of disease (Fox, 1992). The role of androgens was further highlighted by the observation that female NOD mouse thymocytes were shown to have decreased apoptosis compared to male mice, and when male mice were castrated, thymocyte responses to apoptotic signals were reduced (Casteels et al., 1998). This suggested T cell development or selection was affected by androgens. More recently, this gender dichotomy has been further investigated with both androgens and gut microbiota capable of modifying NOD diabetes susceptibility (Yurkovetskiy et al., 2013, Markle et al., 2013a). In addition, only male NOD mice develop autoimmune dacryoadenitis, where cells infiltrate the lachrymal glands, however both castration and testosterone treatment of male NOD mice increased the incidence (Takahashi et al., 1997). This suggests that androgens may have different effects in relation to different autoimmune diseases.

Similarly, human diabetes involves cellular infiltration in the pancreas of patients with juvenile diabetes mellitus (Gepts, 1965), with macrophages, T cells ($CD4^{+}$ and $CD8^{+}$) and B cells shown to infiltrate the islets of patients with type 1 diabetes (Foulis et al., 1986, Foulis, 1993, Willcox et al., 2009, Coppieters et al., 2012). Although the patterns of infiltration may be different, nevertheless, there are sufficient parallels in the NOD mouse diabetes that indicate that the NOD mouse may give important insights to some aspects of human disease.

1.2.2.3 GENETIC SUSCEPTIBILITY TO DIABETES IN THE NOD MOUSE

The most important genetic susceptibility factor in NOD mice is the MHC. NOD mice express MHC molecules H-2K^{d}D^{b} and I-A^{g7}, with a lack of the MHCII I-E molecule, due to a deletion in the promoter region of the α chain, associated with susceptibility to diabetes (Hattori et al., 1986, Nishimoto et al., 1987, Lund et al., 1990, O'Shea et al., 2006). In addition, NOD mice express I-A^{g7} containing a serine at position 57 (i.e. a non-aspartic acid residue) of the IA-β chain (Acha-Orbea and McDevitt, 1987), thus altering the charge enabling a site for auto-antigens to bind e.g. WE14 peptide of chromogranin A (Stadinski et al., 2010b). This susceptibility is also seen in humans (Sato et al., 1999). When I-A^{g7} was introduced into NOD mice with the wild type proline at position 56 instead of the histidine expressed in NOD mice, it protected them from disease (Lund et al., 1990). Like NOD mice, the most important genetic susceptibility in human type 1 diabetes comes from the MHC, encoded in the Insulin Dependent Diabetes Mellitus 1 (IDDM1) locus. The MHCII HLA DR3/4-DQ8 haplotypes provide the greatest genetic susceptibility to type 1 diabetes, with other HLA-DR and DQ alleles providing protection (Aly et al., 2006, Erlich et al., 2008). In addition, to MHCII susceptibilities, there are also MHCI genetic susceptibilities (Nejentsev et al., 2007).

The second most important genetic susceptibility is a region upstream of the proinsulin gene, known as the insulin-dependent diabetes mellitus 2 (IDDM2) locus. In humans, a variable number of tandem repeats (VNTRs) related to the insulin gene, give rise to protection or susceptibility depending on the number of repeats (140->200 repeats vs 26-63 repeats respectively) (Vafiadis et al., 1997). The greater the number of insulin VNTRs an individual has, the greater the level of thymic proinsulin expression, and thus auto-reactive T cells are more likely to be negatively selected, providing protection against type 1 diabetes (Pugliese et al., 1997). By generating NOD mice with graded insulin levels, it was shown that the more insulin was expressed in the thymus, the greater the degree of immune tolerance seen (Chentoufi and Polychronakos, 2002).

In addition to these genetic susceptibilities, there are other immune function genes that contribute to susceptibility to type 1 diabetes. These include genes encoding CTLA-4, which competes with CD28 for CD80/86 on the APC to induce T cell deactivation. NOD mice are protected from developing diabetes when splice variants are expressed (Vijayakrishnan et al., 2004, Gerold et al., 2011) and the variant encoding CTLA-4 is believed to contribute significantly to genetic susceptibility contained within the *Idd5.1* locus (Hunter et al., 2007). Idd3 and 5 are both required to restore complete tolerance to anti-islet reactive T cells by Tregs through preventing accumulation within the pancreatic lymph nodes (Martinez et al., 2005, Hamilton-Williams et al., 2012). In addition, Idd3 also provides protection from both spontaneous and cyclophosphamide-induced diabetes (Wicker et al., 1994b). Interestingly, genetic susceptibility at the Idd9 locus alters the $CD8^+$ T cell response to islet antigens (Chamberlain et al., 2006) and provides protection from late expansion of pathogenic $CD8^+$ IGRP-specific T cells within the pancreas and draining lymph nodes (Hamilton-Williams et al., 2010). There are many more genetic susceptibilities, but they are all involved in immune function, insulin secretion and metabolism, some of which have candidate/known genes, others currently do not.

In humans, multiple genetic regions are also implicated in the susceptibility to type 1 diabetes (Concannon et al., 2009). These include similar genetic susceptibilities to the NOD mouse, such as genes associated with immune function and pancreatic β cell function, including the MHC (the most important genetic susceptibility factor), CTLA-4 and insulin expression (reviewed in (Polychronakos and Li, 2011)). Historically, only those at high genetic risk would develop T1D, however, individuals who are less genetically susceptible are now developing T1D (Gillespie et al., 2004). These changes have occurred too quickly to be due to genetic shift and therefore the environment has been suggested to play a role.

1.2.2.4 ENVIRONMENTAL FACTORS INFLUENCING DIABETES IN NOD MICE

In human diabetes, environmental factors have been implicated in the pathogenesis of T1D due for a number of reasons. These include the studies on

concordance of monozygotic twins with T1D where both twins developed diabetes in fewer than 30% of twin pairs (Hyttinen et al., 2003). If genetics were the sole factor in causing diabetes, the concordance would be 100%. In addition, geographical variation and migration also affect the incidence of T1D (Harjutsalo et al., 2008b, Hjern and Söderström, 2008), suggesting that environmental factors modify disease susceptibility. Furthermore, the incidence of type 1 diabetes worldwide is rising (Gillespie et al., 2004, Harjutsalo et al., 2008b, Evertsen et al., 2009, Ehehalt et al., 2010), suggesting that something other than genetic susceptibility factors, such as environmental factors, are involved in disease pathogenesis.

In the NOD mouse, environmental factors have been known to influence diabetes susceptibility. These include dietary factors (Schmid et al., 2004, Maurano et al., 2005, Marietta et al., 2013), infections (Cooke et al., 1999, Zaccone et al., 2004, Drescher et al., 2004), antibiotics and the gut microbiota (Hansen et al., 2012, Mor and Cohen, 2013, Tormo-Badia et al., 2014). Interestingly, these factors are also similar to those impacting human diabetes (reviewed in (Akerblom et al., 2002, Knip and Simell, 2012)). While many environmental factors cannot be controlled in humans, NOD mice can be housed in specific conditions, enabling assessment of the environmental factor(s) on disease. In order to assess environmental factors modifying disease susceptibility in humans, a large international study is currently underway investigating the environmental determinants of diabetes in the young (TEDDY), following a cohort of children over time (Group, 2008).

In diabetes in both NOD mice and humans, the gut microbiota appears to play a key role with many environmental factors having direct or indirect effects on the gut microbiota. While it is unknown as to what triggers the autoimmune process, the role of gut microbiota has become more recently favoured.

1.2.2.4.1 THE EFFECT OF GUT MICROBIOTA ON THE INCIDENCE OF TYPE 1 DIABETES

During any immune response, the innate immune cells are the first to respond, interacting with components of foreign organisms, such as bacteria, through Toll-like receptors (TLRs). There are currently 12 TLR family members, of which TLRs 3, 7, 8 and 9 are expressed intracellularly and TLRs 1, 2, 4, 5 and 6 are expressed extracellularly (reviewed by (Akira et al., 2006)). Many TLRs use MyD88, an adaptor protein, for downstream signalling, resulting in stimulation of the production of NF-κB-dependent proinflammatory cytokines and chemokines, as well as costimulation molecule expression (Medzhitov et al., 1997). TLRs are expressed on many cell types, including antigen-presenting cells such as DCs and macrophages, which upon TLR signalling, can differentiate and become activated (Krutzik et al., 2005).

Both TLRs and MyD88 signalling are important in shaping the immune response to gut microbiota through stimulating antimicrobial peptide release (reviewed in (Ganz, 2003)), IgA secretion (Shang et al., 2008), epithelial cell proliferation (Fukata et al., 2006) and ensuring epithelial tight junctions are maintained (Cario et al., 2004). These cellular responses maintain gut homeostasis and prevent opportunistic pathogen infections.

As discussed TLR signalling is important for keeping invading organisms from infecting the host and causing disease. However, to understand the role that these TLRs play, TLR knock out mice were generated. For example, *TLR2*$^{-/-}$ mice had increased bacterial loads, associated with increased pathology (Wooten et al., 2002, Echchannaoui et al., 2002), while *TLR4*$^{-/-}$ mice exhibited decreased myosin-specific CD4^{+} T cell proliferation (TCRVβ8.1 and 8.2), due to increased apoptosis compared to TLR4 sufficient mice, suggesting a role for TLR4 signalling in experimental autoimmune myocarditis (Gonnella et al., 2008).

In NOD mice, TLRs have also been implicated in disease. For example, NOD mice lacking TLR2 or TLR9 were protected from the development of autoimmune diabetes whereas TLR3 or TLR4 had no influence on diabetes development (Kim

et al., 2007, Wong et al., 2008). The protective effect of TLR9$^{-/-}$ was mediated through inhibition of the activation of diabetogenic CD8^{+} T cells (Zhang et al., 2010) and expanded CD73^{+} immune cells, which were immunosuppressive (Tai et al., 2013). Diabetes-resistant NOD mice downregulate TLR1 gene expression, resulting in diminished regulatory and effector CD4^{+} T cell proliferation and proinflammatory cytokine production compared to diabetes susceptible NOD mice (Vallois et al., 2007). Interestingly, inducing TLR2 tolerance (through Pam3CSk$_4$) with dipeptidyl peptidase 4 inhibitors, which prevent the destruction of incretin, thereby increasing insulin production, were able to reverse recent-onset diabetes in NOD mice. This was due to increased beta cell mass and proliferation, while reducing BDC2.5 CD4^{+} diabetogenic T cell proliferation in the PLN (Kim et al., 2012).

There have also been human studies investigating the role of TLRs in diabetes. For example, a Korean study showed humans with a particular TLR2 polymorphism were associated with increased protection from type 1 diabetes (Park et al., 2004). Additionally, TLR2 and 4 expression was increased on monocytes from human type 1 diabetes patients with microvascular complications compared to both patients without complications or normal control subjects (Devaraj et al., 2011a). This association suggested that TLR signalling was exacerbating the proinflammatory response and disease (Devaraj et al., 2011b, Devaraj et al., 2011c). These observations highlight the role of TLR-dependent signalling in containing microbial infections, but also in determining prevention of, or susceptibility to, autoimmunity.

While models investigating TLRs and their individual roles have been discussed, others focused on the downstream signalling molecules e.g. MyD88. *MyD88*$^{-/-}$ mice were protected from diabetes both on the NOD, and the C57BL/6 background, even when the latter expressed islet costimulatory molecules (Wen et al., 2008, Alkanani et al., 2014). Interestingly, specific pathogen free (SPF) NOD*MyD88*$^{-/-}$ mice, were protected from disease but when the mice were rederived into a germ-free environment, nearly all mice developed diabetes by 30 weeks of age (Wen et al., 2008). By repopulating the gut bacteria using specific

commensal bacteria, diabetes was reduced to below 40% (Wen et al., 2008). This suggested that bacteria were involved in stimulating TLR signalling and the subsequent immune responses that develop and importantly, could modify the susceptibility to development of autoimmune diabetes. In addition, those NOD mice lacking MyD88 also had a different bacterial gut composition to those sufficient in MyD88. By transferring the gut microbiota from the protected NOD*MyD88*$^{-/-}$ mice into NOD MyD88 sufficient mice, insulitis was reduced and the onset of diabetes delayed (Peng et al., 2014). Investigation of the microbiota within the gut revealed increases in *Clostridiaceae* and *Lachnospiraceae* with a decrease in *lactobacillaceae*, while also identifying higher concentrations of luminal TGF-β and IgA, associated with increases in CD8αβ^{+} and CD8^{+}CD103^{+} T cells. This work highlighted the importance of gut bacteria and the innate immune system in shaping the diabetogenic potential of the adaptive immune system.

The altered gut microbiota noted in these NOD*MyD88*$^{-/-}$ mice, was also seen in other TLR deficient mice, with the additional observation that this altered microbiota can be maternally transmitted to the offspring (Ubeda et al., 2012).

Bacterial interactions with the innate immune system are important, not only for stimulation of the innate immune response, but also for innate immune cell communication with the adaptive immune system. This connection may therefore be important for responses mediated by the adaptive immune system and lead to immunopathology and autoimmune disease such as type 1 diabetes. In the NOD mouse, it has been shown that diabetogenic T cells can be activated in the gut and pancreatic lymph nodes (Jaakkola et al., 2003) and that this activation is dependent on mucosal addressin cell adhesion molecule-1, which enables lymphocyte homing into mucosal lymphoid tissue (Hänninen et al., 1998). When the mucosal addressin molecule was blocked, the investigators observed a reduction in diabetes incidence from approximately 50% to 9%, but only when the mice were treated before 3 weeks of age. Therefore, diabetogenic T cells can encounter antigen that could be natively expressed or produced by components within the gut. Furthermore, mucosal inflammation can be seen in

NOD mice prior to the development of autoimmune diabetes. This inflammation could lead to a "leaky" mucosal epithelium allowing the microbiota to interact with the immune system, which may also be important (Vaarala et al., 2008). This highlights the adaptive immune system can be activated in the gut and that this activation may be modified by the bacteria present, either directly or indirectly, through modification of the innate immune system.

Other studies investigating the role of the gut microbiota include work in the Bio-Breeding diabetes-prone (BBDP) and diabetes-resistant (BBDR) rats, which also highlighted gut bacterial differences. Here, the investigators found a greater presence of *Lactobacillus* and *Bifidobacterium* in those resistant to developing diabetes (Roesch et al., 2009). Interestingly, these two genera have probiotic activity, unlike the three most abundant genera (*Bacteroides, Eubacterium and Ruminococcus*) found in BBDP rats. Similarly, in humans with T1D, specific bacteria may predispose susceptible individuals to the development of autoimmune diabetes. The proportion of bacteria from the Bacteroidetes phylum was found to be increased (mainly due to *Bacteroides ovatus*) while bacteria from the Firmicutes phylum decreased, compared to microbiota in age and genotyped matched non-T1D individuals (Giongo et al., 2011). In addition, in children with β cell autoimmunity, there was a lack of *Bifidobacterium adolescentis* and *Bifidobacterium pseudocatenulatum* and an increase in the Bacteroides genus when compared to those without β cell autoimmunity (de Goffau et al., 2013).

Antibiotic treatment of NOD mice has also yielded interesting results. NOD female mice treated from birth to 28 days with Vancomycin have showed reduced diabetes incidence (~80% vs 95% in controls) and when treated from 8 weeks also show diminished insulitis in comparison to non-treated controls (Hansen et al., 2012). Investigations into the gut microbiota revealed an increase in Akkermansia muciniphila species (in the Verrucomicrobia phylum), while also increasing proinflammatory $CD4^+$ T cells in the small intestine of neonatally-treated adult NOD female mice. This once again illustrates that altering the gut microbiota reduces diabetes in a polyclonal NOD mouse susceptible to disease.

Furthermore, antibiotic treatment of pregnant female NOD mice was also shown to impact the development of the gut in the offspring (Tormo-Badia et al., 2014).

In addition, oral administration of heat-inactivated *Lactobacillus casei* reduced diabetes incidence in NOD mice treated at 4 weeks, as did treatment with an oral probiotic mix VSL#3 (80% in controls vs 20-25% in the treatment cohort) (Matsuzaki et al., 1997, Calcinaro et al., 2005). Genetically modified *Lactococcus lactis,* engineered to secrete human proinsulin and IL-10, administered with low-dose anti-CD3 treatment to NOD mice, reverted diabetes in approximately 50% of the NOD mice and induced proinsulin-specific tolerance (Takiishi et al., 2012). Similarly, genetic modification of *Lactococcus lactis* to facilitate secretion of $GAD65_{370\text{-}575}$ and IL-10, administered with low-dose anti-CD3 treatment, stabilised insulitis and preserved islet β cell mass as well as reversing hyperglycaemia in recently diagnosed NOD mice (Robert et al., 2014). This prevention of further autoimmunity was shown to be mediated by an increase in the number of $CD4^{+}FoxP3^{+}CD25^{+}$ regulatory T cells present. This work highlights the importance of gut mucosal tolerance and how it can be adapted to develop antigen-specific therapies even after the onset of disease.

As mentioned previously, female NOD mice have a higher incidence of diabetes but when males and female mice are germ-free, or the males are castrated, the incidence of diabetes in both male and female mice is similar (Yurkovetskiy et al., 2013). In addition, upon faecal transfer from male NOD mice into young female NOD mice, there was an alteration in the microbiota with an increase in testosterone, which was associated with decreased islet inflammation and type 1 diabetes protection (Markle et al., 2013a). This suggests that the gut microbiota, androgens and the immune system all interact to help shape protection from, or susceptibility to, type 1 diabetes.

There are a number of mechanisms by which these auto-reactive T cells become activated, including bystander activation, where the T cells become non-specifically activated, and molecular mimicry. In molecular mimicry, a bacterial component mimics a component of self, in order to avoid being destroyed;

however, this can inadvertently lead to T cells becoming activated in response to the bacteria and subsequently cause destruction of the self-antigen expressing target i.e. the pancreatic islets. Interestingly, in human diabetes, rotavirus VP7 peptides have significant sequence similarity to IA-$2_{805-817}$ and $GAD65_{115-127}$ (Honeyman et al., 2010), while Coxsackie virus P2-C peptides have high sequence similarity to $GAD65_{247-279}$ (Atkinson et al., 1994). Both studies showed T cell proliferation to the diabetes-related antigen as well as the mimic; however, it is unknown if this is causal in the development of diabetes.

While these studies have focused on diabetes development, only a small number have focused on auto-antigen-specific T cells; however none have shown the gut microbiota cause diabetes. Therefore, to further understand the role of gut microbiota, more work has to be done to identify which T cells are being affected and if that effect is direct/indirect or specific/non-specific.

1.2.2.5 AUTO-ANTIGENS TARGETED IN NOD MICE

There are many auto-antigen targets of T cells during diabetes development. These targets include insulin (Wegmann et al., 1994, Zekzer et al., 1997, Wong et al., 1999, Lamont et al., 2014), islet glucose-6-phosphatase related subunit protein (IGRP) (Lieberman et al., 2003), GAD65 (Kaufman et al., 1993, Quinn et al., 2001b), Chromogranin A (Stadinski et al., 2010a) and Zinc transporter 8 (ZnT8) (Nayak et al., 2014). Some of the auto-reactive $CD4^+$ and $CD8^+$ T cell clones identified are shown in TABLE 2 and TABLE 3 respectively. Interestingly in humans with type 1 diabetes, similar auto-antigens are targeted including insulin (Schloot et al., 1998, Semana et al., 1999, Arif et al., 2004, Bulek et al., 2012), GAD65 (Panina-Bordignon et al., 1995, Nepom et al., 2001), IGRP (Yang et al., 2006, Jarchum et al., 2008) and ZnT8 (Énée et al., 2012), while also targeting other auto-antigens including islet amyloid precursor protein (IAPP) (Panagiotopoulos et al., 2003) and glial fibrilliary acidic protein (GFAP) (Standifer et al., 2006).

In human diabetes, $CD8^+$ T cell responses to preproinsulin and GAD dominate early in diagnosis but this immunodominance is replaced by subdominant IA-2 and IGRP responses over time (Martinuzzi et al., 2008). Even in healthy newborn

individuals, naïve proinsulin and GAD reactive T cells can be detected (Heninger et al., 2013). In addition, HLA-A*0201 patients with recent onset type 1 diabetes also showed frequently detectable populations of $CD8^+$ T cells reactive to preproinsulin$_{15-24}$, Insulin B_{10-18} and $IGRP_{265-273}$ (Velthuis et al., 2010). However, in NOD mice insulin B_{15-23} reactive $CD8^+$ T cell responses are low, with IGRP-reactive T cells dominating the auto-reactive T cell populations as early as 5 weeks of age (Lieberman et al., 2004). However, these IGRP-reactive $CD8^+$ T cells are dependent on prior insulin autoimmunity, as when NY8.3 TCR transgenic mice (recognising $IGRP_{206-214}$) were crossed to NOD mice over-expressing proinsulin 2, the mice were protected from developing diabetes (Krishnamurthy et al., 2008).

In human type 1 diabetes, B cells were found to recognise a number of auto-antigens resulting in the production and secretion of auto-antibodies to insulin (Palmer et al., 1983), GAD (Baekkeskov et al., 1990), insulinoma antigen 2 (IA-2) (Bonifacio et al., 1995), IA-2β (Lu et al., 1996) and ZnT8 (Wenzlau et al., 2008a, Wenzlau et al., 2008b). In the NOD mice, auto-antibodies were only found against Insulin (Michel et al., 1989), but not to GAD (Velloso et al., 1994) or Insulinoma antigen 2 (IA-2) (DeSilva et al., 1996). While auto-antibodies are present in NOD mice, they provide a marker of inflammation and not necessarily diabetes development (Robles et al., 2003). However, in humans the more auto-antibodies present in an individual, the more likely they will develop disease (Ziegler et al., 2013).

While there are many auto-antigens identified in diabetes, insulin is believed to have a prime role in the development of diabetes.

TABLE 2: AUTO-REACTIVE CD4$^+$ T CELL CLONES AND THEIR EPITOPES

CLONE	ANTIGEN	PEPTIDE SEQUENCE	TCRα CHAIN	TCRβ CHAIN	REFERENCES
2H6	Insulin B Chain $_{12\text{-}25/9\text{-}23}$	VEALYLVCGERGFF/ SHLVEALYLVCGERG	Vα6, Jα45	Vβ14, Jβ2.3	(Zekzer et al., 1997)
BDC4-7.2	Insulin B chain $_{9\text{-}23}$	SHLVEALYLVCGERG	Vα13.3, Jα45	Vβ1, Jβ1.3	(Simone et al., 1997)
BDC6-4.3	Insulin B chain $_{9\text{-}23}$	SHLVEALYLVCGERG	Vα13.3, Jα45	Vβ2, Jβ1.1	(Simone et al., 1997)
BDC6-6.4	Insulin B chain $_{9\text{-}23}$	SHLVEALYLVCGERG	Vα8, Jα48	Vβ10, Jβ2.5	(Simone et al., 1997)
BDC8-1.1	Insulin B chain $_{9\text{-}23}$	SHLVEALYLVCGERG	Vα13.3, Jα47	Vβ12, Jβ2.6	(Simone et al., 1997)
BDC8-1.3	Insulin B chain $_{9\text{-}23}$	SHLVEALYLVCGERG	Vα13.1, Jα34	Vβ6, Jβ1.6	(Simone et al., 1997)
BDC8.1.9	Insulin B chain $_{9\text{-}23}$	SHLVEALYLVCGERG	Vα13.3, Jα34	Vβ4, Jβ1.1	(Simone et al., 1997)
BDC12-1.19	Insulin B chain $_{9\text{-}23}$	SHLVEALYLVCGERG	Vα10, Jα9	Vβ6, Jβ1.1	(Simone et al., 1997)
BDC12-2.35	Insulin B chain $_{9\text{-}23}$	SHLVEALYLVCGERG	Vα1, Jα1	Vβ8.3, Jβ1.6	(Simone et al., 1997)
BDC12-4.1	Insulin B chain $_{9\text{-}23}$	SHLVEALYLVCGERG	Vα13.3, Jα45	Vβ2, Jβ2.6	(Simone et al., 1997)
BDC12-4.4	Insulin B chain $_{9\text{-}23}$	SHLVEALYLVCGERG	Vα13.3, Jα45	Vβ12, Jβ1.3	(Simone et al., 1997)
B16.3	GAD65 $_{286\text{-}300}$	KKGAAAIGIGTDSVI	Vα4.5, Jα6	Vβ1, Jβ2.7	(Chao et al., 1999, Tarbell et al., 2002)
BDC2.5	Chromogranin A WE14 $_{359\text{-}372}$	WSRMDQLAKELTAE	Vα1, Jα17	Vβ4, Jβ1.2	(Candéias et al., 1991a, Katz et al., 1993, Stadinski et al., 2010a)
BDC10.1	Chromogranin A WE14 $_{359\text{-}372}$	WSRMDQLAKELTAE	Vα9.2	Vβ15	(Stadinski et al., 2010a, Burton et al., 2008)
NY4.1	Unknown	Unknown	Vα4.1, Jα33	Vβ11, Jβ2.4	(Schmidt et al., 1997)

NOTE: All CD4$^+$ T cell clones recognise peptides presented by MHC Class II I-A^{g7} due to a lack of I-E.

TABLE 3: AUTO-REACTIVE CD8$^+$ T CELL CLONES AND THEIR EPITOPES IN DIABETES

CLONE	MHC RESTRICTION	ANTIGEN	PEPTIDE SEQUENCE	TCRα CHAIN	TCRβ CHAIN	REFERENCES
P4.10*	Unknown	Proinsulin 2 $_{25–34}$	FYTPMSRREV	Unknown	Unknown	(Ejrnaes et al., 2005)
AI4	H-2D^b	Insulin A Chain $_{14-20}$	YQLENYC	Vα8, Jα52	Vβ2, Jβ1.3	(DiLorenzo et al., 1998, Lamont et al., 2014)
G9C8	H-2K^d	Insulin B Chain $_{15-23}$	LYLVCGERG	Vα18, Jα8	Vβ6, Jβ2.3	(Wong et al., 1996)
A1*	H-2K^d	Insulin B Chain $_{15-23}$	LYLVCGERG	Unknown	Vβ13	(Ejrnaes et al., 2005)
R1*	H-2K^d	GAD65 $_{515-524}$	WFVPPSLRTL	Unknown	Vβ8.2	(Videbaek et al., 2003)
C2*	H-2K^d	GAD67 $_{515-524}$	WYIPQSLRGV	Unknown	Vβ6	(Bowie et al., 1999)
NY8.3	H-2K^d	IGRP $_{206-214}$	VYLKTNVFL	Vα17, Jα42	Vβ8.1, Jβ2.4	(Nagata et al., 1994a, Lieberman et al., 2003)
NY2.3	H-2D^b	Unknown	Unknown	Vα4, Jα45	Vβ11, Jβ2.1	(Nagata et al., 1994a)
YNK1.3	H-2K^d	Unknown	Unknown	Unknown	Vβ8	(Yoneda et al., 1997)

NOTE: * Isolated by peptide immunisations prior to the cloning procedure

1.2.2.5.1 INSULIN

Proinsulin is the prohormone of the active Insulin. This is cleaved to produce the active hormone insulin, composed of 2 chains (A and B) joined by disulphide bonds (FIGURE 7). Insulin, in its metabolic form, is secreted by the β cells in the islets of Langerhans within the pancreas in response to glucose stimulation and is a known auto-antigen in type 1 diabetes. In NOD mice, there are 2 proinsulin genes – Proinsulin 1 and Proinsulin 2, which are highly homologus and differ by only 2 amino acids in the B chain and 3 amino acids in the C peptide. However, they appear to be expressed differently. Within the thymus, proinsulin is expressed under the AIRE promoter (Anderson et al., 2002), enabling developing T cells that would recognise insulin to be negatively selected and thus prevent autoimmunity. This role of proinsulin in T cell selection is believed to be driven by proinsulin 2, as it is predominantly expressed in the thymus and is believed to be important in tolerance (Chentoufi and Polychronakos, 2002, Chentoufi et al., 2004, Faideau et al., 2004, Palumbo et al., 2006). In NOD mice deficient in proinsulin 2, nearly all mice developed robust accelerated diabetes (Thébault-Baumont et al., 2003), while over-expression of proinsulin 2 protected mice from diabetes (French et al., 1997, Jaeckel et al., 2004). In addition, proinsulin 2 mediates tolerance in non-autoimmune mice shown in 129SV/Pas mice, where all insulin-reactive T cells were deleted; however, in proinsulin 2 deficient 129SV/Pas mice immunised with proinsulin 2, a T cell response was detected and islet infiltration was identified (Faideau et al., 2004). Furthermore, the protective effect of proinsulin 2 was shown to be mediated by thymic epithelial cells (Jaeckel et al., 2004, Faideau et al., 2006). However, proinsulin 2 expressed solely in bone-marrow derived cells was not influential in protecting proinsulin 2 deficient NOD mice, suggesting that thymic tolerance was the most important factor in shaping the immune response (Martin-Pagola et al., 2009). However, whether proinsulin 1 is expressed in the thymus remains a source of contention with some studies suggesting it is present, while others do not; although all agree that both proinsulin 1 and 2 are expressed in the pancreas. Unlike, proinsulin 2 deficient mice, proinsulin 1 deficient NOD mice were protected from developing diabetes (Moriyama et al., 2003). Not surprisingly, given the sequence homology between

proinsulin 1 and 2, proinsulin 1-reactive T cells were shown to cross-react with proinsulin 2 epitopes (Jaeckel et al., 2004). However, proinsulin 1 9-23 (B chain) and 49-66 (C chain) peptides were able to stimulate a proliferative response. This suggested that these insulin cross-reactive T cells, expressing specific TCRs, were selected for by proinsulin 2 and that both proinsulins can allow proinsulin-specific populations to be expanded. Recently, NOD mice lacking both proinsulin 1 and 2, but containing a mutant insulin transgene, where position 16 of the insulin B chain was substituted from a tyrosine to an alanine, were generated (Nakayama et al., 2005a). This mutation prevented both insulin B9-23 and insulin B15-23 peptides from being recognised by these insulin-reactive T cells, due to poor MHC binding of the peptide, and these mice were protected from diabetes suggesting that insulin was an important antigen in initiating the auto-reactive T cell response. Furthermore, this mutated insulin was unable to prevent insulin autoimmunity and diabetes when expressed in the thymus of NOD mice lacking proinsulin 2 (Nakayama et al., 2005b). This suggested tolerance was mediated by the native proinsulin epitopes and is required to effectively delete auto-reactive T cells recognising epitopes overlapping the site of mutation in the proinsulin gene.

In spite of the fact, NOD mice express 2 proinsulin genes; insulin-reactive T cells are able to escape from thymic negative selection. For insulin $B_{9\text{-}23}$ reactive $CD4^+$ T cells, it has been suggested the peptide binds to the MHC ($I\text{-}A^{g7}$) in two conformations; register 1-recognising T cells (type A insulin-specific T cells) respond weakly upon TCR stimulation by p:MHC whereas register 2 T cells (type B insulin-specific T cells) react to intra-islet DC presentation of peptide and are capable of inducing diabetes (Mohan et al., 2010). This difference in peptide binding has been suggested as a mechanism for the escape from negative selection of the insulin-reactive $CD4^+$ T cells. For insulin $A_{14\text{-}20}$ reactive $CD8^+$ T cells (AI4), the MHC ($H\text{-}2D^b$) allows peptides lacking C terminal amino acids i.e. the anchor at position 9, to avoid negative selection, yet become activated within the periphery (Lamont et al., 2014). The reason that the insulin B15-23 reactive $CD8^+$ T cells (G9C8) escape negative selection is likely to be due to the low affinity interaction, whereby insulin B15-23 binds weakly to $H\text{-}2K^d$ (Wong et al., 1999).

FIGURE 7: Mus musculus preproinsulin II protein sequence is shown. Letters highlighted in red indicate sequence differences between preproinsulin II and preproinsulin I, while the red box identifies 2 amino acids missing in preproinsulin I. Initially, preproinsulin is translated by a ribosome at the ER, where the leader sequence (in green) is removed by proprotein convertase II (Davidson et al., 1988). This proinsulin molecule is then folded and transported out of the ER via the Golgi. The C peptide is then cleaved (in red) to produce the active hormone insulin, where the A (in blue) and B (in yellow) chains are bound by disulphide bonds. This cleavage is carried out by proprotein convertase I (Davidson et al., 1988). These proprotein convertase enzymes are only able to convert preproinsulin into insulin within the pancreatic β cells (Neerman-Arbez et al., 1994).

FIGURE 7: PREPROINSULIN CLEAVED TO PRODUCE INSULIN

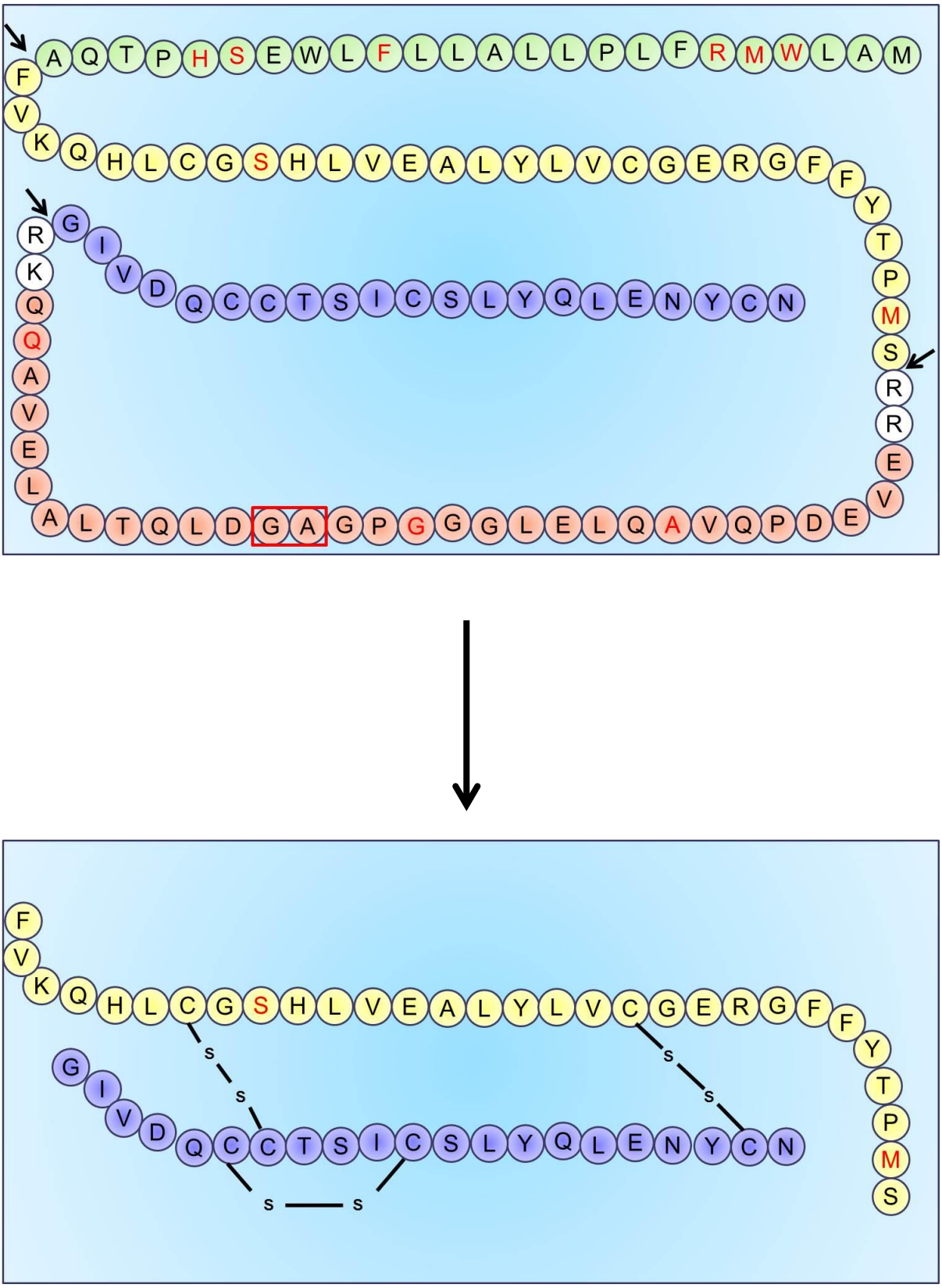

1.2.2.6 G9C8 CLONE

1.2.2.6.1 G9C8 ANTIGEN IDENTIFICATION

G9C8 $CD8^+$ T cell lines were generated from islets of pre-diabetic female NOD mice (Wong et al., 1996). In order to identify the islet antigen recognised by the $CD8^+$ T cell, a NOD-derived pancreatic islet cDNA library was ligated into the pEAX expression vector and transfected into COS cells (Wong et al., 1999). cDNA translation to protein and the subsequent MHC association enabled G9C8 $CD8^+$ T cell hybridomas to recognise their putative antigen. Detection of the clones recognising their antigen was through using a reporter gene, *lacZ*, under the NFAT element of the IL-2 enhancer. Upon addition of X-Gal, the lac-Z encoded β-galactosidase catalysed the conversion of X-Gal, with any positive cells seen as blue-coloured. Any hybridomas recognising antigen were then screened further, eventually identifying peptides from preproinsulin 1 and 2 to be stimulating the cells. Through generating overlapping peptides spanning the length of preproinsulin 1, the G9C8 TCR was found to specifically recognise the insulin B chain amino acids 15-23 (LYLVCGERG).

Insulin B15-23 was shown to be restricted to H-$2K^d$ through *in vitro* cytotoxicity experiments, whereby the G9C8 T cell clones could only respond to antigen presented by NOD and BALB/C islets but not C57BL/6 islets (Wong et al., 1996, Wong et al., 1999). NOD mice express H-$2D^bK^d$, BALB/C mice express H-$2D^dK^d$ and C57BL/6 mice express H-$2D^bK^b$. The only detectable T cell responses were between NOD and BALB/C islets suggesting that the shared H-$2K^d$ was presenting the antigen and not H-$2D^b$. *In vivo* adoptive transfer experiments also confirmed this MHC restriction as the CB17-SCID (H-$2K^dD^d$) developed diabetes but the B6-SCID (H-$2K^bD^b$) mice did not (Wong et al., 1996). Furthermore, using an anti-K^d antibody and subsequently preventing peptide presentation, T cell proliferation and cytokine production were inhibited (Wong et al., 1999).

The G9C8 TCR was initially characterised through monoclonal antibodies identifying the TCRVβ chain as Vβ6 (later referred to as TRBV-19*01). Further sequence analysis revealed that the G9C8 TCRβ chain expressed TCR Vβ6, Dβ1.1,

Jβ2.3 (later referred to as TRBV-19*01, TRBD1.1, TRBJ2-3), while the partnered TCRα chain was identified as Vα15 initially due to homology with the published TCRα chain designated Vα15. This TCRα chain was later renamed Vα18 with Jα8 (later redesignated as TRAV8-1*01 and TRAJ9) (Wong et al., 1996).

Interestingly, Insulin B chain 15-23 (LYLVCGERG) binds poorly to H-2K^{d}, reducing the avidity of the TCR:p:MHC interaction (Wong et al., 2002). By introducing single alanine mutations at positions 1, 2, 3, 4 and 6 along the cognate peptide, T cell recognition was lost with a mutation at position 8 very weakly stimulating the T cells. However, alanine mutations at positions 5, 7 and 9 were able to stimulate almost equivalent T cell recognition to the native peptide. Through modelling the p:MHC, a tyrosine at position 2 of the cognate peptide was identified as the primary anchor with a glycine at position 9 providing a secondary anchor. At the amino terminus of the peptide, several MHC derived heavy chain residues enable the peptide to bind and interact with many polar residues. Peptide interactions with MHCI amino acids 97R-99F and the 74F/116F pair force the insulin peptide backbone to curve upwards (in relation to the β sheet of the MHC groove) enabling the small glycine at position 9 to bind, but not fill, the MHCI groove. This binding is enhanced through hydrogen bonds between residues 143T and 146K. In a later modelling paper, it was suggested that MHC amino acids 73W and 147W create a barrier, which forces the peptide to curve upwards instead (Petrich de Marquesini et al., 2008).

Through molecular modelling, potential TCR contact residues within the p:MHC complex including p3L, p4V, p5C, p6G and p8R with a partial interaction at p1L have been identified (Wong et al., 2002). Depressions at position 3, between positions 5 and 6 and around positions 7 and 9 within the peptide suggest sites the TCR may bind. It is believed that little interaction between the TCR and peptide p7E can occur due to the amino acid pointing towards the MHCI α2 helix (Petrich de Marquesini et al., 2008). Interactions between p:MHCI force the insulin peptide backbone to curve enabling the TCR to make contacts with both p6G and p8R, both of which are required for TCR selection as no substitutions at these positions in the peptide allow the G9C8 T cells to become stimulated

(Wong et al., 2002, Petrich de Marquesini et al., 2008). However, while modelling is useful, without a specific p:MHC:TCR structure to analyse, it may not be entirely accurate.

Recently this p:MHC structure was crystallised revealing that the amino acids at position 1, 3, 6, 7 and 8 of the peptide were exposed potentially for TCR recognition (Motozono et al, in submission). Interestingly, glutamic acid and arginine (positions 7 and 8 of the peptide) extended the furthest out of the MHC groove, suggesting that these amino acids are most likely to contact the TCR. However, further work is needed to crystallise the TCR in order to identify how the p:MHC:TCR interact with one another.

1.2.2.6.2 G9C8 HETEROCLITIC PEPTIDE INTERACTIONS

The cognate Insulin B15-23 glycine at position 9 is small and unable to completely fill the binding pocket within the MHCI (Wong et al., 2002). This weak interaction can be enhanced through substituting the amino acid at p9 with A/V/L/I, which stabilise binding through van der Waals interactions. Modelling these substitutions does not displace the peptide backbone structure and thus the interactions with MHC/TCR are equal or enhanced. Identification of the minimal cognate peptide also identified a weak decamer (LYLVCGERGF) capable of stimulating G9C8 T cell clones but at higher concentrations to the cognate nonamer. In addition, proliferation and IFN-γ production were reduced approximately 10-fold, as was the cytotoxic response, requiring 25 times more peptide to obtain a similar response to the cognate nonamer (Wong et al., 2002).

Primary TCR anchor contacts within the cognate B15-23 peptide involve p6G and p8R (Wong et al., 2002). Through substituting these amino acids, antagonism can be induced whereby T cell function can be altered in a non-competitive MHC-binding way between native and altered peptides (Petrich de Marquesini et al., 2008). Altered peptide ligands with substitutions at p6 (G6H, G6I, G6L) induced over 50% antagonism at 0.1μg/ml, resulting in IFN-γ inhibition. Antagonism was also induced, albeit to a lesser extent in substitutions involving p8 (R8L). These altered peptide ligands correspond to reduced TCR affinity and thus antagonism

through changing TCR main contacts i.e. p6H reduces the contact space for the TCR to engage and raises the p8R side chain making it difficult for the cognate TCR to interact. Even in peptides encoding p8L, where the only difference between cognate peptide and altered peptide is the lack of a guanidine group with a charged nitrogen, reduced TCR recognition.

Through p:MHC crystallisation, it was noted between the native LYLVCGERG and altered LYLVCGERV peptides, there are similar interactions at the C terminal end of the peptide to the MHC, however; the avidity is altered due to reduced hydrogen bonding at the N terminus of the peptide (Motozono et al, in submission). Furthermore, the arginine at postion 84 of the MHCα1 chain, accompanied by the tyrosine at position 84, were able to adopt a different confirmation enabling the phenylalanine at position 10 of the LYLVCGERGF peptide to fit into the groove. This movement is likely to reduce the stabilisation of the p:MHC.

1.2.2.6.3 G9C8 T CELL PHENOTYPE AND FUNCTIONAL ABILITIES

Monoclonal antibodies to a panel of activation and adhesion cell surface markers revealed G9C8 $CD8^+$ T cells expressed activation markers CD28 and CD44, and adhesion molecules α-4 integrin and ICAM-1 but were HSA and CD69 negative (Wong et al., 1996).

In vitro, G9C8 T cells could be stimulated by NOD islets to express proinflammatory cytokines, IFN-γ, TNF-α and TNF-β, and the effector molecule perforin (Wong et al., 1996). In addition, other cytokines were tested for by RT-PCR but were shown not to be expressed by the G9C8 clone, including IL-2, IL-4, IL-5, IL-12 and TGF-β. In order to assess, the G9C8 T cells ability to destroy antigen-specific targets, mimicking the *in vivo* ability to destroy the insulin-producing β cells, a cytotoxicity assay was set up. This involved culturing G9C8 T cells with MHC-K^d expressing pancreatic islets, which were specifically destroyed, while the control target was unaffected (Wong et al., 1996). In addition Insulin B chain 15-23 loaded P815 cells (PKH labelled target cells) could also be specifically lysed by the G9C8 T cells (Wong et al., 1999, Wong et al., 2002).

In addition, G9C8 T cells could be identified using tetrameric complexes expressing MHC-K^d bound to Insulin B chain 15-23 with an attached fluorescent dye detected using a flow cytometer (Wong et al., 1999). Studies with the tetramer p:MHC complex showed that predominant insulin B15-23 tetramer positive G9C8-like populations were detectable in 4-week old NOD islets but were shown to decrease with age, as other antigen specificities became immunodominant (Wong et al., 1999, Lieberman et al., 2004).

In adoptive transfer studies, activated G9C8 T cells were able to cause rapid diabetes in irradiated NOD mice without $CD4^+$ T cell help within 10 days (Wong et al., 1996). Investigation of these NOD islets revealed extensive islet destruction with all cells expressing Vβ6. In addition, fluorescent labelled G9C8 T cells homed to, and invaded, the islets within 24 hours post-transfer, confirming that the cells clearly targeted the islets, contributing to their highly diabetogenic phenotype.

1.2.2.7 G9Cα$^{-/-}$ TRANSGENIC MICE

1.2.2.7.1 DEVELOPMENT OF G9Cα$^{-/-}$ TRANSGENIC MICE

Cloned G9C8 T cell genomic DNA was isolated identifying the G9C8 TCR comprising TCR Vα18 and Jα8 (TRAV8-1*01TRAJ9) and TCRβ chain Vβ6, Dβ1.1 and Jβ2.3 (TRBV19*01TRBD1-1TRBJ2-3) (Wong et al., 1996). Each chain of the TCR was purified and cloned into individual TCR cassette vectors (Kouskoff et al., 1995), with expression dependent on natural TCR regulatory elements. Single TCR transgenic founders were generated through injection of the constructs into NOD ova, producing three independent single chain TCRα and TCRβ founders, which were then crossed to generate G9C8 transgenic mice (Wong et al., 2009) (FIGURE 8).

FIGURE 8: SCHEMATIC REPRESENTATION OF THE DEVELOPMENT OF G9Cα$^{-/-}$ TRANSGENIC MICE

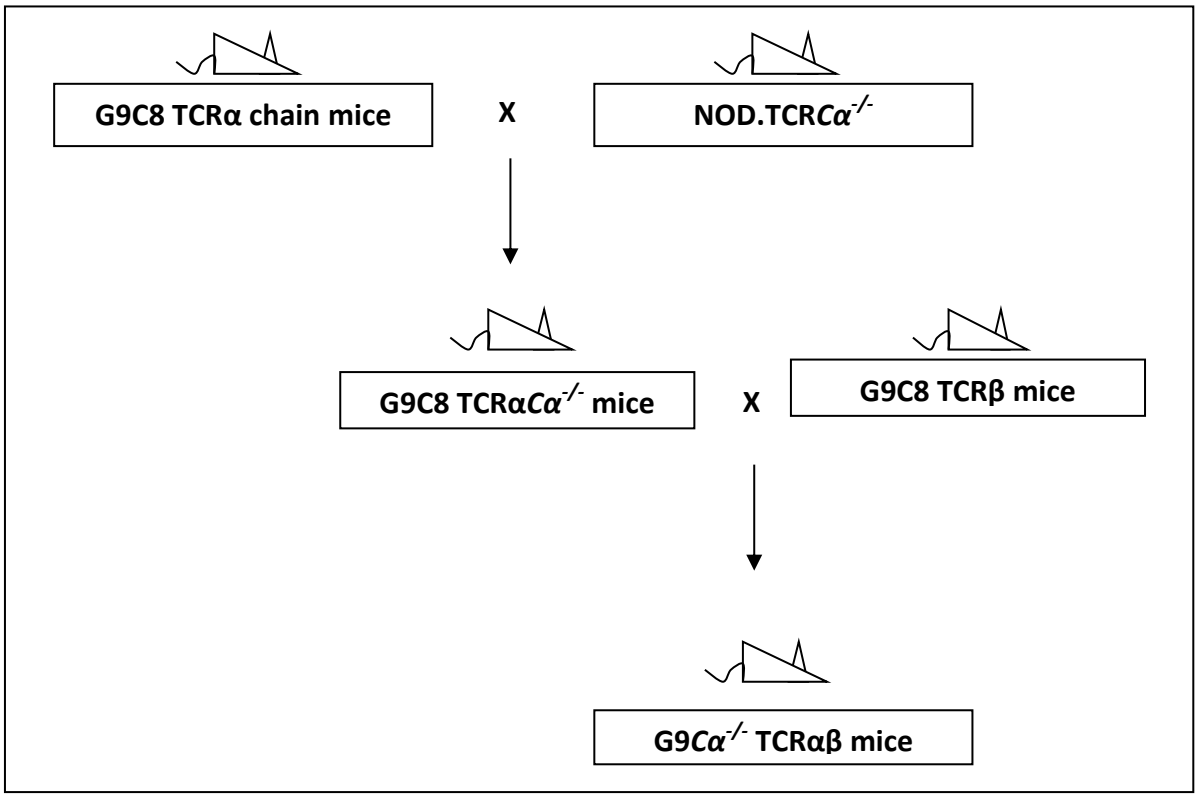

FIGURE 8: NOD mice expressing the G9C8 TCRα chain (G9C8 TCRα chain mice) were crossed to NOD mice lacking TCRα chains (NOD.TCRCα$^{-/-}$ mice). This generated single chain G9C8 TCRα mice that only expressed the clonotypic TCRα chain. These mice were then crossed to G9C8 TCRβ restricted NOD mice (lacking other TCRβ chains) to generate the clonotypic G9C8 TCR-expressing NOD mice (G9Cα-/-TCRαβ mice).

1.2.2.7.2 T CELL SELECTION IN G9*Cα*$^{-/-}$ TRANSGENIC MICE

Despite natural thymic proinsulin expression, T cells in G9*Cα*$^{-/-}$ mice are selected in the thymus and expand in the peripheral tissues (Wong et al., 2009). These transgenic mice exhibit a CD8^{+} T cell bias both in the thymus and the periphery (TABLE 4). Interestingly, even when these G9*Cα*$^{-/-}$ mice were crossed with mice deficient in proinsulin 1 or proinsulin 2 or mice lacking native insulin and expressing the mutant proinsulin with alanine replacing tyrosine at position 16 in the B chain (see section 1.2.2.5.1), preventing the G9 TCR epitope from being recognised, all mice exhibited a CD8^{+} T cell bias and there was no difference in the frequency of G9C8 CD8^{+} T cells that were selected in the thymus (Terri Thayer, personal communication, manuscript in progress). Thus, there was no evidence of negative selection of the G9C8 CD8^{+} T cells in the thymus. Even when G9*Cα*$^{-/-}$ mice were crossed to mice over-expressing proinsulin 2, there was no apparent deletion of these cells in the thymus; however in the periphery, G9C8 T cells were reduced. This suggests that for this particular antigen specificity, peripheral tolerance is more important than central tolerance.

TABLE 4: CD8^{+} AND CD4^{+} T CELL PROPORTIONS IN G9C8 TCR TRANSGENIC MICE

TISSUE	% CD8^{+}	% CD4^{+}
THYMUS	5.1 (+/- 1.6)	1.43 (+/- 0.42)
SPLEEN	21.14 (+/- 4.62)	8.28 (+/- 1.35)
LYMPH NODES	52.18 (+/- 9.26)	6.28 (+/- 0.57)

1.2.2.7.3 T CELL FUNCTION IN G9*Cα*$^{-/-}$ TRANSGENIC MICE

G9*Cα*$^{-/-}$ T cells isolated directly *ex vivo* can elicit antigen-specific cytotoxicity although this can be greatly enhanced when cells are co-cultured with antigen indicating these T cells are relatively naïve. In addition, similarly to the G9C8 T cell clones, the G9*Cα*$^{-/-}$ derived T cells proliferate in response to Insulin B chain 15-23 and produce IFN-γ and TNF-α in response to stimulation (Wong et al., 1996, Wong et al., 2009). Interestingly, when these G9*Cα*$^{-/-}$ mice were crossed with mice deficient in proinsulin 2 (G9*Cα*$^{-/-}$*PI2*$^{-/-}$ mice) or lacking native insulin expression (G9*Cα*$^{-/-}$*PI1*$^{-/-}$*PI2*$^{-/-}$*Y16A*^{tg} mice), with a transgenic mutant insulin

(where the tyrosine at position 16 of the B chain is replaced by an alanine (Nakayama et al., 2005a)) expressed, there were no differences in T cell selection in the thymus, but there were functional differences (Terri Thayer, personal communication, manuscript in progress). Interestingly in the native proinsulin deficient G9*Cα*$^{-/-}$*PI1*$^{-/-}$*PI2*$^{-/-}$*Y16A*^{tg} mice, the CD8^{+} T cells exhibited the greatest antigen response *in vitro*, in terms of proliferation and cytotoxicity with increased cytokine production, followed by G9*Cα*$^{-/-}$*PI2*$^{-/-}$ mice and finally the native proinsulin expressing G9*Cα*$^{-/-}$ mice. Therefore, while alterations in proinsulin expression do not change the T cell selection, the antigen is important for controlling the functional ability of these T cells.

In the G9*Cα*$^{-/-}$ mice, only mice aged 15 weeks or older showed islet infiltration, with the majority of islets remaining intact (Wong et al., 2009). In addition, no spontaneous diabetes was seen by 35 weeks of age, even when CD4^{+}CD25^{+} T cells (i.e. regulatory T cells) were depleted. However, on immunisation with insulin B15-23 and CpG adjuvant, the naïve phenotype was altered (downregulation of CD62L while CD44 was upregulated) and mice rapidly developed spontaneous diabetes (75-100% incidence 5-15 days post-immunisation) with many islets subject to extensive infiltration and destruction. Enhanced islet expression of the costimulatory molecule B7-1 (under the RIP), was also capable of inducing spontaneous diabetes in G9*Cα*$^{-/-}$ mice with ~90% incidence by 20 weeks (Wong et al., 2009). Even when purified CD4^{+} T cells were transferred from diabetic NOD donors into G9*Cα*$^{-/-}$ mice, spontaneous diabetes could be demonstrated (in ~75% mice) suggesting a requirement for activated, polyclonal CD4^{+} T cell help (Wong et al., 2009). However, CD4^{+} T cell independent diabetes could be induced when G9*Cα*$^{-/-}$ CD8^{+} T cells were activated *in vitro* (3 day co-culture with bone marrow-derived DCs presenting antigen) and subsequently transferred into NODscid mice. However, naïve CFDA-SE-labelled G9*Cα*$^{-/-}$ CD8^{+} T cells, used directly *ex vivo* were unable to induce spontaneous diabetes when transferred into 4-6 week old NOD mice, although they showed specific homing and CD69^{+} T cell proliferation solely within the pancreatic lymph nodes.

1.3 THESIS INTRODUCTION

T cell development involves the rearrangement of the T cell receptor (TCR) gene segments forming the mature TCR, which mediates the antigen specificity of the responding T cell. It is important that T cells develop with a broad TCR repertoire in order to protect the host from any potential infection; however, this broad repertoire may also include T cells with TCRs that recognise self-antigens. While there are processes to reduce likelihood that the repertoire of T cells in the periphery are not reactive to self-antigens, through central and peripheral tolerance, some T cells escape this control and may cause disease. One example, of many auto-reactive T cells, is the insulin B15-23 reactive G9C8 T cell, discussed in the previous sections, which can cause autoimmune diabetes in the NOD mouse. Insulin B15-23 peptide is specifically recognised by this T cell through its TCR comprising TRAV8-1*01TRAJ9 and TRBV19*01TRBD1-1TRBJ2-3, however, the recognition is weak, enabling the T cell to escape both negative and peripheral selection processes. As discussed in the previous section, proinsulin is thymically expressed, yet this expression alone, fails to stop all proinsulin/insulin-reactive T cells from escaping. However, central and peripheral tolerance are able to control proinsulin/insulin reactive T cells through deletion, anergy or inducing regulatory T cells. Therefore, antigen is important for shaping the TCR repertoire, whether through inducing protective responses or in the G9C8 T cell, leads to a proinflammatory response causing the destruction of the insulin-producing β cells in the islets of Langerhans within the pancreas. Therefore, understanding the role proinsulin plays in the T cell developmental process is important as it may identify novel ways to control inappropriate T cell activation and may enable new therapies leading to the prevention of autoimmune diabetes. In addition, even though antigen drives the immune response, other factors exist, which help control or prevent inappropriate responses from taking place. This may include regulatory cell subsets, the location the antigen is expressed (i.e. thymus, draining lymph nodes etc.) and factors influencing antigen expression, e.g. insulin responds to glucose stimulus and therefore factors affecting metabolism are important such as the gut microbiota.

The G9C8 T cell is a single insulin B15-23 reactive T cell and studies of this T cell has provided valuable insight into how the T cell causes diabetes and how proinsulin expression affects T cell development. However, it is only one T cell and it is highly likely, there are other insulin B15-23 reactive $CD8^+$ T cells that have not been studied. Therefore, this study focuses on identifying other insulin B15-23 reactive T cells and examining how proinsulin expression is able to alter the TCR repertoire of those T cells which develop. This was investigated in single chain TRAV8-1*01TRAJ9 NOD transgenic mice, which utilised the same TCRα chain as the G9C8 T cell. Previous work on $CD4^+$ insulin-reactive T cells revealed that the TCRα chain was more important in dictating antigen specificity than its TCRβ chain partner, but this has not been shown for insulin-reactive $CD8^+$ T cells. In addition, using a known insulin-reactive TCRα chain would also enable us to potentially increase the number of insulin-reactive T cells compared to a non-TCR transgenic wild-type NOD mouse.

The hypothesis for this study was:

Genetically-manipulating proinsulin expression will mediate significant T cell receptor repertoire selection pressure on insulin B15-23 reactive T cells, while also influencing the functional development and/or the control of these auto-reactive T cells in single chain TRAV8-1*01TRAJ9 transgenic NOD mice.

This was be addressed by using single chain TCR transgenic NOD mice (expressing TRAV8-1*01TRAJ9), the same TCRα chain used by the insulin-reactive G9C8 T cell. These mice were then crossed to other NOD mice, lacking TCRα chains (*TCRCα*$^{-/-}$) that were also genetically deficient in proinsulin 1 or 2, deficient in proinsulin 1 and 2 with a mutant transgene expressed, or over-express proinsulin 2 under the MHCII promoter. By generating these mice we were able to answer:

1. Does the expression of proinsulin influence the selection of the TCRβ chain paired to the restricted TCRα chain? This was investigated through flow cytometric methods using TCR monoclonal antibodies to the TCRVβ chains, as discussed in Chapter 3.

2. Does the expression of proinsulin influence the selection of the TCRβ chain paired to the restricted TCRα chain in insulin B15-23 reactive $CD8^+$ T cells? This was investigated through molecular methods identifying the sequence of the TCRβ chain used by the insulin B15-23-reactive $CD8^+$ T cells, as discussed in Chapter 3.
3. Does the expression of proinsulin influence the function of the insulin B15-23-reactive $CD8^+$ TCRs selected? This was investigated by cytokine production, proliferative ability and cytotoxicity responses of insulin B15-23-reactive $CD8^+$ T cells, as discussed in Chapter 4.
4. Does altering the gut microbiota influence the TCR repertoire or the functional capabilities of the insulin B15-23 reactive T cells? This was investigated through flow cytometric methods using TCR monoclonal antibodies to the TCRVβ chains and memory markers, as well as through the detection of spontaneous autoimmune diabetes in the single chain TCRα restricted NOD mice, as discussed in Chapter 5.

CHAPTER 2: MATERIALS AND METHODS

2.1 MICE

2.1.1 GENERATION

Single TCRα chain, *A22Cα*$^{-/-}$ mice, were generated using a transgene for the G9C8 TCRα chain (TRAV8-1*01TRBJ9 referred to in this thesis as A22, deriving from mouse line 22) and a *TCRCα* gene knock out, preventing endogenous TCRα chain expression (Wong et al., 2009). *A22*$^{+/+}$ NOD mice, were generated using TRAV8-1*01TRBJ9 DNA expressed in a TCR vector (originally provided by D.Mathis) (Kouskoff et al., 1995) and injected into NOD ova. The mice were crossed with *TCRCα*$^{-/-}$ NOD mice, derived from backcrossing *TCRCα*$^{-/-}$ mice on the B6/129 background (Philpott et al., 1992) to the NOD background, to generate *A22Cα*$^{-/-}$ mice. The breeding for the generation of these mice (FIGURE 9), shows that within 3 generations, both *A22*$^{+/+}$ and *TCRCα*$^{-/-}$ genes were homozygous in 25% of the offspring. Interbreeding of these homozygous mice resulted in fixing both genes to homozygousity. All mice used were on the NOD background and had native insulin 1 and 2 expression. To further generate mice expressing altered proinsulin levels, these *A22Cα*$^{-/-}$ mice were bred with other strains. For the generation of *A22Cα*$^{-/-}$*PI2*^{tg} mice, which over-expressed proinsulin 2 as a transgene under the MHCII promoter, *A22Cα*$^{-/-}$ mice were bred with NOD*PI2*^{tg} mice, which were provided by L. Harrison, WEHI, Australia (French et al., 1997). For *A22Cα*$^{-/-}$*PI1*$^{-/-}$ mice and *A22Cα*$^{-/-}$*PI2*$^{-/-}$ mice, the *A22Cα*$^{-/-}$ mice were bred with NOD*PI1*$^{-/-}$ or NOD*PI2*$^{-/-}$ mice, purchased from the Jackson Laboratory, respectively (Paronen et al., 2003). Finally, for the generation of *A22Cα*$^{-/-}$*PI1*$^{-/-}$*PI2*$^{-/-}$*Y16A*^{tg} mice, the *A22Cα*$^{-/-}$ mice were bred with NOD*PI1*$^{-/-}$*PI2*$^{-/-}$*Y16A*^{tg} mice, purchased from the Jackson Laboratory (Nakayama et al., 2005a). All these mice had already been generated at the start of this work.

2.1.2 ANIMAL HUSBANDRY

All mice were bred in specific pathogen-free isolators, except those used in Chapter 5, which were bred in scantainer facilites. All other mice, post-weaning, were then transferred to scantainers or filter top cages which were specific

pathogen-free. All procedures were carried out according to the Home Office guidelines, under PPL number 30/2766 and PIL number 30/9655.

2.2 MOLECULAR TECHNIQUES

2.2.1 GENOTYPING

2.2.1.1 DNA ISOLATION

Mice ear/tail clippings were placed into individual 1.5ml microfuge tubes, and were incubated in a Digest Buffer with 10µg pronase per sample overnight in a water bath at 55°C. Samples were then cooled at 4°C for 5 minutes, prior to the addition of 200µl saturated sodium chloride (~5.5M), which was mixed well and left to incubate for a further 5 minutes at 4°C. Samples were then centrifuged (14000rpm, 20 minutes, 4°C) with the nucleic acid-containing supernatant aliquotted into a new 1.5ml microcentrifuge tube. To this 80µg Ribonuclease A was then added (to remove RNA contamination), tubes were then inverted and incubated at 37°C for 15-20 minutes. 500µl of 100% ice-cold ethanol was then added to each tube before centrifugation. The supernatant was then discarded and the DNA pellet was then washed with 500µl of 70% ethanol (diluted in deionised water). The supernatant was discarded and tubes were left to dry at room temperature before resuspension in 50µl deionised water. Samples were then stored at 4°C until required.

2.2.1.2 POLYMERASE CHAIN REACTION (PCR)

A PCR mastermix comprising; deionised water, 10x Buffer, Primers, dNTPs and Taq DNA Polymerase was added to DNA pipetted into a 96 well plate. Plates were briefly centrifuged and placed into a PCR thermal cycler. Genotyping the mice required PCR reactions for different genes (2.9.2.3.1) which required different amplification programmes (2.9.2.3.2).

2.2.1.3 GEL ELECTROPHORESIS

An appropriate agarose gel was made in 1xTAE buffer for the PCR product of interest (2.9.2.3.4). The solution was microwaved at medium heat until the agarose was fully dissolved and allowed to cool to approximately 55-60°C prior to the addition of ethidium bromide (stains DNA). The solution was mixed well and

poured into an electrophoresis gel tray to further cool and solidify. Post-PCR, Orange G (DNA loading dye) was added to the PCR product and then loaded onto the agarose gel, with a 100bp ladder. The DNA was electrophoresed for 50 minutes at 100V and subsequently visualised and photographed on a UV transilluminator. The band appearance and size was then used to determine the genotype of the given mouse.

2.2.2 TCR CLONOTYPING

Cells were sorted as described in 2.3.5.1 on a BD FACS ARIA into RNAlater®.

2.2.2.1 mRNA ISOLATION

Cells were thawed quickly at room temperature, then immediately pelleted by centrifugation (15000xg, 7 minutes, 4°C). The supernatant was then removed and replaced with 900µl Lysis/Binding buffer, provided in the µMACS isolation kit (2.9.1.4). Samples were then vortexed at high intensity for 1 minute and centrifuged (13000xg, 2 minutes, room temperature). Lysate was then transferred to a Lysateclear® column placed on top of a centrifugation tube and centrifuged (13000xg, 3 minutes, room temperature). 50µl Oligo(dT) beads per ml of lysate were added and mixed well prior to transfer onto a pre-rinsed MACS µ column enabling mRNA to bind. The column was then washed twice with Lysis/Binding buffer to remove proteins and DNA and then four times with Wash buffer (removing DNA and rRNA). mRNA was then eluted using two additions of 70°C heated Elution buffer; an initial 27µl pre-elution to remove all Wash Buffer and then a 30µl addition, containing the mRNA. Samples were stored in a 1.5ml screw-topped microtube at -80°C until required.

2.2.2.2 cDNA SYNTHESIS

Into a 1.5ml screw-topped microtube, 1µl 5'CDS primer (oligo dT primer) and 6µl mRNA were added. The tubes were then incubated at 72°C for 3 minutes to denature the RNA, and then cooled to 42°C for 2 minutes to allow the primer to anneal. Post-incubation 7µl of the cDNA mastermix was added and mixed before further incubating at 42°C for 2 hours. The reverse transcriptase was then

deactivated by the addition of Tricine Buffer and incubated for 8 minutes at 72°C. cDNA was then stored at -80°C until required.

2.2.2.3 AMPLIFICATION OF TCRβ CHAIN BY PCR

Into a 0.2ml microcentrifuge tube, 13µl of cDNA was added to the TCRβ chain mastermix (to make a total volume of 50µl) and mixed well by pipetting. The sample was then incubated in a PCR thermal cycler on programme "TCRβ CHAIN AMPLIFICATION" (2.9.2.3.2) which amplified the TCRβ chain from the TCRβ constant region.

2.2.2.4 ELECTROPHORESING TCRβ CHAIN cDNA PRODUCT ON A 1% AGAROSE TAE GEL

After the TCRβ chain has been amplified, TrackIt buffer was added to each sample, mixed by pipetting and then all the samples was loaded into individual wells of a 1% agarose TAE gel with a 1Kb ladder. The samples were then electrophoresed at 65V at 180mA (per gel) for 50 minutes. Post-electrophoresis, 15µl of SYBR Gold was added to the gel and 1xTAE solution and the sample was then covered with aluminium foil to protect the light-sensitive SYBR Gold. The gel and solution were then mixed on a plate rocker at approximately 25-30 rotations per minute for 25 minutes, allowing the SYBR Gold to bind to the DNA. The gel was then visualised under low UV light for approximately 3 seconds with positive bands identified between 500-700bp.

2.2.2.5 GEL EXTRACTION OF TCRβ CHAIN cDNA

The TCRβ chain DNA band was removed from the 1% agarose TAE gel using a sterile scalpel on a UV Box set to minimum intensity to avoid damaging the DNA. The gel was then placed into a sterile 1.5ml microtube, which were then weighed. To this, 2 volumes of NT1 buffer for every 1 volume of gel (i.e. 200µl per 100mg gel) were added. Samples were then incubated at 50°C for 10 minutes and vortexed every 2-3 minutes to dissolve the agarose. The NT1/Agarose solution was then pipetted onto a DNA binding column and centrifuged (11000xg, 30 seconds, room temperature), with the flow-through discarded. The column was then washed using 700µl of NT3 buffer (containing ethanol) and centrifuged as

before, discarding the flow-through. The tube was then centrifuged again (11000xg, 1 minute, room temperature) to remove excess wash buffer. The DNA was then eluted into a clean microtube by the addition of 30µl of NE Buffer onto the filter prior to centrifugation as before. The eluted DNA from the column was then stored at -80°C until required.

2.2.2.6 TCRβ CHAIN LIGATION INTO TOPO TA DH5α PLASMID VECTOR

In a 1.5ml microtube 4µl of DNA was added to 1µl of salt solution and 1µl of Topo vector. The solution was mixed and incubated at room temperature for 30 minutes, allowing each TCRβ chain amplicon, from the heterogeneous population, to be ligated into a vector. Following the incubation, the tubes were placed on ice to stop the reaction and samples were then prepared for immediate bacterial transformation.

2.2.2.7 TCRβ CHAIN AMPLIFICATION USING CHEMICALLY COMPETENT E.COLI

Max efficiency DH5α-T1^{R} *E.Coli* were defrosted on ice and once thawed; 50µl was removed and added to the ligation mix prepared in the previous step. Samples were mixed gently and then incubated on ice for 30 minutes. Cells were then heat shocked for 30 seconds at 42°C and immediately placed on ice for a further 2 minutes. Using sterile technique, 950µl of SOC media was then added to each tube with the samples then placed in a thermomixer at 750rpm for 90 minutes. 100µl was then removed from each sample and spread over a pre-warmed 37°C LB-AIX plate using a glass L-shaped spreader (2 plates per sample). Plates were then inverted and incubated overnight (16-24 hours) in a 37°C incubator.

2.2.2.8 FURTHER AMPLIFICATION OF TCRβ CHAIN CDR3 REGION

The TCRβ chain amplicon was then amplified by PCR using the Colony PCR mastermix, in a 96-well PCR plate. Individual white bacterial colonies were then picked and transferred into a 96 well PCR plate with the PCR mastermix solution. The PCR plate was then sealed with a film lid, vortexed and centrifuged briefly and then placed in the PCR thermal cycler following the Colony PCR programme. After the PCR amplification, the wells were diluted 1:2 using sterile water, with

half then transferred into a new PCR plate. Plates were then sealed with foil lids and stored at -80°C.

2.2.2.9 SEQUENCING TCRβ CHAIN CDR3 REGION

The TCRβ chain was sequenced by single-pass PCR DNA sequencing (Beckman Coulter Genomics in Danvers, MA (USA)). Data were then analysed using Sequencher (Gene Codes Corporation), whereby sequences were aligned against the TCR genome using the IMGT website. Post-identification, sequences with their relative proportions were then calculated.

2.2.3 BACTERIAL DNA EXTRACTION, SEQUENCING AND IDENTIFICATION

Faecal pellets were collected from mice in Baytril-treated observational studies as discussed (see section 2.8). Samples were then shipped to Yale University for Bacterial DNA isolation, sequencing and classification. The following methods were conducted by Dr Jian Peng in Dr Li Wen's laboratory.

2.2.3.1 BACTERIAL DNA EXTRACTION

Faecal pellets were resuspended in TE Buffer, vortexed and then digested with Proteinase K (200µg/ml) at 37°C. 0.3g of zirconium beads (diameter 0.1mm) were then added to the samples, which were then beaten with a mini bead beater shaker at 5000rpm for 3 minutes in a 50% phenol-chloroform isoamyl (PCI) solution. Samples were then pelleted and DNA was precipitated with isopropanol and subsequently washed in 70% ethanol.

2.2.3.2 16S rRNA GENE SEQUENCING

Bacterial DNA was amplified using primers specifically for the V2 region of the 16S rRNA gene. Post-PCR, DNA was electrophoresed in a 1.2% agarose gel containing ethidium bromide and subsequently the DNA was cut from the gel using a sterile scalpel on a UV transilluminator. PCR products were then gel extracted (as discussed in 2.2.2.5) and DNA was quantified using a Nanodrop spectrophotometer. DNA was then resuspended at $1x10^9$ molecules/µl in TE Buffer. 20µl of DNA was then used for pyrosequencing on a GS Junior Titanium Series 454 sequencing system (Roche).

2.2.3.3 BACTERIAL IDENTIFICATION

Sequencing data were analysed using QIIME software version 1.6 where operational taxonomic units were assigned and low quality samples removed. Beta diversity was then calculated to enable comparisons between microbial communities. Data were then plotted as a principal component analysis (PCA). Post-sequencing data analysis identified bacterial phyla, shown as pie charts.

2.2.4 QUANTITATIVE PCR (qPCR)

2.2.4.1 ISOLATION AND DIGESTION OF CELLS FROM THE THYMUS AND PLN

Thymus and PLN were removed from NOD mice aged 8 weeks (n=8-9) under sterile conditions and were placed in RPMI complete media. Cell suspensions were then made as outlined in 2.3.2, however, the entire stromal tissue was also used for the subsequent digestion. Cells were then pelleted (400xg, 5 minutes, 4°C) and resuspended in Liberase-DNase I containing RPMI complete media. Cells were then incubated for 2 hours at 37°C, mixing frequently, with half the solution removed and placed into a 50ml tube on ice containing MACS Buffer. To the original tube, an equal volume of fresh enzyme solution was added. Post-incubation, similar tissue and gender samples were pooled together. The cells were then pelleted as before and resuspended in MACS buffer for counting. Cells were then pelleted again and the CD45 MACS Miltenyi kit method was followed, depleting leukocytes. Briefly, cells were resuspended in 90µl MACS Buffer and 10µl CD45 microbeads per 10^7 cells. Cells were incubated for 15 minutes at 4°C, then washed in MACS Buffer. Cells were then resuspended in MACS Buffer and then loaded onto a LS column held by a magnet. $CD45^-$ cells were found in the flow-through and the column was washed three times. The $CD45^-$ cells were then pelleted, resuspended in 500µl of Tri-reagent and frozen at -80°C overnight.

2.2.4.2 RNA EXTRACTION

Samples were defrosted on ice slowly and then 100µl of 1-bromo-3-chloropropane was added. Samples were then vortexed and incubated at room temperature for 5 minutes and subsequently pelleted (12000xg, 15 minutes, 4°C). The upper colourless layer (containing RNA) was removed and transferred to a

new 1.5ml tube, to which 500µl of isopropanol was then added. Samples were then incubated for 5 minutes at room temperature and then pelleted as before. Supernatant was discarded and the RNA pellet was washed in 75% ethanol. Samples were vortexed and then pelleted (7500xg, 5 minutes, 4°C), from which the supernatant was removed and samples were incubated at room temperature for 5 minutes, enabling any remaining alcohol to evaporate. Samples were then resuspended in 20µl of ddH_2O and measured on a Nanodrop spectrophotometer for their concentration and purity.

2.2.4.3 GENERATION OF cDNA FROM RNA

cDNA was made from 2.5µg RNA and superscript VILO mastermix (Invitrogen) and made up to 20µl using ddH_2O. Samples were then incubated at 25°C for 10 minutes, 42°C for 60 minutes and to terminate the reaction, 85°C for 5 minutes.

2.2.4.4 qPCR REACTION

cDNA was then plated in quadruplicate, into wells of a 96 well plate, where duplicates were assessed for Insulin 1 or Insulin 2 with either 18S or GAPDH expression using a qPCR mastermix. A total volume of 20µl was loaded into each well of the plate. An adhesive film lid was then placed over the wells and samples were then vortexed and briefly centrifuged. Plates were then loaded onto a ViiA7 real-time qPCR machine for 100 minutes following the qPCR programme.

2.2.4.5 QPCR ANALYSIS

Data were analysed using Expression Suite software version 1.0.3 and plotted showing the change in reaction fluorescence concentration.

2.3 FLOW CYTOMETRIC TECHNIQUES

2.3.1 GENOTYPING *TCRCα*$^{-/-}$ AND *G9Cα*$^{-/-}$ MICE

Mice were bled from the tail tip into Blood Buffer. Cells were then pelleted by centrifugation (400xg, 4°C, 5 minutes) and the supernatant was discarded. The genotyping antibody mastermix in FACS buffer (2.9.3.3.1) was then added and the cells were incubated at 4°C for 30 minutes. This antibody mastermix panel containing antibodies to CD8, CD19, TCRValphas and TCRVβ6, would identify if the *TCRCα*$^{-/-}$ was present and the degree of TCRβ restriction for the G9 T cells. 1ml

of prediluted (1:10) Lysis Buffer was then added and cells were further incubated for 10 minutes at room temperature in the dark. Cells were then washed in FACS Buffer and centrifuged as before with the supernatant discarded and the pellet resuspended in 100µl FACS Buffer. Samples were then stored at 4°C until measured on the BD FACS Calibur with data analysed using Flowjo version 7.6.5 software (Treestar).

2.3.2 STANDARD TRBV PHENOTYPING

Thymus, spleen, pancreatic, mesenteric and para-aortic lymph nodes were removed from mice aged 4-7 weeks, 8-10 weeks and 12-16 weeks. Tissues were placed into 5mls of 1xPBS with the exception of the lymph nodes which were teased open in petri dishes using a 30G needle and pipetted into 4mls 1xPBS. Thymus and spleen were homogenised using loose-fit glass homogenisers. Cells were washed in 1xPBS and pelleted by centrifugation at 400xg for 5 minutes at 4°C. Cells were then resuspended in FACS buffer, except the spleen, which required red blood cell lysis in 900µl H_2O followed quickly by the addition of 100µl 10xPBS and resuspended in 5mls 1xPBS. Post-lysis, the remaining cells were then washed, centrifuged as before and resuspended in FACS buffer. 100µl of each tissue were pipetted into each FACS tube, with the appropriate antibody mastermix (2.9.3.3.2). Cells were then stained at 4°C for 30 minutes prior to the addition of 500µl FACS FIX buffer and a further 30 minute incubation at 4°C. Post-incubation, FACS buffer was added to each tube to remove any excess antibody. Cells were then pelleted as before and resuspended in 100µl FACS buffer and kept at 4°C until ready to be measured on a BD FACS CANTO II instrument.

2.3.2.1 TRBV PHENOTYPING ANALYSIS

Data were analysed using Flowjo software (Treestar), Version 7.6.5. FIGURE 10 and FIGURE 11 show the gating strategy used to identify live single cell lymphocytes (both $CD4^+$ and $CD8^+$), from which the TRBV repertoire was then investigated within the T cell subsets. Data were then plotted in GraphPad Version 4 software.

2.3.2.2 TRBV PHENOTYPING STATISITCAL ANALYSIS

Analyses were carried out using the statistical software, R (version 2.13.2, R Development Core Team 2012, Vienna, Austria), whereby an analysis of variance was conducted using gender, age, strain and tissue as variables with a stringent Bonferroni correction. This correction was calculated using the data below:

Mice (6) x Gender (2) x Strains (5) x Age (2.69*****) x Tissues (4.83******) x CD4/CD8 (2) x TCRVβ chains (14) = 21827.736

For p=<0.05 then values below **0.0000022907** are significant (0.05/21827.736)

For p=<0.01 then values below **0.0000004581** are significant (0.01/21827.736)

*****While 3 strains have 3 age groups, the *A22Cα*$^{-/-}$*PI1*$^{-/-}$ and the *A22Cα*$^{-/-}$*PI1*$^{-/-}$*PI2*$^{-/-}$ *Y16A*^{tg} mice were only analysed at 2 age groups. Therefore a total of 13 age groups were compared resulting in an average of 2.69 age groups in total and therefore, this value was used.

**In all strains, except the *A22Cα*$^{-/-}$*PI1*$^{-/-}$ mice, 5 tissues were analysed and therefore, an average was taken of the total amount of tissues giving 4.83.

2.3.3 PEYER'S PATCH TRBV PHENOTYPING

As for 2.3.2, the PLN and MLN were prepared as discussed; however, they were kept in PP Buffer rather than 1xPBS. For isolation of the Peyer's patches, the small intestine was dissected and flushed twice using 20mls PP Buffer injected using a 20G needle and syringe intra-luminally. Post-flush, Peyer's patches were identified and removed from the small intestine using scissors and placed into a petri dish containing 1ml PP Buffer. Peyer's patches were then teased open using a 30G needle, with excess tissue removed and pipetted into 3mls PP Buffer. Cells were then pelleted (400xg, 5 minutes, 4°C) and resuspended in 500µl FACS Buffer with 100µl aliquots transferred into new FACS tubes. The antibody mastermix was then added (2.9.3.3.3) and cells were fixed, washed and resuspended in FACS buffer as 2.3.2. Samples were kept at 4°C until ready to be measured on a BD FACS CANTO II instrument.

2.3.3.1 PEYER'S PATCH TRBV PHENOTYPING ANALYSIS

Data were analysed as 2.3.2.1, however for Peyer's patch TRBV repertoire staining there was an additional gate post-CD4 and CD8 gating, in which, CD8α vs CD8β was plotted enabling gating on the double positive $CD8\alpha\beta^+$ lymphocytes. These cells were then investigated for the TRBV repertoire or activation status. TRBV data were then adjusted to X number of cells per 10^4 $CD8\alpha\beta^+$ T cells in order to adjust for the proportional differences between the Peyer's patches and the MLN and PLN. Data were then plotted using GraphPad Version 4 software.

2.3.3.2 PEYER'S PATCH TRBV PHENOTYPING STATISITCAL ANALYSIS

Analysis of variance was conducted using gender, age, strain and tissue as variables using the statistical software R (version 2.13.2, R Development Core Team 2012, Vienna, Austria). Data were then corrected using a stringent Bonferroni correction, calculated using the data below:

Mice (5) x Gender (2) x Strains (1) x Tissues (3) x CD4/CD8 (2) x TCRVβ chains (14) = 840

For p=<0.05 then values below **0.0000595238** are significant (0.05/840)

For p=<0.01 then values below **0.00001190476** are significant (0.01/840)

2.3.4 PEPTIDE:MHC TETRAMER STAINING

Tissues were collected and prepared as in 2.3.2 or 2.3.3; however, Tetramer Wash Buffer was used instead of FACS Buffer. Live cells were then counted using a haemocytometer with Trypan blue staining, enabling exclusion of dead cells. $1x10^6$ cells were pipetted into FACS tubes, pelleted (400xg, 5 minutes, 4°C) and resuspended in Tetramer Wash Buffer containing Dasatinib (final concentration of 50nM). Cells were then incubated at 37°C for 30 minutes to allow Dasatinib to enter the cells and inhibit protein kinases, particularly Lck (Lee et al., 2010), and thus TCR recycling, allowing maximal detection of tetramer-reactive T cells. Post-incubation cells were pelleted, supernatant was removed and cells were resuspended in 100µl Tetramer Wash Buffer containing 1µg tetramer. BV421-conjugated tetramers were kindly provided by the Tetramer Core Facility, NIH,

USA. Cells were incubated for 15 minutes at 37°C and were subsequently washed in Tetramer Wash Buffer, to remove excess unbound tetramer, pelleted and resuspended in 100µl of antibody mastermix (2.9.3.3.5). Cells were antibody stained, fixed, washed and resuspended as 2.3.2 and then stored at 4°C until measured on a BD FACS CANTO II instrument.

2.3.4.1 PEPTIDE:MHC TETRAMER STAINING ANALYSIS

Data were analysed using the Flowjo (Treestar) Version 7.6.5 software. FIGURE 12 shows the gating strategy for identifying live single cell lymphocytes which were $CD8^{+}CD19^{-}CD11b^{-}CD4^{-}Tetramer^{+}$. Data were then corrected by subtracting the minimal binding tetramer from the native insulin B15-23 peptide tetramer and then plotted in GraphPad Version 4 software.

2.3.5 FLOW CYTOMETRY SORTING

2.3.5.1 PEPTIDE:MHC TETRAMER FLOW CYTOMETRY SORTING

Splenocytes were prepared and stained as above (2.3.2) using panel 1 (2.9.3.3.5). Once the 30-minute antibody incubation had passed, cells were washed and taken for fluorescent activated cell sorting. Stringent gates were used to ensure the only cells sorted were tetramer positive (FIGURE 13). Cells were sorted on a BD FACS ARIA into RNAlater® and stored at -80°C.

2.3.5.2 $CD8^{+}TRBV19^{+}$ (TCRVβ6) ANTIBODY BASED FLOW CYTOMETRY SORTING

As 2.3.5.1; however, cells were sorted into RPMI complete media under sterile conditions prior to cell culture.

2.4 CELL CULTURE

2.4.1 PEPTIDE PREPARATION

2.4.1.1 INSULIN B CHAIN AMINO ACIDS 15-23 PEPTIDE PREPARATION

Peptide stock (5mg/ml) was diluted in RPMI complete media to 20µg/µl. This was then added to a round-bottomed 96-well plate/FACS tube and diluted 1:4 to provide a top peptide concentration of 5µg/µl.

2.4.1.2 DENATURED WHOLE INSULIN PREPARATION

Actrapid Insulin (100 IU/ml equivalent to 3.5mg/ml, see 2.9.1.5) was diluted using ddH2O and heated to 60°C for 5 minutes. Post-denaturation, insulin was then further diluted, as mentioned for Insulin B15-23 peptide (2.4.1.1).

2.4.2 ANTIGEN PRESENTING CELL PREPARATION

2.4.2.1 HARVESTING AND CULTURING DENDRITIC CELLS

Hind legs were dissected from NOD mice aged 6-10 weeks using sterile technique. Muscle was removed and clean bones were placed into a 5ml tube containing RPMI complete media. Bones were placed in a tissue culture dish in a laminar flow hood and then dissected at the knee joint and the ends of the bones to reveal the red bone marrow pulp using a scalpel. RPMI complete media was then injected into the bone cavity, using a 30G needle, flushing out the bone marrow into a new tissue culture dish. A single cell suspension was then made by flushing the cells through a clean 25G needle into a 50ml centrifuge tube containing a 40µm filter. Cells were then pelleted (400xg, 5 minutes, 4°C), resuspended in RPMI complete media and transferred into 75cm^2 tissue culture flasks and incubated for 2 hours at 37°C. Post-incubation, the cell solution was carefully removed and transferred into a new 50ml tube. The tissue culture flask was gently washed ensuring no adherent cells were removed and then the cells were pelleted and counted using Trypan blue. Cells were then resuspended at 5x10^6/ml and pipetted into a 6-well plate. RPMI complete media was added containing Granulocyte macrophage colony stimulating factor (GM-CSF) to a final concentration of 1x10^6/ml cells and 1.5ng/ml of GM-CSF. RPMI complete GM-CSF media was half-changed every three days.

2.4.2.2 ACTIVATING AND PREPARING DENDRITIC CELLS FOR ASSAY

6-9 days post-dendritic cell culture, RPMI complete GM-CSF-containing media was half changed with the addition of Lipolysaccharide (LPS: final concentration of 1µg/ml). Cells were then incubated for 18 hours at 37°C and then removed from each well using a cell scraper. Collected cells were then pelleted (400xg, 5 minutes, 4°C) and washed in RPMI complete media twice to remove excess LPS.

DCs were then irradiated (3000 grays), pelleted and resuspended in RPMI complete media and counted. Dendritic cells were then plated at $0.2x10^6$/ml.

2.4.2.3 WHOLE SPLENOCYTE PREPARATION

Single cell suspensions of splenocytes were freshly prepared (see 2.3.2) and irradiated (as in 2.4.2.2). Cells were then pelleted and resuspended in RPMI complete media for counting and resuspended at $1x10^6$/ml.

2.4.2.4 CULTURING P815 CELLS

P815 cells (a murine lymphoblast-like mastocytoma cell line) were removed from liquid nitrogen storage and quickly thawed at room temperature. Pre-warmed (37°C) RPMI Complete media was then added to the tube and all cells were transferred into a new 10ml tube. Cells were then pelleted (400xg, 5 minutes, room temperature), supernatant was discarded and cells were washed with pre-warmed RPMI complete media to remove DMSO contaminant from storage. Cells were then resuspended in pre-warmed media, transferred into a $25cm^2$ cell culture flasks and incubated at 37°C with 5% CO_2 until the next day. Cells were checked daily under a light microscope and split i.e. diluted 1:10 when the cells reached approximately 80% confluency using pre-warmed RPMI complete media. Cells were grown until sufficient numbers were obtained for the required cytotoxicity assay.

2.4.3 ISOLATION OF $CD8^+$ T CELLS

$CD8^+$ T cells were isolated from the spleen or PLN and single cell suspensions were prepared as in 2.3.2. Isolated, viable $CD8^+$ T cells were then counted, washed in MACS Buffer, and pelleted (400xg, 5minutes, 4°C). Supernantant was then discarded and $CD8^+$ T cells were isolated using the MACS Miltenyi $CD8^+$ T cell isolation protocol. Briefly, 10^7 cells were resuspended in 40µl MACS Buffer and 10µl Biotin-antibody cocktail (containing anti-mouse monoclonal antibodies to CD4, CD11b, CD11c, CD19, CD45R (B220), CD49b (DX5), CD105, MHC Class II, Ter-119, and TCRγ/δ) and the cells were incubated for 5 minutes at 4°C. Post-incubation, 30µl MACS Buffer and 20µl anti-biotin microbeads were then added to the cells, which were then further incubated for 10 minutes at 4°C. Cells were

then pelleted as before, resuspended in 500µl per 10^7 cells and added to pre-washed MACS columns held by a magnet. The $CD8^+$ T cells flowed through the column, which was washed 3 times. Cells were counted and resuspended at $1x10^6$/ml.

2.4.4 CYTOTOXICITY ASSAY

This method was adapted from (Lee-MacAry et al., 2001). P815 cells were removed from the tissue culture flask and transferred into a 50ml falcon tube. Cells were pelleted (400xg, 5 minutes, room temperature), supernatant was discarded and cells were resuspended in serum-free RPMI media. Viable P815 cells were counted using a haemocytometer and Trypan blue, with the required number of cells transferred into a new 50ml falcon tube (excess P815 cells were kept for use as compensation controls for flow cytometry) and washed in serum-free RPMI media. Supernatant was then discarded and P815 cells were labelled by resuspension in PKH-26 cell dye diluted (1:250) in diluent C. Cells were then wrapped in aluminium foil, to protect from light, and incubated at room temperature for 90 seconds. Post-incubation, cell labelling was terminated by the addition of 500µl of sterile FBS per $1x10^6$ cells. Cells were then incubated for a further minute at room temperature in the dark, then washed twice in 10mls of RPMI complete media. Cells were then resuspended in RPMI complete media, counted and resuspended at $0.2x10^6$/ml. 10,000 P815 cells were then transferred into sterile FACS tubes. P815 cells and isolated $CD8^+$ T cells (1:10) were incubated with Insulin B15-23 peptide for 16 hours overnight at 37°C in duplicate prior to assessment for cytotoxicity by flow cytometry on a BD FACS CANTO II. 20 seconds prior to measurement of cytotoxicity, TOPRO-3, a viability marker, was added to the FACS tubes. 5,000 PKH-26^+ cells were recorded for each sample. Data were then analysed using Flowjo software Version 7.6.5 (Treestar) gating on single PKH-26^+TOPRO-3^+ cells indicating the proportion of P815 target cells lysed. Data were adjusted for background using the P815 cells and T cells without peptide. GraphPad Prism software Version 4 was then used to plot the data.

2.4.5 *IN VITRO* ^{3}H-THYMIDINE INCORPORATION PROLIFERATION ASSAYS

Insulin B15-23 peptide or whole insulin (2.4.1), $CD8^+$ T cells (2.4.3) and Dendritic cells (2.4.2) were plated into a 96-well round bottomed plate at final concentrations of 100,000 T cells, 10,000 DCs and 5µg/ml peptide (prior to serial dilution). Cells were then incubated for 48 hours at 37°C. At this point half the supernatant was removed and stored in sterile 1.5ml microcentrifuge tubes at -20°C for later analysis. 18.5KBq of ^{3}H-thymidine were then added to each well and cells were then incubated for a further 18 hours at 37°C. Post-incubation, cells were harvested onto a filter mat, which was dried overnight. Wax was then melted onto the filter, in a heated cabinet, at 75°C for 3-4 minutes, prior to counting on a microbeta counter with ^{3}H-thymidine incorporation measured in counts per minute (cpm). Counts were then corrected for background subtracting the cpm values for T cells and DCs without peptide. Data were plotted using GraphPad Prism Version 4 software.

2.4.6 GENERATING INSULIN B15-23 REACTIVE $CD8^+$ T CELL OLIGOCLONAL LINES

2.4.6.1 ISOLATION AND INITIAL GROWING OF $CD8^+TRBV19^+$ T CELLS

$CD8^+$ T cells were isolated from murine splenocytes (see 2.4.3) and once purified, were antibody-stained and sorted by FACS for $TRBV19^+$ (TCRVβ6) as outlined in 2.3.5.2. Post-sorting, cells were resuspended RPMI complete media, resuspended at $1x10^6$/ml and transferred into a 6-well plate containing 20,000/ml irradiated DCs (prepared as outlined in 2.4.2) and 80,000/ml irradiated whole splenocytes. The next day, insulin B15-23 peptide was added at a final concentration of 1µg/ml and the day after 20U/ml IL-2 and 2µg/ml IL-7 were also added into the cultures. Cells were cultured for 3 weeks with half media changes (containing IL-7 and IL-2) every 3 days with fresh irradiated DCs, splenocytes and peptide added every 6 days.

2.4.6.2 LIMITING DILUTION OF CD8⁺TRBV19⁺ T CELLS

At 3 weeks, a limiting dilution of the $CD8^+TRBV19^+$ T cells was carried out. Cells were then pelleted (400xg, 5 minutes, 4°C), counted and resuspended at 300 cells/ml, (30 cells/well) and diluted to 100 cells/ml (10 cells/well), 30 cells/ml (3 cells/well) and 10 cells/ml (1 cell/well). The cells were then transferred into a 96-well round-bottomed plate. Cells remaining from the limiting dilution were set up as bulk cultures in a 6-well plate and cultured as in 2.4.6.1.

2.4.6.3 EXPANSION OF CD8⁺TRBV19⁺ T CELLS

Any individual well cultures showing significant expansion were removed using a plastic Pasteur pipette and expanded into a larger 48-well plate with fresh media (and APCs if prepared). Cells expanding further were then plated into 24-, 12-, or 6-well plates depending on the plate they were removed from. Once the oligoclonal lines were plated in 6-well plates, samples were frozen down and assessed for insulin B15-23 reactivity.

2.4.6.4 NOMENCLATURE OF THE CD8⁺TRBV19⁺ OLIGOCLONAL CELL LINES

Oligoclonal lines were named based upon the strain, the plate and the well they were derived from e.g. a culture from *A22Cα*$^{-/-}$ 30 cells/well plate, well D4 became *A22Cα*$^{-/-}$ 30D4.

2.4.6.5 PREPARATION OF CD8⁺TRBV19⁺ OLIGOCLONAL CELL LINES FOR FUNCTIONAL ASSAYS

Cells were removed from the 6-well cultures and pelleted (400xg, 5 minutes, room temperature). They were then washed twice, resuspended in RPMI complete media and incubated at room temperature for 20 minutes (to ensure removal of the cytokines) prior to pelleting as before. Cells were then counted and resuspended at $1x10^6$/ml.

2.4.6.6 FREEZING CD8⁺TRBV19⁺ OLIGOCLONAL CELL LINES

Cells were prepared as 2.4.6.5 except the cells were resuspended at 1-2x106/ml in Freezing medium and transferred into a 1.8ml cryotube. Tubes were then placed into an isopropanol-containing freezing box to ensure cells were gradually

frozen down to -80°C. The next day, tubes were removed from the -80°C freezer and transferred into liquid nitrogen for long-term storage.

2.5 CYTOKINE ASSAYS

2.5.1 ENZYME-LINKED IMMUNOSORBENT ASSAY (ELISA)

2.5.1.1 MACROPHAGE INFLAMMATORY PROTEIN-1β (MIP-1β)

A 96-well Maxisorp immuno plate was coated with 4µg/ml capture antibody and incubated overnight at room temperature. The next day, plates were washed with ELISA Wash Buffer three times using a plate washer and blotted against paper towels to fully remove any buffer. Plates were then blocked using Reagent Diluent for 1 hour at room temperature. During this time, standards and samples (supernatants from cell culture experiments) were thawed, with the standards diluted in Reagent Diluent to the appropriate concentration (2.9.5.3). Plates were washed and blotted as above and standards/samples were then added to the wells and incubated for 2 hours at room temperature. Post-incubation, plates were washed and blotted as before followed by the addition of the detection antibody (0.8µg/ml). Plates were further incubated for 2 hours at room temperature, then washed and blotted as before. Diluted streptavidin-HRP was then added to the wells and incubated in the dark for 20 minutes at room temperature. Plates were then washed and blotted dry. TMB Substrate Solution was then added to each well and incubated for 15-20 minutes until sufficient colour change was seen. Further substrate conversion was then prevented through the addition of 2N H_2SO_4. Optical density (OD) was then determined using a plate reader set to 450nm with a reference at 570nm (to subtract any optical imperfections within the plate).

2.5.1.2 IFN-γ

Protocol as above except; capture antibody was diluted in Carbonate Buffer and incubated at 4°C overnight, plates were blocked at 37°C for 1 hour and the detection antibody was incubated for 1 hour at room temperature.

2.5.1.3 ELISA ANALYSIS

A standard curve was plotted using the OD values and the known concentrations of the standards. From this, the concentration of the samples was calculated by a linear regression. Samples were then corrected for the background using the concentration of cytokines in the absence of peptide.

2.6 HISTOLOGY

2.6.1 FIXING AND CRYOPRESERVING TISSUE

Pancreas, salivary gland and partial spleen were fixed in PLP overnight at 4°C. The tissue was then washed using PB Buffer and infused with 10% sucrose-PB Buffer solution for 30 minutes at 4°C to cryoprotect the tissue. The tissue was then incubated for an additional 30 minutes at 4°C using 20% sucrose-PB Buffer solution. Tissue was then removed from the solution, transferred to a tissue mould, embedded in OCT embedding matrix, and frozen using an isopentane ice bath. Tissue blocks were then stored at -80°C.

2.6.2 SECTIONING TISSUE BLOCKS

8µm sections were cut using a cryostat with the following settings: cryobar -45°C, chamber temperature -25°C and the specimen at -19°C. Sections were then transferred to poly-lysine coated slides and were stored at -80°C.

2.6.3 IMMUNOHISTOCHEMISTRY STAINING

Slides were defrosted at room temperature until dry. A hydrophobic border was then drawn around the tissue using a PAP pen and when dry, the specimens were rehydrated for 45 minutes with 1xPBS. Solution was then removed and replaced with 1% hydrogen peroxide in 1xPBS, to neutralise endogenous peroxidise activity, for 15 minutes. Slides were then washed 3 times using Histology Wash Buffer and, to prevent non-specific binding, FC receptors were blocked using 5% rat serum in Histology Wash Buffer and incubated for 20 minutes at room temperature. Slides were then washed in Histology Wash Buffer prior to the addition of 2-3 drops of Avidin per section. Slides were incubated for 15 minutes at room temperature, rinsed with Histology Wash Buffer, then 2-3 drops of biotin per section were added and slides were incubated for a further 15 minutes. Slides

were then immersed in Histology Wash Buffer for 5 minutes and then incubated for 90 minutes with the appropriate primary biotinylated antibody (2.9.6.3), diluted in 1xPBS. Post-incubation, slides were immersed once in Histology Wash Buffer and twice more in 0.1M Tris Buffer (pH7.4) for 5 minutes each to remove excess unbound primary antibody. Slides were then incubated with 0.1M Tris Buffer (pH7.4) diluted Streptavidin-Alkaline Phosphatase (1:300) for 45 minutes and then washed three times in 0.1M Tris Buffer (pH7.4), incubating each wash for 5 minutes. The colour was then developed using an alkaline phosphatase substrate kit (diluted in 0.1M Tris, pH8.4), with slides incubated for 20 minutes in the dark at room temperature. Slides were then washed in 0.1M Tris Buffer (pH7.4) and incubated for 5 minutes and then in water for 5 minutes. Haematoxylin counter stain was conducted by submerging the slides in haematoxylin for 30 seconds; submerging in water for 5 minutes and then submerging in 1% ammonium chloride in water for 30 seconds prior to a 5 minute wash in water. Slides were then dried overnight followed by section dehydration in 70% ethanol, then 100% ethanol and finally in Histo-Clear. Sections were then mounted with a coverslip using DPX.

2.6.4 HISTOLOGY SCORING

Islets were counted and scored using a scale of 0-4 as follows: no cellular infiltration, score 0, peri-insulitis (cellular infiltration around the islet), score 1, <25% infiltration, score 2, <50% infiltration, score 3, >50% infiltration score 4. Scoring was blinded with 2 independent scorers. Data were then collated and presented in GraphPad Prism Version 4 software.

2.6.5 HISTOLOGY IMAGING

Slides were visualised using an Olympus BX51 light microscope and Axiovision LE software, with help kindly provided by Dr Christopher Von Ruhland within the Central Biotechnology Services of Cardiff University.

2.7 COMPETITIVE INSULIN AUTOANTIBODY RADIOIMMUNOASSAY

2.7.1 SERUM PREPARATION

Mice were culled by cervical dislocation with blood extracted by cardiac puncture using a 25G needle and syringe. Blood was left to clot at room temperature for 3 hours, then stored overnight at 4°C. Blood was then centrifuged (2000xg, 10 minutes, 4°C) and the serum was removed and transferred to a fresh microcentrifuge tube to be stored at -20°C.

2.7.2 INSULIN ^{125}I LABEL

2.7.2.1 DILUTION OF STOCK INSULIN ^{125}I LABEL

^{125}I insulin label stock (50μCi) was diluted in TBT buffer and left at room temperature for 30 minutes. The diluted stock was then aliquotted into 400μl aliquots and stored at -80°C in a lead container until needed.

2.7.2.2 DILUTION OF INSULIN ^{125}I LABEL FOR COMPETITION ASSAY

^{125}I insulin aliquots were thawed at room temperature within a lead container and once defrosted, ^{125}I-labelled insulin was diluted in TBT-BSA. A 25μl sample was removed and counted for 3 minutes on a gamma counter. Once the counts per minute reached 16,500 (+/- 500 counts), half the solution was transferred to a new universal tube. To this new tube, 80μl/ml of cold insulin i.e. non ^{125}I-labelled insulin was added, while an equal volume of TBT-BSA buffer was added to the original diluted tube. A 25μl sample of each solution was then counted as before with counts between 14,000-15,500cpm (+/- 500 counts of each other).

2.7.3 PROTEIN G SEPHAROSE BEADS

Protein G Sepharose (PGS) beads were blocked in ethanolamine. When required, PGS beads were washed 3 times (500xg, 4°C, 3 minutes) in TBT Buffer, to remove excess ethanolamine, and then resuspended in TBT and stored at 4°C until needed.

2.7.4 COMPETITIVE INSULIN AUTOANTIBODY RADIOIMMUNOASSAY

5μl of sample/standard/quality control serum was plated twice in duplicates into a 96-deep-well plate. To each well 25μl of ^{125}I-labelled insulin (“hot”) or ^{125}I-

labelled insulin + non-labelled insulin ("cold") was added. Plates were centrifuged (500xg, 4°C, 3 minutes) and then incubated at 4°C for 72 hours. Washed PGS beads were then added to the labelled plates and shaken on a digital plate shaker at 700rpm for 1 hour and 45 minutes. After PGS incubation, wells were washed with TBT Buffer and centrifuged as before. Wells were then manually aspirated and washed with TBT Buffer 4 times. Upon completion, wells were resuspended in 100µl of TBT Buffer, vortexed briefly and then the solution was transferred into 1.2ml microtubes for counting on the gamma counter for 10 minutes/tube.

2.7.4.1 ANALYSIS

Standard counts per minute were plotted against their concentration to create a standard curve and using linear regression, samples and quality control serum competitive insulin autoantibody (cIAA) results were calculated. Values over 0.0103 cIAA units were deemed positive with quality controls falling within their designated range. This threshold was set using the mean background level (plus 3 standard deviations), detected in serum from C57BL/6 mice, which do not develop diabetes. Data were then presented in GraphPad Prism Version 4 software.

2.8 *IN VIVO* EXPERIMENTS

2.8.1 NATURAL HISTORY OF DIABETES

Post-weaning, mice were placed into observation groups and monitored bi-weekly for glycosuria from 3 weeks of age using Glucostix strips. If positive, the mice were retested the next day and diabetes confirmed with a blood glucose reading, over 13.9mmol/L. In addition, for the gut microbiota experiments, weekly faecal pellets were also taken and placed into 1.5ml microcentrifuge tubes and stored at -80°C. Upon development of diabetes (6-10 weeks of age) or termination of the observation group (12-20 weeks of age), the pancreas, salivary gland and partial spleen were taken for histology and blood was collected for serum. Data were then presented using GraphPad Version 4 software.

2.8.2 PEPTIDE IMMUNISATIONS

Mice were immunised with 50µl of Incomplete Freund's Adjuvant (IFA) added to an equal volume of saline containing 50µg of CpG and 50µg of Insulin B15-23 peptide/denatured insulin. The solution was then emulsified by vortex and then injected subcutaneously at the base of the tail into mice.

2.8.3 SPLENOCYTE TRANSFERS

Spleens were harvested from mice, homogenised using a loose glass homogenisers, lysed with 900µl of water, followed by the addition of 100µl of 10xPBS (producing a 1xPBS solution). Cells were then resuspended in 9mls of 1xPBS and then pelleted (400xg, 5 minutes, 4°C). Splenocytes were then resuspended and washed twice in sterile saline and counted. Cells were then resuspended at 10-20x10^6 per 200µl and injected intravenously into the tail vein of donor mice. Mice were then monitored for diabetes as detailed in 2.8.1.

2.8.3.1 CFDA-SE LABELLED SPLENOCYTE TRANSFER

Single cell splenocyte suspensions were prepared and counted as 2.8.3. $CD8^+$ T cells were then isolated (2.4.3), pelleted (400xg, 5 minutes, 4°C) and resuspended in pre-warmed (37°C) sterile 1xPBS containing the CFDA-SE probe (5µM). Cells were then incubated at 37°C for 15 minutes in a waterbath. Post-incubation, cells were pelleted as before, and resuspended in pre-warmed (37°C) RPMI complete media to ensure complete modification of the probe. Cells were then further incubated for 30 minutes at 37°C, pelleted, washed in sterile saline twice, counted and resuspended at 10-20x10^6 cells per 200µl. They were then intravenously injected into the tail vein of recipient NOD*PI2*^{tg} mice.

2.8.3.2 CFDA-SE IN VIVO PROLIFERATION ASSESSMENT

Thymus, spleen, PLN and MLN were taken from the NOD*PI2*^{tg} mice, which received CFDA-SE labelled $CD8^+$ T cells. Single cell suspensions were prepared, stained and fixed as 2.3.2, with the panel of antibodies as shown in 2.9.3.3.1. Cells were then measured on a BD FACS CANTO II and analysed on Flowjo (Treestar) Version 7.6.5 software, gating on $CD8^+$CFDA-SE^+ T cells. To assess those proliferating cells, a gate was placed on the cells with reduced CFDA-SE staining

i.e. proliferating cells, while excluding unproliferated, bright CFDA-SE labelled cells (FIGURE 14). Data were then presented using GraphPad Prism Version 4 Software.

2.8.4 BAYTRIL ADMINISTRATION

Baytril (containing the active antibiotic enrofloxacin) was diluted 1:250 in sterile, autoclaved tap water. Water was changed bi-weekly with fresh Baytril-containing water made each time. In addition water bottles were replaced every week.

2.8.5 INTRA-PERITONEAL GLUCOSE TOLERANCE TESTS (IPGTT)

Mice were fasted overnight for a period of up to 16 hours. At this point, fasting blood glucose was measured using a blood glucose monitor and all mice were weighed. Sterile glucose (1.5g/kg) was then injected intra-peritoneally into the mice. At time points, 0, 15, 30, 60 and 90 minutes post-injection, mice were bled from a superficial cheek vein and blood glucose tested. At the end of the experiment mice were culled by cervical dislocation. Data were then presented using GraphPad Prism Version 4 software.

2.9 REAGENT DETAILS

2.9.1 GENERAL REAGENT DETAILS

2.9.1.1 IN-HOUSE BUFFERS

BUFFER/SOLUTION NAME	CONSTITUENTS
BAYTRIL-CONTAINING WATER	1:250 BAYTRIL DILUTED IN AUTOCLAVED TAP WATER
BLOOD BUFFER	5% FBS, 0.02M EDTA, 0.08% SODIUM AZIDE IN 500ml 1xPBS
CARBONATE BUFFER (0.05M)	1 TABLET/100mls DEIONISED WATER (pH9.6)
DASATINIB SOLUTION	100nM DASATINIB IN TETRAMER WASH BUFFER
DIGEST BUFFER	0.05M TRIS (pH8), 0.02M EDTA, 2% SDS IN DEIONISED WATER
dNTPs	DEIONISED WATER CONTAINING 5mM OF EACH dNTP
ELISA WASH BUFFER	1xPBS in 0.05% TWEEN (pH7.2-7.4)
ETHANOL (70%)	70% ETHANOL IN MOLECULAR BIOLOGY GRADE STERILE WATER
ETHANOL (75%)	75% ETHANOL IN MOLECULAR BIOLOGY GRADE STERILE WATER
FACS BUFFER	5g/L BSA, 0.01% SODIUM AZIDE in 1xPBS (pH7.3 (+/-0.1))
FACS FIX	1% PARAFORMALDEHYDE IN 1xPBS (pH7.4)
GENE RULER (100bp)	0.083µg/µl DNA LADDER IN 1xLOADING DYE
HISTOLOGY WASH BUFFER	0.01% TRITON X-100 IN 1xPBS (pH7.3 (+/-0.2))
LYSIS BUFFER	1:10 DILUTION OF 10x FACS LYSING SOLUTION IN DEIONISED WATER
MACS BUFFER	2mM EDTA, 0.5% BSA in 1xPBS
ORANGE G (6x)	2.5mg/ml ORANGE G IN 30% GLYCEROL IN DEIONISED WATER
PB BUFFER (0.1M)	3 PARTS 0.1M MONO-BASIC SODIUM PHOSPHATE (NaH_2PO_4), 1 PART 0.1M DI-BASIC SODIUM PHOSPHATE (NA_2HPO_4) (pH7.6)
PLP	0.075M LYSINE, 1% PARAFORMALDEHYDE, IN 100ml OF 0.1M PB BUFFER. ONCE pH7.1, 0.212g SODIUM META-PERIODATE ADDED
PP BUFFER	0.015M HEPES in 1xHBSS (pH7.2)
REAGENT DILUENT	1% BSA in 1xPBS (pH7.2-7.4)
TAE (1x)	0.02M TRIS, 1mM EDTA (pH8), 0.4% ACETIC ACID IN DEIONISED WATER
TBT	50mM/L TRIS, 1% TWEEN in DEIONISED WATER (pH8.0)
TBT-BSA	50mM/L TRIS, 1% TWEEN, 1% BSA in DEIONISED WATER (pH8.0)
TETRAMER WASH BUFFER	2% FBS in 1xPBS

2.9.1.2 IN-HOUSE MEDIA

MEDIA NAME	CONSTITUENTS
FREEZING MEDIA	60% FBS, 30% RPMI 1640 MEDIA, 10% DIMETHYL SULFOXIDE (DMSO)
LB-AIX AGAR MEDIUM	32 AGAR CAPSULES/L (CONTAINING 10g TRYPTONE, 5g YEAST EXTRACT, 10g NaCl & 15g), 8µg/ml AMPICILLIN, 40µg/ml X-GAL
RPMI COMPLETE MEDIA	2mM L-GLUTAMINE, 5000 UNITS PENICILLIN, 0.1mg/ml STREPTOMYCIN, 5% FBS, 0.05mM 2-MERCAPTOETHANOL IN RPMI 1640 MEDIA
SERUM-FREE RPMI MEDIA	2mM L-GLUTAMINE, 5000 UNITS PENICILLIN, 0.1mg/ml STREPTOMYCIN, 0.05mM 2-MERCAPTOETHANOL IN RPMI 1640 MEDIA

2.9.1.3 OTHER CHEMICALS AND SOLUTIONS

REAGENT	SUPPLIER	ITEM NUMBER
ETHANOL	THERMO FISHER SCIENTIFIC	M/4400/17
DOUBLE DEIONISED WATER (MOLECULAR BIOLOGY GRADE)	THERMO FISHER SCIENTIFIC	BP2819-1
SODIUM CHLORIDE (99.85%)	ACROS ORGANICS	7647-14-5
100% GLACIAL ACETIC ACID	SIGMA-ALDRICH	27225
SODIUM DODECYL SULPHATE (SDS)	SIGMA-ALDRICH	L3771
EDTA	SIGMA-ALDRICH	E7889
1x PHOSPHATE BUFFERED SALINE (PBS)	LIFE TECHNOLOGIES	10010023
ISOPROPANOL	SIGMA-ALDRICH	I9516
HYCLONE TRYPAN BLUE	THERMO SCIENTIFIC	SV30084.01
PHENOL-CHLOROFORM ISOAMYL (PCI) ALCOHOL MIX	SIGMA-ALDRICH	77617
TRI-REAGENT	SIGMA-ALDRICH	T9424
1-BROMO-3-CHLOROPROPANE	SIGMA-ALDRICH	B62404
1M HEPES	GIBCO	15630-056
10xHBSS WITHOUT Ca^{2+}, Mg^{2+} & SODIUM BICARBONATE	SIGMA-ALDRICH	H4385
DMSO	SIGMA-ALDRICH	D2650
ISOPENTANE	SIGMA-ALDRICH	M32631
TRIS BASE	SIGMA-ALDRICH	252859
PARAFORMALDEHYDE	SIGMA-ALDRICH	P-6148
TWEEN® 20	FISHER SCIENTIFIC	BP337-500

2.9.1.4 REAGENT KITS

KIT	CONSTITUENTS	SUPPLIER	ITEM NUMBER
AVIDIN/BIOTIN BLOCKING KIT	AVIDIN SOLUTION, BIOTIN SOLUTION	VECTOR LABORATORIES	SP-2001
ALKALINE PHOSPHATASE SUBSTRATE KIT I	REAGENT 1, REAGENT 2, REAGENT 3	VECTOR LABORATORIES	SK-5100
CD8α⁺ T CELL ISOLATION KIT	$CD8\alpha^+$ T CELL BIOTIN-ANTIBODY COCKTAIL, ANTI-BIOTIN MICROBEADS	MACS MILTENYI BIOTEC	130-104-075
GEL EXTRACTION KIT	CLEAN UP COLUMNS, 2ml COLLECTION TUBES, WASH BUFFER, STABILISATION BUFFER, ELUTION BUFFER	QIAGEN	28706
µMACS mRNA ISOLATION KIT	OLIGO dT MICROBEADS, LYSIS/BINDING BUFFER, WASH BUFFER, ELUTION BUFFER, µMACS ISOLATION COLUMNS, LYSATECLEAR COLUMNS	MACS MILTENYI BIOTEC	130-075-201
MOUSE CCL4/MIP-1β DUOSET ELISA DEVELOPMENT SYSTEM	CAPTURE ANTIBODY, DETECTION ANTIBODY, STANDARD, STREPTAVIDIN-HRP	R&D SYSTEMS	DY451
NUCLEOSPIN GEL AND PCR CLEAN UP KIT	NUCLEOSPIN GEL CLEAN UP COLUMNS, 2ml COLLECTION TUBES, BUFFER NT1, BUFFER NT2, WASH BUFFER NT3, ELUTION BUFFER NE	MACHERY-NAGEL	740609.50
PKH-26 RED FLUORESCENT CELL LINKER KIT FOR GENERAL CELL MEMBRANE LABELING	PKH-26 DYE, DILUENT C	SIGMA-ALDRICH	PKH26GL-1KT
SMART™ RACE cDNA AMPLIFICATION KIT	5'CDS PRIMER (OLIGO dT PRIMER), REVERSE TRANSCRIPTASE, RNase INHIBITIOR, TRICINE BUFFER, dNTPs, 10x REACTION BUFFER, UNIVERSAL PRIMER MIX	CLONTECH LABORATORIES	634924
TOPO TA CLONING KIT FOR SEQUENCING, WITH ONE SHOT MAX EFFICIENCY DH5α-T1ᴿ *E.Coli*	pCR™4-TOPO® TA VECTOR, SALT SOLUTION, PCR BUFFER, dNTPS, CONTROL TEMPLATE, PRIMERS, STERILE WATER, ONE SHOT® CHEMICALLY COMPETENT *E. coli*, S.O.C MEDIUM	INVITROGEN	K4595-01

2.9.1.5 PEPTIDES AND PROTEINS

REAGENT	SUPPLIER	ITEM NUMBER
125-LABELLED RECOMBINANT HUMAN INSULIN	PERKIN-ELMER	NEX420050UC
ACTRAPID INSULIN	NOVO NORDISK	8-0201-01-203-3
INSULIN B15-23 PEPTIDE	GL BIOCHEM (SHANGHAI) LTD	068592

2.9.1.6 REAGENT TUBES

REAGENT	SUPPLIER	ITEM NUMBER
0.2ml PCR TUBES	THERMO SCIENTIFIC	AB-0337
1.2ml MICROTUBES	STAR LAB	I14127400
1.5ml MICROCENTRIFUGE	EPPENDORF	0030119460
1.8ml CRYOTUBE	THERMO SCIENTIFIC	375418
2ml MICROTUBE	SARSTEDT	72.609
5ml STERILE POLYSTYRENE ROUND-BOTTOMED FACS TUBES	BD	352054
15ml FALCON TUBE	VWR	734-0451
20ml STERILIN UNIVERSAL TUBE	GREINER BIO-ONE	201151
50ml CENTRIFUGE TUBE	SIGMA-ALDRICH	CLS430291

2.9.1.7 NEEDLES AND SYRINGES

REAGENT	SUPPLIER	ITEM NUMBER
1ml SYRINGE	BD	309628
10ml SYRINGE	BD	SYR188
20G NEEDLE	BD	305175
20ml SYRINGE	BD	301625
25G NEEDLE	BD	300600
27G NEEDLE	BD	305109
30G NEEDLE	BD	304000
MYJECTOR U100 INSULIN 1ml SYRINGE	TERUMO	BS=05M2713

2.9.1.8 GENERAL MISCELLANEOUS REAGENTS

REAGENT	SUPPLIER	ITEM NUMBER
20mm TISSUE CULTURE DISHES	FISHER SCIENTIFIC	08-772-E
300mm PLASTIC PASTEUR PIPETTE	FISHER SCIENTIFIC	12827625
40µm CELL FILTER	BD	352340
BOVINE SERUM ALBUMIN	FISCHER SCIENTIFIC	BP 1600-100
GLASS PASTEUR PIPETTE	FISHER SCIENTIFIC	12710756
LS COLUMNS	MACS MILTENYI BIOTEC	130-042-401
MS COLUMNS	MACS MILTENYI BIOTEC	130-042-201
PBS TABLETS (DULBECCO A)	OXOID	BR0014
STERILE DISPOSABLE SCALPEL	SWANN MORTON	05XX

2.9.1.9 GENERAL EQUIPMENT

REAGENT	SPECIFICATION	SUPPLIER
CENTRIFUGE	EPPENDORF CENTRIFUGE 5415R	EPPENDORF
HAEMOCYTOMETER	BRIGHT-LINE	HAUSSER SCIENTIFIC
TISSUE HOMOGENISER	LOOSE FIT	FISHER SCIENTIFIC
INCUBATOR	HERAcell 150i	THERMO SCIENTIFIC
MICROCENTRIFUGE	5415 R	EPPENDORF
VORTEX	VORTEX GENIE 2	SCIENTIFIC INDUSTRIES
WATER BATH	ISOTEMP 215	FISHER SCIENTIFIC

2.9.2 MOLECULAR REAGENTS AND EQUIPMENT

2.9.2.1 MOLECULAR REAGENTS

REAGENT	SUPPLIER	ITEM NUMBER
1Kb LADDER	THERMO SCIENTIFIC	SM0313
10mM dNTP MIX	LIFE TECHNOLOGIES	18427088
10x PCR BUFFER	SIGMA-ALDRICH	P2192
6x TRACKIT CYAN/ORANGE BUFFER	INVITROGEN	10482-028
96-WELL MICROAMP OPTICAL REACTION PLATES	APPLIED BIOSYSTEMS	4346906
ADVANTAGE 2 POLYMERASE MIX	CLONTECH LABORATORIES	639201
AMPICILLIN	INVITROGEN	11593-027
DNaseI	ROCHE	11284932001
dNTPs	THERMO FISHER SCIENTIFIC	10234683
ETHIDIUM BROMIDE	SIGMA ALDRICH	E1510
GENERULER™ 100BP DNA LADDER	THERMO FISHER SCIENTIFIC	11873953
GLYCEROL	SIGMA-ALDRICH	G5516
LB AGAR MEDIUM	MP	3002-231
LIBERASE TM RESEARCH GRADE	ROCHE	05401119001
MICROAMP OPTICAL ADHESIVE FILM	APPLIED BIOSYSTEMS	4311971
ORANGE G	SIGMA-ALDRICH	O-3756
PCR PLATES (STANDARD)	THERMO FISHER SCIENTIFIC	14-230-232
PCR PLATE STRIP CAPS	THERMO FISHER SCIENTIFIC	3418F
PRONASE	SIGMA-ALDRICH	P6911
PROTEINASE K	SIGMA-ALDRICH	P4850
qPCR PRIMERS	LIFE TECHNOLOGIES	N/A
RIBONUCLEASE A (FROM BOVINE PANCREAS)	SIGMA-ALDRICH	R4642
RNAlater	SIGMA-ALDRICH	R0901
RNAse OUT	INVITROGEN	10777019
SUPERSCRIPT II	INVITROGEN	18064-014
SUPERSCRIPT VILO MASTERMIX	INVITROGEN	11755050
SYBR GOLD	INVITROGEN	S11494
TAQ DNA POLYMERASE (FROM *THERMUS AQUATICUS*)	SIGMA-ALDRICH	D1806
TAQMAN UNIVERSAL MASTERMIX II, NO UNG (URACIL-N GLYCOSYLASE)	APPLIED BIOSYSTEMS	4440040
TRIS-EDTA BUFFER (TE BUFFER)	SIGMA-ALDRICH	93283
ULTRAPURE AGAROSE	INVITROGEN	16500-500
ULTRAPURE X-GAL (5-BROMO-4-CHLORO-3-INDOLYL-β-D-GALACTOSIDE)	INVITROGEN	15520-034
ZIRCONIUM BEADS	BIOSPEC	11079105z

2.9.2.2 MOLECULAR EQUIPMENT

REAGENT	SPECIFICATION	SUPPLIER
BEAD BEATER SHAKER	MINI	BIOSPEC PRODUCTS
GEL ELECTROPHERESIS POWER SUPPLY	POWER 608	FISHER SCIENTIFIC
GEL TANKS	DNA PLUS	USA SCIENTIFIC
GENE AMP PCR THERMOCYCLER	9700	APPLIED BIOSYSTEMS
HEATING BLOCKS	SBH130DC	STUART
MICROWAVE	MICROCHEF SM11	PROLINE
NANODROP SPECTROPHOTOMETER	ND-1000	NANODROP
PCR THERMAL CYCLER	PTC-200	MJ RESEARCH
qPCR MACHINE	Viia-7	APPLIED BIOSYSTEMS
SEQUENCING SYSTEM	GS JUNIOR TITANIUM SERIES 454	ROCHE
THERMOMIXER	COMFORT	EPPENDORF
UV ILLUMINATOR	BIODOC-IT IMAGING SYSTEM	UVP

2.9.2.3 POLYMERASE CHAIN REACTION REACTIONS, PROGRAMMES, MASTERMIXES AND PRIMERS

2.9.2.3.1 PCR GENOTYPING REQUIRED FOR EACH STRAIN

STRAIN	PCR REACTIONS REQUIRED
A22Cα$^{-/-}$	*TCRCα$^{-/-}$, TRAV8-1*01*
A22Cα$^{-/-}$PI1$^{-/-}$	*TCRCα$^{-/-}$, PI1, PI1$^{-/-}$, TRAV8-1*01*
A22Cα$^{-/-}$PI2^{tg}	*TCRCα$^{-/-}$, PI2^{tg}, TRAV8-1*01*
A22Cα$^{-/-}$PI2$^{-/-}$	*TCRCα$^{-/-}$, PI2/PI2$^{-/-}$, TRAV8-1*01*
A22Cα$^{-/-}$PI1$^{-/-}$PI2$^{-/-}$Y16A^{tg}	*TCRCα$^{-/-}$, TRAV8-1*01, PI1, PI1$^{-/-}$, PI2/PI2$^{-/-}$, Y16A^{tg}*
NOD*PI2^{tg}*	*PI2^{tg}*

2.9.2.3.2 PCR PROGRAMME LIST

PROGRAMME FOR PCR REACTIONS	PROGRAMME DETAILS		
	TEMPERATURE (°C)	TIME (SECONDS)	REPEATS
TRAV8*1-01 ***PI1$^{-/-}$*** ***PI2$^{-/-}$*** ***PI2^{tg}*** ***Y16A^{tg}***	94 94 55 72 72 8	180 60 60 60 300 600	} 35x
TCRCα$^{-/-}$ ***PI1***	94 94 60 72 72 8	180 45 45 45 600 600	} 35x
TCRβ CHAIN AMPLIFICATION	95 95 72 95 70 72 95 68 72 4	30 5 120 5 10 120 5 10 120 Forever	} 5x } 5x } 35x
COLONY PCR	95 57 68 4	30 30 180 Forever	} 35x
qPCR	50 95 95 60	120 600 15 60	} 40x

2.9.2.3.3 PCR MASTERMIX CONSTITUENTS

MASTERMIX NAME	CONSTITUENTS PER SAMPLE
cDNA	1µl SMARTer OLIGO, 2µl 5xRT BUFFER, 1µl DTT, 1µl RNAse OUT (RNAse INHIBITOR), 1µl SUPERSCRIPT II (REVERSE TRANSCRIPTASE)
COLONY PCR	250µl 10x BUFFER, 50µl dNTPS, 100µl MI3R PRIMER, 100µl MI3F PRIMER, 5µl ADVANTAGE 2 TAQ, 1995µl ddH_2O
qPCR MASTERMIX	45% TAQMAN UNIVERSAL MASTERMIX II, 10% PRIMERS (5% OF EACH PRIMER), 45% cDNA
TCRβ CHAIN	5µl 10x BUFFER, 10µl UNIVERSAL PRIMER MIX, 1µl MuMBC PRIMER, 1µl dNTPs, 1µl ADVAN TAQ 2, 19µl ddH_2O

2.9.2.3.4 GENOTYPING PRIMER SEQUENCES, BAND SIZE AND AGAROSE GEL REQUIREMENT

GENE OF INTEREST	PRIMER	PRIMER SEQUENCE (5' – 3')*	EXPECTED BAND SIZE	AGAROSE GEL (%)
TCRCα$^{-/-}$	F	GCG GGA TCC AGA ACC CAG AAC CTG CTG TG	900bp	3%
	R	GGC GAA TTC CTG AAC TGG GGT AGG TGG CG		
TRAV8*1-01	F	ATG CAC AGC CTC CTG GGG TTG TTG	650bp	1%
	R	AAC AGC ACC GAA AGC CAC A		
PI1	F	AGA CCT AGC ACC AGG CAA GTG T	970bp	1%
	R	TTG GGC AGG AAG CAG AAT TCC AGA		
PI1$^{-/-}$	F	GAG ATG CAA CCA GGT ATT	350bp	1%
	R	CTA TCA GGA CAT AGC GTT		
PI2/PI2$^{-/-}$	1	GGC AGA GAG GAG GTG CTT TG	PI2: 400bp PI2$^{-/-}$: 470bp	3%
	2	AGA AAA CCA GGG TAG TTA GC		
	3	ATT GAC CGT AAT GGG ATA GG		
PI2^{tg}	F	CCA CTG CCA AGG TCT GAA GGT CAC C	950bp	1%
	R	TTG TTA ATT CTG CCT CAG TCT GCG		
Y16A^{tg}	F	CTA TCT TCC AGG TCA ACT CG	318bp	3%
	R	ATC TAC AAT GCC ACG CTT CT		
	ITC F	CAA ATC TTG CTT GTC TGG TG	200bp	
	ITC R	GTC AGT CGA GTG CAC AGT TT		

*PRIMERS SYNTHESISED BY THERMO FISHER SCIENTIFIC

2.9.2.3.5 TCR CLONOTYPING AND BACTERIAL SEQUENCING PRIMER/OLIGO SEQUENCES

PRIMER NAME	SEQUENCE 5'-3'	FINAL CONCENTRATION	SUPPLIER
5'CDS PRIMER	$(T)_{25}$VN	10µM	CLONTECH LABORATORIES
SMARTer OLIGO	AAG CAG TGG TAT CAA CGC AGA GTA CXX XXX	12µM	CLONTECH LABORATORIES
UNIVERSAL PRIMER MIX	CTA ATA CGA CTC ACT ATA GGG CAA GCA GTG GTA TCA ACG CAG AGT CTA ATA CGA CTC ACT ATA GGG C	0.08µM 0.4µM	CLONTECH LABORATORIES
MuMBC PRIMER	TGG CTC AAA CAA GGA GAC CT	5µM	INVITROGEN
MI3F PRIMER	TTT TCC CAG TCA CGA C	1µM	INVITROGEN
MI3R PRIMER	CAG GAA ACA GCT ATG AC	1µM	INVITROGEN
16S V2 rRNA FORWARD PRIMER	CAT GCT GCC TCC CGT AGG AGT	0.24µM	SIGMA-ALDRICH
16S V2 rRNA REVERSE PRIMER	CAG AGT TTG ATC CTG GCT CAG	0.24µM	SIGMA-ALDRICH

2.9.2.3.6 qPCR PRIMER DETAILS

PRIMER NAME	ASSAY ID	AMPLICON LENGTH
GAPDH	Mm99999915_g1 VIC	107bp
INSULIN 1	Mm01950294_s1 FAM	80bp
INSULIN 2	Mm00731595_gH FAM	99bp

2.9.3 FLOW CYTOMETRY REAGENTS AND EQUIPMENT

2.9.3.1 FLOW CYTOMETRY REAGENTS

REAGENT	SUPPLIER	ITEM NUMBER
DASATINIB	AXON MEDCHEM	1392
LYSIS BUFFER (10x)	BD	349202
RNAlater	SIGMA-ALDRICH	R0901
SODIUM AZIDE	SIGMA ALDRICH	438456

2.9.3.2 NIH PROVIDED PEPTIDE:MHC BV421 TETRAMERS

PEPTIDE	SEQUENCE	MHC RESTRICTION
INSULIN B CHAIN 15-23	LYLVCGERG	H2-K^d
MINIMAL BINDING INSULIN B CHAIN 15-23	AYAAAAAAV*	H2-K^d

*This minimal binding insulin B15-23 peptide enables MHC loading due with Tyrosine at position 2 and provides optimal anchorage with Valine at position 9.

2.9.3.3 FLOW CYTOMETRY-BASED ANTIBODY STAINING PANELS

2.9.3.3.1 GENERALISED FLOW CYTOMETRY-BASED ANTIBODY STAINING PANELS

FLOW CYTOMETRY PANEL NAME	ANTIBODIES
GENOTYPING ANTIBODY PANEL	CD8 APC, CD19 PerCp/Cy5.5, TCRVα2 FITC, TCRVα3.2 FITC, TCRVα8.3 FITC, TCRVα11.1 FITC, TCRVα11.2 FITC*****, TCRVβ6 PE
TRBV PHENOTYPING ORIGINAL 5-COLOUR ANTIBODY PANEL	CD4 APC, CD8 PE/Cy7, VIABILITY DYE eFluor780, CD19 PE, TCRVβ3-14 FITC******
TRBV PHENOTYPING UPDATED 8-COLOUR ANTIBODY PANEL	CD8 BV510, CD4 PE/Cy7, VIABILITY DYE eFluor780 (WITH TCRVβ2-14, 17 AND CD19)*******
CFDA-SE** ANTIBODY PANEL**	CD4 BV421, CD8 V510, CD19 PerCp/Cy5.5, CD44 APC, CD69 PE/Cy7, VIABILITY DYE eFluor780

*****All TCRVα antibodies are added in order exclude any mice that lack the fixed *TCRCα*$^{-/-}$, as mice with the desired *TCRCα*$^{-/-}$ will have no staining for any TCRValpha and will have a small proportion of staining for TCRVβ6 (as the mice have endogenous TCRβ chains).

****** Individual TRBV FITC antibodies were added to each tube (12 tubes per tissue in total). All tubes received CD4, CD8, Live/Dead and CD19 antibodies.

******* The TRBV and CD19 antibodies were split between 4 panels, using a number of different fluorochromes (2.9.3.3.3 and 2.9.3.3.4)

******** CFDA-SE is detected in the FITC channel

2.9.3.3.2 TRBV NOMENCLATURE

CURRENT IMGT NOMENCLATURE	PREVIOUS NOMENCLATURE
TRBV1	TCRVβ2
TRBV2	TCRVβ4
TRBV3	TCRVβ16
TRBV4	TCRVβ10
TRBV5	TCRVβ1
TRBV12-1	TCRVβ5.2
TRBV12-2	TCRVβ5.1
TRBV12-3	TCRVβ5.3
TRBV13-1	TCRVβ8.3
TRBV13-2	TCRVβ8.2
TRBV13-3	TCRVβ8.1
TRBV14	TCRVβ13
TRBV15	TCRVβ12
TRBV16	TCRVβ11
TRBV17	TCRVβ9
TRBV19	TCRVβ6
TRBV20	TCRVβ15
TRBV21	TCRVβ19
TRBV23	TCRVβ20
TRBV24	TCRVβ17
TRBV26	TCRVβ3
TRBV29	TCRVβ7
TRBV30	TCRVβ18
TRBV31	TCRVβ14

2.9.3.3.3 STANDARD TRBV PHENOTYPING FLOW CYTOMETRY MODIFIED 8-COLOUR ANTIBODY PANEL

ANTIBODY	FLUOROCHROME	PANEL 1	PANEL 2	PANEL 3	PANEL 4
CD4	PE/Cy7	☑	☑	☑	☑
CD8	V500/V510	☑	☑	☑	☑
Live/Dead	eFluor 780	☑	☑	☑	☑
CD19	eFluor 450/BV421		☑		
TCRVβ2	AlexaFluor 647	☑			
TCRVβ3	PE	☑			
TCRVβ4	FITC		☑		
TCRVβ5.1, Vβ5.2	APC			☑	
TCRVβ6	APC		☑		
TCRVβ7	PE			☑	
TCRVβ8.1, Vβ8.2	FITC	☑			
TCRVβ9	eFluor 450	☑			
TCRVβ10b	PE		☑		
TCRVβ11	PerCp eFluor 710		☑		
TCRVβ12	PerCp eFluor 710			☑	
TCRVβ13	PerCp eFluor 710	☑			
TCRVβ14	FITC			☑	
TCRVβ17	FITC				☑

2.9.3.3.4 PEYER'S PATCH TRBV PHENOTYPING FLOW CYTOMETRY MODIFIED 8-COLOUR ANTIBODY PANEL

ANTIBODY	FLUOROCHROME	PANEL 1	PANEL 2	PANEL 3	PANEL 4	PANEL 5
CD4	eFluor 450				☑	☑
CD4	APC	☑	☑	☑		
CD8α	V510	☑	☑	☑	☑	☑
CD8β	PE/Cy7	☑	☑	☑	☑	☑
CD19	eFluor 450/BV421	☑		☑		
CD44	FITC	☑				
CD62L	PerCp/Cy5.5	☑				
Live/Dead	eFluor 780	☑	☑	☑	☑	☑
TCRVβ2	Alexa Fluor 647					☑
TCRVβ3	PE		☑			
TCRVβ4	FITC			☑		
TCRVβ5.1, Vβ5.2	APC				☑	
TCRVβ6	PE	☑				☑
TCRVβ7	PE				☑	☑
TCRVβ8.1, Vβ8.2	FITC		☑			
TCRVβ9	eFluor 450		☑			
TCRVβ10b	PE			☑		
TCRVβ11	PerCp eFluor 710			☑		
TCRVβ12	PerCp eFluor 710				☑	
TCRVβ13	PerCp eFluor 710		☑			
TCRVβ14	FITC				☑	
TCRVβ17	FITC					☑

2.9.3.3.5 PEPTIDE:MHC TETRAMER STAINING FLOW CYTOMETRY ANTIBODY PANELS

ANTIBODY	FLUOROCHROME	STANDARD TETRAMER STAIN 1	STANDARD TETRAMER STAIN 2	PEYER'S PATCH TETRAMER STAIN
CD4	APC		☑	
CD4	PE/Cy7	☑		
CD8α	FITC	☑	☑	
CD8α	BV510			☑
CD8β	PE/Cy7			☑
CD11b	APC	☑		
CD19	eFluor 450			☑
CD19	PerCp/Cy5.5	☑	☑	
CD44	FITC			☑
CD62L	PerCp/Cy5.5			☑
CD69	PE/Cy7		☑	
TCRVβ6	PE	☑	☑	☑
TETRAMER	APC			☑
TETRAMER	BV421	☑	☑	
Live/Dead	eFluor 780	☑	☑	☑

2.9.3.4 FLOW CYTOMETRY NON-T CELL RECEPTOR ANTIBODY LIST

ANTIBODY	CLONE	REACTIVITY	SUPPLIER	FLUOROCHROME	CONCENTRATION	DILUTION	USE
CD4	RM-5	Rat α-mouse	BioLegend	BV421	0.2mg/ml	1:400	C
			eBioscience	APC	0.2mg/ml	1:400	T, TR
				eFluor 450	0.2mg/ml	1:400	TR
				PE/Cy7	0.2mg/ml	1:400	T, TR
CD8a	53-6.7	Rat α-mouse	eBioscience	APC	0.2mg/ml	1:20	G
			BD	FITC	0.5mg/ml	1:200	T
				PE/Cy7	0.2mg/ml	1:200	TR
				V500	0.2mg/ml	1:200	TR
			BioLegend	V510	0.1mg/ml	1:200	C, T, TR
CD8β	YTS156.7.7	Rat α-mouse	BioLegend	PE/Cy7	0.2mg/ml	1:200	T, TR
CD11b	M1/70	Rat α-mouse	BD	APC	0.2mg/ml	1:200	T
CD19	6D5	Rat α-mouse	BioLegend	BV421	0.025mg/ml	1:200	TR
	1D3		eBioscience	eFluor 450	0.2mg/ml	1:200	T, TR
	6D5			PerCp/Cy5.5	0.2mg/ml	1:20	C, G, T
CD44	IM7	Rat α-mouse	BioLegend	APC	0.2mg/ml	1:200	C
				FITC	0.2mg/ml	1:200	T, TR
CD62L	MEL-14	Rat α-mouse	BioLegend	PerCp/Cy5.5	0.2mg/ml	1:200	T, TR
CD69	H1.2F3	Hamster α-mouse	BioLegend	PE/Cy7	0.2mg/ml	1:200	C, T
VIABILITY DYE	N/A	N/A	eBioscience	eFluor 780	N/A	1:1000	C, G, T, TR

USE: C = CFDA-SE staining, G = Genotyping, T = Tetramer staining, TR = T cell Receptor Repertoire staining

2.9.3.5 FLOW CYTOMETRY T CELL RECEPTOR ANTIBODY LIST

ANTIBODY	CLONE	REACTIVITY	SUPPLIER	FLUOROCHROME	CONCENTRATION	DILUTION	USE
TCRVα2	B20.1	Rat α-mouse	BioLegend	FITC	0.5mg/ml	1:100	G
TCRVα3.2	RR3-16	Rat α-mouse	BD	FITC	0.5mg/ml	1:100	G
TCRVα8.3	B21.14	Rat α-mouse	BioLegend	FITC	0.5mg/ml	1:100	G
TCRVα11.1, Vα11.2	RR8-1	Rat α-mouse	BD	FITC	0.5mg/ml	1:100	G
TCRVβ2	B20.6	Rat α-mouse	BioLegend	Alexa Fluor 647	0.5mg/ml	1:100	TR
TCRVβ3	KJ25	Hamster α-mouse	BD	FITC	0.5mg/ml	1:200	TR
				PE	0.2mg/ml	1:200	TR
TCRVβ4	KT4	Rat α-mouse	BD	FITC	0.5mg/ml	1:200	TR
TCRVβ5.1, Vβ5.2	MR9-4	Mouse α-mouse	BioLegend	APC	0.2mg/ml	1:200	TR
			BD	FITC	0.5mg/ml	1:200	TR
TCRVβ6	RR4-7	Rat α-mouse	eBioscience	APC	0.2mg/ml	1:200	TR
			BD	FITC	0.5mg/ml	1:200	TR
			BioLegend	PE	0.2mg/ml	1:200	G, T
TCRVβ7	TR310	Rat α-mouse	BD	FITC	0.5mg/ml	1:200	TR
				PE	0.2mg/ml	1:200	TR
TCRVβ8.1, Vβ8.2	KJ16-133	Rat α-mouse	eBioscience	FITC	0.5mg/ml	1:200	TR
TCRVβ9	MR10	Mouse α-mouse	eBioscience	eFluor 450	0.2mg/ml	1:200	TR
			BD	FITC	0.5mg/ml	1:200	TR
TCRVβ10b	B21.5	Rat α-mouse	BD	FITC	0.5mg/ml	1:200	TR
			eBioscience	PE	0.2mg/ml	1:200	TR
TCRVβ11	RR3-15	Rat α-mouse	BD	FITC	0.5mg/ml	1:200	TR
	123		eBioscience	PerCp eFluor 710	0.2mg/ml	1:200	TR
TCRVβ12	MR11-1	Mouse α-mouse	BD	FITC	0.5mg/ml	1:200	TR
			eBioscience	PerCp eFluor 710	0.2mg/ml	1:200	TR
TCRVβ13	MR12-3	Mouse α-mouse	BD	FITC	0.5mg/ml	1:200	TR
			eBioscience	PerCp eFluor 710	0.2mg/ml	1:200	TR
TCRVβ14	14-2	Rat α-mouse	BD	FITC	0.5mg/ml	1:200	TR
TCRVβ17	KJ23	Mouse α-mouse	BD	FITC	0.5mg/ml	1:100	TR

USE: G = Genotyping, T = Tetramer staining, TR = T cell Receptor Repertoire staining

2.9.4 TISSUE CULTURE REAGENTS AND EQUIPMENT

2.9.4.1 TISSUE CULTURE REAGENTS

REAGENT	SUPPLIER	ITEM NUMBER
2-MERCAPTOETHANOL (50mM)	LIFE TECHNOLOGIES	31350-010
6-WELL PLATE	THERMO SCIENTIFIC	140685
12-WELL PLATE	THERMO SCIENTIFIC	150628
24-WELL PLATE	THERMO SCIENTIFIC	142485
25cm^2 TISSUE CULTURE FLASK	THERMO SCIENTIFIC	156340
48-WELL PLATE	THERMO SCIENTIFIC	152640
75cm^2 TISSUE CULTURE FLASK	THERMO SCIENTIFIC	156472
96-WELL PLATE	THERMO SCIENTIFIC	163320
DEAE FILTER MAT	PERKIN ELMER	1450-522
FETAL BOVINE SERUM (FBS)	SIGMA-ALDRICH	F7524
GRANULOCYTE MACROPHAGE COLONY STIMULATING FACTOR (GM-CSF)	WONG LAB	N/A
IL-2 SUPERNATANT	WONG LAB	N/A
IL-7	R&D SYSTEMS	407-ML-005
L-GLUTAMINE (200mM)	LIFE TECHNOLOGIES	25030-024
LIPOPOLYSACCHARIDES (LPS) *E.coli* 026:B6	SIGMA-ALDRICH	L2654
MELTILEX FILTER WAX	PERKIN ELMER	1450-441
MR FROSTY FREEZING CONTAINER	THERMO SCIENTIFIC	5100-0001
NUNC CELL SCRAPER	THERMO SCIENTIFIC	179693
P815 CELLS	WONG LAB	N/A
PENICILLIN-STREPTOMYCIN	SIGMA-ALDRICH	P0781
RPMI 1640	GE HEALTHCARE	E15-039
THYMIDINE	PERKIN ELMER	NET027E001MC
TOPRO-3	LIFE TECHNOLOGIES	T3605

2.9.4.2 TISSUE CULTURE EQUIPMENT

REAGENT	SPECIFICATION	SUPPLIER
CELL HARVESTER	96 MACH	TOMTEC
CELL HARVESTER PUMPS	DYMAX 30	CHARLES AUSTEN PUMPS
HYBRIDIZATION OVEN	N/A	AMERSHAM LIFE SCIENCE
MICROBETA COUNTER	2450 MICROPLATE COUNTER	PERKIN ELMER

2.9.5 ELISA REAGENTS AND EQUIPMENT

2.9.5.1 ELISA REAGENTS

REAGENT	SUPPLIER	ITEM NUMBER
2N SULPHURIC ACID (H_2SO_4)	SIGMA-ALDRICH	35276
96-WELL MAXISORP NUNC IMMUNO PLATE	THERMO SCIENTIFIC	439454
BOVINE SERUM ALBUMIN, FRACTION V	SIGMA-ALDRICH	85040C
CAPTURE ANTIBODY: RAT ANTI-MOUSE IFN-γ	BD	551216
CARBONATE-BICARBONATE BUFFER CAPSULES	SIGMA-ALDRICH	C3041-100CAP
DETECTION ANTIBODY: BIOTIN RAT ANTI-MOUSE IFN-γ	BD	554410
STANDARD: RECOMBINANT MOUSE IFN-γ	BD	555138
STREPTAVIDIN-HORSE RADISH PEROXIDASE	INVITROGEN	SA1007
TMB SUBSTRATE REAGENT SET	BD	555214

2.9.5.2 ELISA EQUIPMENT

REAGENT	SPECIFICATION	SUPPLIER
ELISA PLATE READER	MULTISKAN SPECTRUM	THERMO LABORATORIES
ELISA PLATE WASHER	VP SERIES	KNF NEUBERGER

2.9.5.3 ELISA ANTIBODY AND STANDARD CONCENTRATIONS

ANTIBODY/STANDARD	INITIAL CONCENTRATION	DILUTION	DILUENT	FINAL CONCENTRATION
CAPTURE ANTIBODY: RAT ANTI-MOUSE MIP-1β	720µg/ml	1:180	1xPBS	4µg/ml
CAPTURE ANTIBODY: RAT ANTI-MOUSE IFN-γ	1mg/ml	1:500	CARBONATE BUFFER	2µg/ml
DETECTION ANTIBODY: BIOTINYLATED GOAT ANTI-MOUSE MIP-1β	144µg/ml	1:180	REAGENT DILUENT	0.8µg/ml
DETECTION ANTIBODY: BIOTIN RAT ANTI-MOUSE IFN-γ	0.5mg/ml	1:1000	REAGENT DILUENT	0.5µg/ml
STANDARD: RECOMBINANT MOUSE MIP-1β	0.11µg/ml	1:55	REAGENT DILUENT	0.002µg/ml*
STANDARD: RECOMBINANT MOUSE IFN-γ	1µg/ml	1:250	REAGENT DILUENT	0.004µg/ml**
STREPTAVIDIN-HORSE RADISH PEROXIDASE FOR MIP-1β	N/A	1:200	REAGENT DILUENT	N/A
STREPTAVIDIN-HORSE RADISH PEROXIDASE FOR IFN-γ	N/A	1:4000	REAGENT DILUENT	N/A

*MIP-1β ELISA standard was serially diluted 1:2 with Reagent Diluent to generate a standard curve with standard concentrations at 0.002µg/ml (2000pg/ml), 1000pg/ml, 500pg/ml, 250pg/ml, 125pg/ml, 62.5pg/ml and 31.25pg/ml.

** IFN-γ ELISA standard was serially diluted 1:2 with Reagent Diluent to generate a standard curve with standard concentrations at 0.004µg/ml (4000pg/ml), 2000pg/ml, 1000pg/ml, 500pg/ml, 250pg/ml, 125pg/ml and 62.5pg/ml.

2.9.6 HISTOLOGY REAGENTS AND EQUIPMENT

2.9.6.1 HISTOLOGY REAGENTS

REAGENT	SUPPLIER	ITEM NUMBER
COVERSLIPS (24x50mm)	VWR INTERNATIONAL	631-0147
DPX	SIGMA-ALDRICH	06522
HAEMATOXYLIN	VECTOR LABORATORIES	H-3401
HISTO-CLEAR	NATIONAL DIAGNOSTICS	HS-200
HYDROGEN PEROXIDE 30%	BDH LABORATORY SUPPLIES	285194F
L(+) LYSINE MONOHYDROCHLORIDE, 99%+	ACROS ORGANIC	125221000
LEVAMISOLE SOLUTION	VECTOR LABORATORIES	SP-5000
OCT EMBEDDING MATRIX	CELLPATH	KMA-0100-00A
PAP PEN (IMMEDGE PEN)	VECTOR LABORATORIES	H-4000
RAT SERUM	SIGMA-ALDRICH	R9759
SODIUM META-PERIODATE	THERMO SCIENTIFIC	20504
SODIUM PHOSPHATE DIBASIC	SIGMA-ALDRICH	S-0876
SODIUM PHOSPHATE MONOBASIC	SIGMA-ALDRICH	S-0751
SUCROSE	FISHER SCIENTIFIC	S/8600/60
SUPERFROST PLUS SLIDES	VWR	48311-703
TISSUE MOULDS	FISHER SCIENTIFIC	22-363-554
TRIS BUFFER pH7.4	BRISTOL UNIVERSITY	N/A
TRIS BUFFER pH8.4	BRISTOL UNIVERSITY	N/A
TRITON X-100	SIGMA-ALDRICH	X-100

2.9.6.2 HISTOLOGY EQUIPMENT

REAGENT	SPECIFICATION	SUPPLIER
CAMERA	AXIOVISION LE	ZEISS
CRYOSTAT	CRYOTOME FSE	THERMO ELECTRON CORPORATION
MICROSCOPE	BX51	OLYMPUS

2.9.6.3 HISTOLOGY BIOTINYLATED ANTIBODY LIST

ANTIBODY	CLONE	REACTIVITY	SUPPLIER	CONCENTRATION	DILUTION
CD4	GK1.5	Rat α-mouse	BioLegend	0.5mg/ml	1:10
CD8a	53-6.7	Rat α-mouse	BD	0.5mg/ml	1:10
CD45R/ B220	RA3-6B2	Rat α-mouse	BD	0.5mg/ml	1:30
RAT IgG2a λ ISOTYPE CONTROL	B39-4	N/A	BD	0.5mg/ml	1:10

2.9.7 INSULIN AUTOANTIBODY ASSAY REAGENTS AND EQUIPMENT

2.9.7.1 INSULIN AUTOANTIBODY ASSAY REAGENTS

REAGENT	SUPPLIER	ITEM NUMBER
4 FAST FLOW PROTEIN G SEPHAROSE	GE HEALTHCARE	17-0618-05
5M HYDROCHLORIC ACID	VWR	30018.360
96-WELL 1.2ml MEGABLOCK PLATES	SARSTEDT	82.1970.002
ETHANOLAMINE	SIGMA-ALDRICH	E9508

2.9.7.2 INSULIN AUTOANTIBODY ASSAY EQUIPMENT

REAGENT	SPECIFICATION	SUPPLIER
DIGITAL PLATE SHAKER	IKA MTS 2/4	IKA
GAMMA COUNTER	WALLAC WIZARD 1470 AUTOMATIC GAMMA COUNTER	PERKIN-ELMER
PLATE WASHER	HANDIWASH	DYNATECH

2.9.8 *IN VIVO* REAGENTS AND EQUIPMENT

2.9.8.1 IN VIVO REAGENTS

REAGENT	SUPPLIER	ITEM NUMBER
BAYTRIL	BAYER CORPORATION	BABAY14
BLOOD GLUCOSE STAT STRIPS	NOVA BIOMEDICAL	N/A
CpG 1826 OLIGONUCLEOTIDES	INVIVOGEN	tlrl-1826-1
D-(+)-GLUCOSE SOLUTION	SIGMA-ALDRICH	G8769
DIASTIX (URINE STRIPS)	BAYER CORPORATION	2804
INCOMPLETE FREUND'S ADJUVANT (IFA)	SIGMA-ALDRICH	F5506
STERILE SODIUM CHLORIDE 0.9% w/v (SALINE)	BAXTER HEALTHCARE LIMITED	FKE1323
VYBRANT® CFDA-SE CELL TRACER KIT	INVITROGEN	V12883

2.9.8.2 IN VIVO EQUIPMENT

REAGENT	SPECIFICATION	SUPPLIER
BLOOD GLUCOSE MONITOR	STAT STRIP GLUCOSE XPRESS METER	NOVA BIOMEDICAL
WEIGHING SCALES	CS SERIES	OHAUS

FIGURE 9: *TRAV8-1*01TRBJ9* (*A22*) NOD mice were crossed to *TCRCα*$^{-/-}$ (*Cα*$^{-/-}$) NOD mice in the first generation to generate *A22* and *Cα*$^{-/-}$ heterozygous mice (*A22*$^{+/-}$*Cα*$^{+/-}$). These mice were then fixed for the *TCRCα*$^{-/-}$ mutation through breeding *A22*$^{+/-}$*Cα*$^{+/-}$ and *TCRCα*$^{-/-}$ (*Cα*$^{-/-}$) NOD mice together. This produced *A22*$^{+/-}$ *Cα*$^{-/-}$ mice, which could then be bred in the third generation to produce 25% of mice homozygous for both *A22*$^{+/+}$ and *Cα*$^{-/-}$ (*A22*$^{+/+}$*Cα*$^{-/-}$). These mice could then be further crossed to produce offspring with 50% homozygosity for *A22*$^{+/+}$ and *Cα*$^{-/-}$. After successive generations, the *A22* and *Cα*$^{-/-}$ genes were homozygous.

FIGURE 9: GENERATION OF THE SINGLE CHAIN TRAV8-1*01 TRANSGENIC (*A22Cα$^{-/-}$*) NOD MICE

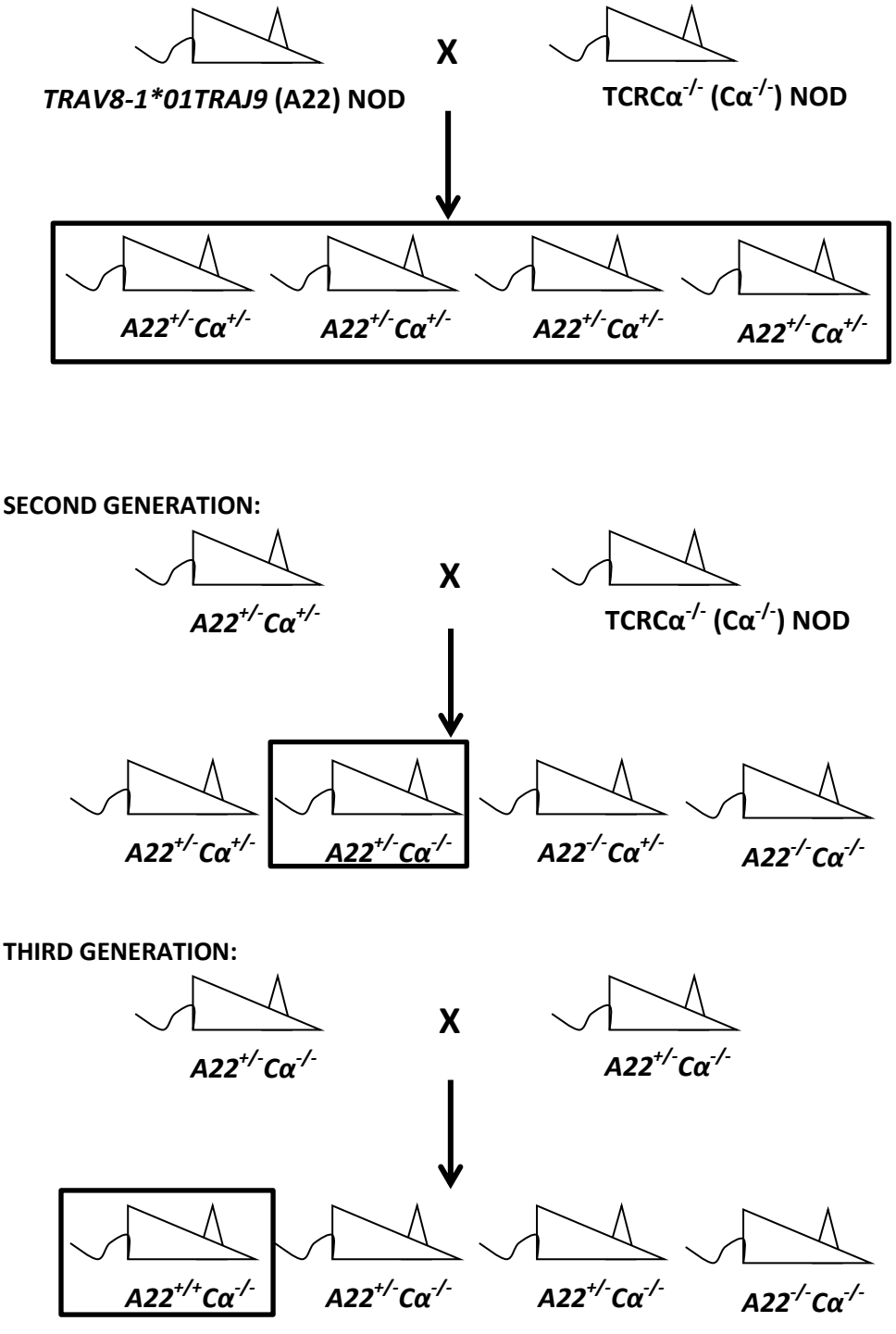

FIGURE 10: Single cell suspensions were prepared from thymi, spleen, pancreatic lymph nodes (PLN) and mesenteric lymph nodes (MLN). These cells were then stained with the TRBV phenotyping panels (see 2.9.3.3), fixed and measured on a BD FACS CANTO II. Data were analysed on Flowjo Version 7.6.5 software gating on cell populations for live single $CD8^+$ T cells as shown above. The same gating was used for all strains and tissues except the thymus, where only the single positive $CD4^+$ and $CD8^+$ T cells were gated.

FIGURE 10: GATING STRATEGY FOR LIVE SINGLE CELL CD8^{+} T CELLS FOR TRBV REPERTOIRE

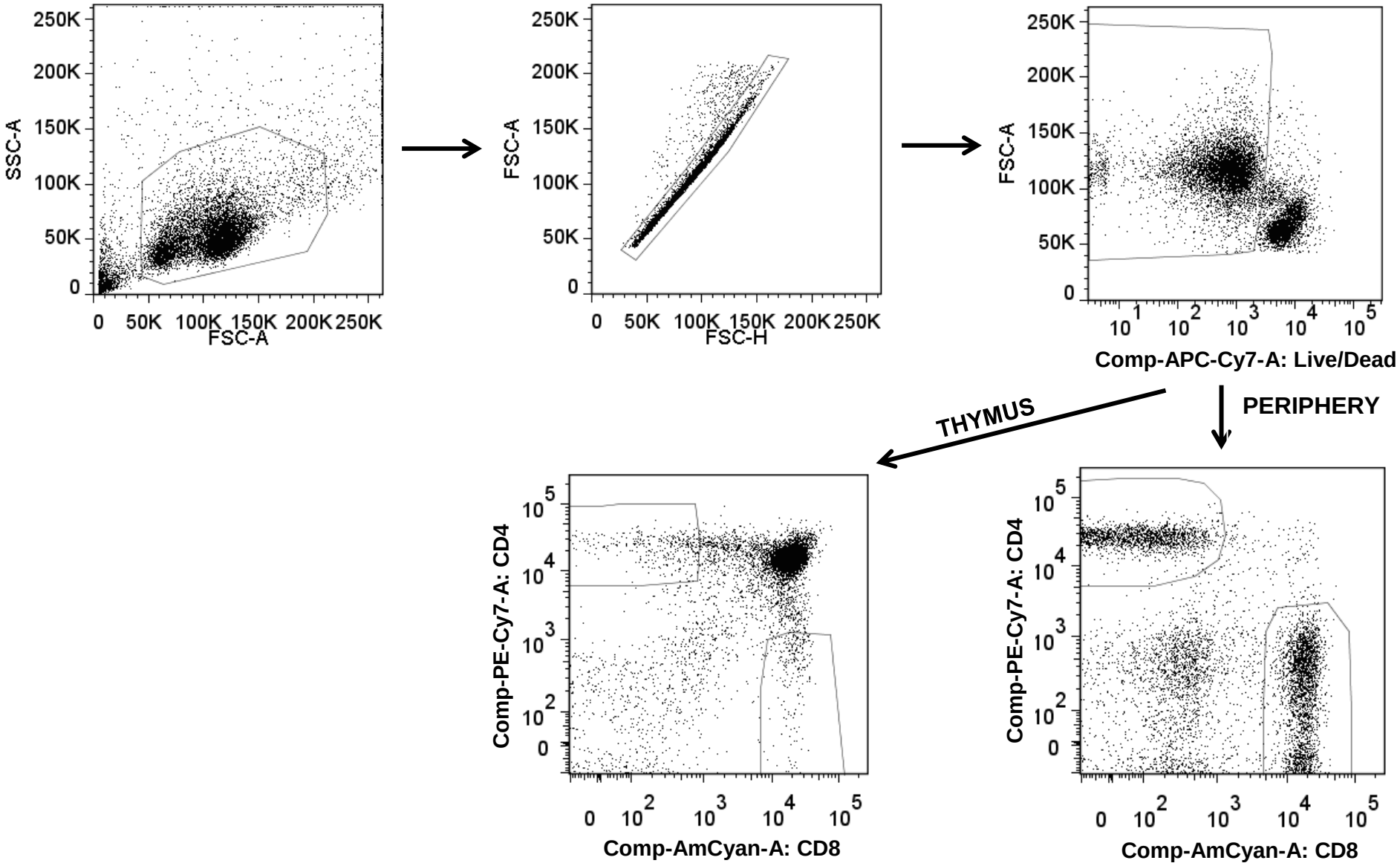

FIGURE 11**:** Single cell suspensions were prepared from thymi, spleen, pancreatic lymph nodes (PLN) and mesenteric lymph nodes (MLN). These cells were then stained with the TRBV phenotyping panels (see 2.9.3.3), fixed and measured on a BD FACS CANTO II. Data were analysed on Flowjo Version 7.6.5 software where cell populations were gated for live single $CD8^+$ T cells as shown (FIGURE 10). Within the $CD8^+$ T cell population, gates were assigned for each of the TCRVβ chains as shown above. The same gating was used for all strains and tissues.

FIGURE 11: GATING STRATEGY FOR CD8$^+$ TRBV REPERTOIRE

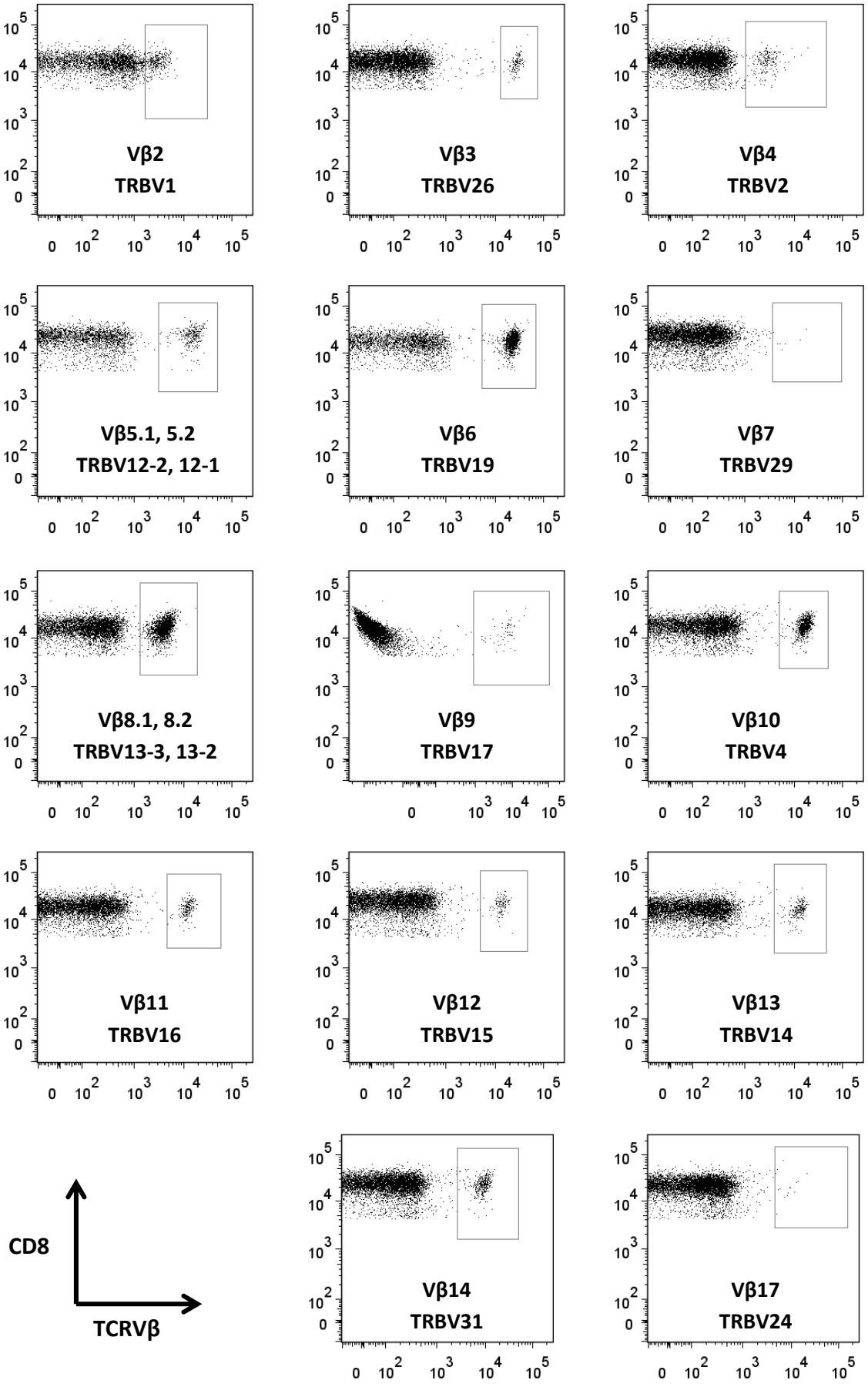

FIGURE 12: Cells were isolated from the thymus, spleen, PLN, MLN or Peyer's patches. Single cell suspensions were made and cells were counted. $1x10^6$ cells were then aliquotted and cells were pre-incubated with Dasatinib for 30 minutes at 37°C. Cells were then washed and resuspended in Tetramer Wash Buffer containing 1µg of peptide:MHC tetramer. Cells were stained separately for Insulin B15-23:$H2K^d$ tetramers and for the minimally binding peptide control AYAAAAAAV:$H2K^d$ tetramer and incubated for 15 minutes at 37°C. Cells were then washed and stained for monoclonal antibodies to CD4, CD8, CD11b, CD19 and viable cells for 30 minutes at 4°C, followed by cell fixation for a further 30 minutes at 4°C. Cells were then washed and resuspended in Tetramer Wash Buffer and were measured on a BD FACS CANTO II. Data were subsequently analysed using Flowjo Version 7.6.5 software (Treestar) using the gating strategy shown to obtain live single cell $CD8^+CD19^-CD11b^-CD4^-Tetramer^+$ T cells, with the Tetramer gate based on the G9C8 positive control. The minimally binding tetramer control was then deducted from the raw tetramer stain. Data shown are from a single male *A22Cα*$^{-/-}$*PI2*$^{-/-}$ mouse PLN, however, it is representative of all mice and tissues stained.

FIGURE 12: GATING STRATEGY FOR LIVE SINGLE CELL $CD8^{+}CD19^{-}CD11b^{-}CD4^{-}$ $TETRAMER^{+}$ T CELLS FOR IDENTIFYING INSULIN B15-23 REACTIVE CELLS

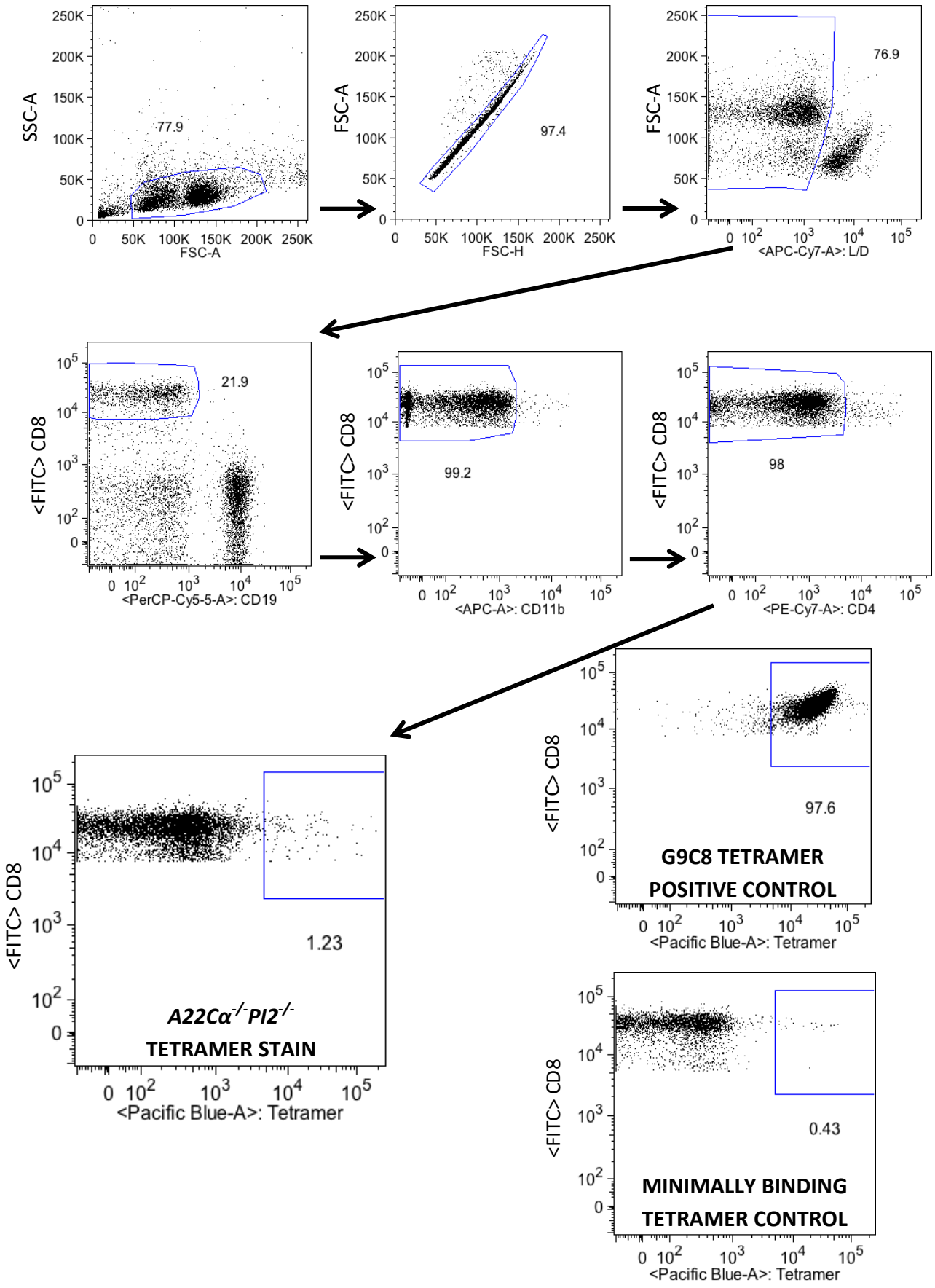

FIGURE 13: Splenocytes were harvested from mice and a single cell suspension was made. The cell suspension was then stained with Insulin B15-23 tetramer (13A) and/or monoclonal antibodies to CD4, CD8, CD11b, CD19, TCRVβ6 (TRBV19) and a viability marker (13A and 13B). 13A shows the gating for the tetramer-based flow cytometry sorting on live single $CD8^{+}CD19^{-}CD11b^{-}CD4^{-}Tetramer^{+}$ T cells into RNAlater from a male *A22Cα*$^{-/-}$*PI1*$^{-/-}$*PI2*$^{-/-}$*Y16A*^{tg} mouse PLN. 13B has the same gating strategy as 13A, whereby cells were gated on $CD8^{+}CD19^{-}CD11b^{-}CD4^{-}$, however, instead of tetramer, $TCRV\beta6^{+}$ T cells were gated and sorted into RPMI complete media. Sample 13B derives from a male *A22Cα*$^{-/-}$ mouse PLN. Both gating strategies are representative of all tetramer and antibody flow cytometry-based cell sorting done.

FIGURE 13: FLOW CYTOMETRY BASED TETRAMER/TCRVβ ANTIBODY SORTING STRATEGY

A

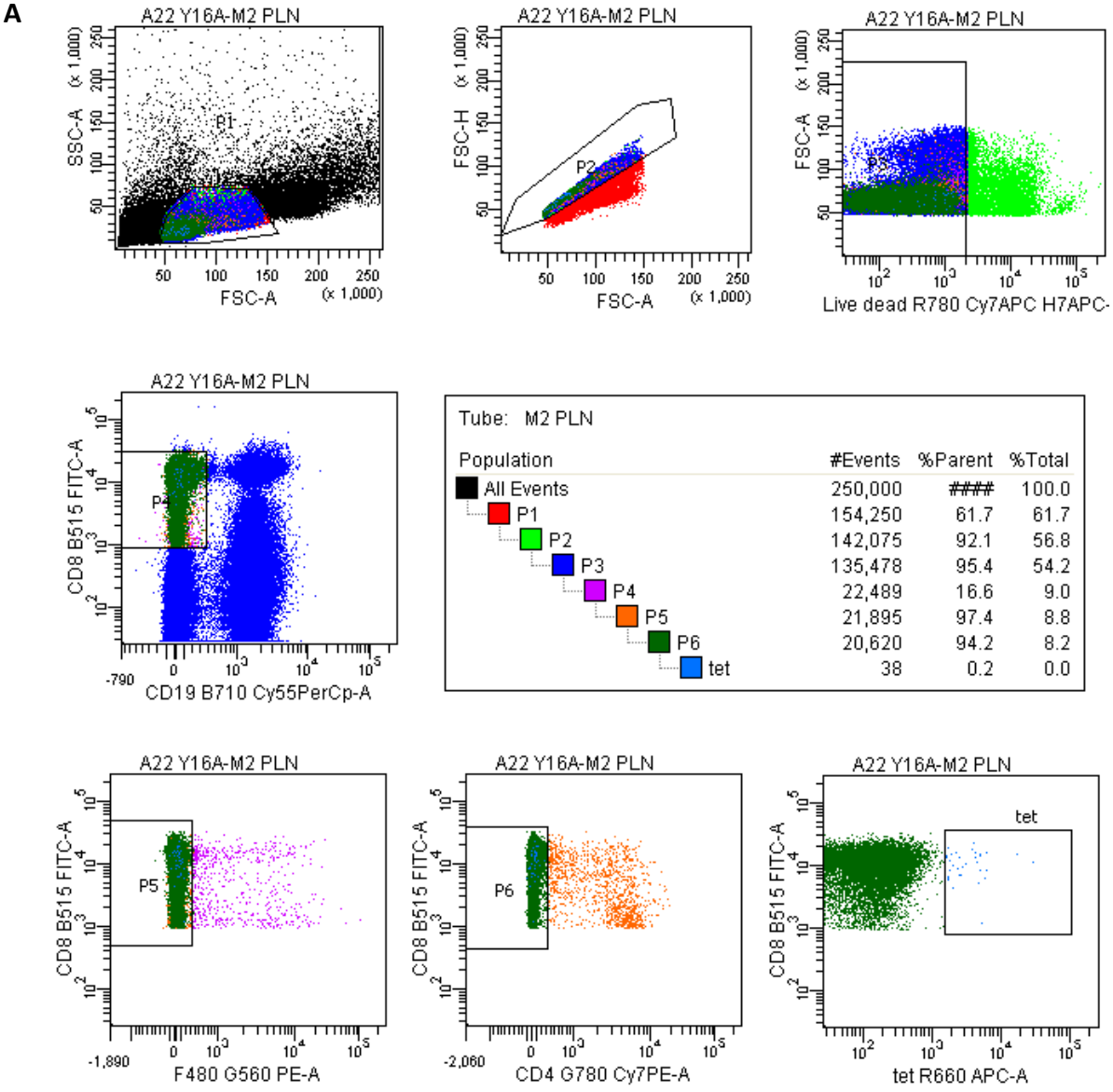

B

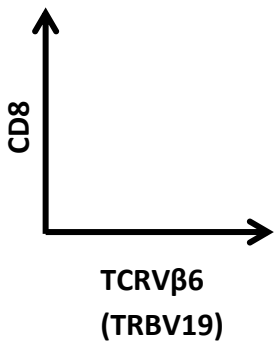

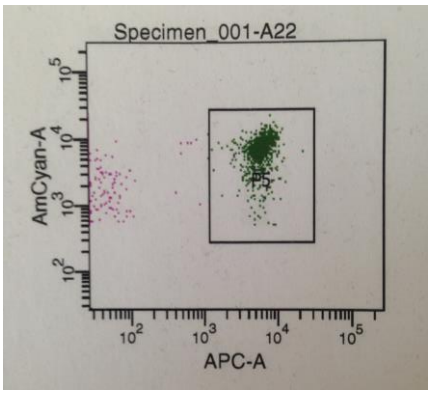

FIGURE 14: Cells were isolated from the thymus, spleen, PLN or MLN. Single cell suspensions were made and cells were counted. $CD8^+$ T cells were then isolated from the tissues using a MACS Miltenyi $CD8^+$ Isolation kit. $CD8^+$ T cells were then labelled with CFDA-SE at 37°C and washed to remove excess dye. Cells were then counted and resuspended at 10-20x10^6 per 200µl and transferred intravenously into NOD*PI2*^{tg} mice. Tissues were harvested four days later, single cell suspensions were made and cells were stained by monoclonal antibodies against CD4, CD8, CD19, CD44, CD69 and a viability marker for 30 minutes at 4°C. Cells were then fixed and washed prior to measurement on a BD FACS CANTO II. Post-measurement, cells were analysed as outlined, gating live single cell $CD8^+CD4^-$ CFDA-SE^+ T cells. Cells were then gated for proliferating CFDA-SE^+ T cells (i.e. those with reduced CFDA staining).

FIGURE 14: GATING STRATEGY FOR CFDA-SE LABELLED CD8$^+$ T CELL PROLIFERATION ASSAYS

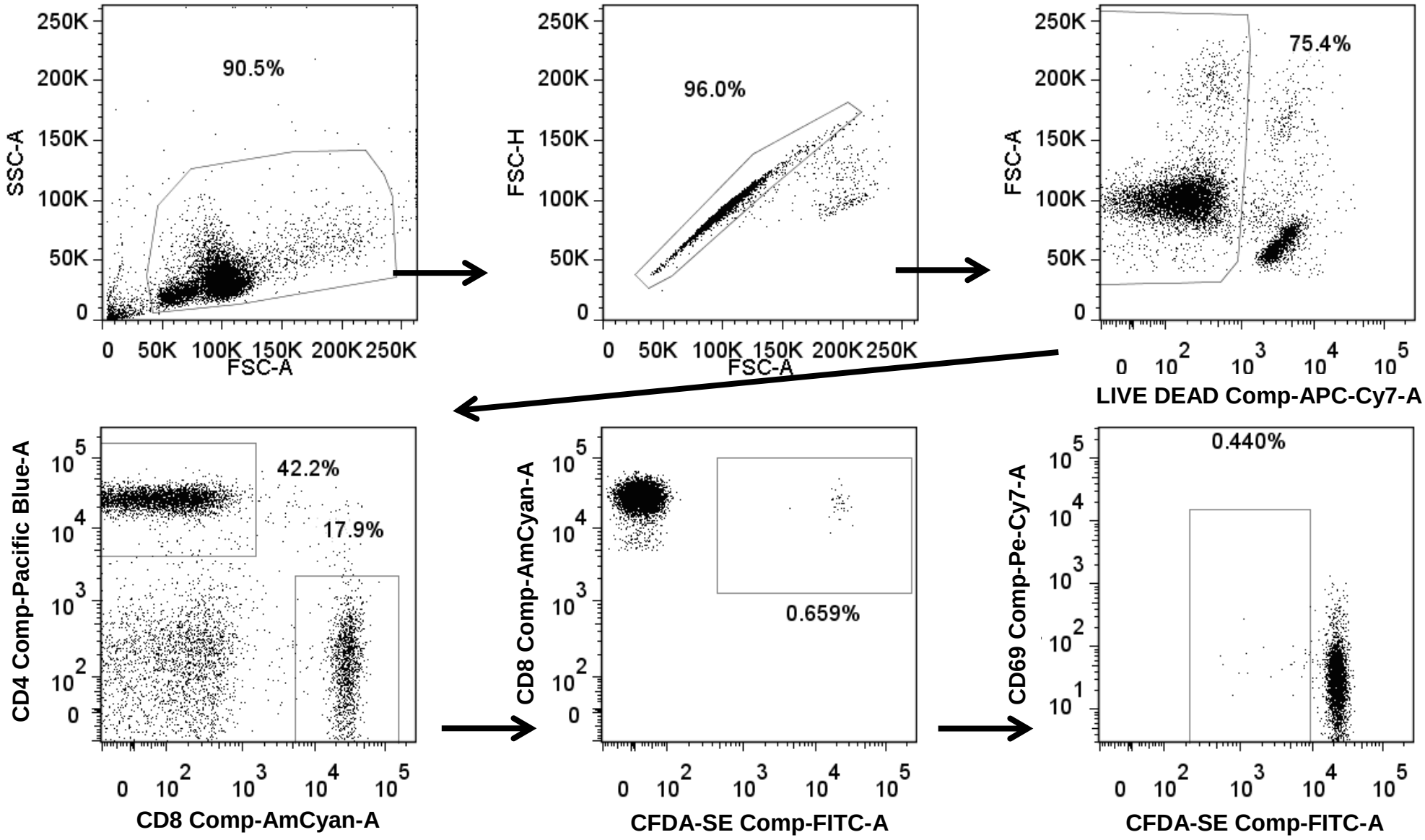

CHAPTER 3: ANALYSIS OF THE T CELL RECEPTOR VARIABLE BETA CHAIN REPERTOIRE OF INSULIN B15-23 REACTIVE CD8$^+$ T CELLS IN SINGLE CHAIN TRANSGENIC TRAV8-1*01TRAJ9 NOD MICE EXPRESSING VARYING LEVELS OF PROINSULIN 1 AND 2

3.1 INVESTIGATION OF THE T CELL VARIABLE BETA CHAIN RECEPTOR REPERTOIRE IN SINGLE CHAIN TRANSGENIC TRAV8-1*01TRAJ9 NOD MICE EXPRESSING VARIABLE LEVELS OF PROINSULIN

3.1.1 RATIONALE, AIMS & HYPOTHESIS

The T cell receptor (TCR) repertoire is initially selected during thymic selection, with those TCRαβ chains that are able to strongly recognise tissue-restricted antigens being negatively selected. Furthermore, TCR repertoire selection also continues extra-thymically. There are many factors that are able to preferentially select specific TCR-expressing T cell responses and these apply to T cell responses to foreign antigens, tumour antigens and self-antigens. The main pressure on peripheral TCR repertoire is antigen expression. More specifically, the TCR repertoire is changed through the presence of antigen, preferentially selecting for the appropriate T cells to respond to the antigen (Cose et al., 1995, Hayashi et al., 1995, Verdaguer et al., 1996, Wong et al., 2007b, Fanning et al., 2013, Koning et al., 2013, Sun et al., 2014), or promoting cross-reactive T cell responses (Smith et al., 2014, Nguyen et al., 2014). Furthermore, how the peptide is presented is also important (Messaoudi et al., 2002, Gras et al., 2009). In addition to antigen expression, peripheral regulation can also affect the TCR repertoire, for example through deletional tolerance (Fairchild et al., 1991) or through TCR repertoire biased regulatory T cell expansion (Quinn et al., 2001a, Sainz-Perez et al., 2012, Myers et al., 2013, Okuno et al., 2013). Interestingly, regulatory T cells have different TCR repertoires compared to conventional T cells, suggesting that conventional T cells are not converted into Tregs (Wong et al., 2007a, Hindley et al., 2011, Relland et al., 2012). There are also regional TCR repertoire differences found in the T cell populations (Weidmann et al., 1992, Halapi et al., 1993, Emerson et al., 2013, Sherwood et al., 2013). While some studies have shown

preferential TCR repertoire bias in the TCRα chain (Davies et al., 1991, Kobayashi et al., 2008), others have shown it is the TCRβ chain (Berschick et al., 1993, Cose et al., 1995, Hayashi et al., 1995, DiLorenzo et al., 1998, Quinn et al., 2001a), while some studies have shown no/little TCR repertoire bias (Lund et al., 1990, Olive et al., 1991, Sioud et al., 1992, Davies et al., 1992, Mathoulin et al., 1993, Parish et al., 1993). These differences are likely to have arisen due to the restricted availability of anti-TCR chain antibodies, particularly to the TCRVα chain (currently there are only 4 available antibodies), as well as the fact that TCR repertoire bias has been studied globally instead of investigating the antigen-specific T cell populations. However, in order to maintain health, a diverse TCR repertoire is important, enabling T cells to stimulate a pathogenic or protective immune response as required (Ferreira et al., 2009, Manuel et al., 2012). This TCR diversity is affected by age (Naylor et al., 2005, Pfister et al., 2006, Yager et al., 2008, Rudd et al., 2011, Vong et al., 2011, Britanova et al., 2014) and can make immunisations difficult, particularly in the elderly. However, some therapies have been developed using anti-TCRVβ monoclonal antibodies leading to protection from disease or disease reduction e.g. collagen-induced arthritis (Osman et al., 1993), experimental autoimmune encephalomyelitis (EAE) (Zaller et al., 1990) and autoimmune diabetes (Edouard et al., 1993, Liu et al., 2012). Therefore, understanding how this TCR repertoire develops is important, not only for developing successful immunisations but it also enables investigators to identify factors that affect the promotion or reduction of T cell populations, based on their TCR, and how they impact disease survival or progression (reviewed by (Miles et al., 2011).

As discussed earlier, antigen expression and presentation dictates the T cells, expressing a specific TCR, that are recruited during an immune response. In some studies, foreign antigens were expressed as self-antigens under the rat insulin promoter (Oldstone et al., 1991, Ohashi et al., 1991, Kurts et al., 1997). These studies highlighted the fact that auto-reactive $CD8^+$ T cells were still selected, regardless of thymic antigen expression. However, the level of antigen expressed in the thymus dictated the avidity of the T cells selected (von Herrath et al., 1994,

Zehn and Bevan, 2006). Interestingly, these auto-reactive $CD8^+$ T cells were unable to cause disease unless additional antigen was administered e.g. by infection in both polyclonal mice (Oldstone et al., 1991, Ohashi et al., 1991) and single TCRβ (Vβ5.2/TRBV12-1) transgenic mice (Dillon et al., 1994, Zehn and Bevan, 2006). These studies utilised a foreign antigen, expressed as a self-antigen, and they may not be representative of T cell responses in a natural self-antigen system such as the role of proinsulin expression on the development of an auto-reactive $CD8^+$ TCR repertoire.

In autoimmune diabetes, it has been shown that numerous TRBV chains may be important in disease, although many of these studies were done simply using flow cytometric methods and were non-antigen specific. However, with respect to insulin autoimmunity it has been shown that for insulin B9-23 reactive $CD4^+$ T cells, the TCRα chain (TRAV5D-4*04) was shown to be important for conserving insulin autoimmunity, while able to pair to a number of TCRβ chains (Kobayashi et al., 2008, Zhang et al., 2009). This suggested a more permissive role for the TCRβ chain. However, it is unknown whether insulin-reactive $CD8^+$ T cells show any TCR repertoire bias, with the only Insulin B15-23 reactive T cell known to utilise TRAV8-1*01TRAJ9 and TRBV19*01TRBD1-1TRBJ2-3 (previously named TCRVα15Jα8 and TCRVβ6Dβ1.1Jβ2.3 (Wong et al., 1996) and later, the TCRα chain was re-designated TCRVα18S1 (Wong et al., 1999)).

In order to investigate the role of proinsulin expression in shaping the auto-reactive $CD8^+$ TCR repertoire, single chain transgenic mice were generated whereby the TCRα chain was restricted to the sole use of TRAV8-1*01TRAJ9 from the Insulin B15-23 reactive T cell, G9C8. As the TCRα chain in $CD4^+$ Insulin B9-23 reactive T cells dictated the development of insulin autoimmunity we chose to restrict the TCRα chain, allowing any endogenous TCRβ chains to pair (Kobayashi et al., 2008, Zhang et al., 2009). In addition, restriction of the TCRα chain also enabled us, in the first instance, to investigate the TCR repertoire by flow cytometry by using anti-TRBV antibodies, enabling us to identify the majority of TRBV chains (14 chains out of a total of 24).

HYPOTHESIS:

Proinsulin expression will specifically alter the insulin-reactive $CD8^+$ TCR repertoire, thus affecting the recognition of p:MHC, and the development of Insulin autoimmunity, including the ability to develop spontaneous autoimmune diabetes.

AIMS:

1. To investigate the total $CD8^+$ T cell TRBV chain repertoire in single TRAV8-1*01TRAJ9 chain transgenic mice aged 4-7 weeks, 8-10 weeks and 11-16 weeks in the context of different levels of proinsulin 1 and 2 expression within the thymus and the periphery.
2. To determine the frequency, the diabetogenicity and TCRβ chain repertoire of the Insulin B15-23 reactive $CD8^+$ T cells in these mice expressing various levels of proinsulin 1 and 2

The mice to be used for this investigation, including simplified names, which will be used throughout this work, are summarised in TABLE 5 below.

TABLE 5: STRAIN NAMES AND INSULIN EXPRESSION OF MICE TO BE STUDIED

NOD STRAIN NAME	STRAIN SIMPLIFIED NAME	PROINSULIN 1	PROINSULIN 2
TRAV8-1*01TRAJ9Cα$^{-/-}$ PI1$^{+/+}$PI2$^{+/+}$	*A22Cα$^{-/-}$*	++	++
TRAV8-1*01TRAJ9Cα$^{-/-}$ PI1$^{+/+}$PI2$^{+/+}$PI2^{tg}	*A22Cα$^{-/-}$PI2^{tg}*	++	+++
#TRAV8-1*01TRAJ9Cα$^{-/-}$ PI1$^{-/-}$PI2$^{+/+}$	*A22Cα$^{-/-}$PI1$^{-/-}$*	--	++
TRAV8-1*01TRAJ9Cα$^{-/-}$ PI1$^{+/+}$PI2$^{-/-}$	*A22Cα$^{-/-}$PI2$^{-/-}$*	++	--
TRAV8-1*01TRAJ9Cα$^{-/-}$ PI1$^{-/-}$PI2$^{-/-}$Y16A^{tg}	*A22Cα$^{-/-}$PI1$^{-/-}$PI2$^{-/-}$ Y16A^{tg}*	--	--

#Note: The data generated for the *TRAV8-1*01TRAJ9Cα$^{-/-}$PI1$^{-/-}$PI2$^{+/+}$* (*A22Cα$^{-/-}$PI1$^{-/-}$*) was generated in part by Miss Amy Phillips, an undergraduate, under my supervision. The designation A22 for the TCRα chain related to the selection of the transgenic mouse line 22 from a number of TCRα chain transgenic mice that had been generated.

3.2 PROINSULIN EXPRESSION IN POLYCLONAL NOD MICE

During the development of the mice expressing varying levels of proinsulin, it was important to not only have genetic typing results but also to quantify the level of proinsulin expression. This provided useful data to confirm that the model was valid for further assessment as well as identifying any differences between the genders. Polyclonal NOD mice were used as a baseline for proinsulin expression.

3.2.1 PROINSULIN 1 AND 2 ARE EXPRESSED IN THE THYMUS AND PLN

NOD mice (both males and females) were investigated for the expression of proinsulin 1 and 2 within the thymus and the PLN. FIGURE 15 shows that the control GAPDH gene was present in all samples, with the largest amplification noted in the thymus, then the PLN and finally the islets. In all cases, both males and females were similar (thymus GAPDH amplification seen between cycles 20-22 and PLN GAPDH between cycles 26-28) to each other suggesting similar amounts of RNA were present in the samples. In regard to proinsulin 1 and 2 expression, the islets (positive control) highly expressed both proinsulin 1 and 2. The NOD mouse PLNs also expressed proinsulin 1 and 2; however, there was greater amplification of both proinsulin 1 and 2 in the males than in the female NOD PLN. As for thymus, proinsulin 1 was just detectable, with higher levels of proinsulin 2 noted. In both males and females, the thymic proinsulin expression was similar. This data derived from pooled tissues from 8-9 mice; however it is only representative of a single experiment, which could not be repeated at the point of writing this report, due to time restrictions.

FIGURE 15: Thymus and PLN were taken from polyclonal NOD male and female mice, separately, at 8 weeks of age (n=8-9). Thymus and PLN samples were homogenised/teased open to create a single cell suspension prior to enzymatic digestion at 37°C using Liberase/DNAse I enzymes. Post-digestion, cells were then depleted of $CD45^+$ cells using a Miltenyi MACS kit and column (purity >99%) and frozen overnight in Tri Reagent at -80°C. The cells were defrosted and RNA was extracted. 2µg RNA was then used to make cDNA using Superscript VILO mastermix (Life Technologies). cDNA was then amplified for proinsulin 1, 2 and GAPDH using gene-specific primers and a Taqman mastermix (Life Technologies) on a Viia7 Real-Time PCR machine and analysed using ExpressionSuite software version 1.0.3. F=female, M=male. Control has everything except DNA.

FIGURE 15: PROINSULIN 1 AND 2 EXPRESSION WITHIN POLYCLONAL NOD ISLETS, THYMUS AND PANCREATIC LYMPH NODES (PLN) AS ASSESSED BY qPCR

A: GAPDH

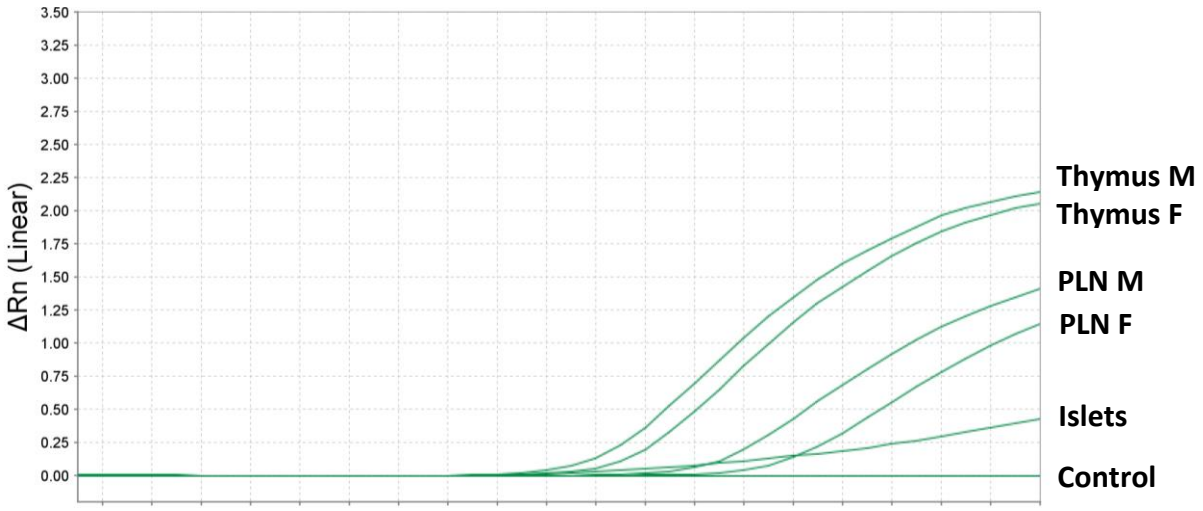

B: PROINSULIN 1

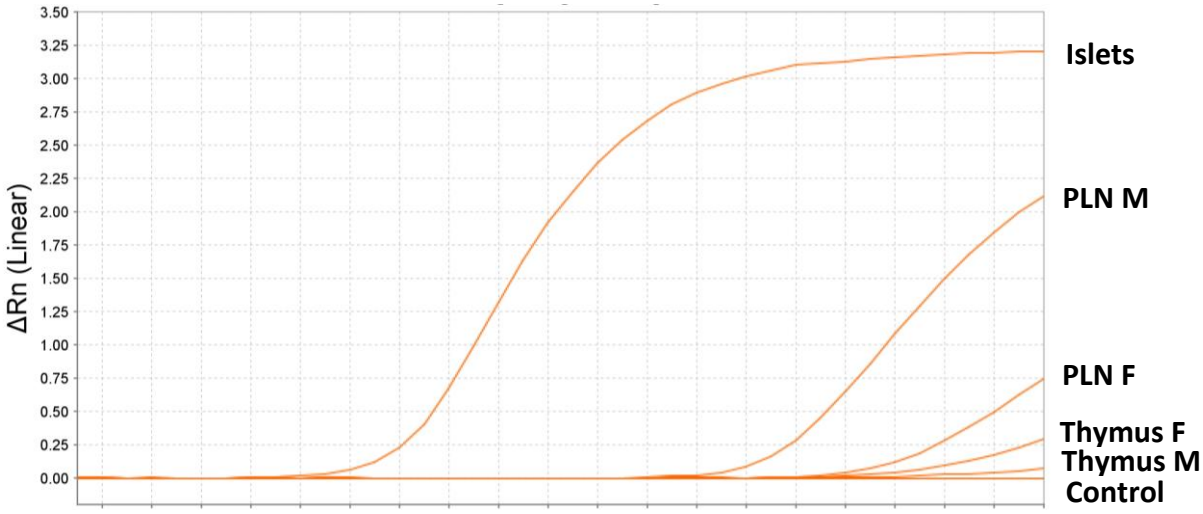

C: PROINSULIN 2

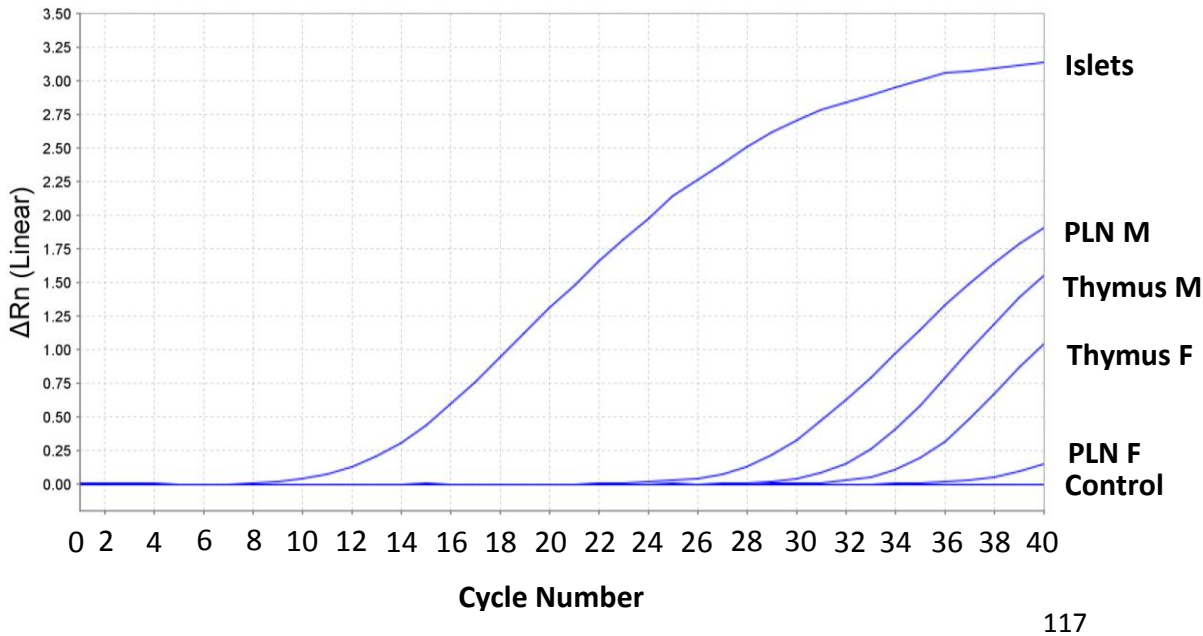

3.3 THE EFFECT OF PROINSULIN EXPRESSION ON CELL POPULATIONS

After confirmation of the models and documentation of the proinsulin expression levels, the next question to address was the role that proinsulin expression may have on the total population of T cells present in these mice. Therefore, lymphoid tissues were harvested and counted with single cell suspensions from the various lymphoid tissues analysed by flow cytometry for their $CD4^+$ and $CD8^+$ T cell populations.

3.3.1 TOTAL CELL NUMBER IS INDEPENDENT OF PROINSULIN EXPRESSION

Total thymi and splenocyte cells from mice aged 4-7 weeks, 8-10 weeks (see appendix) and 11-16 weeks were counted. The data in FIGURE 16 shows that at 4-7 weeks, the *A22Cα*$^{-/-}$ mice had fewer cells in the spleen compared to A22*Cα*$^{-/-}$*PI1*$^{-/-}$*PI2*$^{-/-}$*Y16A*^{tg} mice; however by 11-16 weeks there were no differences seen between the strains. In addition, there were a greater number of cells in the thymus of the NOD mice than in the TCR-restricted counterparts (apart from those over-expressing Proinsulin 2) by 11-16 weeks. Furthermore, all strains showed a significant change in thymic ($p=<0.01$) and splenic cell number ($p=<0.01$) with age, except for the spleen cell numbers for the *A22Cα*$^{-/-}$*PI2*^{tg} and the A22*Cα*$^{-/-}$*PI1*$^{-/-}$*PI2*$^{-/-}$*Y16A*^{tg} mice.

FIGURE 16: Thymocyte and splenocyte cells were harvested and homogenised. The red blood cells were lysed in the splenocyte populations and resuspended in 10mls FACS Buffer for counting. Cell number was determined through exclusion of non-viable cells by Trypan blue using a haemocytometer. Data were analysed by ANOVA using R software. Data were shown to be significant (**) if it reached the p=<0.01 level; Thymocytes at 11-16 weeks: NOD vs *A22Cα*$^{-/-}$ p=0.0002996, NOD vs *A22Cα*$^{-/-}$*PI1*$^{-/-}$ p=0.0000518, NOD vs *A22Cα*$^{-/-}$*PI2*$^{-/-}$ p=0.0015271, NOD vs *A22Cα*$^{-/-}$*PI1*$^{-/-}$*PI2*$^{-/-}$*Y16A*^{tg} p=0.0000158, Splenocytes at 4-7 weeks: *A22Cα*$^{-/-}$ vs *A22Cα*$^{-/-}$*PI1*$^{-/-}$*PI2*$^{-/-}$*Y16A*^{tg} p=0.0091656. Each dot represents an individual mouse with the horizontal lines indicating the mean.

FIGURE 16: THYMOCYTE AND SPLENOCYTE TOTAL CELL COUNTS IN SINGLE CHAIN TRANSGENIC TRAV8-1*01TRAJ9 NOD MICE EXPRESSING VARYING PROINSULIN LEVELS

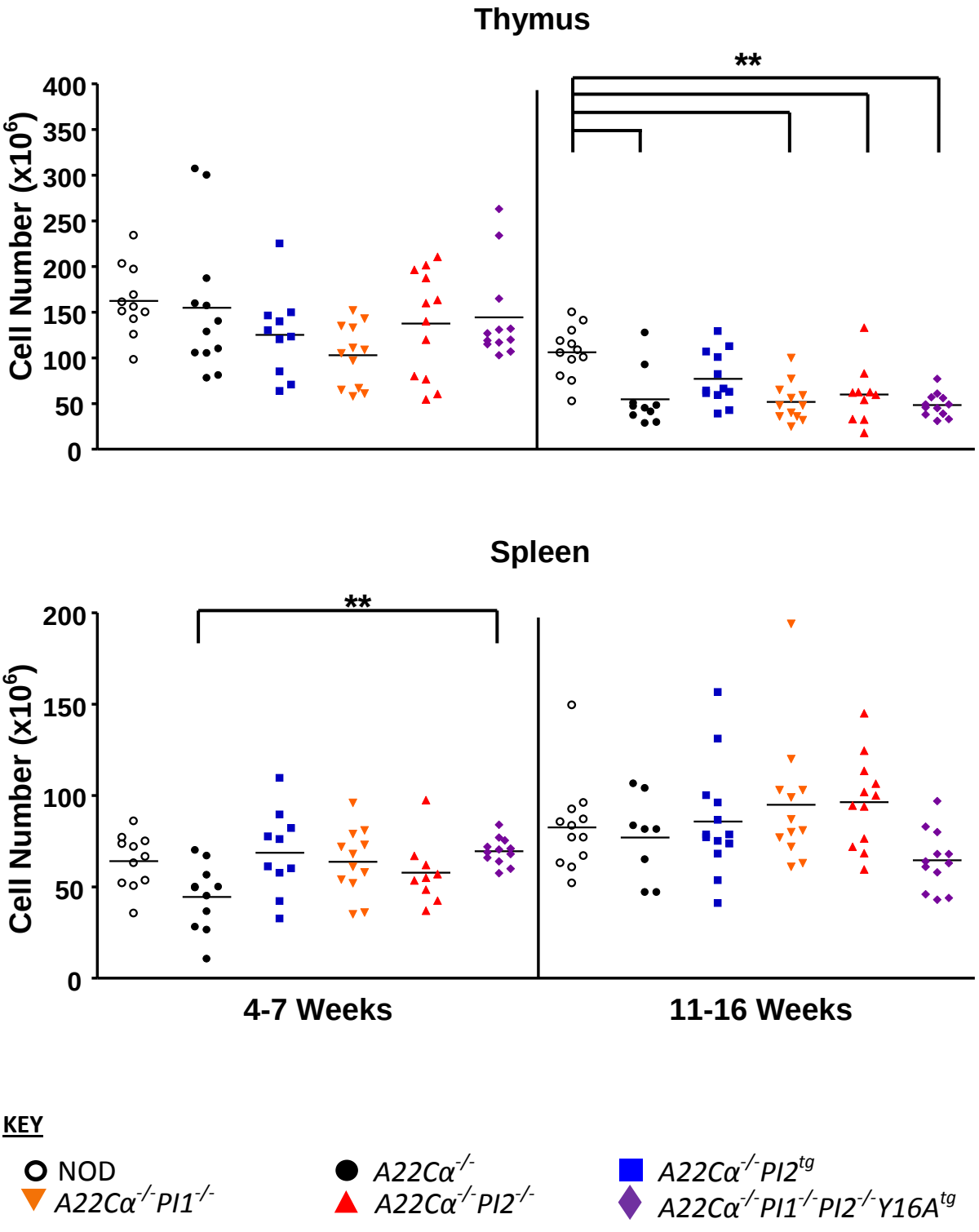

3.3.2 CD4/CD8 T CELL RATIO IS AFFECTED BY PROINSULIN EXPRESSION

The next question was to identify the role of proinsulin expression on the T cell compartment. Therefore, the proportion of $CD4^+$ and $CD8^+$ T cells were investigated by flow cytometric methods. FIGURE 17 illustrates the $CD4^+$ (A&B) and $CD8^+$ (C&D) T cell proportions at both 4-7 weeks and 11-16 weeks. Comparing the groups of 4-7 week old mice (17A), there were statistically significant differences in the $CD4^+$ populations within the thymus between the *A22Cα*$^{-/-}$*PI2*$^{-/-}$ mice, which had a greater proportion of $CD4^+$ T cells, and both *A22Cα*$^{-/-}$*PI1*$^{-/-}$ mice and *A22Cα*$^{-/-}$*PI1*$^{-/-}$*PI2*$^{-/-}$*Y16A*^{tg} mice; however by 11-16 weeks (17B) these differences were no longer seen. Interestingly, by 11-16 weeks the mice exhibited more statistically significant differences in the periphery, particularly when proinsulin 2 was deficient. Within the $CD8^+$ T cell compartment there were only statistically significant differences between the *A22Cα*$^{-/-}$*PI2*$^{-/-}$ mice, which have fewer $CD8^+$ T cells, and the *A22Cα*$^{-/-}$*PI1*$^{-/-}$ mice within the spleen, PLN and MLN and the *A22Cα*$^{-/-}$*PI1*$^{-/-}$*PI2*$^{-/-}$*Y16A*^{tg} mice within the Spleen at 4-7 weeks of age (17C). However, these differences only appear in the young group. There were also no gender differences in the proportions of $CD4^+$ or $CD8^+$ T cells between these mice, and so males and females were grouped together.

3.4 THE EFFECT OF PROINSULIN EXPRESSION ON TOTAL $CD8^+$ T CELL VARIABLE BETA CHAIN RECEPTOR REPERTOIRE

The next question to answer was - did the level of proinsulin expression have any effect on the $CD8^+$ T cells selecting a specific TCRβ chain? For this, lymphoid tissues were harvested, stained with monoclonal antibodies using a multi-colour antibody staining panel (2.9.3.3 in Chapter 2), and analysed by flow cytometry.

FIGURE 17: CD4 and CD8 Single cell suspensions were prepared from thymi, spleen, pancreatic lymph nodes (PLN) and mesenteric lymph nodes (MLN). These cells were then stained with the TRBV phenotyping panels (see 2.9.3.3), fixed and measured on a BD FACS CANTO II. Data were analysed using Flowjo Version 7.6.5 software and results were then collated for all mice. These box plots show the median with the first and third quartile indicated by the top and bottom of the box, with the maximum and minimum values indicated by the arms above and below the box. Strains were compared by ANOVA using R software with data shown to be statistically significant at the $p=<0.05$ (*) or at the $p=<0.01$ level (**).

FIGURE 17: CD4 & CD8 T CELL PROPORTIONS IN THE THYMI, SPLEEN, PANCREATIC LYMPH NODE (PLN) AND MESENTERIC LYMPH NODE (MLN) IN SINGLE CHAIN TRANSGENIC TRAV8-1*01TRAJ9 NOD MICE EXPRESSING VARYING PROINSULIN LEVELS

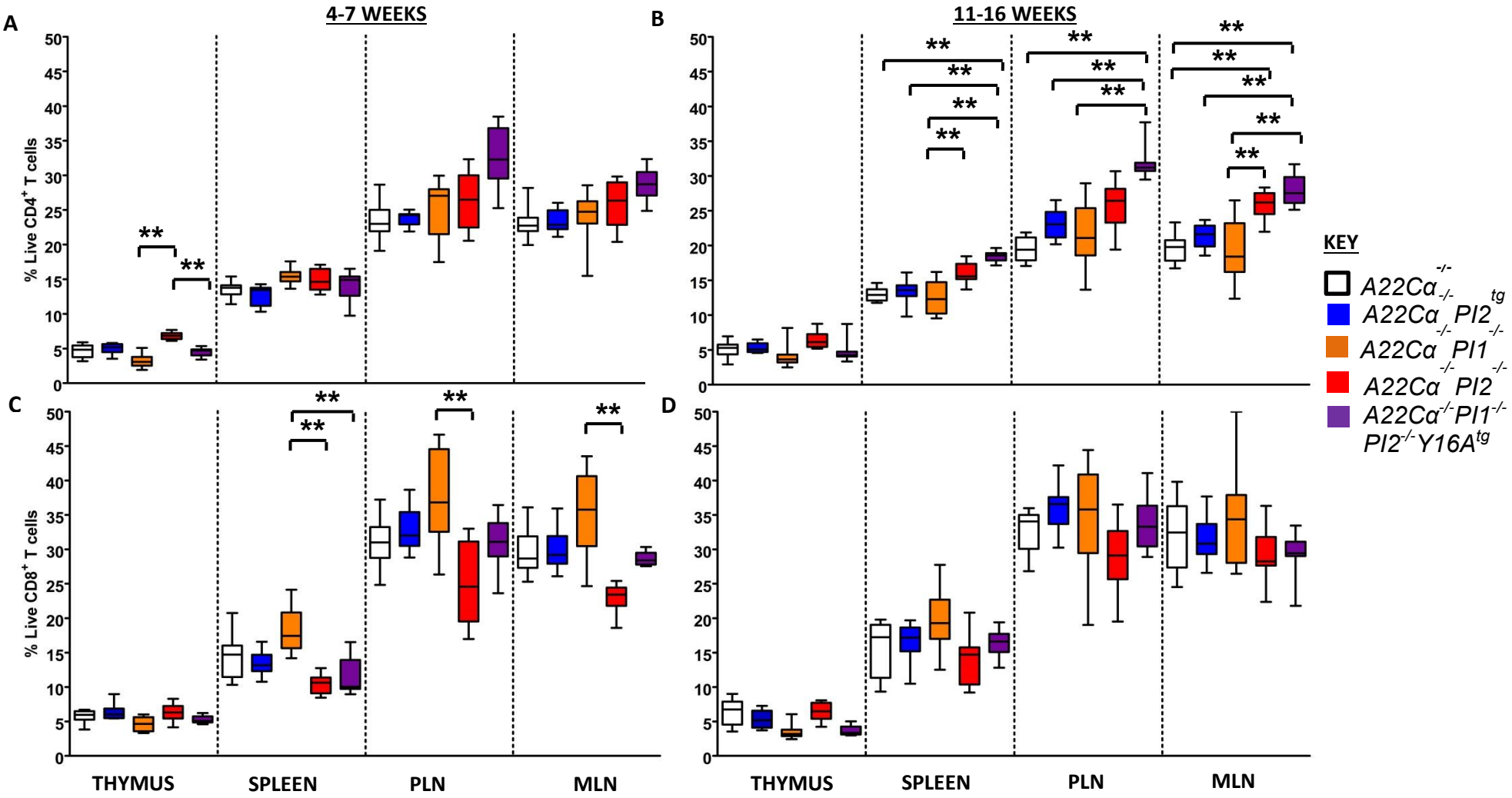

3.4.1 TRBV19 EXPRESSING CD8+ T CELLS ARE REDUCED BY EXPRESSION OF BOTH PROINSULIN 1 AND 2

One of the TRBV chains affected by proinsulin expression was TRBV19 (also known as TCRVβ6), as FIGURE 18 illustrates. This figure shows that when either Proinsulin 1 (*A22Cα*$^{-/-}$*PI1*$^{-/-}$), Proinsulin 2 (*A22Cα*$^{-/-}$*PI2*$^{-/-}$) or both (*A22Cα*$^{-/-}$*PI1*$^{-/-}$*PI2*$^{-/-}$*Y16A*^{tg}) are absent, there is no change in the proportion of CD8^{+} T cells expressing TRBV19 with age. However, in mice that have normal levels of Proinsulin 1 and 2 (*A22Cα*$^{-/-}$), there is a small decrease with age (n.s), but increasing the level of Proinsulin 2 results in a greater reduction and significant differences between the strains at both 4-7 weeks and 11-16 weeks. The differences between the *A22Cα*$^{-/-}$ mice and the other strains are summarised in TABLE 6. Interestingly, the TRBV19^{+} T cells in the *A22Cα*$^{-/-}$ mice differ significantly from only the *A22Cα*$^{-/-}$*PI2*^{tg} mice both at 4-7 and 11-16 weeks of age, with the differences limited to peripheral lymphoid tissues. The comparisons between the other strains are shown in the appendix, but the only significant differences observed were between the *A22Cα*$^{-/-}$*PI2*^{tg} mice and the mice lacking either or both of proinsulin 1 or proinsulin 2. In addition, there were no differences within the lymphoid tissues of each strain, no differences with age and, as mentioned previously, no gender differences.

AGE (WEEKS)	STRAIN NAME	DIFFERENT TO	TISSUE	P VALUE
4-7	***A22Cα*$^{-/-}$**	*A22Cα*$^{-/-}$*PI2*^{tg}	PLN	0.0000004
		A22Cα$^{-/-}$*PI2*^{tg}	MLN	0.0000000
11-16		*A22Cα*$^{-/-}$*PI2*^{tg}	Spleen	0.0000000

TABLE 6: SIGNIFICANT DIFFERENCES IN TRBV19 ASSOCIATION BETWEEN NATIVE PROINSULIN EXPRESSING SINGLE CHAIN TRANSGENIC TRAV8-1*01TRAJ9 NOD MICE AND ALL OTHER STRAINS EXPRESSING VARYING LEVELS OF PROINSULIN

NOTE: All strains were compared for TRBV19 differences but only the *A22Cα*$^{-/-}$*PI2*^{tg} mice were significantly different to the wildtype *A22Cα*$^{-/-}$ mice. For all other comparisons between the strains see the Appendix Tables.

3.4.2 OTHER TRBV RESULTS

TRBV19 showed the most dramatic TRBV repertoire changes in relation to proinsulin expression. However, proinsulin-specific effects were also seen with TRBV29 and TRBV16. In Proinsulin 2 deficient *A22Cα*$^{-/-}$*PI2*$^{-/-}$ mice, the CD8^{+} T cells have an increased proportion of TRBV29 in the PLN, compared to all other strains, at 11-16 weeks, as shown in FIGURE 19. There were also significant differences between the tissues of the *A22Cα*$^{-/-}$*PI2*$^{-/-}$ mice and the other strains, as shown. As for TRBV16, mice deficient in Proinsulin 1, Proinsulin 2 or both showed an increase in TRBV16 expression, as shown in FIGURE 20. As shown, at 4-7 weeks, there is a significant difference between the mice lacking both Proinsulin 1 and 2 (*A22Cα*$^{-/-}$*PI1*$^{-/-}$*PI2*$^{-/-}$*Y16A*^{tg}) and those lacking Proinsulin 1 (*A22Cα*$^{-/-}$*PI1*$^{-/-}$) when compared to the other strains, particularly in the PLN and MLN. At 11-16 weeks, those mice deficient in Proinsulin 2 (*A22Cα*$^{-/-}$*PI2*$^{-/-}$), also show significant differences to those mice expressing native levels of proinsulin (*A22Cα*$^{-/-}$) and mice over-expressing proinsulin 2 (*A22Cα*$^{-/-}$*PI2*^{tg}) in the PLN and MLN. In addition to proinsulin-specific TRBV repertoire changes, significant changes were also noted with age. The proportion of TRBV4^{+} CD8^{+} T cells, shown in FIGURE 21, shows strain differences primarily in the thymus. However, it is the differences in the peripheral tissues between 4-7 weeks and 11-16 weeks, within each strain that show significant TRBV4 expansions ($p=<0.01$).

The most striking results are discussed above, with the results for the other TCRVβ chains shown in the appendix. However, other statistically significant differences between the strains at different ages (TABLE 7 and TABLE 8), with age (TABLE 9) and between the tissues (TABLE 10 and TABLE 11) are shown below. In general, these results show greater variation between the strains at 4-7 weeks than at 11-16 weeks. In addition, these results also show that the thymus has the most significant differences when compared to the spleen or lymph nodes. Unfortunately, due to small numbers, the repertoire results for TRBV24 could not be compared.

FIGURE 18: Lymphoid cells were harvested from thymus, spleen, PLN and MLN of mice aged 4-7 weeks or 11-16 weeks. These cells were stained using a multi-colour antibody staining panel, measured on a BD FACS CANTO II and analysed later using Flowjo Version 7.6.5 software. Data were then plotted using GraphPad Version 4 software. Each shape represents an individual mouse (n=8-13), with unfilled shapes representing those aged 4-7 weeks and filled shapes those aged 11-16 weeks. The median is shown for each data set by a horizontal line with statistically significant differences at p=<0.05 (*) and p=<0.01 (**) between the strains shown following an ANOVA analysis using R software.

FIGURE 18: CD8^{+}TRBV19^{+} T CELL PROPORTIONS IN THE THYMI, SPLEEN, PANCREATIC LYMPH NODE (PLN) AND MESENTERIC LYMPH NODE (MLN) IN SINGLE CHAIN TRANSGENIC TRAV8-1*01TRAJ9 NOD MICE EXPRESSING VARYING PROINSULIN LEVELS

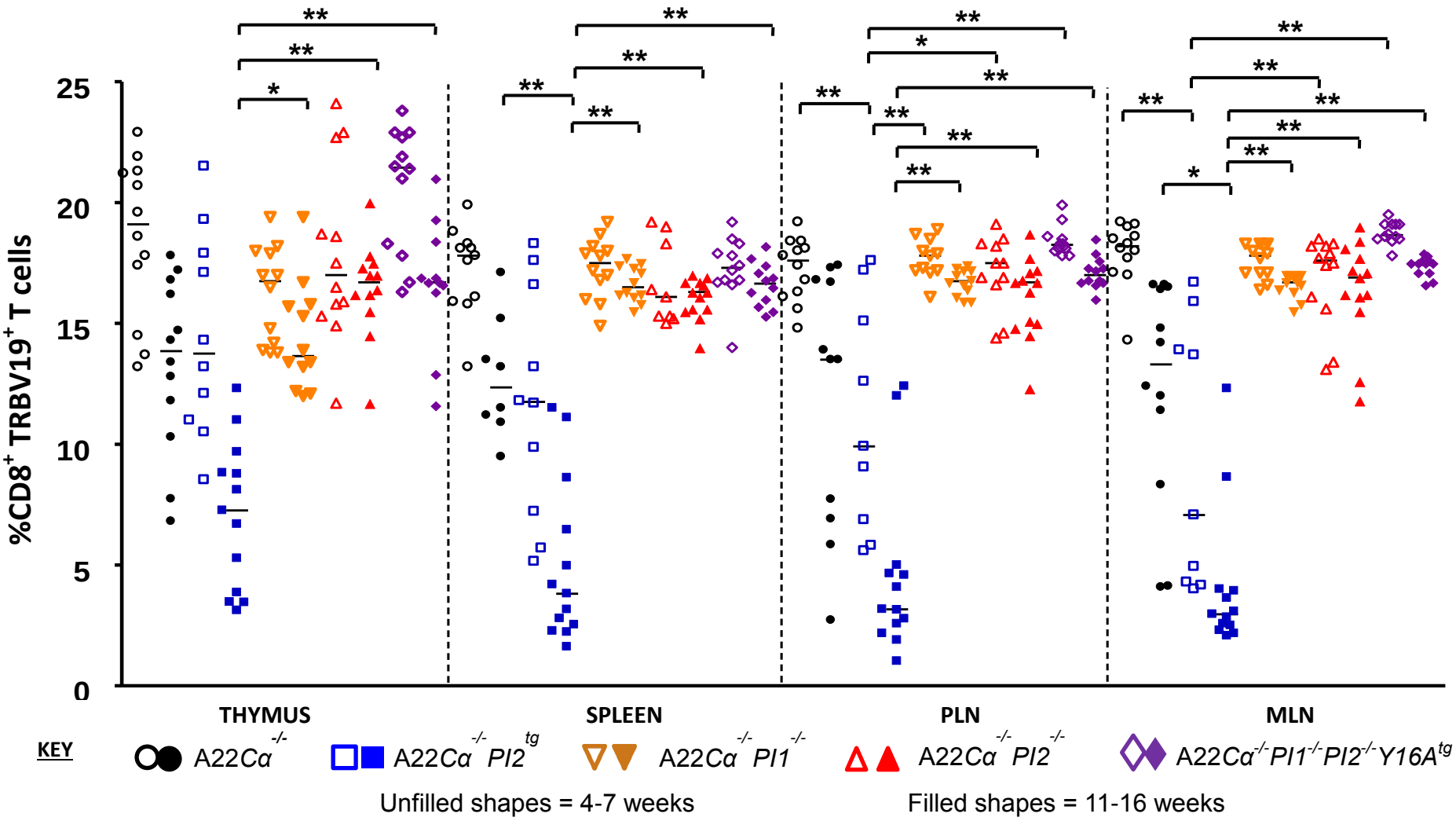

FIGURE 19: Lymphoid cells were harvested from thymus, spleen, PLN and MLN of mice aged 4-7 weeks or 11-16 weeks. These cells were stained using a multi-colour antibody staining panel and measured on a BD FACS CANTO II to be analysed later using Flowjo Version 7.6.5 software. Data were then plotted using GraphPad Version 4 software. Each shape represents an individual mouse (n=8-13), with unfilled shapes representing those aged 4-7 weeks and filled shapes those aged 11-16 weeks. The median is shown for each data set by a horizontal line with statistically significant differences at p=<0.05 (*) and p=<0.01 (**) between the strains shown following an ANOVA analysis using R software.

FIGURE 19: CD8$^+$TRBV29$^+$ T CELL PROPORTIONS IN THE THYMI, SPLEEN, PANCREATIC LYMPH NODE (PLN) AND MESENTERIC LYMPH NODE (MLN) IN SINGLE CHAIN TRANSGENIC TRAV8-1*01TRAJ9 NOD MICE EXPRESSING VARYING PROINSULIN LEVELS

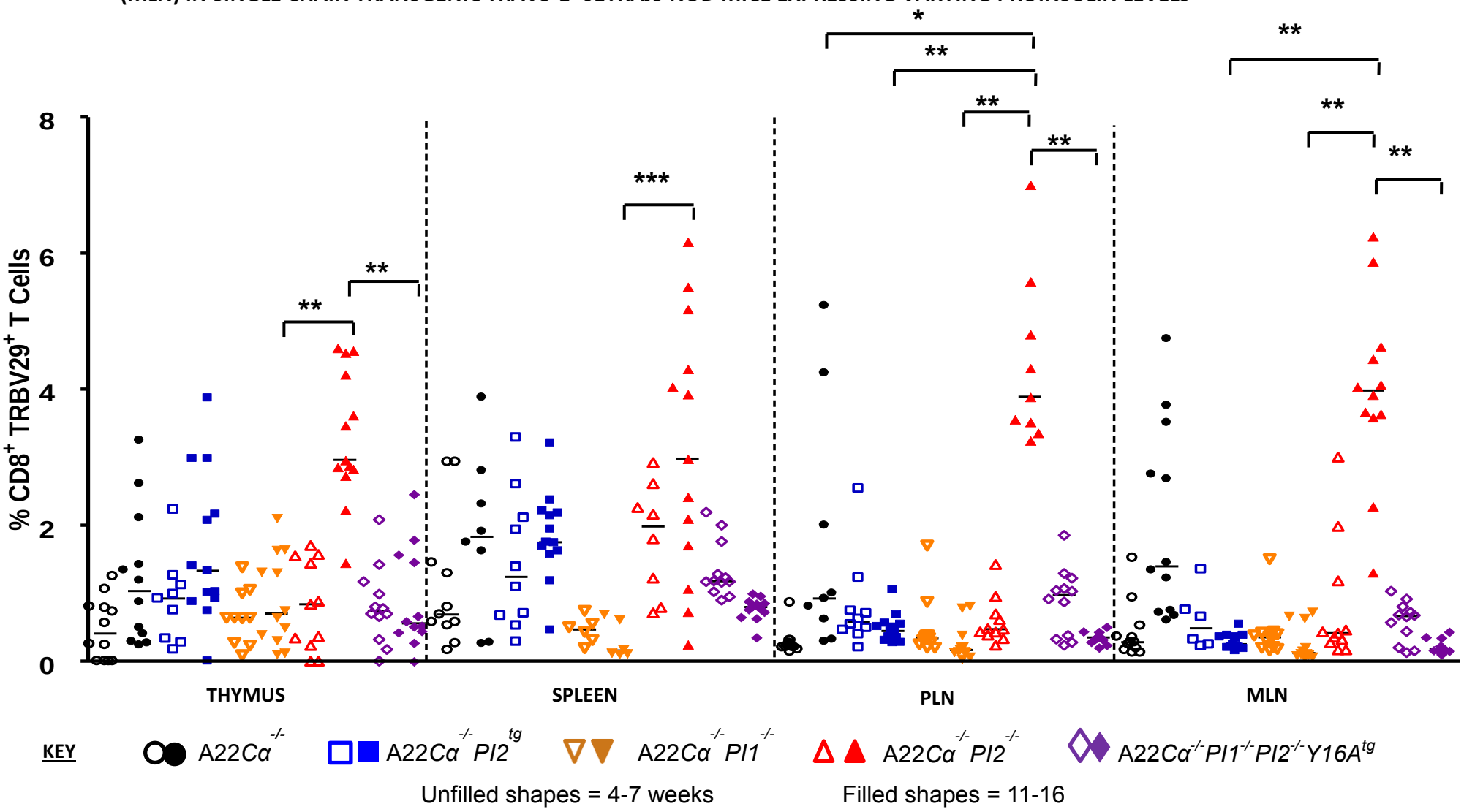

FIGURE 20: Lymphoid cells were harvested from thymus, spleen, PLN and MLN of mice aged 4-7 weeks or 11-16 weeks. These cells were stained using a multi-colour antibody staining panel and measured on a BD FACS CANTO II to be analysed later using Flowjo Version 7.6.5 software. Data were then plotted using GraphPad Version 4 software. Each shape represents an individual mouse (n=8-13), with unfilled shapes representing those aged 4-7 weeks and filled shapes those aged 11-16 weeks. The median is shown for each data set by a horizontal line with statistically significant differences at $p=<0.05$ (*) and $p=<0.01$ (**) between the strains shown following an ANOVA analysis using R software.

FIGURE 20: CD8$^+$TRBV16$^+$ T CELL PROPORTIONS IN THE THYMI, SPLEEN, PANCREATIC LYMPH NODE (PLN) AND MESENTERIC LYMPH NODE (MLN) IN SINGLE CHAIN TRANSGENIC TRAV8-1*01TRAJ9 NOD MICE EXPRESSING VARYING PROINSULIN LEVELS

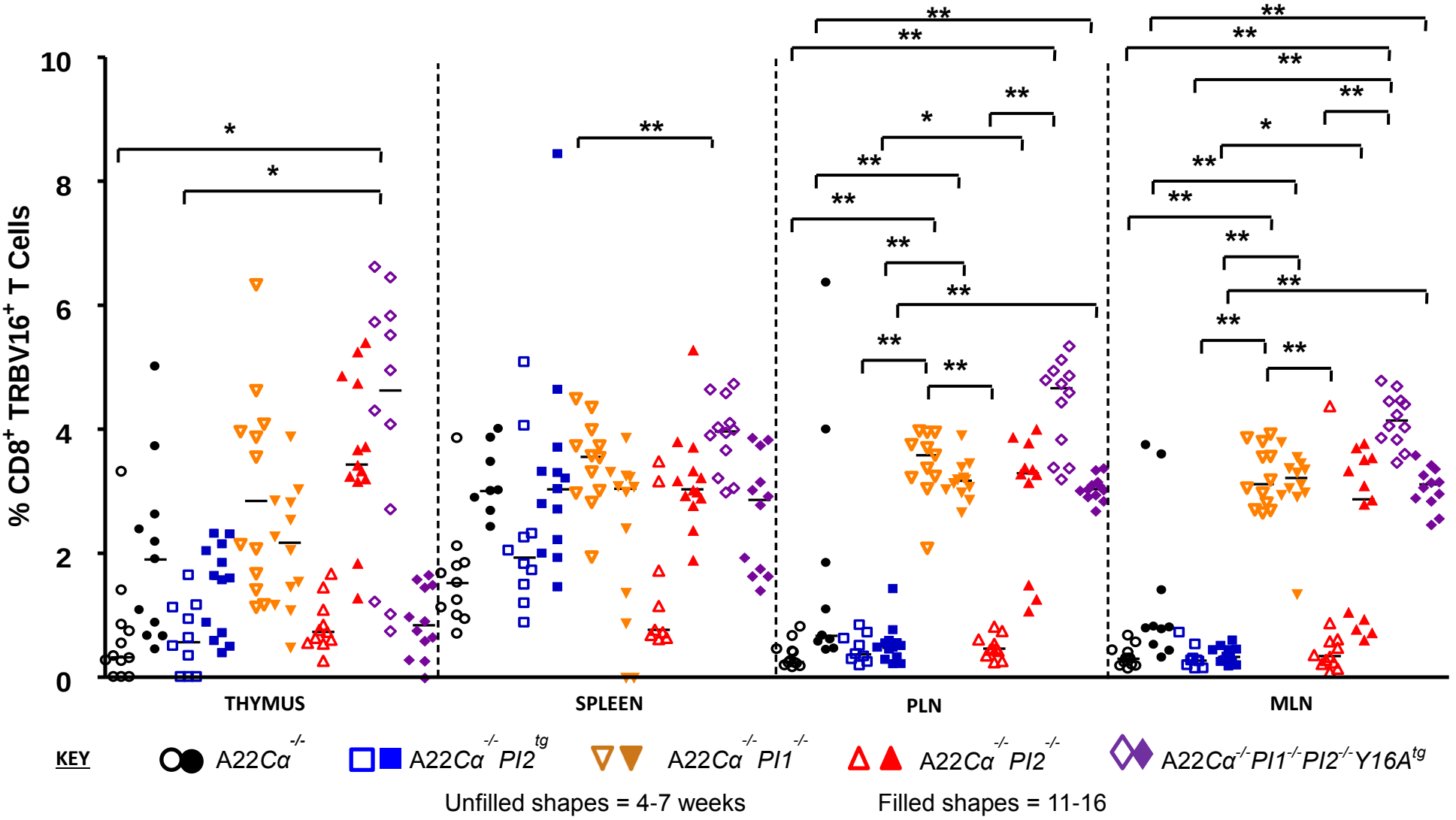

FIGURE 21: Lymphoid cells were harvested from thymus, spleen, PLN and MLN of mice aged 4-7 weeks or 11-16 weeks. These cells were stained using a multi-colour antibody staining panel and measured on a BD FACS CANTO II to be analysed later using Flowjo Version 7.6.5 software. Data were then plotted using GraphPad Version 4 software. Each shape represents an individual mouse (n=8-13), with unfilled shapes representing those aged 4-7 weeks and filled shapes those aged 11-16 weeks. The median is shown for each data set by a horizontal line with statistically significant differences at p=<0.05 (*) and p=<0.01 (**) between the strains shown following an ANOVA analysis using R software.

FIGURE 21: CD8^{+}TRBV4^{+} T CELL PROPORTIONS IN THE THYMI, SPLEEN, PANCREATIC LYMPH NODE (PLN) AND MESENTERIC LYMPH NODE (MLN) IN SINGLE CHAIN TRANSGENIC TRAV8-1*01TRAJ9 NOD MICE EXPRESSING VARYING PROINSULIN LEVELS

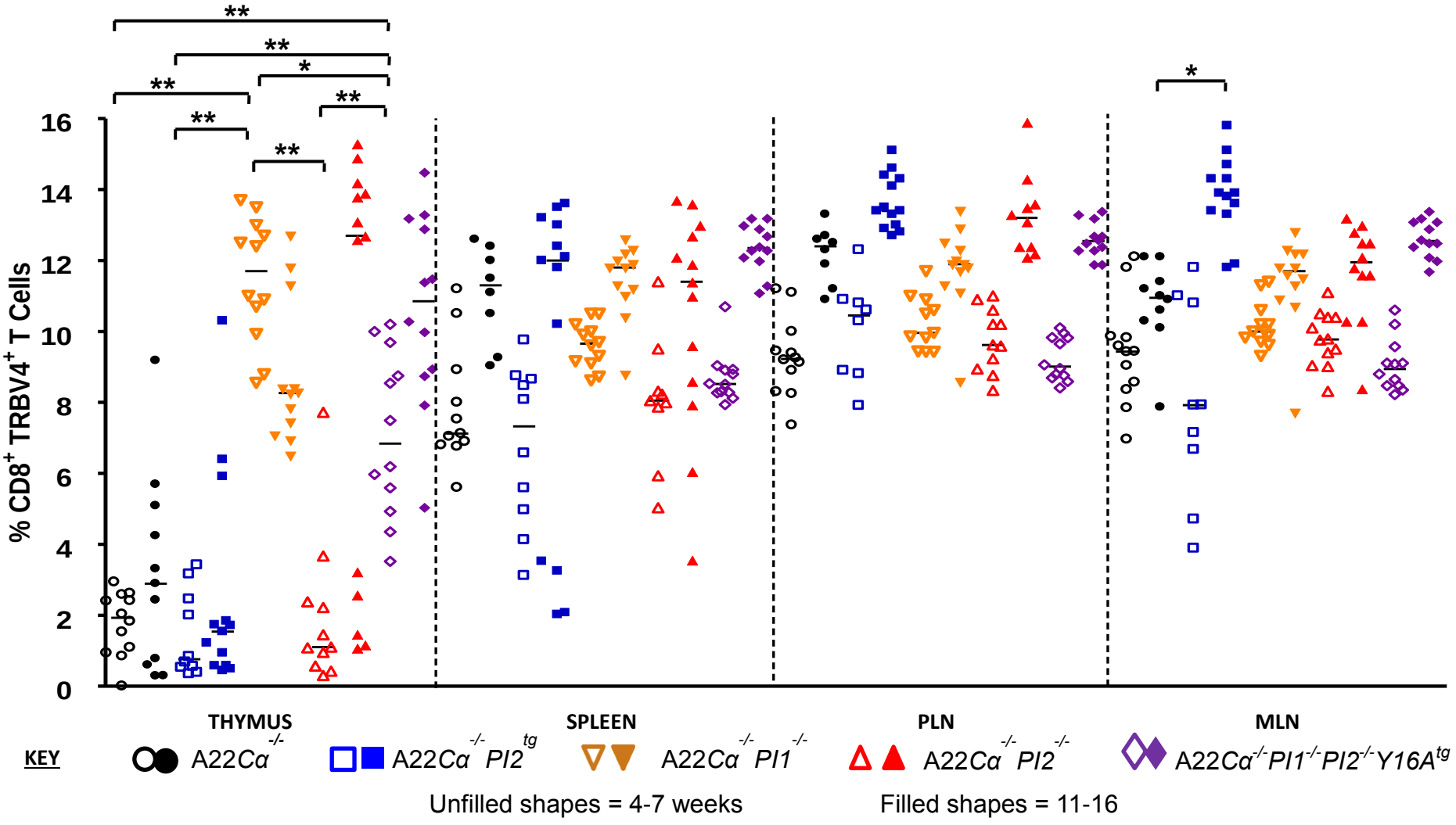

TRBV CHAIN	STRAIN	DIFFERENT TO	TISSUE	P VALUE
TRBV2	*A22Cα$^{-/-}$PI2^{tg}*	*A22Cα$^{-/-}$PI1$^{-/-}$*	Spleen	0.0000005
		A22Cα$^{-/-}$PI1$^{-/-}$PI2$^{-/-}$Y16A^{tg}	Spleen	0.0000001
		A22Cα$^{-/-}$PI1$^{-/-}$PI2$^{-/-}$Y16A^{tg}	PLN	0.0000016
TRBV13-2/13-3	*A22Cα$^{-/-}$PI1$^{-/-}$PI2$^{-/-}$Y16A^{tg}*	*A22Cα$^{-/-}$PI2^{tg}*	Thymus	0.0000000
TRBV14	*A22Cα$^{-/-}$PI1$^{-/-}$PI2$^{-/-}$Y16A^{tg}*	*A22Cα$^{-/-}$*	Thymus	0.0000000
		A22Cα$^{-/-}$PI2$^{-/-}$		0.0000000
		A22Cα$^{-/-}$PI2^{tg}		0.0000004
		A22Cα$^{-/-}$	Spleen	0.0000000
		A22Cα$^{-/-}$PI2$^{-/-}$		0.0000000
		A22Cα$^{-/-}$PI2^{tg}		0.0000000
	A22Cα$^{-/-}$PI1$^{-/-}$	*A22Cα$^{-/-}$*		0.0000000
		A22Cα$^{-/-}$PI2^{tg}		0.0000000
	A22Cα$^{-/-}$PI1$^{-/-}$PI2$^{-/-}$Y16A^{tg}	*A22Cα$^{-/-}$*	PLN	0.0000000
		A22Cα$^{-/-}$PI2$^{-/-}$		0.0000000
		A22Cα$^{-/-}$PI2^{tg}		0.0000000
	A22Cα$^{-/-}$PI1$^{-/-}$	*A22Cα$^{-/-}$*		0.0000000
		A22Cα$^{-/-}$PI2^{tg}		0.0000000
	A22Cα$^{-/-}$PI1$^{-/-}$PI2$^{-/-}$Y16A^{tg}	*A22Cα$^{-/-}$*	MLN	0.0000000
		A22Cα$^{-/-}$PI2$^{-/-}$		0.0000000
		A22Cα$^{-/-}$PI2^{tg}		0.0000000
	A22Cα$^{-/-}$PI1$^{-/-}$	*A22Cα$^{-/-}$*		0.0000000
		A22Cα$^{-/-}$PI2$^{-/-}$		0.0000000
		A22Cα$^{-/-}$PI2^{tg}		0.0000000
TRBV15	*A22Cα$^{-/-}$PI1$^{-/-}$PI2$^{-/-}$Y16A^{tg}*	*A22Cα$^{-/-}$*	MLN	0.0000000
		A22Cα$^{-/-}$PI2$^{-/-}$		0.0000000
		A22Cα$^{-/-}$PI2^{tg}		0.0000001
	A22Cα$^{-/-}$PI1$^{-/-}$	*A22Cα$^{-/-}$*		0.0000000
		A22Cα$^{-/-}$PI2$^{-/-}$		0.0000000
		A22Cα$^{-/-}$PI2^{tg}		0.0000000
TRBV26	*A22Cα$^{-/-}$PI1$^{-/-}$PI2$^{-/-}$Y16A^{tg}*	*A22Cα$^{-/-}$*	Thymus	0.0000002
		A22Cα$^{-/-}$PI2$^{-/-}$		0.0000000
		A22Cα$^{-/-}$PI2^{tg}		0.0000003

TABLE 7: OTHER TRBV SIGNIFICANT DIFFERENCES BETWEEN SINGLE CHAIN TRANSGENIC TRAV8-1*01TRAJ9 NOD MICE EXPRESSING VARYING LEVELS OF PROINSULIN AT 4-7 WEEKS OF AGE

TRBV CHAIN	STRAIN	DIFFERENT TO	TISSUE	P VALUE
TRBV2	*A22Cα$^{-/-}$PI1$^{-/-}$*	*A22Cα$^{-/-}$*	Spleen	0.0000009
	A22Cα$^{-/-}$PI1$^{-/-}$PI2$^{-/-}$Y16A^{tg}	*A22Cα$^{-/-}$*		0.0000002
		A22Cα$^{-/-}$PI2^{tg}		0.0000004
	A22Cα$^{-/-}$PI2$^{-/-}$	*A22Cα$^{-/-}$*		0.0000002
		A22Cα$^{-/-}$PI2^{tg}		0.0000004
	A22Cα$^{-/-}$PI1$^{-/-}$PI2$^{-/-}$Y16A^{tg}	*A22Cα$^{-/-}$*	PLN	0.0000000
		A22Cα$^{-/-}$PI2^{tg}		0.0000004
	A22Cα$^{-/-}$PI2$^{-/-}$	*A22Cα$^{-/-}$*		0.0000000
	A22Cα$^{-/-}$	*A22Cα$^{-/-}$PI2$^{-/-}$*	MLN	0.0000002
		A22Cα$^{-/-}$PI1$^{-/-}$PI2$^{-/-}$Y16A^{tg}		0.0000002
TRBV12-2/12-1	*A22Cα$^{-/-}$PI1$^{-/-}$PI2$^{-/-}$Y16A^{tg}*	*A22Cα$^{-/-}$PI2^{tg}*	Spleen	0.0000002
TRBV15	*A22Cα$^{-/-}$PI2^{tg}*	*A22Cα$^{-/-}$PI1$^{-/-}$*	PLN	0.0000001
		A22Cα$^{-/-}$PI1$^{-/-}$PI2$^{-/-}$Y16A^{tg}		0.0000000
TRBV26	*A22Cα$^{-/-}$PI1$^{-/-}$PI2$^{-/-}$Y16A^{tg}*	*A22Cα$^{-/-}$PI2$^{-/-}$*	Spleen	0.0000000
		A22Cα$^{-/-}$PI2^{tg}		0.0000000
	A22Cα$^{-/-}$PI1$^{-/-}$	*A22Cα$^{-/-}$PI2$^{-/-}$*		0.0000001
		A22Cα$^{-/-}$PI2^{tg}		0.0000000

TABLE 8: OTHER TRBV SIGNIFICANT DIFFERENCES BETWEEN SINGLE CHAIN TRANSGENIC TRAV8-1*01TRAJ9 NOD MICE EXPRESSING VARYING LEVELS OF PROINSULIN AT 11-16 WEEKS OF AGE

STRAIN	TRBV CHAIN	TISSUE	P VALUE
A22Cα$^{-/-}$PI2^{tg}	TRBV15	PLN	0.0000000
	TRBV31		0.0000018
	TRBV15	MLN	0.0000000
	TRBV17		0.0000000
A22Cα$^{-/-}$PI2$^{-/-}$	TRBV26	Thymus	0.0000002
A22Cα$^{-/-}$PI1$^{-/-}$PI2$^{-/-}$Y16A^{tg}	TRBV26	MLN	0.0000000

TABLE 9: OTHER TRBV SIGNIFICANT DIFFERENCES WITHIN SINGLE CHAIN TRANSGENIC TRAV8-1*01TRAJ9 NOD MICE EXPRESSING VARYING LEVELS OF PROINSULIN WITH AGE

STRAIN	TRBV CHAIN	TISSUE	DIFFERENT TO	P VALUE
A22Cα$^{-/-}$	TRBV13-3/13-2	Thymus	Spleen	0.0000000
			PLN	0.0000000
			MLN	0.0000000
	TRBV14	Spleen	PLN	0.0000008
			MLN	0.0000015
	TRBV26	Thymus	PLN	0.0000001
			MLN	0.0000000
A22Cα$^{-/-}$PI2^{tg}	TRBV13-3/13-2	Thymus	Spleen	0.0000000
			PLN	0.0000000
			MLN	0.0000000
	TRBV26	Thymus	PLN	0.0000000
			MLN	0.0000000
A22Cα$^{-/-}$PI1$^{-/-}$	TRBV13-3/13-2	Thymus	Spleen	0.0000001
			PLN	0.0000000
			MLN	0.0000000
A22Cα$^{-/-}$PI2$^{-/-}$	TRBV13-3/13-2	Thymus	Spleen	0.0000006
	TRBV26	Thymus	PLN	0.0000000
			MLN	0.0000000
A22Cα$^{-/-}$PI1$^{-/-}$PI2$^{-/-}$Y16A^{tg}	TRBV12-2/12-1	Thymus	Spleen	0.0000000
			PLN	0.0000000
			MLN	0.0000000
	TRBV13-3/13-2	Thymus	PLN	0.0000000
			MLN	0.0000000
	TRBV31	Thymus	Spleen	0.0000001
			PLN	0.0000022
			MLN	0.0000001

TABLE 10: OTHER TRBV SIGNIFICANT DIFFERENCES BETWEEN THE TISSUES IN SINGLE CHAIN TRANSGENIC TRAV8-1*01TRAJ9 NOD MICE EXPRESSING VARYING LEVELS OF PROINSULIN AT 4-7 WEEKS OF AGE

STRAIN	TRBV CHAIN	TISSUE	DIFFERENT TO	P VALUE
A22Cα$^{-/-}$PI2^{tg}	TRBV2	Spleen	Thymus	0.0000000
			PLN	0.0000000
			MLN	0.0000000
	TRBV13-3/13-2	Thymus	Spleen	0.0000000
			PLN	0.0000000
			MLN	0.0000000
	TRBV26	Thymus	PLN	0.0000000
			MLN	0.0000000
		Spleen	PLN	0.0000000
			MLN	0.0000000
A22Cα$^{-/-}$PI1$^{-/-}$	TRBV13-3/13-2	Thymus	MLN	0.0000020
A22Cα$^{-/-}$PI2$^{-/-}$	TRBV13-3/13-2	Thymus	Spleen	0.0000006
			PLN	0.0000001
			MLN	0.0000002
A22Cα$^{-/-}$PI1$^{-/-}$PI2$^{-/-}$Y16A^{tg}	TRBV13-3/13-2	Thymus	Spleen	0.0000000
			PLN	0.0000000
			MLN	0.0000000

TABLE 11: SIGNIFICANT DIFFERENCES BETWEEN THE TISSUES IN SINGLE CHAIN TRANSGENIC TRAV8-1*01TRAJ9 NOD MICE EXPRESSING VARYING LEVELS OF PROINSULIN AT 11-16 WEEKS OF AGE

3.5 THE EFFECT OF PROINSULIN EXPRESSION ON INSULIN B15-23 AUTOIMMUNITY IN SINGLE CHAIN TRANSGENIC TRAV8-1*01TRAJ9 NOD MICE

The next question we wanted to address was whether the level of proinsulin expression had any effect on the development of insulin autoimmunity. This was addressed specifically, in the T cell compartment, by insulin B15-23 reactivity using peptide:MHC tetramers.

3.5.1 THE EFFECT OF PROINSULIN EXPRESSION ON INSULIN B15-23-REACTIVE CD8+ T CELL VARIABLE BETA CHAIN RECEPTOR REPERTOIRE

The above sections report the results for total $CD8^+$ TCRVβ chain repertoire in mice expressing the TRAV8-1*01TRAJ9, the TCRα chain from the G9C8 T cell clone (Wong et al., 1996), related to proinsulin expression. However, no knowledge was known of their antigen specificity and therefore given the antigen specificity of G9C8, we then sought to identify the TCRβ repertoire of the Insulin B15-23 reactive $CD8^+$ T cells in these mice with different levels of proinsulin.

*3.5.1.1 PROINSULIN 1 AND 2 DEFICIENCY INCREASES THE PROPORTION OF INSULIN B15-23 REACTIVE CD8+ T CELLS WITHIN THE PLN IN SINGLE CHAIN TRANSGENIC TRAV8-1*01TRAJ9 NOD MICE*

Using insulin H-$2K^d$-B15-23 peptide tetramers (NIH tetramer facility), single cell suspensions from the thymus, spleen, pancreatic lymph node (PLN) and mesenteric lymph node (MLN) were stained. This allowed us to address the role of proinsulin expression on the development of those antigen-specific $CD8^+$ T cells. Interestingly, when mice lacked Proinsulin 2 (*A22Cα*$^{-/-}$*PI2*$^{-/-}$), there was a significant increase in the proportion of insulin B15-23 reactive $CD8^+$ T cells in comparison to the TCRα restricted mice (*A22Cα*$^{-/-}$) expressing normal insulin levels within the spleen (p=0.0134) and the PLN (p=0.0466) as shown in FIGURE 22. In addition, within the PLN there was also a significant increase in H-$2K^d$-B15-23 peptide tetramer positive cells, seen in those mice deficient in Proinsulin 1 (*A22Cα*$^{-/-}$*PI1*$^{-/-}$) and polyclonal NOD mice when compared to the *A22Cα*$^{-/-}$ mice (p=0.0296 and p=0.003 respectively). The *A22Cα*$^{-/-}$*PI2*$^{-/-}$ mice also had a greater proportion of insulin B15-23 reactive $CD8^+$ T cells within the thymus than the polyclonal NOD mice. There were no other significant differences in the thymus and none seen at all within the MLN.

FIGURE 22: PROINSULIN B15-23 REACTIVE CD8$^+$ T CELL PROPORTIONS IN THE THYMI, SPLEEN, PANCREATIC LYMPH NODE (PLN) AND MESENTERIC LYMPH NODE (MLN) IN POLYCLONAL NOD MICE AND SINGLE CHAIN TRANSGENIC TRAV8-1*01 NOD MICE EXPRESSING VARYING PROINSULIN LEVELS

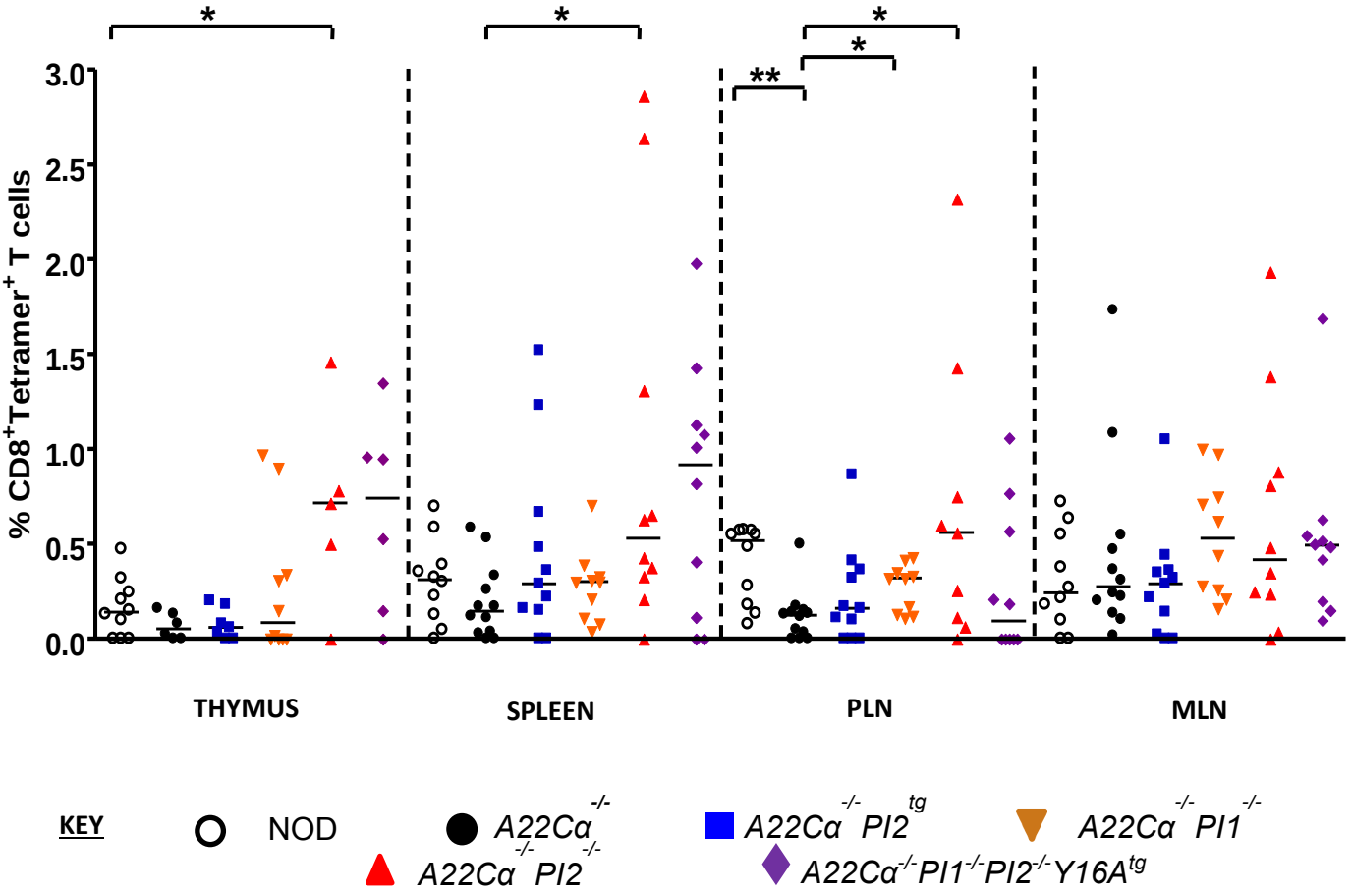

FIGURE 22: Cells were harvested from thymus, spleen, PLN and MLN of mice aged 4-8 weeks. These cells were stained using a multi-colour antibody staining panel (see 2.9.3.3) and measured on a BD FACS CANTO II to be analysed later using Flowjo Version 7.6.5 software. Data were then plotted using GraphPad Version 4 software. Each shape represents an individual mouse (n=5-10). The median is shown for each data set by a horizontal line with statistically significant differences at p=<0.05 (*) and p=<0.01 (**) between the strains shown following a Mann Whitney comparison test between the strains.

*3.5.1.2 SINGLE CHAIN TRANSGENIC TRAV8-1*01TRAJ9 NOD MICE EXHIBIT INDIVIDUAL INSULIN B15-23 REACTIVE CD8+ T CELL CLONAL EXPANSIONS WITHIN THE PLN*

In order to isolate the insulin B15-23 reactive $CD8^+$ T cells, cells from the PLN were harvested and sorted using a BD FACS ARIA for live single $CD8^+CD4^-CD11b^-CD19^-H\text{-}2K^d$- B15-23 peptide $Tetramer^+$ cells. These cells were then clonotyped for their TCRβ chain identifying the CDR3 region, which is used by the TCR to contact the peptide:MHC complex.

Focussing initially on the TRBV chain, there were 14 different TRBV genes that pair with the specific TCRα chain in these insulin B15-23 reactive $CD8^+$ T cells; however when analysed by strain, the TRBV gene selection was more restricted. As can be seen from FIGURE 23, although the numbers are small there was a trend with the greatest number of TRBV genes found in the Proinsulin 2 deficient mice (*A22Cα$^{-/-}$PI2$^{-/-}$*; n=6), then the *A22Cα$^{-/-}$* mice (n=4), with the *A22Cα$^{-/-}$PI1$^{-/-}$PI2$^{-/-}$Y16A^{tg}* mice following (n=3) and finally the *A22Cα$^{-/-}$PI2^{tg}* mice (n=1). Interestingly, the highest proportion of $TRBV19^+H\text{-}2K^d$-B15-23 peptide $tetramer^+$ cells was found in the mice deficient in both Proinsulin 1 and 2 (61%), followed by those that lack Proinsulin 2 (13%) and finally those with normal levels of proinsulin (4%) while not being detected in those mice over-expressing Proinsulin 2. TRBV4 and TRBV13-2 were also shared by 3/4 of the strains analysed, while 9/14 TRBV genes were restricted to only 1 strain.

There are 14 TRBJ chains that can be used in conjunction with a TRBV chain and 9 of these were identified by sequencing in these insulin B15-23 reactive $CD8^+$ T cells. However, there were only 2 TRBJ segments that appeared in 3/4 strains of mice (see TABLE 12); these included TRBJ2-7 found in all strains except the *A22Cα$^{-/-}$PI2^{tg},* and TRBJ1-1 found in all but the *A22Cα$^{-/-}$PI2$^{-/-}$* mice. TRBJ2-7 was the most prevalent in the *A22Cα$^{-/-}$* mice (49.86%), the second most prevalent in the *A22Cα$^{-/-}$PI1$^{-/-}$PI2$^{-/-}$Y16A^{tg}* mice (30.49%) and the third in the *A22Cα$^{-/-}$PI2$^{-/-}$* mice (20.39%). The TRBJ2-3 utilised by the G9C8 T cell clone for recognition of insulin B15-23 was found in approximately the same proportion in both *A22Cα$^{-/-}$* mice (12.97%) and the *A22Cα$^{-/-}$PI2$^{-/-}$* mice (12.94%) but not in the other strains.

FIGURE 23: Lymphoid cells were harvested from the PLN from individual mice aged 4-8 weeks, stained with H-2K^{d}-B15-23 peptide tetramer and sorted using a BD FACS ARIA. RNA was then extracted from the cells and TCRβ chain cDNA was generated, purified, cloned into a vector and amplified using recombinant *E.coli*. Individual colonies were then sequenced for their TCRβ chain. Data were then plotted as a percentage of all the sequences obtained within that strain, with each TCRβ chain colour coded to highlight similarities. Data shown are from *A22Cα*$^{-/-}$ (**A** – 2F & 2M), *A22Cα*$^{-/-}$*PI2*^{tg} (**B** – 1F), *A22Cα*$^{-/-}$*PI2*$^{-/-}$ (**C** – 2F & 4M) and *A22Cα*$^{-/-}$*PI1*$^{-/-}$*PI2*$^{-/-}$*Y16A*^{tg} (**D** – 1F & 2M) mice.

FIGURE 23: PROINSULIN B15-23 REACTIVE CD8^{+} T CELL RECEPTOR VARIABLE BETA CHAIN PROPORTIONS SINGLE CHAIN TRANSGENIC TRAV8-1*01 NOD MICE EXPRESSING VARYING PROINSULIN LEVELS

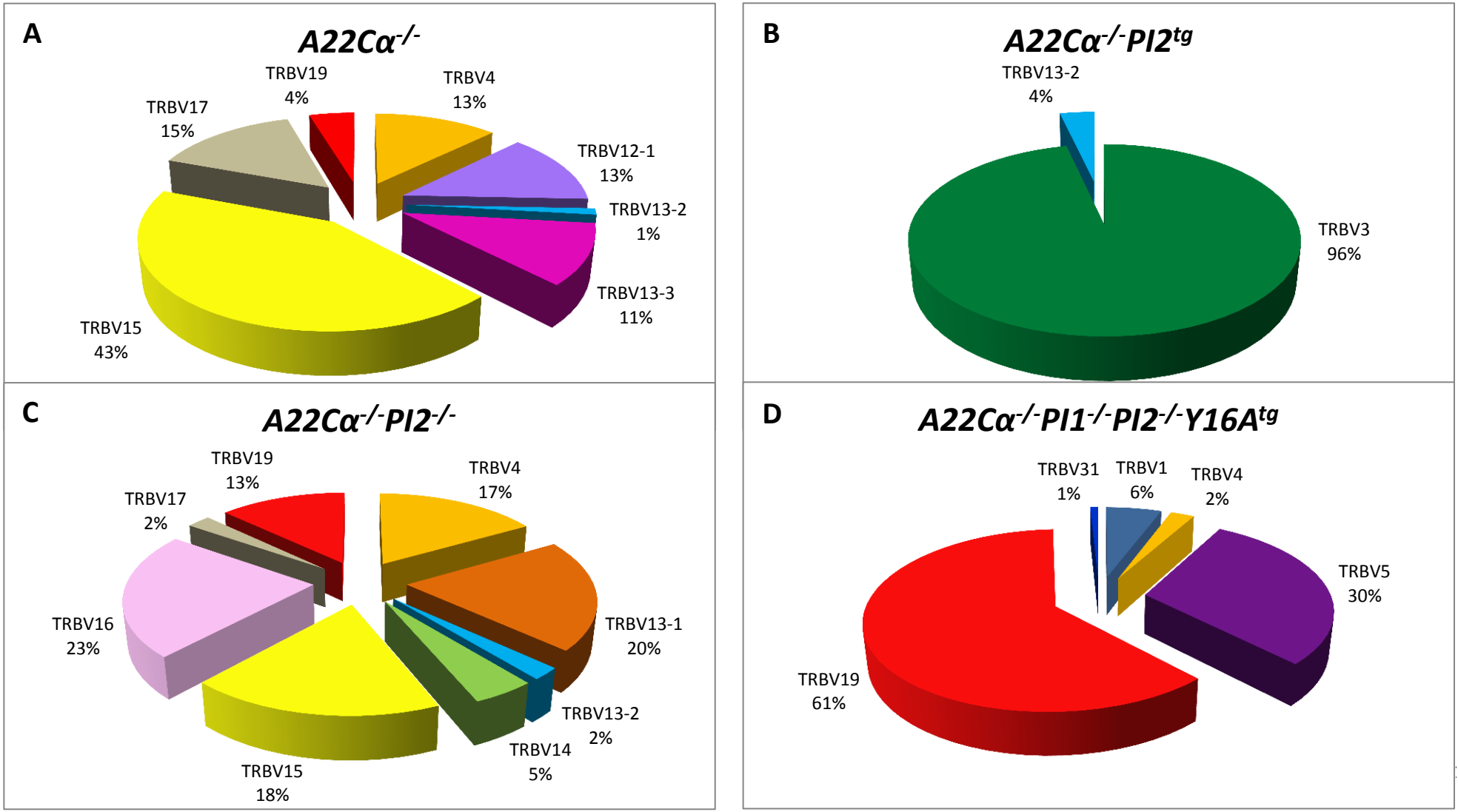

TRBJ CHAIN	STRAIN FOUND IN	PROPORTION (%)
TRBJ1-1	*A22Cα*$^{-/-}$	17.29
	A22Cα$^{-/-}$*PI2*^{tg}	3.57
	A22Cα$^{-/-}$*PI2*$^{-/-}$	19.08
TRBJ1-3	*A22Cα*$^{-/-}$*PI2*$^{-/-}$	2.41
TRBJ1-6	*A22Cα*$^{-/-}$*PI2*^{tg}	96.43
TRBJ2-1	*A22Cα*$^{-/-}$	12.68
	A22Cα$^{-/-}$*PI1*$^{-/-}$*PI2*$^{-/-}$*Y16A*^{tg}	38.62
TRBJ2-2	*A22Cα*$^{-/-}$	0.58
	A22Cα$^{-/-}$*PI1*$^{-/-}$*PI2*$^{-/-}$*Y16A*^{tg}	2.44
TRBJ2-3	*A22Cα*$^{-/-}$	12.97
	A22Cα$^{-/-}$*PI2*$^{-/-}$	12.94
TRBJ2-4	*A22Cα*$^{-/-}$*PI2*$^{-/-}$	20.61
	A22Cα$^{-/-}$*PI1*$^{-/-}$*PI2*$^{-/-}$*Y16A*^{tg}	28.46
TRBJ2-5	*A22Cα*$^{-/-}$	6.63
	A22Cα$^{-/-}$*PI2*$^{-/-}$	24.56
TRBJ2-7	*A22Cα*$^{-/-}$	49.86
	A22Cα$^{-/-}$*PI2*$^{-/-}$	20.39
	A22Cα$^{-/-}$*PI1*$^{-/-}$*PI2*$^{-/-}$*Y16A*^{tg}	30.49

TABLE 12: INSULIN B15-23 REACTIVE CD8^{+} T CELL RECEPTOR JOINING BETA CHAIN PROPORTIONS IN SINGLE CHAIN TRANSGENIC TRAV8-1*01 NOD MICE EXPRESSING VARYING PROINSULIN LEVELS

Taking into account the entire clonotyping results i.e. the CDR3 sequence for individual mice within a strain, there was clearly an expansion of different clonotypes associated with the insulin B15-23 reactive $CD8^+$ T cells. As TABLE 13 and TABLE 14 show, each mouse has a different clonal expansion regardless of proinsulin expression with only 1 identical sequence found between the *A22Cα*$^{-/-}$ mice (1 male and 1 female) and one male *A22Cα*$^{-/-}$*PI2*$^{-/-}$ mouse. This sequence was CASSLGGYEQY (highlighted in yellow), utilising TRBV15 and TRBJ2-7 and was the dominant clonotype within these mice. A similar clonotype to this sequence was found in a male *A22Cα*$^{-/-}$*PI2*$^{-/-}$ mouse; however, the single amino acid difference was for a different amino acid group (E to G, see TABLE 15). The only other identical sequence identified was CASSRVPGEQY (highlighted in orange) and was found in 2 male *A22Cα*$^{-/-}$ mice as a sub-dominant clonotype utilising TRBV17 and TRBJ2-7. 2 clonotypes with 1 amino acid substitution were also found within a male *A22Cα*$^{-/-}$ mouse. While one of these substitutions involves a similar amino acid substitution (V to A), the other substitution is different (S to G).

TABLE 15 shows that half of the single amino acid differences within the clonotype involved a similar valine to alanine substitution. Taking this into account identified 7 CDR3 sequences, which were shared or involved similar amino acid substitutions to another sequence.

All the other clonotypes were unique with each mouse exhibiting a different dominant clonotype. Due to time restraints, the *A22Cα*$^{-/-}$*PI1*$^{-/-}$ mice were not analysed.

STRAIN	GENDER	TRBV CHAIN	CDR3 SEQUENCE	TRBJ CHAIN	PROPORTION (%)	TOTAL SAMPLES
A22Cα$^{-/-}$	M	15	CASSLGGYEQY	2-7	47.78	43
		15	CASSQDRSNTEVF	1-1	27.78	25
		17	CASSRVPGEQY	2-7	22.22	20
		17	CASSRAPGEQY	2-7	1.11	1
		17	CAGSRVPGEQY	2-7	1.11	1
		12-1	CASLVETLY	2-3	48.89	44
		17	CASSRVPGEQY	2-7	32.22	29
		13-3	CASSDAWAGGQDTQY	2-5	21.11	19
		12-1	CASLAETLY	2-3	1.11	1
	F	15	CASSLGGYEQY	2-7	95.18	79
		13-2	CASGDWGGYQDTQY	2-5	4.82	4
		4	CASSFILGGYAEQF	2-1	54.32	44
		13-3	CASSDYGDANTEVF	1-1	23.46	19
		19	CASTRHHTEVF	1-1	19.75	16
		15	CASTGNTGQLY	2-2	2.47	2
A22Cα$^{-/-}$*PI2*^{tg}	F	3	CASRRDIYNSPLY	1-6	96.43	81.00
		13-2	CASGPGTGGFTEVF	1-1	3.57	3.00

TABLE 13: INSULIN B15-23 REACTIVE CD8^{+} T CELL RECEPTOR CDR3 CLONOTYPES FROM INDIVIDUAL SINGLE CHAIN TRANSGENIC TRAV8-1*01TRAJ9 NOD MICE EXPRESSING NORMAL LEVELS OF PROINSULIN OR OVER-EXPRESSING PROINSULIN 2

STRAIN	GENDER	TRBV CHAIN	CDR3 SEQUENCE	TRBJ CHAIN	PROPORTION (%)	TOTAL SAMPLES
A22Cα$^{-/-}$PI2$^{-/-}$	M	19	CASSIRESGAETLY	2-3	65.56	59
		17	CASSRDNTEVF	1-1	12.22	11
		16	CASSLVSQDTQY	2-5	11.11	10
		13-2	CASGDAVEQY	2-7	11.11	10
		15	CASSLGGYEQY	2-7	65.96	62
		15	CASSLGGYGQY	2-7	22.34	21
		13-1	CASRSGGTGNTLY	1-3	10.64	10
		13-1	CASRSGGPGNTLY	1-3	1.06	1
		16	CASSLDRNQNTLY	2-4	100.00	94
		14	CASSYRGPNQDTQY	2-5	100.00	21
	F	4	CASSHRGNTEVF	1-1	93.42	71
		4	CVSSHRGNTEVF	1-1	5.26	4
		4	CASSHRGNTEAF	1-1	1.32	1
		13-1	CASSEGQGGDTQY	2-5	98.77	80
		13-1	CAGSEGQGGDTQY	2-5	1.23	1
A22Cα$^{-/-}$PI1$^{-/-}$PI2$^{-/-}$Y16A^{tg}	M	19	CASSPAGSTLY	2-4	92.11	70
		4	CASSLTGNTGQLY	2-2	7.89	6
		5	CASSPDNYEQY	2-7	83.91	73.00
		1	CTCSADYAEQF	2-1	16.09	14.00
	F	19	CASSGDYAEQF	2-1	97.59	81
		31	CAWSLAGGGQY	2-7	2.41	2

TABLE 14: INSULIN B15-23 REACTIVE CD8^{+} T CELL RECEPTOR CDR3 CLONOTYPES FROM INDIVIDUAL SINGLE CHAIN TRANSGENIC TRAV8-1*01TRAJ9 NOD MICE DEFICIENT IN PROINSULIN 2 OR LACKING BOTH NATIVE PROINSULIN 1 AND PROINSULIN 2

STRAIN	GENDER	CDR3 SEQUENCE FROM MOUSE 1	CDR3 SEQUENCE FROM MOUSE 2	SIMILAR/ DIFFERENT	EXPLANATION OF SIMILARITY OR DIFFERENCE
A22Cα $^{-/-}$	M	CASSRVPGEQY*	CASSRAPGEQY	SIMILAR	VALINE & ALANINE BOTH HAVE NONPOLAR SIDE CHAINS
		CASSRVPGEQY*	CAGSRVPGEQY	DIFFERENT	SERINE HAS AN UNCHARGED POLAR SIDE CHAIN WHEREAS GLYCINE HAS A NONPOLAR SIDE CHAIN
		CASLVETLY	CASLAETLY	SIMILAR	VALINE & ALANINE BOTH HAVE NONPOLAR SIDE CHAINS
A22Cα $^{-/-}$ ***PI2*** $^{-/-}$	F	CASSHRGNTEVF	CVSSHRGNTEVF	SIMILAR	VALINE & ALANINE BOTH HAVE NONPOLAR SIDE CHAINS
		CASSHRGNTEVF	CASSHRGNTEAF	SIMILAR	VALINE & ALANINE BOTH HAVE NONPOLAR SIDE CHAINS
		CASSEGQGGDTQY	CAGSEGQGGDTQY	DIFFERENT	SERINE HAS AN UNCHARGED POLAR SIDE CHAIN WHEREAS GLYCINE HAS A NONPOLAR SIDE CHAIN
	M	CASSLGGYEQY**	CASSLGGYGQY	DIFFERENT	GLUTAMIC ACID HAS AN ACIDIC SIDE CHAIN WHEREAS GLYCINE HAS A NONPOLAR SIDE CHAIN
		CASRSGGTGNTLY	CASRSGGPGNTLY	DIFFERENT	THREONINE HAS AN UNCHARGED POLAR SIDE CHAIN WHEREAS PROLINE HAS A NONPOLAR SIDE CHAIN

TABLE 15: INSULIN B15-23 REACTIVE CD8^{+} T CELL RECEPTOR CDR3 CLONOTYPE AMINO ACID COMPARISON FROM INDIVIDUAL SINGLE CHAIN TRANSGENIC TRAV8-1*01TRAJ9 NOD MICE EXPRESSING NORMAL PROINSULIN LEVELS OR DEFICIENT IN PROINSULIN 2

*****This CDR3 sequence also appears in another male *A22Cα*$^{-/-}$ mouse.

****** This CDR3 sequence also appears in one male and one female *A22Cα*$^{-/-}$ mouse.

3.6 SPONTANEOUS DIABETES SEEN ONLY IN PROINSULIN 2 DEFICIENT SINGLE CHAIN TRANSGENIC TRAV8-1*01TRAJ9 NOD MICE

Having identified numerous clonotypes within the strains of mice, we asked whether any of these strains developed spontaneous autoimmune diabetes. Interestingly, no *A22Cα*$^{-/-}$ mice or *A22Cα*$^{-/-}$*PI2*^{tg} mice developed spontaneous autoimmune diabetes (n=20 males and females). However, as FIGURE 24 shows, 3/12 *A22Cα*$^{-/-}$*PI2*$^{-/-}$ male mice, but no females, developed spontaneous diabetes (p=0.0377). This onset was accelerated compared to polyclonal NOD female and male mice (10 weeks vs 17 and 19 weeks respectively) and reached 25% vs 88.89% and 16.67% respectively. While the highest incidence of diabetes was seen in the NOD female mice overall, comparing the male *A22Cα*$^{-/-}$*PI2*$^{-/-}$ and male NOD mice there is both an acceleration and an increase in incidence.

3.7 ALL SINGLE CHAIN TRANSGENIC TRAV8-1*01TRAJ9 NOD MICE DEVELOP INSULIN AUTO-ANTIBODIES WITH AGE

Mice at 4-7, 8-10 and 11-16 weeks of age were investigated for the presence of insulin auto-antibodies in the serum. As FIGURE 25 shows there are similar insulin autoantibody results between male and female mice at all ages and the different strains of mice. Interestingly, the *A22Cα*$^{-/-}$*PI1*$^{-/-}$*PI2*$^{-/-}$*Y16A*^{tg} mice had the fewest number of mice with insulin auto-antibodies at 4-7 weeks with only 1/6 female mice and 0/6 male mice seen to have insulin auto-antibodies. However, insulin autoantibody prevalence in these mice had increased to 5/5 female and 3/3 male mice by 11-16 weeks. All mice shown in FIGURE 25 are non-diabetic, however 3/4 male diabetic *A22Cα*$^{-/-}$*PI2*$^{-/-}$ mice were shown to have insulin auto-antibodies present (see appendix).

FIGURE 24: THE INCIDENCE OF SPONTANEOUS DIABETES IN SINGLE CHAIN TRANSGENIC TRAV8-1*01TRAJ9 NOD MICE DEFICIENT IN PROINSULIN 2 AND POLYCLONAL NOD MICE

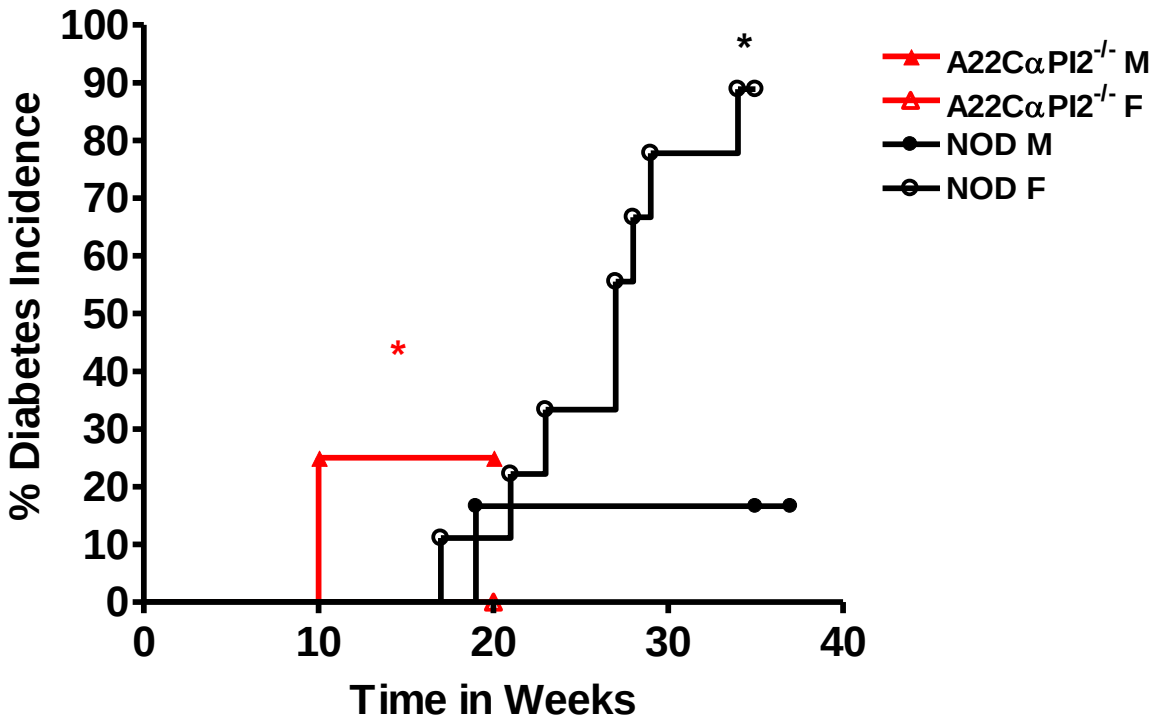

FIGURE 24: *A22Cα$^{-/-}$PI2$^{-/-}$* mice (12 males and 16 females) and NOD mice (6 males and 9 females) were placed into an observation group from weaning (3 weeks) and left to develop diabetes over a period of 20 weeks and 35-37 weeks respectively. Mice were tested bi-weekly for glycosuria and if positive were confirmed the next day by a blood glucose test. Diabetes was diagnosed only when the blood glucose level was above 13.9mmol/L. Data were then plotted using GraphPad Version 4 software. Survival curves were compared using a log rank test with significant differences at p=<0.05 between the *A22Cα$^{-/-}$PI2$^{-/-}$* male and female mice (* p=0.0377) and the NOD male and female mice (* p=0.0177).

FIGURE 25: THE PREVALENCE OF INSULIN AUTO-ANTIBODIES IN SINGLE CHAIN TRANSGENIC TRAV8-1*01TRAJ9 NOD MICE EXPRESSING VARYING PROINSULIN LEVELS

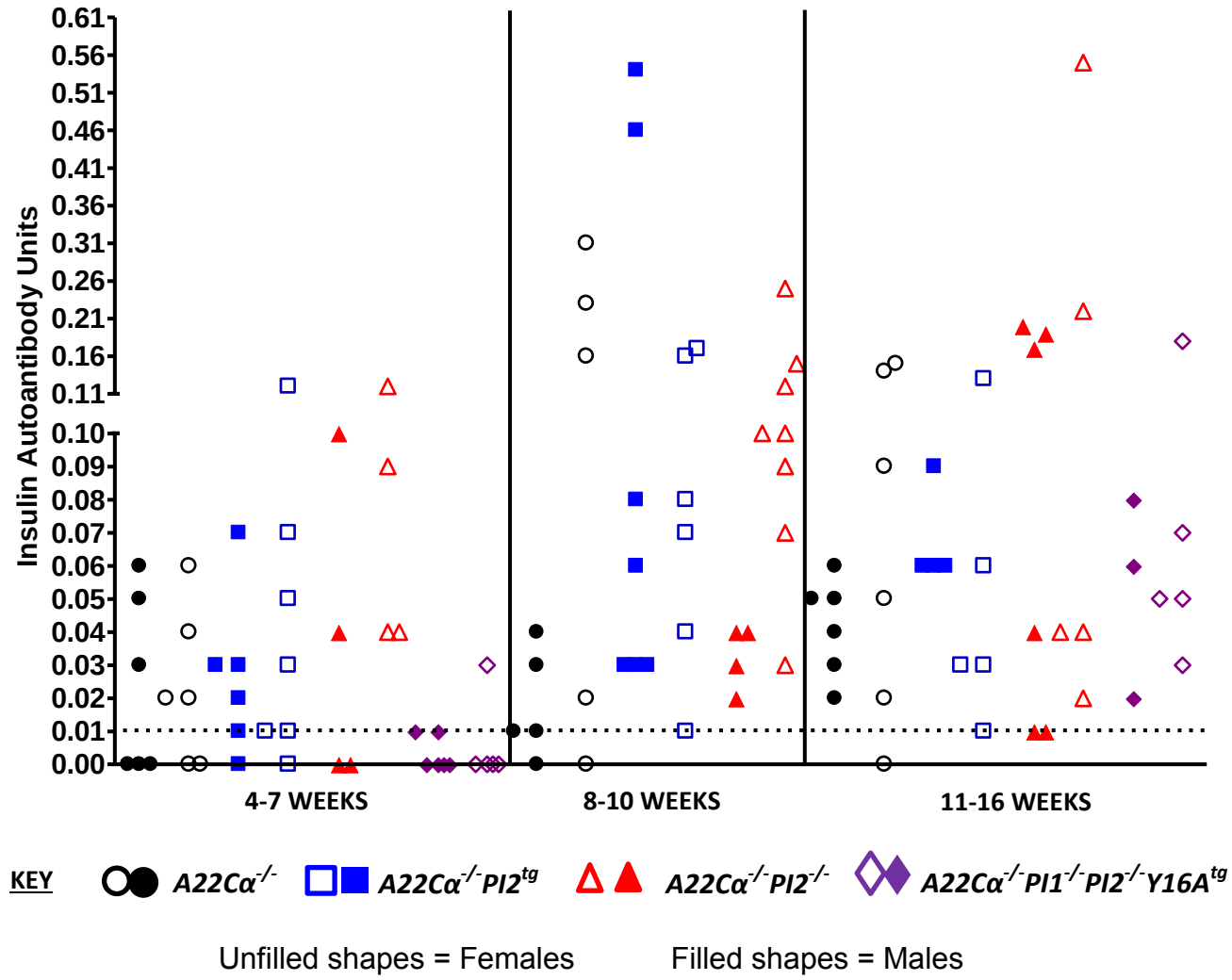

FIGURE 25: Serum was harvested from the blood from 4-7 week, 8-10 week (except the *A22Cα*$^{-/-}$*PI1*$^{-/-}$*PI2*$^{-/-}$*Y16A*^{tg} mice) and 11-16 week old mice. Insulin auto-antibodies were then measured in a competitive insulin radioimmunoassay. Data were then plotted using GraphPad Version 4 software. Each shape represents an individual mouse (n=3-8 per group), with males and females shown separately. Anything above the dotted line (over 0.0103) was deemed positive. Positivity was based on the mean plus 3 standard deviations from control C57BL/6 serum.

FIGURE 26: CD8^{+} T CELL AND B CELL INFILTRATION IN THE PANCREATIC ISLETS OF DIABETIC *A22Cα$^{-/-}$PI2$^{-/-}$* MICE

A

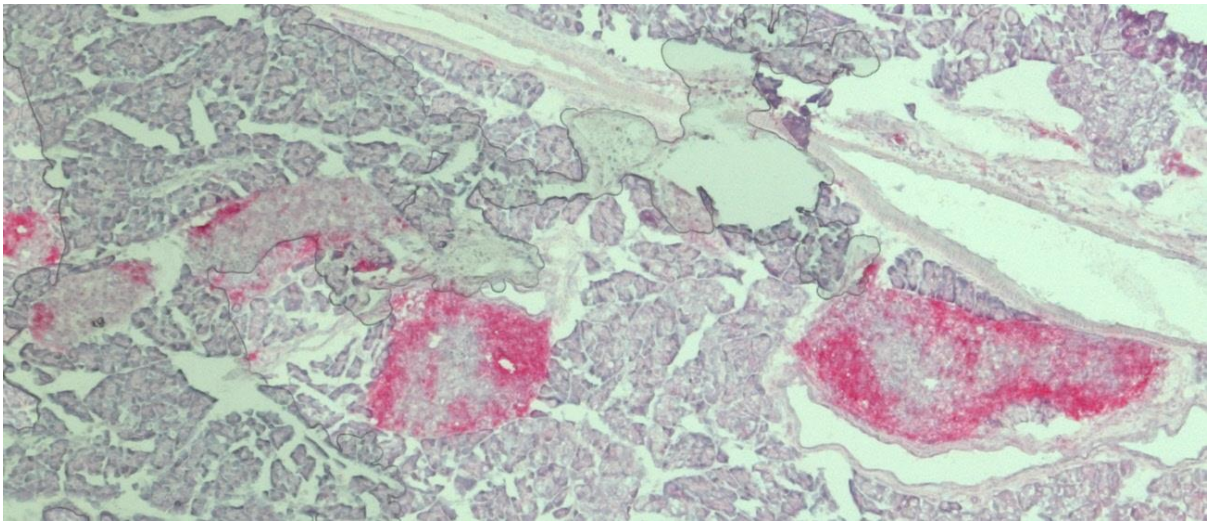

B

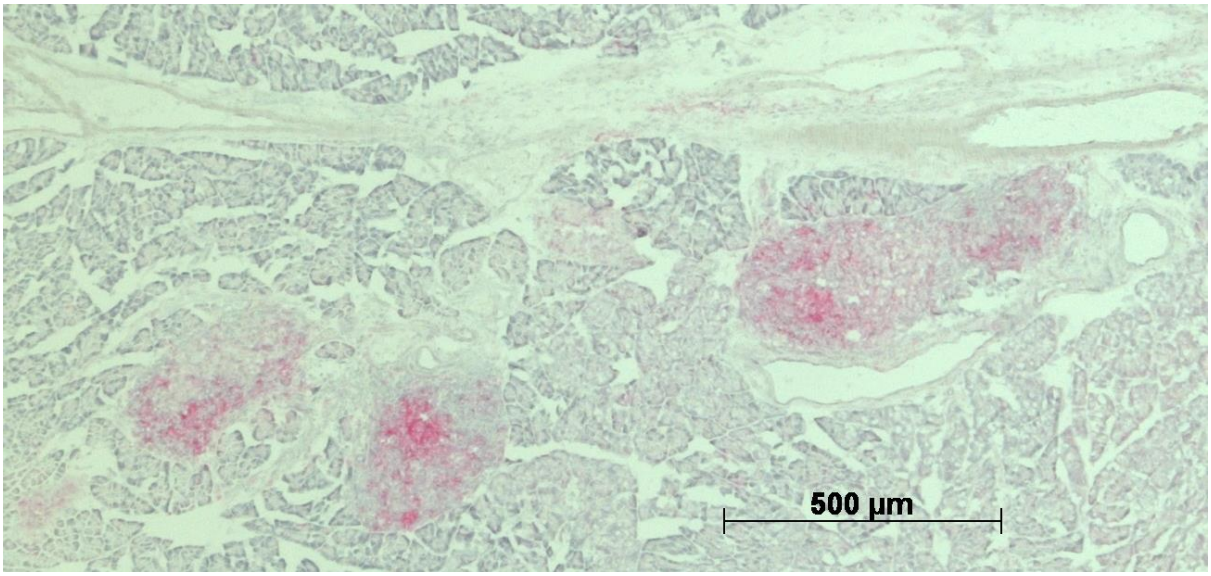

FIGURE 26: Pancreata were taken from male diabetic *A22Cα$^{-/-}$PI2$^{-/-}$* mice at 10 weeks and placed into PLP fixative overnight at 4°C. The next day samples were infused with 10% then 20% sucrose and frozen in OCT embedding matrix in an isopentane ice bath. 8µm sections were then cut and transferred onto histology slides. Sections were then stained for B220 (**A**) and CD8 (**B**) using biotinylated antibodies, which were detected using a streptavidin phosphatase. Slides were then counter-stained using haematoxylin and 1% ammonium chloride prior to dehydration in ethanol and Histo-clear. Coverslips were then mounted on the sections and once dry were imaged on an Olympus BX51 microscope using Axiovision LE Software (Zeiss).

3.8 PROINSULIN 2 DEFICIENT SINGLE CHAIN TRANSGENIC TRAV8-1*01TRAJ9 NOD MICE EXHIBITED GREATER INSULITIS

Observing that 25% of male Proinsulin 2 deficient mice only developed spontaneous diabetes, immunohistochemistry on frozen sections of pancreas was carried out to identify the degree on infiltration in the mice. As FIGURE 26 shows, both CD8 and B cell infiltration in *A22Cα*$^{-/-}$*PI2*$^{-/-}$ mice was detected. However, only a small number of islets were analysed for pancreatic infiltrating cells and therefore the level of infiltration can not be compared between the strains. However, further investigation is needed to identify the difference in infiltration in relation to proinsulin expression between the mice, while also identifying the TCRβ chains of those infiltrating T cells. This may suggest differences in T cell recruitment and therefore the provide evidence for why some mice lacking proinsulin 2 develop diabetes while others do not. In addition, a full natural history study of these mice, identifying when they develop infiltration, would be useful as it may indicate if proinsulin expression can alter how quickly the pancreas becomes infiltrated.

3.9 DISCUSSION

In this chapter, three principal findings are reported. Firstly, proinsulin expression affected the CD8$^+$ TRBV repertoire in mice that expressed a transgenic TCRα chain from an insulin-reactive CD8$^+$ T cell clone. In particular CD8$^+$TRBV19$^+$ cells were reduced significantly upon exposure to both proinsulin 1 and 2, while removing either proinsulin gene alone did not change the frequency of this population. Other TRBV changes were also noted, including proinsulin specific effects on TRBV29 and TRBV16, with age-specific increases seen with TRBV4 expression. Secondly, in those mice lacking proinsulin 1 or 2 there were significant increases in insulin B15-23-reactive CD8$^+$ T cells in the draining lymph node for the pancreas (PLN). However, thirdly, investigation of the CDR3β sequence of these cells identified minimal shared sequences between the different proinsulin-expressing strains with each mouse having an individual dominant clonotype.

This entire work takes into account thousands of data points and therefore when analysing the data for the TRBV repertoire work by ANOVA, it was decided to use

a stringent Bonferroni correction. This corrected for all the comparisons done, while also minimising any non-specific and spurious results. Therefore any data reported as significant at the p=<0.05 level, in fact had a p value of less than 0.0000022907, while significance reported at the p=<0.01 level related to a p value less than 0.0000004581. While this means there was a 5% or 1% probability of this result being found by chance, it is important to remember that while something may not reach statistical significance it may be biologically relevant. In other data analysed, such as the cell counts and tetramer data, the uncorrected values were reported, as strain comparisons only were performed. In addition, for H-2K^{d}-B15-23 peptide tetramer staining, the data were corrected by subtracting the background staining using an irrelevant tetramer control.

3.9.1 PROINSULIN EXPRESSION AND THE EFFECT ON CELL NUMBER

The baseline of proinsulin 1 and 2 expression in the polyclonal NOD mice (all the animal models used in this study were developed on the NOD genetic background), was measured using qPCR. As the data showed, proinsulin 1 and 2 were detectable at high levels in the islets, as expected. In the PLN, males had higher levels of proinsulin 1 and 2 than their female counterparts, even though they had similar levels of GAPDH. The result may suggest that the males express more proinsulin immunologically than the females, potentially providing more antigen to activate the T cells to cause diabetes, although this experiment needs to be repeated to draw this conclusion. In addition, the thymus was found to have low levels of proinsulin 1 and higher levels of proinsulin 2 with similar levels noted in males and females. This confirms previous findings suggesting proinsulin 2 is predominantly expressed within the thymus (Chentoufi and Polychronakos, 2002, Chentoufi et al., 2004, Palumbo et al., 2006); however, this study also shows minimal thymic proinsulin 1 expression. While some studies support proinsulin 1 expression in the thymus (Chentoufi and Polychronakos, 2002, Chentoufi et al., 2004, Palumbo et al., 2006), other studies report it is not present (Nakayama et al., 2005b). The presence of proinsulin 1 in the thymus is much discussed but from data generated here, it is clear there is a small amount present. In addition, the data shows there is more proinsulin 2 detectable than

proinsulin 1 in the periphery, which agrees with previous work (Chentoufi and Polychronakos, 2002, Chentoufi et al., 2004, Palumbo et al., 2006). Proinsulin 2 is known to be important from a tolerogenic perspective (French et al., 1997, Chentoufi and Polychronakos, 2002, Thébault-Baumont et al., 2003, Jaeckel et al., 2004); however, it is also important metabolically, as NOD mice lacking proinsulin 1 are protected from developing diabetes (Moriyama et al., 2003).

In our model we investigated whether the expression of proinsulin altered the total cell numbers. Although we had not expected any differences between the single chain transgenic strains, we found that the wildtype *A22Cα*$^{-/-}$ mice had fewer spleen cells than the *A22Cα*$^{-/-}$*PI1*$^{-/-}$*PI2*$^{-/-}$*Y16A*^{tg} mice at 4-7 weeks. This difference was not seen in the older 11-16 week group. Although it is possible that the age at which the mice were studied was responsible, it is unlikely as the average age for each strain was 4.3 and 4.7 weeks respectively. Therefore, it is more likely that this effect was proinsulin-specific; expression of both proinsulin 1 and 2 may have reduced the cell expansion in the periphery or may have induced deletion of T cells that have escaped negative selection. If this were the case, we would expect the Proinsulin 2 over-expressing mice to have even fewer cells. However, the numbers in the *A22Cα*$^{-/-}$*PI2*^{tg} mice were comparable, although this could be a compensatory change. As expected, at 11-16 weeks the polyclonal NOD mouse with no TCRα chain restriction had a greater number of thymic cells than the restricted TCRα mice. This is most likely to be due to the lack of TCR restriction in the polyclonal NOD mouse, producing many more different TCR combinations and thus the thymus atrophies at a slower pace, eventhough the NOD thymus is morphologically different and does not involute the same as other mice (Savino et al., 1991, Savino et al., 1993).

3.9.2 PROINSULIN EXPRESSION AND THE CD4/CD8 T CELL RATIO

Having restricted the TCRα chain from a proinsulin B15-23 reactive CD8$^+$ T cell we investigated the effect on the CD4$^+$ and CD8$^+$ T cell populations within these different proinsulin-expressing mice. At 4-7 weeks, the mice lacking proinsulin 2 (*A22Cα*$^{-/-}$*PI2*$^{-/-}$ mice) had a greater number of thymic CD4$^+$ T cells than the *A22Cα*$^{-/-}$*PI1*$^{-/-}$ mice and the *A22Cα*$^{-/-}$*PI1*$^{-/-}$*PI2*$^{-/-}$*Y16A*^{tg} mice, while having decreased

peripheral $CD8^+$ T cells when compared to the *A22Cα*$^{-/-}$*PI1*$^{-/-}$ mice. However, at 11-16 weeks the *A22Cα*$^{-/-}$*PI2*$^{-/-}$ mice have more $CD4^+$ T cells present in the spleen and MLN than the *A22Cα*$^{-/-}$*PI1*$^{-/-}$ mice, while still showing a trend in the reduction in $CD8^+$ T cells within the periphery compared to other strains. This difference in peripheral $CD8^+$ T cells in the *A22Cα*$^{-/-}$*PI2*$^{-/-}$ mice may be due to a lack of tolerance (lack of proinsulin 2) allowing auto-reactive $CD8^+$ T cells to escape into the periphery and begin infiltrating the islets, resulting in a peripheral reduction in the 4-7 week old mice, as some of these mice developed spontaneous autoimmune diabetes. As for the peripheral expansion of $CD4^+$ T cells in the *A22Cα*$^{-/-}$*PI1*$^{-/-}$*PI2*$^{-/-}$*Y16A*^{tg} mice compared to the *A22Cα*$^{-/-}$ mice, the *A22Cα*$^{-/-}$*PI2*^{tg} mice and the *A22Cα*$^{-/-}$*PI1*$^{-/-}$ mice in the spleen, PLN and MLN, this may be due to a lack of antigen enabling more auto-reactive $CD4^+$ T cells to develop (the original model was generated to study this), or it may be that $CD4^+$ T cells are more resilient and receive non-antigen survival signals or that they can expand better than the $CD8^+$ T cells. At 11-16 weeks, the *A22Cα*$^{-/-}$*PI2*$^{-/-}$ mice have a non-significant reduction in peripheral $CD8^+$ T cells and an increased proportion of $CD4^+$ T cells and therefore if those $CD8^+$ T cells are entering the pancreas (as observed in the single chain TRBV13-3 transgenic NOD mouse recognising a peptide of IGRP (Verdaguer et al., 1996, Lieberman et al., 2003)), this may allow the $CD4^+$ T cells to expand and "fill the space". It is noted, however, that in the TRBV13-3 transgenic NOD mouse, no differences were noted in the $CD4^+$ T cell population (Verdaguer et al., 1996).

3.9.3 THE EFFECT OF PROINSULIN ON TOTAL $CD8^+$ TCR REPERTOIRE

Within the $CD8^+$ T cell population, the TRBV repertoire was investigated for any proinsulin-specific biases. Interestingly TRBV19, the same TRBV chain utilised by the G9C8 clone, was reduced in proportion with age but only when proinsulin 1 and 2 were both present; when either or both genes were deleted, there was no effect on the population of $TRBV19^+CD8^+$ T cells. This reduction also correlated with the amount of antigen available, with a greater reduction seen in those mice which over-expressed proinsulin 2. TRBV19 has also been detected by clonotyping the $CD8^+$ T cells in the *A22Cα*$^{-/-}$ mice, the *A22Cα*$^{-/-}$*PI2*$^{-/-}$ mice and the

A22Cα$^{-/-}$*PI1*$^{-/-}$*PI2*$^{-/-}$*Y16A*^{tg} mice. The role of proinsulin 2 has been established and shown to promote tolerance (French et al., 1997, Chentoufi and Polychronakos, 2002, Jaeckel et al., 2004, Faideau et al., 2004) and when NOD mice are deficient in proinsulin 2, the mice develop accelerated diabetes (Thébault-Baumont et al., 2003). However, NOD mice lacking proinsulin 1 do not develop autoimmune diabetes, believed to be due to the expression of proinsulin 2, tolerising the T cells (Moriyama et al., 2003), although this has not been fully investigated. The reduction in proportion of TRBV19 is seen in the thymus where proinsulin 2 is believed to be predominantly expressed; however, there is even more reduction within the periphery where proinsulin 1 and 2 are expressed (Chentoufi and Polychronakos, 2002, Chentoufi et al., 2004, Palumbo et al., 2006). This data suggests that both proinsulin 1 and 2 have tolerogenic properties and that they synergistically eliminate or prevent the development of T cells with potentially auto-reactive TCRs. While proinsulin 1 and 2 were able to reduce the proportion of CD8^{+}TRBV19^{+} T cells by approximately 5% (in *A22Cα*$^{-/-}$ mice) in all tissues, fewer than 1% of the total CD8^{+} T cells were insulin B15-23 reactive with even fewer that expressed TRBV19 (shown by clonotyping). This non-specific TRBV19 deletion may be due to potential tolerance. If the TCR CDR1 and CDR2 regions are important for MHC recognition with CDR3 important for dictating specificity, the combination of TRBV19 with the transgenic TCRα chain could result in the deletion of those G9-like CD8^{+} T cells. The level of proinsulin expressed may also contribute to the deletion of T cells with different avidity for the p:MHC complex. Numerous studies have shown that auto-reactive T cells with high avidity are deleted within the thymus, providing the antigen is expressed, while lower avidity T cells can escape into the periphery (Zehn and Bevan, 2006, Enouz et al., 2012). The spectrum of TCR avidity may therefore correlate to the level of antigen i.e. the more antigen that is expressed, the more likely the T cell will interact with it and therefore those with a lower avidity may also be deleted over time. In addition, it is possible that the expression of proinsulin 2 may increase the presence and function of regulatory cells to eliminate more auto-reactive T cells, but there is currently no evidence for this.

Proinsulin-specific effects were also seen in TRBV29 expression in the *A22Cα*$^{-/-}$*PI2*$^{-/-}$ mice. At 11-16 weeks, there was an increased TRBV29 proportion present in these mice when compared to all other strains within the PLN. In addition, the *A22Cα*$^{-/-}$*PI1*$^{-/-}$ mice had statistically lower TRBV29 proportions in the thymus, spleen and MLN compared to the *A22Cα*$^{-/-}$*PI2*$^{-/-}$ mice, while the *A22Cα*$^{-/-}$*PI1*$^{-/-}$*PI2*$^{-/-}$*Y16A*^{tg} mice also had reduced TRBV29 proportions in the thymus and MLN in comparison to the *A22Cα*$^{-/-}$*PI2*$^{-/-}$ mice. TRBV29 has not been identified as a proinsulin B15-23 reactive TRBV chain from the clonotyping or from previous data in NOD mice and is therefore likely to have arisen from a balancing effect in the TRBV repertoire; when one TRBV chain increases another is reduced. However, TRBV16 is increased when one or both proinsulins are deficient, while those mice with normal or over-expressed proinsulin levels do not show any expansion for TRBV16^{+} CD8^{+} T cells. Unlike TRBV29, clonotyping has shown that insulin B15-23 reactive CD8^{+} T cell receptors utilise TRBV16 In the *A22Cα*$^{-/-}$*PI2*$^{-/-}$ mice. Therefore, this suggests when proinsulin is lacking; these auto-reactive CD8^{+} T cells are able to expand. TRBV4, on the other hand, expands in all strains, regardless of proinsulin expression, with age. Some of the increases in receptor frequencies are greater, whereas others show only a small rise. Therefore, there are factors in all these mice allowing the cells to expand. Interestingly, the clonotyping data revealed a proinsulin-reactive TRBV4^{+} clonotype. This expansion does not seem to be proinsulin-specific as it is seen in the *A22Cα*$^{-/-}$ mice, the *A22Cα*$^{-/-}$*PI2*$^{-/-}$ mice and the *A22Cα*$^{-/-}$*PI1*$^{-/-}$*PI2*$^{-/-}$*Y16A*^{tg} mice, which lack native proinsulin expression. Although it is possible that these T cells are selected on a different proinsulin epitope, present in all the mice, it is more likely the T cells expand because of cross-reactivity to a different antigen.

Investigating other TRBV repertoire differences revealed that the *A22Cα*$^{-/-}$*PI1*$^{-/-}$*PI2*$^{-/-}$*Y16A*^{tg} mice appeared to be more different than any of the other strains, particularly at 4-7 weeks with significant differences reported with respect to TRBV13-2/13-3, TRBV14, TRBV15 and TRBV26. However, with age, these differences became less pronounced and there were fewer TRBV repertoire differences between the strains. While some of these differences were observed

in all the tissues, others tend to differ, particularly within the thymus. Within the strains there were also differences between the thymus and periphery, which is not surprising, given that the thymus is constantly changing and forming new T cells with different TCRs and both the thymus and periphery have different mechanisms to control the TCR repertoire.

3.9.4 PROINSULIN EXPRESSION AND INSULIN B15-23 REACTIVE CD8$^+$ T CELLS

Given that these mice only have a restricted TCRα chain, but not TCRβ chain, and therefore a more polyclonal repertoire than TCRαβ transgenic mice, the proportion of those T cells that recognise insulin B15-23 are low and at similar levels to a polyclonal NOD mouse. This may suggest that this TCRα chain is utilised by many TCRs to recognise insulin B15-23 and would therefore agree with the Eisenbarth group suggesting that the TCRα chain is vital for insulin autoimmunity, although they investigated this in CD4$^+$ T cells (Kobayashi et al., 2008, Nakayama et al., 2012). However, it is also possible that forcing the TCR to have this TCRα chain also increases the proportion of the insulin B15-23 reactive T cells. When proinsulin 2 is deficient, these mice have significantly elevated levels of insulin B15-23 reactive CD8$^+$ T cells in the thymus, spleen and PLN. Given that proinsulin 2 is important in central tolerance (Chentoufi and Polychronakos, 2002, Chentoufi et al., 2004, Faideau et al., 2004, Palumbo et al., 2006), it is not surprising that the auto-reactive T cells are increased in these mice. Interestingly, in the PLN, the proinsulin 1 deficient mice also have increased proportions of proinsulin B15-23 reactive CD8$^+$ T cells, providing further evidence that both proinsulin 1 and 2 may be important in tolerising auto-reactive T cells.

3.9.5 PROINSULIN EXPRESSION AND THE TCRβ CHAIN REPERTOIRE OF INSULIN B15-23 REACTIVE CD8$^+$ T CELLS

By sorting these insulin B15-23 reactive CD8$^+$ T cells and sequencing their CDR3β sequences, we learnt a number of important things. Firstly, while we may have expected TRBV19 to be predominantly expressed, it was only expressed in a small number of mice and was one of 14 TRBV chains utilised by the auto-reactive repertoire. This may be explained, as mentioned earlier, by the TCRα chain having greater importance in dictating insulin autoimmunity. Secondly, there was only 1

shared sequence between the strains and 1 other within a strain detected. Although more mice should be examined, the data shows that each mouse has its own individual clonal expansion. This is interesting as it illustrates how complex the interactions are in shaping the auto-reactive TCR repertoire. This data may also suggest a reason as why only some male proinsulin 2 deficient mice develop diabetes, because if one dominant clonotype can expand, it may be able to surmount the threshold of activation, leading to β cell specific destruction and the onset of autoimmune diabetes. However, the question to ask would be - what is driving that expansion of these individual clonotypes? One possibility addressed in Chapter 5, is the role of microbiota in the gut, which may influence the capabilities of these clonotypes to expand through molecular mimicry or in directly through the microbiota altering the metabolism and therefore changing the level of insulin produced. It could also be due to a diminished regulatory response in controlling the auto-reactive T cells; however, in the G9C8 transgenic mice, there were no additional regulatory populations found causing the lack of diabetes (Wong et al., 2009). However, the G9C8 transgenic mice also had a restricted TCRβ chain, whereas in the mice in this study, the TCRα chain can pair with any endogenous TCRβ chain and therefore direct comparison may not be applicable here. It is worth noting that the $CD4^+$ T cells are also forced to have the same TCR that originates in a $CD8^+$ T cell and therefore, in these single chain transgenic mice, the normal function of $CD4^+$ T cells may be impeded and they may not function as normal polyclonal $CD4^+$ T cells.

Previous investigations of islet-infiltrating TRBV repertoire in NOD mice, indicated that TRBV12 coupled with TRBJ2-6 was important (Berschick et al., 1993); however, while TRBV12 was detected in this study, it was seen in association with TRBJ2-3. The same report also suggested TRBV13 was important, which is not surprising, given that this is the most common TRBV chain in the NOD mouse; however, they showed that there was no selection pressure on the TRBJ chain, similarly to this work. In addition, while data in the Bio-Breeding diabetes prone rat and Lewis rat showed treatment with anti-TRBV14 monoclonal antibodies was able to reduce and prevent autoimmune diabetes (Liu et al., 2012), it may also be

useful in the NOD mouse, as TRBV14 was the TCR found as the only insulin B15-23 reactive clone in a male *A22Cα*$^{-/-}$*PI2*$^{-/-}$ mouse. The previously published clonotyping data also revealed different TRBV chains associated with other auto-reactive clones in diabetes. In addition to TRBV19, utilised by the insulin B15-23 reactive G9C8 clone (Wong et al., 1996, Wong et al., 1999), TRBV1 was utilised by the AI4 T cell clone that recognises the insulin A chain (DiLorenzo et al., 1998, Lamont et al., 2014), TRBV16 was utilised by the NY8.2 T cell clone (Nagata et al., 1994b), TRBV13-3 was utilised by the IGRP reactive NY8.3 CD8^{+} T cell clone (Nagata et al., 1994b, Lieberman et al., 2003) and TRBV13 was used by the islet-reactive YNK1.3 T cell (Yoneda et al., 1997). While these clones used other TCRα chains and other TRBJ chains, except the G9C8 clone, a limited number of TRBV chains are found. This raises an interesting question as to whether some TCRβ chains form TCRs that are more auto-reactive, or even more promiscuous than others, or even that the level of proinsulin expression may be enough to drive other auto-reactive T cells to develop. However, it is important to clarify that the CDR3β repertoire work in this study refers solely to insulin B15-23 reactivity.

The difference in immunodominance seen in each mouse from the CDR3β data may have arisen due to a difference in the amount of antigen present. In viral studies, the viral dose is associated with a change in the immunodominance and avidity of the T cell as well as antigen presentation and the number of viral reactive CD8^{+} T cells (Luciani et al., 2013). In relation to this work, metabolic insulin is dependent on the level of blood glucose, which can be affected by diet, exercise and environmental factors, which are different in each mouse. Therefore, individual mice may have different blood glucose levels, which result in increased insulin secretion, which in turn may provide additional antigen for presentation. The increase in insulin secretion may alter the immunodominance and avidity of those T cells present, enabling 25% of those male proinsulin 2 deficient mice to develop autoimmune diabetes.

3.9.6 PROINSULIN EXPRESSION AND THE DEVELOPMENT OF INSULIN AUTOIMMUNITY AND DIABETES

As mentioned, only a small proportion of male *A22Cα*$^{-/-}$*PI2*$^{-/-}$ mice develop autoimmune diabetes. However, all mice regardless of proinsulin expression have detectable insulin auto-antibodies present and therefore exhibit insulin autoimmunity; however, this does not seem to be affected by the level of proinsulin expression. Insulin auto-antibodies in NOD mice are associated with islet inflammation but are not predictive of diabetes development (Robles et al., 2003). Interestingly, previous work had shown NOD mice that lack native proinsulins but express the mutated Y16A transgene do not have any islet auto-antibodies (Nakayama et al., 2005a). However, in the presence of a restricted TCRα chain, the *A22Cα*$^{-/-}$*PI1*$^{-/-}$*PI2*$^{-/-}$*Y16A*^{tg} mice have detectable insulin auto-antibodies suggesting that this TCR chain may be important in inducing insulin autoimmunity and islet inflammation.

The only TCRα chain transgenic mice here that developed spontaneous autoimmune diabetes, lacked proinsulin 2 and when the TCRα chain was not restricted in NOD mice, they develop accelerated diabetes with nearly 100% incidence in males and females (Thébault-Baumont et al., 2003, Moriyama et al., 2003). This acceleration, due to a lack of proinsulin 2, may also explain the earlier onset of diabetes in the *A22Cα*$^{-/-}$*PI2*$^{-/-}$ mice, which would enable high avidity auto-reactive T cells to escape. As discussed the different dominant clonotypes may predispose/prevent those mice from developing diabetes. Unusually, there was a gender difference in diabetes development in these *A22Cα*$^{-/-}$*PI2*$^{-/-}$ mice. While there were no gender differences in total TRBV repertoire, these T cells within these strains may function differently or may be better controlled. Interestingly, in data discussed in the fifth chapter, we noted males tended to have a higher blood glucose level than their female counterparts and when challenged with glucose in an intra-peritoneal glucose tolerance test, they appeared to take longer to return to normal. One may speculate that this difference could result in a greater amount of insulin being produced and therefore more antigen available to activate the T cells in the males; however, these experiments have not been done.

Investigation of the islet infiltrating T cells within the pancreas revealed some infiltration of CD4, CD8 and B cells in the islets. However, the degree of infiltration was quite small and the frequency of islets in the *A22Cα*$^{-/-}$*PI2*$^{-/-}$ male mice was also reduced when compared to other strains. This is similarly seen in the G9 TCR transgenic mice deficient in PI2 (Terri Thayer, personal communication, manuscript in progress). This may suggest that the mice may be insulin resistant, although we are yet to formally test this with an insulin tolerance test (see Chapter 5), or that proinsulin 2 is important for islet development.

3.9.7 SUMMARY

Together, this data highlights that proinsulin expression is capable of altering the total and insulin B15-23 reactive TRBV repertoire and that these cells may have different functional capabilities given that 25% male *A22Cα*$^{-/-}$*PI2*$^{-/-}$ mice develop diabetes. This has also raised questions as to the nature of factors other than antigen that may affect the development of the auto-reactive repertoire, in addition to the roles of both proinsulin 1 and 2 in shaping this repertoire.

In this work, the TRBV repertoire, and more specifically, the CDR3β repertoire of insulin B15-23 reactive CD8^{+} T cells has been investigated. However, the functional capabilities of these cells in the different proinsulin environments have not been addressed in this chapter. As only 25% of the male *A22Cα*$^{-/-}$*PI2*$^{-/-}$ mice develop diabetes, this warrants further investigation. In the next chapter, we ask what is the role of proinsulin expression in shaping the function of these insulin B15-23 reactive CD8^{+} T cells?

CHAPTER 4: THE EFFECT OF PROINSULIN EXPRESSION ON THE FUNCTION OF PROINSULIN-SPECIFIC CD8$^+$ T CELL RESPONSES IN SINGLE CHAIN TRANSGENIC TRAV8-1*01TRAJ9 NOD MICE EXPRESSING VARYING LEVELS OF PROINSULIN 1 AND 2

4.1 AIMS, RATIONALE AND HYPOTHESIS

Having investigated the repertoire of these insulin-specific CD8$^+$ T cells, the question remained about if and how proinsulin expression affected the way the cells functioned.

In the OT-1 RIPmOva model, the investigators showed that the CD8$^+$ T cells escape negative selection. By expressing the ovalbumin antigen in Listeria and then infecting the mice with the antigen-expressing Listeria, the OT-1 cells became activated and caused diabetes (Zehn and Bevan, 2006, Zehn et al., 2009, Enouz et al., 2012). In addition, in this artificial self-antigen model, they showed that the T cells could become activated by weak interactions at a similar, or lower, affinity/avidity threshold to that used during thymic negative selection, but that strong and maintained TCR interactions were needed to enable the CD8$^+$ T cells to expand (Zehn et al., 2009, Enouz et al., 2012). However, this model utilises a foreign antigen expressed as a self-antigen. Here, we studied how auto-reactive CD8$^+$ T cells developed and became activated in response to their native antigen.

In a separate project using the transgenic G9C8 mice, whereby all the T cells express both the TCRα and β chain from the insulin B15-23 specific CD8$^+$ T cell clone, functional differences in the G9C8 CD8$^+$ T cells were found dependent on how much proinsulin was expressed (Terri Thayer, personal communication, manuscript in preparation). While the thymus was important, to some extent, the periphery had a greater role in continuing to shape the functional abilities of these T cells and their ability to respond to cognate peptide. The CD8$^+$ T cells, which developed in the G9C8 mice that lacked both proinsulin 1 and 2 but had a mutant proinsulin expressed (Y16A transgene), showed that on encounter with insulin peptide, they responded significantly faster and stronger than the G9C8

$CD8^+$ T cells that developed in proinsulin 1 and 2 sufficient mice. The G9C8 T cells from G9C8 transgenic mice lacking proinsulin 2 responded at levels between the mutant proinsulin mice and the wild type mice. Therefore, this indicated the importance of cognate antigen expression shaping the diabetogenic potential of an insulin-specific $CD8^+$ T cell.

As discussed in Chapter 3, 25% of TCRα chain transgenic male mice lacking proinsulin 2 (*A22Cα*$^{-/-}$*PI2*$^{-/-}$ mice) developed spontaneous autoimmune diabetes, suggesting functional differences in the insulin B15-23-specific $CD8^+$ T cells. This was similar to the diabetes incidence in male G9C8 transgenic mice discussed above. In this current study, as discussed in the previous chapter, there were multiple TCRs capable of recognising insulin B15-23 in the TCRα restricted mice and therefore the functional ability of these cells warrants investigation, as some may have had stronger or weaker functional avidities (i.e. the overall strength of the interaction between the TCR and p:MHC) than the clonotypic G9C8 TCR.

Hypothesis:

Alterations in endogenous proinsulin expression will alter the functional ability of the insulin B15-23-reactive $CD8^+$ T cells.

Aim:

To assess the functional abilities, of the insulin B15-23 specific $CD8^+$ T cells, both *in vitro* and *in vivo*, in single chain transgenic TRAV8-1*01TRAJ9 NOD mice expressing variable levels of proinsulin.

4.2 *IN VITRO* ASSESSMENT OF THE FUNCTION OF DIRECTLY *EX VIVO* ISOLATED CD8+ T CELLS FROM SINGLE CHAIN TRANSGENIC TRAV8-1*01TRAJ9 NOD MICE EXPRESSING VARIABLE LEVELS OF PROINSULIN

$CD8^+$ T cells were isolated from mice expressing native proinsulin (*A22Cα*$^{-/-}$ mice), those over-expressing proinsulin 2 (*A22Cα*$^{-/-}$*PI2*^{tg}), those lacking proinsulin 2 (*A22Cα*$^{-/-}$*PI2*$^{-/-}$) and those deficient in native proinsulin 1 and 2 (*A22Cα*$^{-/-}$*PI1*$^{-/-}$*PI2*$^{-/-}$ *Y16A*^{tg}) to assess their potential to recognise insulin B15-23 peptide and denatured whole insulin, directly *ex vivo*. The methods used to investigate this included ^{3}H-thymidine incorporation proliferation assays, cytokine ELISAs and cytotoxicity assays. Due to time restrictions, no current functional data was obtained for the *A22Cα*$^{-/-}$*PI1*$^{-/-}$ mice.

4.2.1 INSULIN B15-23-REACTIVE CD8+ T CELL PROLIFERATIVE RESPONSES TO INSULIN B15-23 PEPTIDE OR DENATURED WHOLE INSULIN WERE NOT DETECTED IN WHOLE CD8+ T CELL POPULATIONS IN SINGLE CHAIN TRANSGENIC TRAV8-1*01TRAJ9 NOD MICE EXPRESSING VARYING LEVELS OF PROINSULIN

In order to assess the functional capabilities of these insulin-reactive $CD8^+$ T cells from the various TCRα chain transgenic mice upon cognate peptide recognition, $CD8^+$ T cells were initially isolated and cultured *in vitro* to determine their proliferative ability through using a ^{3}H-thymidine incorporation assay. As FIGURE 27 shows, the proliferative responses to both insulin B15-23 peptide and denatured whole insulin were variable both within the spleen and the PLN. Insulin B15-23 peptide responses were seen at low levels at 0.04μg/ml insulin B15-23 peptide in all mice in the spleen but only the *A22Cα*$^{-/-}$*PI2*$^{-/-}$ mice and the *A22Cα*$^{-/-}$*PI1*$^{-/-}$*PI2*$^{-/-}$*Y16A*^{tg} mice showed any response in the PLN. However, overall the counts per minute (cpm) were very low except at 5μg peptide in the *A22Cα*$^{-/-}$ *PI1*$^{-/-}$*PI2*$^{-/-}$*Y16A*^{tg} mice. As for whole denatured insulin responses, these were lower than with peptide in the spleen and PLN with the *A22Cα*$^{-/-}$*PI1*$^{-/-}$*PI2*$^{-/-}$*Y16A*^{tg} mice showing a greater response at 25μg/ml. In the PLN, the *A22Cα*$^{-/-}$*PI2*$^{-/-}$ mice show a larger response at 0.2μg/ml, which was maintained at similar levels regardless of the concentration of denatured insulin. The data shown is from 1 experiment; however, upon repeating and changing the peptide concentrations (titrating down as far as 0.0016μg/ml) the results were highly variable and failed

to show the same trend more than once. In all experiments, although no or low proliferative responses were seen to insulin or insulin peptide, α-CD3 stimulation was used as a positive control and on each occasion, proliferation was seen (cpm: 50,000+). In addition, a G9C8 $CD8^+$ T cell control was also included, showing proliferation of these cells with counts reaching as high as 120,000 cpm. Therefore, the proliferation responses were deemed too low in these single chain TRAV8-1*01TRAJ9 mice to detect the insulin-specific responses.

4.2.2 NO DETECTABLE CYTOKINE RESPONSES TO INSULIN B15-23 PEPTIDE OR DENATURED WHOLE INSULIN FROM WHOLE $CD8^+$ T CELL POPULATIONS IN SINGLE CHAIN TRANSGENIC TRAV8-1*01TRAJ9 NOD MICE EXPRESSING VARYING LEVELS OF PROINSULIN

Supernatants were removed 48 hours post-incubation from the proliferation assays and assessed for MIP-1β and IFN-γ production. As FIGURE 28 shows, MIP-1β cytokine responses were produced at very low levels with a peptide concentration specific increase seen in all strains in response to denatured insulin and insulin B15-23 peptide; however the *A22Cα*$^{-/-}$*PI2*^{tg} mice exhibited no increase in response to insulin B15-23 peptide. The greatest MIP-1β production was seen in the *A22Cα*$^{-/-}$*PI2*$^{-/-}$ mice reaching 175pg/ml at 25μg/ml of insulin B15-23 peptide. The *A22Cα*$^{-/-}$*PI2*$^{-/-}$ mice also produced the greatest amount of IFN-γ reaching approximately 1750pg/ml at 5μg of insulin B15-23 peptide. All other strains had much lower IFN-γ production in response to insulin B15-23 peptide compared to the *A22Cα*$^{-/-}$*PI2*$^{-/-}$ mice. MIP-1β and IFN-γ responses were very similar in all the strains in response to insulin B15-23 peptide or to denatured insulin, although the *A22Cα*$^{-/-}$*PI2*$^{-/-}$ mice had lower responses to denatured whole insulin when compared to insulin B15-23 peptide responses. The data in FIGURE 28 shows the best responses detected but similar to the proliferation data, upon repeating these experiments and varying the peptide concentration; the results were variable and followed no general trend.

FIGURE 27: $CD8^+$ T cells were isolated from the spleen (**A** & **B**) or the PLN (**C** & **D**) by magnetic negative selection from mice aged 4-8 weeks. T cells were then cultured with bone-marrow derived DCs at a 10:1 T cell:APC ratio with varying concentrations of Insulin B15-23 peptide (**A** & **C**) or denatured insulin (**B** & **D**). Cells were incubated at 37°C for 48 hours, then 120µl of supernatant was removed and 18.5KBq of thymidine was added to the plate which was incubated for a further 18 hours. Cells were then harvested onto a filter mat and counted in a Microbeta counter (Perkin Elmer). Mean data were then plotted using GraphPad Prism software where the counts per minute (cpm) were corrected for the background of proliferation without peptide.

FIGURE 27: THE EFFECT OF PROINSULIN EXPRESSION ON THE PROLIFERATIVE CAPABILITIES OF CD8^{+} T CELLS ISOLATED FROM THE SPLEEN OR PANCREATIC LYMPH NODE (PLN) FROM SINGLE CHAIN TRANSGENIC TRAV8-1*01TRAJ9 NOD MICE

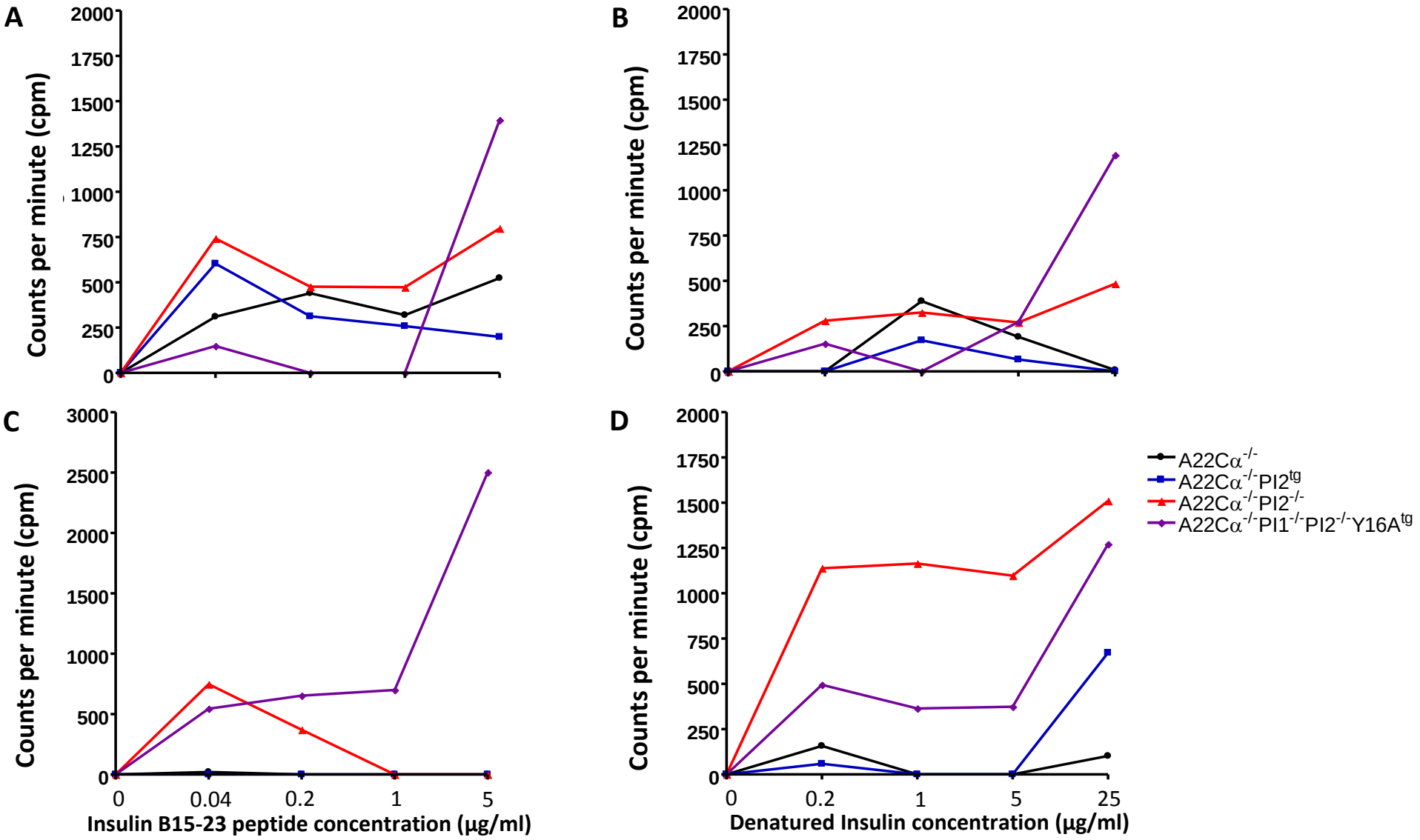

FIGURE 28: $CD8^+$ T cells were isolated from the PLN by magnetic negative selection from mice aged 4-8 weeks. T cells were then cultured with bone-marrow derived DCs at a 10:1 T cell:APC ratio with varying concentrations of Insulin B15-23 peptide (**A** & **C**) or denatured insulin (**B** & **D**). Cells were incubated at 37°C for 48 hours, then 120µl of supernatant was removed. Supernatants were tested for MIP-1β and IFN-γ production by ELISA (R&D Systems or BD ELISA kit). A plate reader was then used to detect the optical density (OD) values at a wavelength of 450nm with a reference at 570nm. Data were then plotted using GraphPad Prism Version 4 software where the OD values were used to generate a standard curve. The concentration of the samples were then calculated by a linear regression and corrected for the background without peptide.

FIGURE 28: THE EFFECT OF PROINSULIN EXPRESSION ON THE ABILITY TO PRODUCE PROINFLAMMATORY CYTOKINES IN RESPONSE TO DENATURED INSULIN AND INSULIN B15-23 PEPTIDE OF $CD8^+$ T CELLS ISOLATED FROM THE PANCREATIC LYMPH NODE (PLN) FROM SINGLE CHAIN TRANSGENIC TRAV8-1*01TRAJ9 NOD MICE

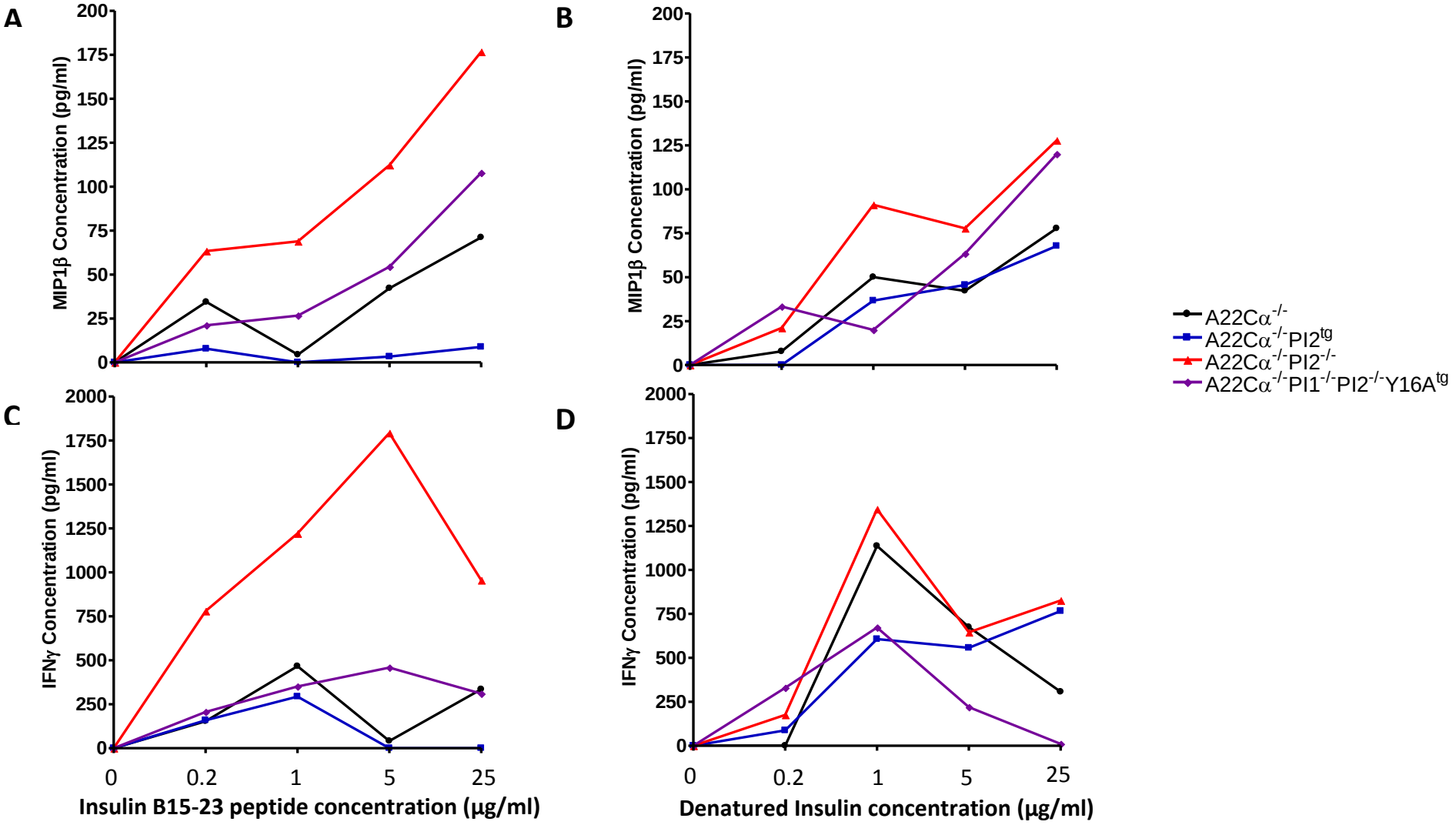

4.2.3 NO DETECTABLE INSULIN B15-23-REACTIVE CD8$^+$ T CELL CYTOTOXICITY IN RESPONSE TO INSULIN B15-23 PEPTIDE COATED P815 TARGETS FROM WHOLE CD8$^+$ T CELL POPULATIONS IN SINGLE CHAIN TRANSGENIC TRAV8-1*01TRAJ9 NOD MICE EXPRESSING VARYING LEVELS OF PROINSULIN

Having seen no clear evidence for proliferative responses, the T cells were tested in a cytotoxicity assay for their ability to kill target cells expressing Insulin B15-23 peptide. This assay utilised PKH-labelled P815 cells, a murine mastocytoma that expresses appropriate H-2K^d MHC to present insulin B15-23 as targets in a non-radioactive assay adapted from the assay by Lee-MacAry and colleagues (Lee-MacAry et al., 2001). As FIGURE 29 shows, the spontaneous lysis of the target cells (P815 cells) is low at approximately 5%. However, no T cells from any of the strains showed peptide-specific cytotoxicity with between 13-23% P815 lysis without peptide and between 12-25% with peptide. As discussed previously, repeating this experiment and altering the effector:target ratios and peptide concentrations yielded similar results to the data shown in FIGURE 29 where no consistent cytotoxicity was seen.

FIGURE 29: THE EFFECT OF PROINSULIN EXPRESSION ON THE CYTOTOXIC CAPABILITIES OF CD8$^+$ T CELLS ISOLATED FROM THE SPLEEN FROM SINGLE CHAIN TRANSGENIC TRAV8-1*01TRAJ9 NOD MICE

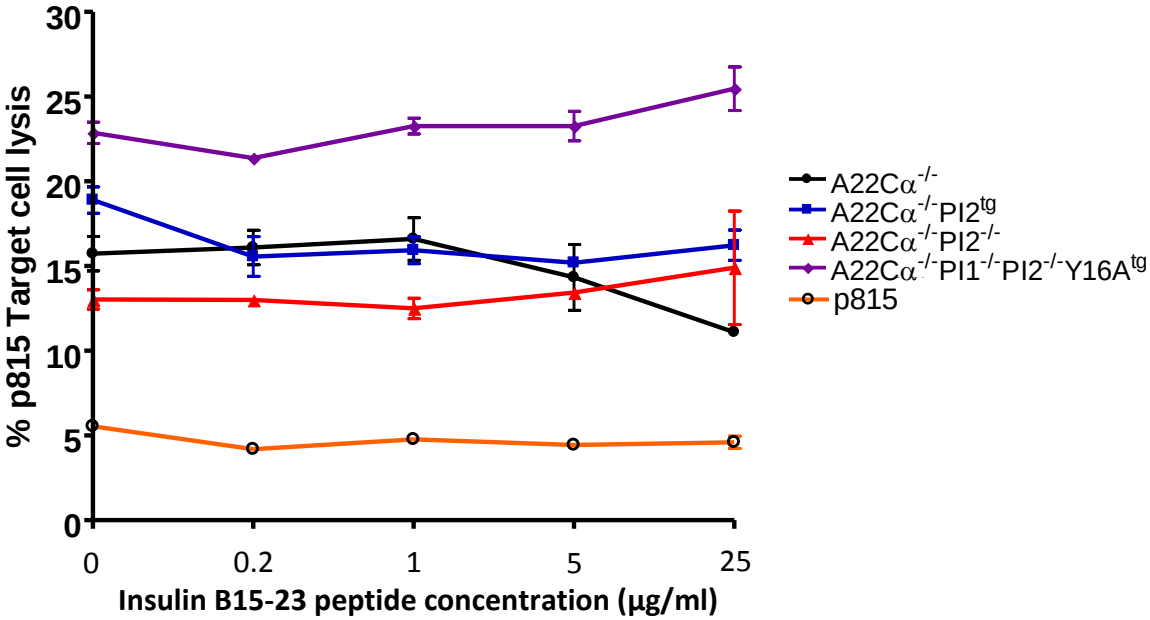

FIGURE 29: CD8$^+$ T cells were isolated from the spleen by magnetic negative selection from mice aged 4-8 weeks. T cells were then cultured with P815 cells at a 20:1 effector:target ratio with varying concentrations of Insulin B15-23 peptide. Cells were incubated overnight for 16 hours at 37°C. Cells were then measured on a BD FACS CANTO II flow cytometer with the addition of TOPRO (a viability dye) 20 seconds before cell acquisition on the cytometer. Data were then analysed using Flowjo Version 7.6.5 (gated on PKH$^+$TOPRO$^+$ P815s) and P815 lysis was plotted using GraphPad Prism 4 software.

4.3 *IN VIVO* ANTIGEN-SPECIFIC STIMULATION OF CD8+ T CELLS FROM SINGLE CHAIN TRANSGENIC TRAV8-1*01TRAJ9 NOD MICE EXPRESSING VARIABLE LEVELS OF PROINSULIN

As no insulin-specific functional responses were detected in the earlier assays where $CD8^+$ T cells were studied for insulin-specific responses directly *ex vivo*, $CD8^+$ T cell responses were then studied post-immunisation with insulin B15-23 peptide. $CD8^+$ T cells were then isolated for adoptive transfer into NOD mice over-expressing proinsulin 2 (NOD$PI2^{tg}$), to amplify insulin-reactive $CD8^+$ T cell responses. In the NOD$PI2^{tg}$ mice, insulin-reactive T cells will proliferate wherever they encounter antigen-presenting cells, as the APCs constitutively express insulin on the MHCII promoter. This would provide insight into whether increased antigen and general inflammation were able to stimulate the insulin B15-23 reactive $CD8^+$ T cells *in vivo*.

4.3.1 INSULIN B15-23 PEPTIDE IMMUNISATIONS BOOST THE T CELL COMPARTMENT NON-SPECIFICALLY BUT FAIL TO ACTIVATE INSULIN B15-23-REACTIVE CD8+ T CELLS

In order to stimulate the insulin B15-23-reactive $CD8^+$ T cells, young TCRα chain transgenic mice aged 4-8 weeks were immunised with 50µg CpG mixed with, 50µl Incomplete Freund's Adjuvant with or without 50µg Insulin B15-23 peptide. Control mice were immunised with CpG and IFA without peptide. The mice were analysed at various times post-immunisation including days 2, 4, 6 and 9. The results at post-immunisation day 2 (TABLE 16) and day 6 (TABLE 17) showed the most difference and therefore day 4 and 9 results have not been shown. As TABLE 16 and TABLE 17 show, between days 2 and 6 post-immunisation, there was an increase in the proportion of $CD8^+$ T cells present in the ILN (Inguinal lymph node), PLN (pancreatic lymph node) and spleen in both controls and those receiving peptide. This increase in $CD8^+$ T cells was also associated with an increase in CD44 expression, while those cells expressing CD69 decreased by approximately 50%. In addition by day 6 post-immunisation, the total proportion of Insulin B15-23-reactive $CD8^+$ T cells was increased, with a small increase seen in those expressing CD44 and CD69, however, these still remained at low levels (less than 5%). However, there was no difference between the controls and those receiving peptide. The *A22C*$\alpha^{-/-}$*PI2*$^{-/-}$ mice and the *A22C*$\alpha^{-/-}$*PI1*$^{-/-}$*PI2*$^{-/-}$*Y16A*^{tg} mice

receiving peptide had the greatest proportion of Insulin B15-23 reactive $CD8^+$ T cells present. However, there were also no differences seen in responses between peptide-immunised and the control mice.

4.3.2 NO PROLIFERATION OF TOTAL $CD8^+$ T CELLS ISOLATED FROM SINGLE CHAIN TRAV8-1*01TRAJ9 TRANSGENIC NOD MICE EXPRESSING VARIOUS PROINSULIN LEVELS UPON ADOPTIVE TRANSFER INTO NOD MICE OVER-EXPRESSING PROINSULIN 2

A different method of amplifying any insulin-reactive $CD8^+$ T cells from these single chain TRAV8-1*01TRAJ9 transgenic mice expressing variable levels of proinsulin was tested next. $CD8^+$ T cells were harvested from the spleen from immunised or control mice expressing different proinsulin levels and stained with CFDA-SE. $15x10^6$ $CD8^+$ T cells from each strain were then intravenously injected into NOD*PI2*^{tg} mice that over-express proinsulin 2 under the MHCII promoter. Peripheral tissues including spleen, PLN and MLN were then harvested 4 days post-transfer. As TABLE 18 shows there were no detectable differences in the proportion of total $CD8^+$ T cells in the NOD*PI2*^{tg} mice between the cells from control mice and cells from immunised mice. However, there was greater variation in total $CD8^+$ T cell proportion within the PLN (9.72-11.3% in the spleen, 16.5-21.4% in the PLN and 17-18.8% in the MLN). In addition, while the proportions are small and the data was not significantly different, in the NOD*PI2*^{tg} mice receiving cells from immunised *A22Cα*$^{-/-}$ donor mice, there were more $CD8^+$CFDA-SE^+ T cells present in all tissues compared with the NOD*PI2*^{tg} mice receiving control *A22Cα*$^{-/-}$ donor cells. This trend was reversed in both the NOD*PI2*^{tg} mice receiving *A22Cα*$^{-/-}$*PI2*^{tg} or *A22Cα*$^{-/-}$*PI1*$^{-/-}$*PI2*$^{-/-}$*Y16A*^{tg} cells where there were fewer $CD8^+$CFDA-SE^+ T cells present in all tissues when the labelled donor cells were derived from mice that had been immunised prior to transfer. Functional investigations of these transferred $CD8^+$ T cells by observing CD69 upregulation revealed no proportional differences between the control and the immunised cells with few cells expressing CD69. As mentioned previously, there were no differences between the cells from the different strains.

STRAIN	TISSUE	CD8+ (%)	CD8+TETRAMER+ (%)	CD8+CD44+ (%)	*CD8+CD44+TETRAMER+ (%)	CD8+CD69+ (%)	*CD8+CD69+TETRAMER+ (%)
***A22Cα*$^{-/-}$**	ILN	37.7	0.28	5.34	1.3	11.5	0.85
Control	PLN	40.5	2.33	4.05	3.5	11.5	3.01
	SPLEEN	25.3	0.83	8.44	1.21	13.4	1.41
***A22Cα*$^{-/-}$**	ILN	37.85	0.455	4.495	1.455	13.65	0.435
Imm	PLN	40.45	0.64	3.795	0.905	10.975	0.715
	SPLEEN	25.75	0.345	7.94	0.935	11.62	0.39
***A22Cα*$^{-/-}$**	ILN	36.4	0	6.63	0	7.16	0.38
***PI2*^{tg}**	PLN	36.5	0.13	5.27	0	4.4	0
Control	SPLEEN	27.8	0.56	7.24	0.02	4.91	0.31
***A22Cα*$^{-/-}$**	ILN	36.45	0.5	4.725	1.3	13.235	1.18
***PI2*^{tg}**	PLN	36.1	1.105	4.67	1.095	7.38	1.505
Imm	SPLEEN	24.6	0.79	8.645	1.915	8.02	0.86
***A22Cα*$^{-/-}$*PI2*$^{-/-}$**	ILN	29.4	0	9.83	0	5.84	0
	PLN	31.4	0.21	5.61	0.98	3.62	0.65
Control	SPLEEN	14.6	0.22	16.2	0.05	4.61	0
***A22Cα*$^{-/-}$*PI2*$^{-/-}$**	ILN	35.7	0.17	7.08	0.8	7.8	0.34
	PLN	31.4	0.88	6.78	0.47	6.27	0.24
Imm	SPLEEN	22.5	0.01	11.9	1.65	7.43	1.47
***A22Cα*$^{-/-}$*PI1*$^{-/-}$*PI2*$^{-/-}$*Y16A*^{tg}**	ILN	28.4	0.2	4.51	0.28	6.57	0
	PLN	30.9	1	5.59	1.15	4.02	0.8
Control	SPLEEN	23.8	0.51	9.67	1.11	4.77	1.22
***A22Cα*$^{-/-}$*PI1*$^{-/-}$*PI2*$^{-/-}$*Y16A*^{tg}**	ILN	30.9	0.11	5.205	0.89	9.54	0.52
	PLN	30.7	0.31	5.665	0.615	6.525	0.41
Imm	SPLEEN	23.45	0.48	9.66	1.03	6.85	1.11

TABLE 16: THE EFFECT OF INSULIN B15-23 IMMUNISATION ON TOTAL AND INSULIN B15-23-REACTIVE CD8$^+$ T CELLS 2 DAYS POST-IMMUNISATION FROM THE SPLEEN, INGUINAL LYMPH NODE (ILN) AND PANCREATIC LYMPH NODE (PLN) IN SINGLE CHAIN TRANSGENIC TRAV8-1*01TRAJ9 NOD MICE EXPRESSING VARIABLE PROINSULIN LEVELS

*CD8$^+$CD44$^+$TETRAMER$^+$ T cells (%) refers to the percentage of the CD8$^+$CD44$^+$ T cells (%) that were tetramer positive. Likewise, the CD8$^+$CD69$^+$TETRAMER$^+$ T cells (%) refers to the percentage of the CD8$^+$CD69$^+$ T cells (%) that were tetramer positive.

NOTE: Control refers to mice not receiving peptide (n=1 per group), whereas Imm, short for immunised, refers to those mice receiving peptide (n=2 per group).

STRAIN	TISSUE	CD8+ (%)	CD8+TETRAMER+ (%)	CD8+CD44+ (%)	*CD8+CD44+TETRAMER+ (%)	CD8+CD69+ (%)	*CD8+CD69+TETRAMER+ (%)
A22Cα$^{-/-}$	ILN	55.7	1	19.2	1.01	6.34	1.28
Control	PLN	51.7	2.03	11.5	1.76	3.52	2.16
	SPLEEN	31.9	1.54	21.5	1.01	2.65	0.64
A22Cα$^{-/-}$	ILN	54.55	0.395	15.95	0.2	5.675	0.485
Imm	PLN	53.4	1.695	12.45	1.47	5.04	1.535
	SPLEEN	32.65	0.11	22.5	0.25	3.175	0
A22Cα$^{-/-}$PI2^{tg}	ILN	52.1	1.44	13.3	1.41	4.96	1.64
Control	PLN	51.6	0.43	9.89	0.26	3.27	0.58
	SPLEEN	31.2	0	19.4	0	2.09	0
A22Cα$^{-/-}$PI2^{tg}	ILN	53.7	0	12.9	0	4.24	0
Imm	PLN	54.4	1.4	8.95	1.63	2.96	1.82
	SPLEEN	33.9	0	15.6	0	1.7	0
A22Cα$^{-/-}$PI2$^{-/-}$	ILN	37	1.09	15.7	1.75	1.75	1.45
Control	PLN	38.5	0	13.1	0	2.78	0
	SPLEEN	20.5	1.77	19.1	0	0.894	0
A22Cα$^{-/-}$PI2$^{-/-}$	ILN	42.2	2.27	19.5	3.88	1.91	4.22
Imm	PLN	39.4	0.57	9.84	2.72	1.87	1.83
	SPLEEN	19.6	2.8	24.1	2.44	0.901	5
A22Cα$^{-/-}$PI1$^{-/-}$	ILN	47.8	1.9	23.8	1.59	4.92	1.62
PI2$^{-/-}$Y16A^{tg}	PLN	38.2	1.87	15.3	1.75	2.92	1.55
Control	SPLEEN	21	0.63	30.3	0.42	1.82	0.47
A22Cα$^{-/-}$PI1$^{-/-}$	ILN	46.6	1.52	23.5	1.32	4.87	1.385
PI2$^{-/-}$Y16A^{tg}	PLN	45.05	1.345	11.9	1.195	2.82	1.655
Imm	SPLEEN	24.75	1.92	20.85	1.76	2.23	2.95

TABLE 17: THE EFFECT OF INSULIN B15-23 IMMUNISATION ON TOTAL AND INSULIN B15-23-REACTIVE CD8$^+$ T CELLS 6 DAYS POST-IMMUNISATION FROM THE SPLEEN, INGUINAL LYMPH NODE (ILN) AND PANCREATIC LYMPH NODE (PLN) IN SINGLE CHAIN TRANSGENIC TRAV8-1*01TRAJ9 NOD MICE EXPRESSING VARIABLE PROINSULIN LEVELS

*CD8$^+$CD44$^+$TETRAMER$^+$ T cells (%) refers to the percentage of the CD8$^+$CD44$^+$ T cells (%) that were tetramer positive. Likewise, the CD8$^+$CD69$^+$TETRAMER$^+$ T cells (%) refers to the percentage of the CD8$^+$CD69$^+$ T cells (%) that were tetramer positive.

NOTE: Control refers to mice not receiving peptide (n=1 per group), whereas Imm, short for immunised, refers to those mice receiving peptide (n=2 per group).

DONOR	TISSUE	$CD8^+$ (%)	$CD8^+CFDA^+$ (%)	$CD8^+CFDA+CD69^+$ (%)
A22Cα$^{-/-}$ **Control**	SPLEEN	11.3	0.406	4.2
	PLN	16.5	0.502	3.91
	MLN	17	0.438	2.56
A22Cα$^{-/-}$ **Imm**	SPLEEN	10.65	1.16	4.01
	PLN	18.6	1	3.18
	MLN	17.85	1.03	2.92
A22Cα$^{-/-}$PI2^{tg} **Control**	SPLEEN	9.72	1.13	4.14
	PLN	21	1.32	2.51
	MLN	18.8	1.15	1.8
A22Cα$^{-/-}$PI2^{tg} **Imm**	SPLEEN	10.95	0.779	4.24
	PLN	21	0.978	3.67
	MLN	18.65	0.754	7.94
A22Cα$^{-/-}$PI1$^{-/-}$PI2$^{-/-}$Y16A^{tg} **Control**	SPLEEN	11.1	0.577	3.39
	PLN	21.4	0.676	1.79
	MLN	17.4	0.586	1.35
A22Cα$^{-/-}$PI1$^{-/-}$PI2$^{-/-}$Y16A^{tg} **Imm**	SPLEEN	11.6	0.348	2.34
	PLN	18.7	0.442	2.22
	MLN	17.3	0.353	0.938

TABLE 18: THE EFFECT OF INSULIN B15-23 IMMUNISATION ON $CD8^+$ T CELL PROLIFERATION AND ACTIVATION FROM SINGLE CHAIN TRANSGENIC TRAV8-1*01 NOD MICE EXPRESSING VARIOUS PROINSULIN LEVELS POST-ADOPTIVE TRANSFER INTO NOD*PI2^{tg}* MICE OVER-EXPRESSING PROINSULIN 2

NOTE: Control refers to mice not receiving peptide, whereas Imm, short for immunised, refers to those mice receiving peptide. Data above represents the mean from 2 NOD*PI2^{tg}* mice per donor except the *A22Cα$^{-/-}$PI2^{tg}* Imm which is from a single mouse.

4.4 *EX VIVO* EXPANSION OF CD8$^+$TRBV19$^+$ T CELLS FROM SINGLE CHAIN TRAV8-1*01TRAJ9 TRANSGENIC NOD MICE EXPRESSING VARYING LEVELS OF PROINSULIN

In spite of detection of insulin-reactive CD8$^+$ T cells in the different proinsulin-expressing mice shown in Chapter 3, insulin-reactive responses were not seen either *in vivo* or *in vitro,* in proliferative or cytotoxic responses in the total CD8$^+$ T cell populations isolated from the single chain TRAV8-1*01TRAJ9 transgenic mice. Therefore, we embarked on a cloning procedure, by limiting dilution, to identify and expand those specific Insulin B15-23-reactive CD8$^+$ T cells. To do this CD8$^+$ T cells were sorted by flow cytometry for TRBV19$^+$ expression (using an anti-TCRVβ6 antibody) and grown in culture with irradiated splenocytes, bone-marrow derived DCs, Insulin B15-23 peptide and IL-2. IL-7 was also added to help promote survival (Tsuda et al., 2000). Cells were then replated at 1, 3, 10 and 30 cells per well using limiting dilution, enabling isolation of (oligo)clonal lines. A total of 40 cell lines were established through this cloning procedure (TABLE 19).

MOUSE STRAIN	CELL LINE ID
A22Cα$^{-/-}$	10E5, 10F3, 10F11, 10F12 30B6, 30B7, 30C2, 30C4, 30D7, 30F7, 30F11
A22Cα$^{-/-}$PI2$^{-/-}$	1C5, 1F9, 1H9 10F10 30A4, 30A5, 30A6, 30B9, 30D1, 30D4, 30D8, 30E2, 30F6, 30H3
A22Cα$^{-/-}$PI1$^{-/-}$PI2$^{-/-}$Y16A^{tg}	1G3 3D7, 3F11, 3G5 10A12, 10G2 30A8, 30B7, 30B8, 30D9, 30E2, 30E8, 30G3, 30G7, 30H1

TABLE 19: TOTAL OLIGOCLONAL CD8$^+$TRBV19$^+$ INSULIN B15-23-REACTIVE T CELL LINES ISOLATED

4.4.1 CD8$^+$TRBV19$^+$ T CELL LINES FROM SINGLE CHAIN TRAV8-1*01TRAJ9 TRANSGENIC NOD MICE EXPRESSING VARYING LEVELS OF PROINSULIN ARE CYTOTOXIC TO INSULIN B15-23 LOADED P815 TARGETS

In order to assess the function of the expanded oligoclonal CD8$^+$TRBV19$^+$ T cell lines, the cells were tested for their ability to destroy insulin B15-23 loaded P815

target cells. As FIGURE 30 shows, most of the oligoclonal lines were able to lyse Insulin B15-23 loaded targets specifically with cytotoxic activity seen at 0.2µg/ml of peptide and above. The expanded $CD8^+TRBV19^+$ T cells derived from the *A22Cα*$^{-/-}$ mice or *A22Cα*$^{-/-}$*PI1*$^{-/-}$*PI2*$^{-/-}$*Y16A*^{tg} mice responded similarly from around 0.2µg peptide with 70-90% lysis and 50-90% lysis at 5µg peptide respectively. Interestingly, the *A22Cα*$^{-/-}$*PI2*$^{-/-}$ 1F9 oligoclonal line (30B) responded at a lower concentration of 0.04µg/ml peptide and is the most sensitive oligoclonal line. While the *A22Cα*$^{-/-}$*PI2*$^{-/-}$ 1F9, 30D4 and 30A6 lines responded similarly to the other strains, the oligoclonal lines 1C5, 30B9 and 30D8 respond much more weakly. In addition, the *A22Cα*$^{-/-}$*PI2*$^{-/-}$ 30H3 line peaked at 1µg/ml peptide (~40% lysis) prior to a decreased cytotoxic response at 5µg/ml peptide.

4.4.2 $CD8^+TRBV19^+$ T CELL LINES FROM SINGLE CHAIN TRAV8-1*01TRAJ9 TRANSGENIC NOD MICE EXPRESSING VARYING LEVELS OF PROINSULIN PRODUCE PROINFLAMMATORY CYTOKINES IN RESPONSE TO INSULIN B15-23 PEPTIDE PRESENTATION

The cytotoxicity results showed that many oligoclonal lines responded specifically to peptide, and were further tested for production of proinflammatory MIP-1β and IFN-γ cytokines. FIGURE 31 shows the highest secreting cytokine oligoclonal lines for both MIP-1β (A) and IFN-γ (B). Oligoclonal lines *A22Cα*$^{-/-}$ 10F3, *A22Cα*$^{-/-}$*PI2*$^{-/-}$ 1H9, 30D1 and 30E2 and *A22Cα*$^{-/-}$*PI1*$^{-/-}$*PI2*$^{-/-}$*Y16A*^{tg} 30G7 showed high cytokine production for both MIP-1β and IFN-γ. However, some oligoclonal lines secreted more MIP-1β than IFN-γ and vice versa. Interestingly, more oligoclonal lines derived from *A22Cα*$^{-/-}$*PI2*$^{-/-}$ mice produced higher concentrations of IFN-γ and more oligoclonal lines derived from *A22Cα*$^{-/-}$*PI1*$^{-/-}$*PI2*$^{-/-}$*Y16A*^{tg} mice produced higher concentrations of MIP-1β. Similarly to the cytotoxicity results, the oligoclonal lines produced cytokines at either 0.2 or 1µg/ml of peptide. All oligoclonal results for MIP-1β or IFN-γ production are shown in TABLE 20 and TABLE 21 respectively. This data shows that all oligoclonal lines, regardless of strain origin, had similar cytokine responses.

FIGURE 30: $CD8^+TRBV19^+$ T cells were isolated from *A22Cα*$^{-/-}$ mice (**A**), *A22Cα*$^{-/-}$ *PI2*$^{-/-}$ mice (**B**) or *A22Cα*$^{-/-}$*PI1*$^{-/-}$*PI2*$^{-/-}$*Y16A*^{tg} mice (**C**) by flow cytometric sorting using a BD FACS ARIA. These cells were then expanded *ex vivo* with the addition of IL-2, IL-7 and 1µg/ml of Insulin B15-23 peptide and supported by irradiated splenocytes and bone-marrow derived DCs. Expanded cells were then removed, washed three times, counted and then cultured with P815 cells at a 10:1 effector:target ratio with varying concentrations of Insulin B15-23 peptide. Cells were incubated overnight for 16 hours at 37°C. Cells were then run on a BD FACS CANTO II flow cytometer with the addition of TOPRO-3 (a viability dye) 20 seconds before each tube was run. Data were then analysed using Flowjo Version 7.6.5 (gated on PKH^+TOPRO^+ P815 cells) and P815 lysis was corrected for the background (using 0µg/ml) and results analysed using GraphPad Prism 4.

FIGURE 30: THE CYTOTOXIC CAPABILITIES OF CD8$^+$TRBV19$^+$ T CELLS EXPANDED *EX VIVO* FROM SINGLE CHAIN TRAV8-1*01TRAJ9 TRANSGENIC NOD MICE EXPRESSING VARIOUS LEVELS OF PROINSULIN

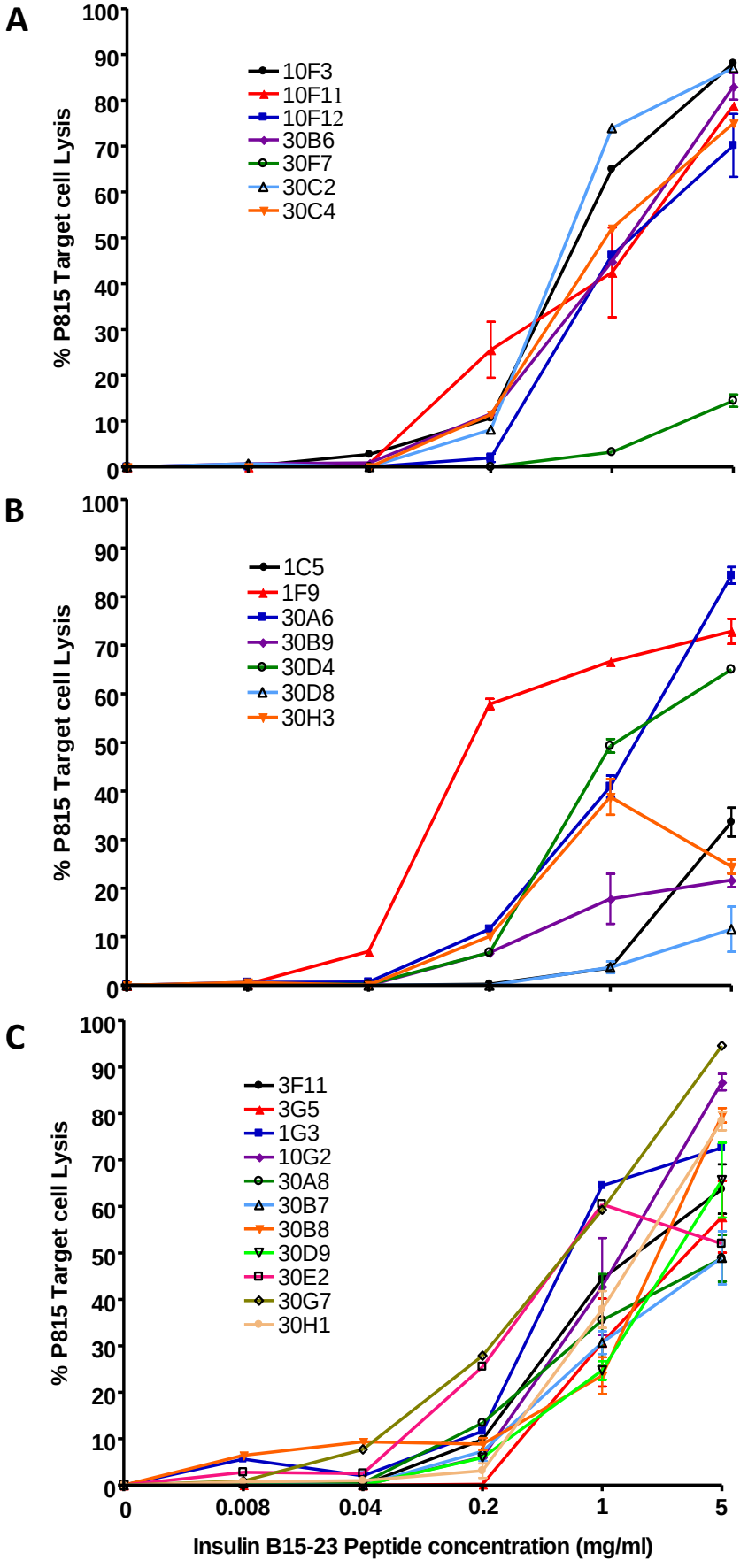

FIGURE 31: $CD8^+TRBV19^+$ T cells were isolated from *A22Cα*$^{-/-}$ mice, *A22Cα*$^{-/-}$*PI2*$^{-/-}$ mice or *A22Cα*$^{-/-}$*PI1*$^{-/-}$*PI2*$^{-/-}$*Y16A*^{tg} mice by flow cytometric sorting using a BD FACS ARIA. These cells were then expanded *ex vivo* with the addition of IL-2, IL-7 and 1µg/ml of Insulin B15-23 peptide and supported by irradiated splenocytes and bone-marrow derived DCs. Expanded cells were then removed, washed three times, counted and then cultured with bone-marrow derived DCs at a 10:1 T cell:APC ratio with varying concentrations of Insulin B15-23 peptide. Cells were then incubated at 37°C for 48 hours then supernatant was removed. Supernatants were tested for MIP-1β (**A**) and IFN-γ (**B**) production by ELISA. A plate reader was then used to detect the optical density (OD) values at a wavelength of 450nm with a reference at 570nm. Data were then plotted using GraphPad Prism 4 where the OD values were used to generate a standard curve. The concentration of the samples were then calculated by a linear regression and corrected for the background cytokine production in the absence of peptide.

FIGURE 31: MIP1β AND IFNγ CYTOKINE PRODUCTION FROM CD8^{+}TRBV19^{+} T CELLS EXPANDED *EX VIVO* FROM SINGLE CHAIN TRAV8-1*01TRAJ9 TRANSGENIC NOD MICE EXPRESSING VARIOUS LEVELS OF PROINSULIN

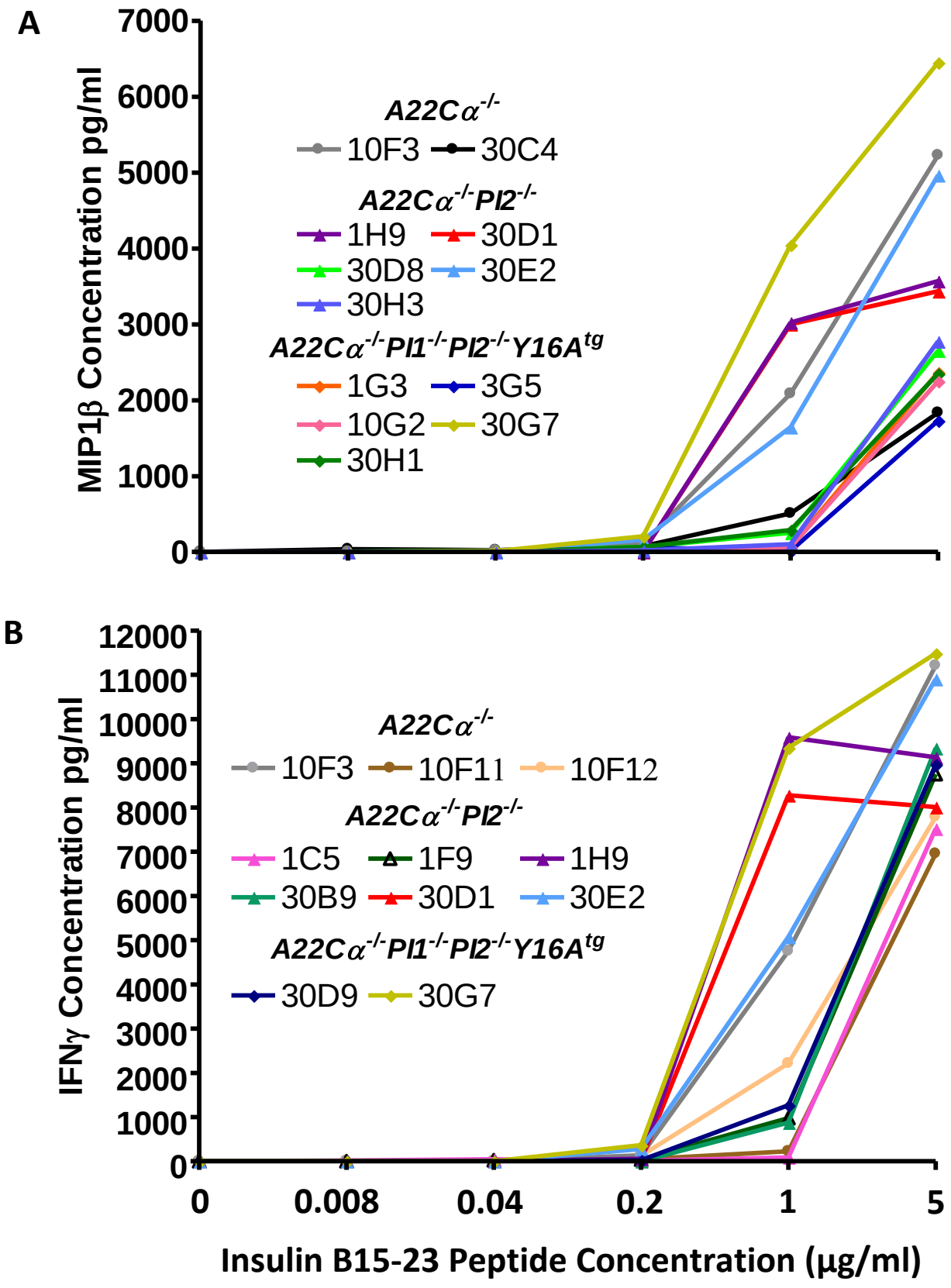

DONOR STRAIN	ID	INSULIN B15-23 PEPTIDE CONCENTRATION (µg/ml)			
		0.04	**0.02**	**1**	**5**
A22Cα$^{-/-}$	10F11	0.00	0.00	0.00	144.22
	10F12	0.00	0.00	17.67	413.45
	30B6	0.00	0.00	0.00	35.04
	30C2	6.60	22.45	269.34	**NT**
	30D7	11.12	11.12	48.91	211.21
	30F7	11.17	4.96	17.37	80.65
A22Cα$^{-/-}$PI2$^{-/-}$	1C5	0.00	0.00	0.00	40.00
	1F9	0.00	0.00	27.59	288.14
	30A6	9.24	9.24	50.17	**NT**
	30B9	0.00	0.00	0.00	226.10
	30D4	0.00	0.00	57.37	135.53
	30F6	0.00	0.00	0.00	151.18
A22Cα$^{-/-}$PI1$^{-/-}$PI2$^{-/-}$Y16A^{tg}	3F11	0.00	0.00	0.00	169.03
	30A8	0.00	0.00	0.00	213.70
	30B7	6.60	33.01	698.44	**NT**
	30B8	0.00	0.00	0.00	123.13
	30D9	0.00	0.00	0.00	306.75
	30E2	0.00	18.48	179.56	662.21

TABLE 20: MIP-1β CYTOKINE PRODUCTION FOR ALL OLIGOCLONAL CD8^{+}TRBV19^{+} T CELL LINES EXPANDED *EX VIVO* FROM SINGLE CHAIN TRAV8-1*01TRAJ9 TRANSGENIC NOD MICE EXPRESSING VARIOUS LEVELS OF PROINSULIN

NT = Not Tested at 5µg/ml of Insulin B15-23 peptide

DONOR STRAIN	ID	INSULIN B15-23 PEPTIDE CONCENTRATION (µg/ml)			
		0.04	**0.02**	**1**	**5**
A22Cα$^{-/-}$	30B6	0.00	0.00	275.14	5015.86
	30C2	0.00	0.00	393.77	**NT**
	30C4	0.00	141.59	1203.24	2210.29
	30D7	0.00	0.00	0.00	670.18
	30F7	0.00	0.00	32.52	2607.10
A22Cα$^{-/-}$PI2$^{-/-}$	30A6	0.00	0.00	23.29	**NT**
	30D4	0.00	0.00	239.22	2604.63
	30D8	0.00	169.61	1122.29	2656.61
	30F6	0.00	0.00	91.40	955.55
	30H3	0.00	0.00	691.16	446.06
A22Cα$^{-/-}$PI1$^{-/-}$PI2$^{-/-}$Y16A^{tg}	1G3	0.00	0.00	113.57	2368.02
	3F11	0.00	0.00	1109.66	2383.26
	3G5	0.00	0.00	45.08	1737.98
	10G2	0.00	0.00	116.69	2251.52
	30A8	0.00	0.00	391.80	2602.83
	30B7	0.00	0.00	1421.17	**NT**
	30B8	0.00	0.00	381.79	**NT**
	30E2	0.00	0.00	241.22	762.00
	30H1	0.00	0.00	51.31	2473.78

TABLE 21: IFN-γ CYTOKINE PRODUCTION FOR ALL OLIGOCLONAL CD8^{+}TRBV19^{+} T CELL LINES EXPANDED *EX VIVO* FROM SINGLE CHAIN TRAV8-1*01TRAJ9 TRANSGENIC NOD MICE EXPRESSING VARIOUS LEVELS OF PROINSULIN

NT = Not Tested at 5µg/ml of Insulin B15-23 peptide

4.4.3 *EX VIVO* EXPANSION OF CD8$^+$TRBV19$^+$ T CELLS FROM SINGLE CHAIN TRAV8-1*01TRAJ9 TRANSGENIC NOD MICE EXPRESSING VARYING LEVELS OF PROINSULIN IDENTIFY OLIGOCLONAL CD8$^+$ T CELL LINES THAT UTILISE TRBV19 IN CONJUNCTION WITH TRBJ2-3

Functional analysis had shown that some of the oligoclonal T cell lines responded better than others. In order to address whether these oligoclonal T cell lines were clonal or not, we investigated the TCR clonotype of these cells. As can be seen from TABLE 22 and TABLE 23, there are 9/20 clonal lines, with 6 shared CDR3 sequences across all strains and 5 unique CDR3 sequences. Two of these were identified in the *A22Cα*$^{-/-}$ derived 30B6 and 30D7 lines and 3 in the *A22Cα*$^{-/-}$*PI2*$^{-/-}$ derived 30B9, 30D4 and 30D8 lines. There were no unique CDR3 sequences in the *A22Cα*$^{-/-}$*PI1*$^{-/-}$*PI2*$^{-/-}$*Y16A*^{tg} derived lines. In addition, it should be noted that there were 2 non-TRBV19 sequences in the 30F7 line derived from the *A22Cα*$^{-/-}$ mice using TRBV24 and the 3F11 line derived from the *A22Cα*$^{-/-}$*PI1*$^{-/-}$*PI2*$^{-/-}$*Y16A*^{tg} mice utilising TRBV4. Interestingly, all the lines utilise TRBJ2-3 except one clone within the 30D7 oligoclonal line (from the *A22Cα*$^{-/-}$ mice) which utilises TRBJ2-7. All the clones identified that use TRBV19 and TRBJ2-3 express 4 amino acids between the TRBV and TRBJ chain in the motif CASS-XXXX-GAETLY.

DONOR STRAIN	ID	TRBV	CDR3 SEQUENCE	TRBJ	FREQUENCY (%)
A22Cα$^{-/-}$	10F11	19	CASSIRTGGAETLY	2-3	100
	10F12	19	CASSMRQGGAETLY	2-3	100
	30B6	19	CASSIRQGGAETLY	2-3	94.74
		19	CASSIRQGDAETLY	2-3	5.26
	30C4	19	CASSMRQGGAETLY	2-3	88.89
		19	CASSRRDRGAETLY	2-3	11.11
	30D7	19	CASSSGLEQY	2-7	93.75
		19	CASSFREEGAETLY	2-3	6.25
	30F7	19	CASSIRTGGAETLY	2-3	94.12
		24	CASSRDSDTEVF	1-1	5.88
A22Cα$^{-/-}$*PI2*$^{-/-}$	1F9	19	CASSIRQGGAETLY	2-3	96
		19	CASSFREEGAETLY	2-3	4
	30A6	19	CASSFREEGAETLY	2-3	100
	30B9	19	CASSMRQGGAETLY	2-3	69.23
		19	CASSFREEGAETLY	2-3	23.08
		19	CASSIREGGAETLY	2-3	7.69
	30D4	19	CASSIRQGGAETLY	2-3	94.12
		19	CASSVRQGGAETLY	2-3	5.88
	30D8	19	CASSFREEGAETLY	2-3	50
		19	CASSIRQGGAETLY	2-3	25
		19	CASSFRQEGAETLY	2-3	16.67
		19	CASSMRQRGAETLY	2-3	8.33
	30H3	19	CASSIRQGGAETLY	2-3	100

TABLE 22: THE TCR CDR3 CLONOTYPE FOR ALL OLIGOCLONAL CD8^{+}TRBV19^{+} T CELL LINES EXPANDED *EX VIVO* FROM SINGLE CHAIN TRAV8-1*01TRAJ9 TRANSGENIC NOD MICE EXPRESSING VARIOUS LEVELS OF PROINSULIN

DONOR STRAIN	ID	TRBV	CDR3 SEQUENCE	TRBJ	FREQUENCY (%)
A22Cα$^{-/-}$PI1$^{-/-}$PI2$^{-/-}$Y16A^{tg}	1G3	19	CASSMRQGGAETLY	2-3	100
	3F11	19	CASSMRQGGAETLY	2-3	63.64
		19	CASSRRDRGAETLY	2-3	31.82
		4	CASSQDGQDTQY	2-5	4.55
	3G5	19	CASSIRQGGAETLY	2-3	100
	10G2	19	CASSMRQGGAETLY	2-3	58.33
		19	CASSFREEGAETLY	2-3	33.33
		19	CASSFRQEGAETLY	2-3	8.33
	30A8	19	CASSMRQGGAETLY	2-3	100
	30B8	19	CASSMRQGGAETLY	2-3	100
	30E2	19	CASSIRTGGAETLY	2-3	61.90
		19	CASSMRQGGAETLY	2-3	33.33
		19	CASSFREEGAETLY	2-3	4.76
	30H1	19	CASSIRQGGAETLY	2-3	100

TABLE 23: THE TCR CDR3 CLONOTYPE FOR ALL OLIGOCLONAL CD8^{+}TRBV19^{+} T CELL LINES EXPANDED *EX VIVO* FROM SINGLE CHAIN TRAV8-1*01TRAJ9 TRANSGENIC NOD MICE EXPRESSING VARIOUS LEVELS OF PROINSULIN

4.5 DISCUSSION

To summarise, functional insulin B15-23-reactive T cell responses, including proliferation, cytokine production and cytotoxicity assays, could not be detected within the heterogeneous population of $CD8^+$ T cells, regardless of the proinsulin expression, in the different single chain TRAV8-1*01TRAJ9 transgenic NOD mice. Immunisation, to pre-activate insulin B15-23 responses, was also not effective in expanding the cells sufficiently to detect the population by the standard methods. Therefore a cloning procedure to amplify the insulin B15-23 responses was done. Through the generation of many $TRBV19^+$ (oligo)clonal lines, insulin B15-23 responses were detected by many clones with low avidity. Clonotyping of these cell lines revealed a requirement, in almost all insulin B15-23 reactive responses, for TRBV19 to be associated with TRBJ2-3, the same TCRβ chain utilised by the original G9C8 T cell clone. Investigation of the CDR3β chain also revealed a conserved 4 amino acid motif between the TCRVβ and TCRJβ chains that seemed to be important for insulin B15-23 recognition. At position 2 of this sequence, arginine was required in all cases.

4.5.1 INSULIN B15-23 FUNCTIONAL RESPONSES WITHIN A HETEROGENEOUS CELL POPULATION

While proinsulin expression can alter the proportion of Insulin B15-23-reactive $CD8^+$ T cells in single chain TRAV8-1*01TRAJ9 transgenic NOD mice, those cells are still a small proportion (generally less than 0.5% of the total $CD8^+$ T cells). Therefore, when assessing the functional capabilities of the insulin B15-23-reactive $CD8^+$ T cell population, we aimed to detect and study the insulin-specific responses above the background level. However, the results were variable for all the strains and there was not any consistent peptide-specific proliferative, cytotoxic or cytokine responses. This may not be surprising as the frequency is low and therefore we may not be able to detect the insulin-specific responses with methods at the limit of sensitivity. In addition, each mouse stained using Insulin B15-23 $H2K^d$ tetramers had a different proportion of insulin B15-23-reactive $CD8^+$ T cells, as well as having different TCR repertoires. As we were unable to detect consistent responses in any of the strains including those lacking either one or both proinsulin genes, it may suggest that these $CD8^+$ T cells are of

low avidity or are tolerised. In addition, the individual dominance in the insulin B15-23 reactive TCR repertoire, coupled with only 25% of male *A22Cα*$^{-/-}$*PI2*$^{-/-}$ mice developing diabetes, may suggest that the variable responses seen depend on which specfic T cell clone or clones expand in any given mouse. Therefore, the lack of response may be due to the diabetes-causing clones not being present in the small number of individual mice studied.

Insulin B15-23-reactive G9C8 CD8^{+} T cells that develop in the G9C8 transgenic mouse are relatively naïve in phenotype and fail to develop spontaneous diabetes (Wong et al., 2009). However, other TCR transgenic mice such as those specific for IGRP (NY8.3) can develop spontaneous autoimmune diabetes (Verdaguer et al., 1997). This may suggest that these insulin B15-23-reactive CD8^{+} T cells are more difficult to activate than other T cells. In addition, the insulin B15-23-reactive T cells are proportionally reduced with age in the unmanipulated NOD mouse (Wong et al., 1999), whereas the IGRP$_{206-214}$-reactive T cells become dominant (Lieberman et al., 2004). This suggests that there may be different intrinsic mechanisms controlling these antigen-specific T cells and their development, which may be related to the level of antigen e.g. proinsulin expressed and may suggest why some *A22Cα*$^{-/-}$*PI2*$^{-/-}$ mice develop diabetes. Proinsulin is known to be expressed ectopically (Anderson et al., 2002, Yip et al., 2009) and this may have an effect to generate peripheral tolerance. However the NY8.3 T cells do not appear to be tolerised by peripheral antigen expression (Wang et al., 2012b). This may be due to the high avidity that these NY8.3 T cells have for IGRP and therefore the individual T cell clone avidity/affinity for antigen is another contributing factor to differences in antigen-specific responses. Currently, although it is clear that there are factors controlling the expansion of these insulin B15-23-reactive CD8^{+} T cells, the nature of these has not been elucidated.

4.5.2 *IN VIVO* IMMUNISATIONS TO AMPLIFY THE INSULIN B15-23-REACTIVE T CELLS

Through immunisations with insulin peptide or protein, we aimed to provide a stronger stimulus to the T cells in the various strains of TCRα transgenic mice to

raise them over their activation threshold and identify their functional responses. However, this also failed to yield any reproducible results, with many non-specific effects seen and very few peptide-specific effects noted. By measuring CD69 expression, an early T cell activation marker (Testi et al., 1989), we saw a decrease in expression over time, post-immunisation. This may have been due to the activated T cells migrating to tissues that were not examined in this study e.g. the pancreas or may be due to peripheral control, preventing T cell activation. With respect to the G9C8 T cell, CD69 expression is not seen prior to activation as the cells are naïve, but once activated, expression is upregulated (Wong et al., 2009). In contrast, CD44 was seen to increase. This was not surprising given that CD44 is a memory marker, which in conjunction with CD62L and CCR7, can distinguish between effector memory ($CD44^+CD62L^-CCR7$-) and central memory T cells ($CD44^+CD62L^+CCR7^+$) (Sallusto et al., 1999); in activated G9C8 T cells CD62L was shown to be decreased (Wong et al., 2009). This may suggest that it is more difficult to raise auto-reactive T cells over their activation threshold, potentially due to better peripheral control and therefore multiple immunisations may be required in order to enable the T cells to respond in a proinflammatory manner. In addition, some vaccinations poorly activate naïve T cells prior to memory T cell development (Lauvau et al., 2001) and therefore this may be what occurs in our model. In the G9C8 transgenic mouse model approximately 70% of mice developed spontaneous autoimmune diabetes after two immunisations (Wong et al., 2009) and therefore more immunisations may be required. In addition, other investigators had shown that immunisation with insulin, the insulin B chain or epitopes B9-23 did not stimulate detectable insulin-specific responses, although their study focused on $CD4^+$ T cells (Daniel and Wegmann, 1996, Halbout et al., 2002).

In the RIPmOva model, ovalbumin, a foreign antigen, is expressed as a self-antigen in the thymus and pancreas under the rat insulin promoter. Infection of these mice with OVA-expressing *Listeria monocytogenes* or vesicular stomatitis virus, increases antigen availability, enabling developing T cells to bypass negative selection and become activated by their antigen at avidities similar to, or lower,

than thymic negative selection to cause disease (Enouz et al., 2012). This contrasts with the work we have done. However, in this current study we are using a naturally expressed self-antigen system whereas the RIPmOva model is artificial and therefore the T cells that can respond to Ova antigen may have a higher avidity than normal self-antigen-reactive $CD8^+$ T cells and subsequently may be capable of getting over the activation threshold more easily or have a lower activation threshold. In addition, if we had substituted the native insulin B15-23 peptide for a heteroclitic peptide e.g. the LYLVCGERV variant, we may had greater functional responses, as seen with the clonotypic G9C8 T cell clone (Wong et al., 2002). However, as this peptide is not naturally expressed, we refrained from using this peptide as we wanted our results to show the T cells activated with the native peptide.

Studying the $CD8^+$ T cells in the single chain TRAV8-1*01TRAJ9 transgenic NOD mice, both directly *ex vivo* and following immunisation, had failed to reliably test the functional capabilities of any insulin B15-23-reactive $CD8^+$ T cells. Therefore, we decided to sort antigen-specific $TRBV19^+$ $CD8^+$ T cells by flow cytometry to amplify proinsulin-specific T cells for further study. In addition, this was also the TRBV chain used by the clonotypic G9C8 T cell clone in conjuction with TRBJ2-3 (Wong et al., 1996). By culturing these cells with IL-2, IL-7 and Insulin B15-23 peptide, the Insulin B15-23-reactive $CD8^+$ T cells expanded well, enabling functional responses to be evaluated.

4.5.3 CLONING $TRBV19^+$ INSULIN B15-23 REACTIVE T CELLS

The oligoclonal lines, generated from the different strains of mice, exhibited peptide-specific cytotoxic behaviour to Insulin B15-23 peptide-loaded P815 targets and were capable of secreting proinflammatory MIP-1β and IFN-γ cytokines. Each oligoclonal line responded to the presence of insulin B15-23 peptide. From the cytotoxicity results, the majority of oligoclonal lines responded similarly to higher concentrations of Insulin B15-23 peptide, with three of the oligoclonal lines having minimal cytolytic capability (*A22Cα*$^{-/-}$ derived 30F7 line and the *A22Cα*$^{-/-}$*PI2*$^{-/-}$ derived 30B9 and 30D8 lines). All the other oligoclonal lines were capable of causing specific lysis of peptide-coated targets above 40% and as

high as 90% at 5µg/ml of Insulin B15-23 peptide, as shown by the G9C8 $CD8^+$ T cell clone (Wong et al., 1999). The finding that most of the oligoclonal lines did not respond to lower peptide concentrations supports the notion that these $CD8^+TRBV19^+$ T cells, recognising Insulin B15-23, were of low functional avidity. It is worth noting that these T cells were isolated from the spleen and therefore it is possible that higher avidity T cells may have been found in the pancreatic lymph nodes. There are several other possibilities for our observation that only low functional avidity T cells were isolated. 1. Higher avidity T cells may have already been activated by the target antigenic peptide and infiltrated the pancreas, destroying the insulin producing β cells. 2. High avidity insulin B15-23 reactive $CD8^+$ T cells were negatively selected in the thymus, similarly to the OVA-reactive $CD8^+$ T cells (Zehn and Bevan, 2006). Expression of one proinsulin gene is sufficient to select against these high avidity T cells, resulting in only low avidity T cells surviving in the different strains of mice due to the presence of one or both proinsulin genes as in the *A22Cα*$^{-/-}$, *A22Cα*$^{-/-}$*PI1*$^{-/-}$, *A22Cα*$^{-/-}$*PI2*^{tg} or *A22Cα*$^{-/-}$*PI2*$^{-/-}$ mice. These possibilities do not apply to the *A22Cα*$^{-/-}$*PI1*$^{-/-}$*PI2*$^{-/-}$*Y16A*^{tg} mice, which lack both native proinsulin genes (with a mutated proinsulin gene expressed). Here, of all the mice, we might have expected development of higher avidity insulin-reactive $CD8^+$ T cell clones. However, in these mice, the insulin B15-23 peptide is mutated and thus, any higher avidity T cells that may initially develop, may not be maintained in the periphery due to a lack of antigen. By creating a conditional native insulin knock out model, where both insulin 1 and 2 are deficient but are prevented from developing metabolic diabetes by expression of Y16A transgene, the insulin 1 and/or 2 genes can be re-expressed at later time points. This would allow T cells to develop without encountering antigen until the proinsulin genes are activated and may identify if high avidity T cells, reactive to Insulin B15-23, can develop but fail to be maintained if the antigen is not expressed.

A number of the oligoclonal lines produced cytokines – the highest concentrations were secreted from the *A22Cα*$^{-/-}$*PI1*$^{-/-}$*PI2*$^{-/-}$*Y16A*^{tg} derived 30G7

line, closely followed by the *A22Cα*$^{-/-}$ derived 10F3 line and the *A22Cα*$^{-/-}$*PI2*$^{-/-}$ derived 1H9 line.

Interestingly, there were more *A22Cα*$^{-/-}$*PI1*$^{-/-}$*PI2*$^{-/-}$*Y16A*^{tg} derived lines that produced higher MIP-1β cytokine production than from any other mouse strains and likewise there are more *A22Cα*$^{-/-}$*PI2*$^{-/-}$ derived lines that produced higher quantities of IFN-γ. Whilst it is possible that this is simply due to biological variation, it may suggest a potential role of antigen expression on the proinflammatory cytokine bias found within these oligoclonal lines derived from the different proinsulin expressing TRAV8-1*01TRAJ9 NOD mice. However, the number of oligoclonal lines is small and this suggestion therefore remains speculative, but from the results it may suggest proinsulin 1 expression may enable greater IFN-γ production and proinsulin 2 expression may enable greater MIP-1β production. This functional difference may also be associated with the presence of other clones in the oligoclonal line, different TRBJ usage and differences within the CDR3 region that contact the insulin B15-23 p:MHC complex. Therefore, we went on to investigate the clonality and repertoire of these insulin B15-23-reactive T cell lines to address these questions.

4.5.4 CLONOTYPING OF THE CD8^{+}TRBV19^{+} OLIGOCLONAL LINES

From data obtained from the clonotyping of these oligoclonal lines, it was clear to see that in order for the insulin B15-23-reactive CD8^{+} T cells to recognise the auto-antigenic peptide using TRBV19, in almost all cases, TRBJ2-3 was selected, which is the same TRBV and TRBJ chains as the G9C8 T cell clone (Wong et al., 1996). Therefore, there is an importance in these two chains associating to allow the insulin peptide to be recognised and that TRBJ2-3 has to be used to stimulate a proinflammatory response. There was one oligoclonal line, the *A22Cα*$^{-/-}$ derived 30D7, that used TRBJ2-7 instead of TRBJ2-3; however, the production of MIP-1β and IFN-γ in response to Insulin B15-23 peptide was quite low and therefore this may suggest that while the T cells may recognise insulin using this TRBJ chain, the interaction is too weak to elicit the functional response. Interestingly, all lines derived from all of the mice have the same TRBJ chain suggesting that these TCRs form regardless of thymic proinsulin expression - even in the *A22Cα*$^{-/-}$ mice

expressing native proinsulin, as well as in the polyclonal NOD mouse from which the G9C8 T cell clone was originally derived. This G9C8 T cell clone was isolated from islets of a 7 week old pre-diabetic NOD female (Wong et al., 1996) suggesting that in mice with normal proinsulin expression the T cells expressing TRBV19 in conjunction with TRBJ2-3 fail to be tolerised and are capable of infiltrating the islets to cause diabetes.

When compared to the TCR repertoires of insulin B15-23 tetramer-sorted cells described in the previous chapter, the TRBV19 expressing T cell clones also associated with TRBJ1-1, TRBJ2-1 and TRBJ2-4, as well as the TRBJ2-3, suggesting TRBV19 is the most important part of the TCRβ chain in recognising insulin B15-23. Therefore, while other TRBJ chains can be used to recognise insulin, only the TRBJ2-3 cells were detected through *ex vivo* expansion. Whilst remaining to be confirmed at this stage, possible reasons for finding this could be: 1. T cell clones using the other TRBJ chains may have a higher avidity and therefore using 1µg/ml of Insulin B15-23 peptide may have resulted in too strong a stimulation and may have caused deletion of high avidity cells. 2. The culture conditions may have limited the expansion of other TRBJ expressing T cells and favoured those of a lower avidity expressing TRBJ2-3, although this does not seem likely.

While some of the oligoclonal lines were in fact clonal, others were not, and there did not seem to be any functional enhancement if only one T cell clone was present or not. The presence of more than one clone in each line is not surprising as limiting dilution was used as a standard cloning procedure and usually requires more than one limiting dilution procedure to isolate a clone. However, there were two lines containing non-TRBV19 T cells. These were the *A22Cα*$^{-/-}$ derived 30F7 (using TRBV24) and the *A22Cα*$^{-/-}$*PI1*$^{-/-}$*PI2*$^{-/-}$*Y16A*^{tg} derived 3F11 (utilising TRBV4). This growth of non-TRBV19^{+} T cells may have arisen because of incomplete exclusion in the initial TRBV19 sorting of the cloned lines to remove contaminated APCs prior to clonotyping. However, it is currently unknown if either of these T cell clones recognise Insulin B15-23, given that these T cells were not sorted using the insulin B15-23 peptide:MHC tetramers and therefore testing the clones for their ability to individually recognise insulin B15-23 will

need to be done. While TRBV24 has not been identified in the previous Insulin B15-23-reactive $CD8^+$ T cell repertoire work, TRBV4 was found in conjunction with TRBJ1-1 or TRBJ2-2 in the *A22Cα*$^{-/-}$*PI2*$^{-/-}$ mice and the *A22Cα*$^{-/-}$*PI1*$^{-/-}$*PI2*$^{-/-}$*Y16A*^{tg} mice respectively.

It was shown in Chapter 3 that only one male *A22Cα*$^{-/-}$*PI2*$^{-/-}$ mouse examined had insulin-reactive tetramer positive $CD8^+$ T cells utilising the TRBV19 and TRBJ2-3 chains and that utilised a CDR3β sequence of CASSIRESGAETLY. This sequence also fits with the 4 amino acids found between CASS and the GAETLY sequence in all of the TRBV19 expanded T cell lines. While the initial G9C8 T cell clone used the 4 amino acid sequence IRDR and the tetramer-sorted clone used IRES, neither of these sequences were identified in the expanded $TRBV19^+$ oligoclonal lines. Instead, IREG, IRQG, IRTG, FREE, FRQE, MRQG, RRDR and VRQG were found. In all of these CDR3β sequences, arginine was conserved in the second position, likely providing a very important contact with the insulin B15-23 peptide. In the first position, non-polar side chain amino acids were preferred (with the exception of arginine), while at the third position either an amino acid with an acidic side chain (aspartic acid (D) or glutamic acid (E)) or an uncharged polar side chain (Glutamine (Q) or Threonine (T)) were preferred, with the last position having little preference for an amino acid type. This demonstrates the potential importance of these amino acids in this CDR3β region for dictating peptide specificity. It is currently unknown as to how these amino acid differences interact with the peptide and if there is an optimal CDR3β sequence.

Unlike the TCR repertoire from Insulin B15-23 tetramer sorted cells discussed in the previous chapter, there are many $TRBV19^+$ expanded oligoclonal lines that have shared CDR3β sequences across all the strains regardless of proinsulin expression. Of the 20 clones sequenced for their CDR3β region, there are 6 shared CDR3β sequences across all strains and 5 unique CDR3 sequences. Two of these unique sequences were identified within the *A22Cα*$^{-/-}$ derived 30B6 and 30D7 lines and 3 within the *A22Cα*$^{-/-}$*PI2*$^{-/-}$ derived 30B9, 30D4 and 30D8 lines. This sequence homology between strains provides further evidence of an intrinsic selection for particular sequences, following the aforementioned motif, which

appears to be essential when using TRBV19 and TRBJ2-3 for recognising insulin B15-23. It should also be noted that these results are from a selection of the more rapidly growing lines, and not all oligoclonal lines could be tested functionally or sequenced for the CDR3β region due to time restrictions.

4.5.5 SUMMARY

To summarise, this study demonstrated a lack of peptide-specific responses from investigation of total $CD8^+$ T cell populations, from the lymphoid tissues of the various TCRα chain restricted, proinsulin-expressing mice. However, when a subset expressing TRBV19 were expanded, insulin B15-23 responses were identified. A number of oligoclonal lines were isolated that were cytotoxic for targets presenting the auto-antigenic peptide, and produced proinflammatory cytokines. Through sequencing the CDR3β region of these oligoclonal lines, we identified a requirement for TRBJ2-3 for insulin recognition with the fixed TRAV8-1*01TRAJ9 and TRBV19. In addition, the oligoclonal lines use the same TRBV and TRBJ chain as the G9C8 T cell clone and showed similarities in a 4 amino acid motif to the other insulin B15-23-reactive TRBV19 expressing cells in the previous tetramer based repertoire work. This study has shown that regardless of proinsulin expression, the insulin B15-23-reactive $CD8^+$ T cells still develop and have a similar avidity for their peptide when they express TRBV19.

4.6 FUTURE WORK

This investigation has yielded many more questions to answer. Firstly, it is important that more data is obtained both in terms of functional assays and in terms of CDR3β clonotyping in order to confirm if the trends identified are confirmed but also to identify any other T cell clones not yet seen i.e. such as those expressing alternative TRBJ chains in the cells sorted by Insulin B15-23 tetramer binding in Chapter 3. In addition, the oligoclonal lines with more than one clone would also need to be further cloned in order to obtain clonal populations.

Secondly, while we initially flow cytometrically sorted for TRBV19-expressing $CD8^+$ T cells, due to the selection pressure placed on that TRBV chain by

proinsulin expression, isolating Insulin B15-23-reactive $CD8^+$ T cells by virtue of their insulin B15-23 reactivity, rather than by TCRβ chain, and studying their TCR repertoires should also be conducted. This would identify other TRBV chains capable of recognising the insulin B15-23 peptide, providing more data on the selection of auto-reactive $CD8^+$ T cells and whether there are other T cell clones of higher avidity that can be activated at lower peptide concentrations. It is possible that TRBV19 itself places limitations on the avidity of interaction with the insulin peptide. Understanding how both the TRBV19 and other TRBV chain expressing insulin B15-23-reactive $CD8^+$ T cells develop would allow comparisons to be made between the chains identifying any common motifs within the CDR3 region. Once these cells have been isolated, the role of proinsulin 1 and 2 may then be fully explored in terms of their ability to expand and transfer diabetes in mice with altered proinsulin levels.

Thirdly, this data focuses on the selection of the TRBV repertoire and therefore we do not fully understand if the TCRα chain makes important contacts within the peptide:MHC and therefore, it would be important to also examine the TCRα restriction in mice expressing various proinsulin levels. While there are few flow monoclonal antibodies against the TCRα chain, sorting for those insulin B15-23-reactive $CD8^+$ T cells with tetramer would enable the T cells to be investigated for their TRAV and TRAJ chains as well as the CDR3α sequence. If insulin B15-23-reactive $CD8^+$ T cells from TRBV19*01TRBD1TRBJ2-3 restricted mice had similar CDR3α sequences to the G9C8 TCRα chain sequence, then this would suggest the TCRα chain is more important for recognising the insulin peptide than the TCRβ chain. The data generated from this prospective study would also enable investigation into how auto-reactive T cells develop and escape negative selection due to the TCRα pairing, and whether high avidity T cells can develop with only the TCRβ chain restricted. In addition, this work would aid our understanding as to the strength of the interaction the TCRα and TCRβ chains individually contribute in recognising Insulin B15-23.

Fourthly, since the immunisation work failed to sufficiently expand the insulin B15-23-reactive $CD8^+$ T cells to facilitate study of the cells from *in vivo* activation,

it may be worth attempting additional immunisations in order to see if these T cells can be stimulated above their threshold. During this work, it would also be useful to identify which cells are capable of preventing these T cells from responding, providing a therapeutic target to enrich in preventing autoimmune diabetes.

Finally, as mentioned in this work and the previous chapter, these mice have a variable proportion of insulin B15-23-reactive $CD8^+$ T cells with individual dominant TCR repertoires. These individual clones may be important functionally as we found that only 25% of male *A22Cα*$^{-/-}$*PI2*$^{-/-}$ mice developed spontaneous autoimmune diabetes. Therefore, investigating this difference in incidence and whether it is linked to specific higher avidity clonotypes remains to be tested.

CHAPTER 5: THE EFFECT OF ANTIBIOTICS AND THE GUT MICROBIOTA ON THE INCIDENCE OF DIABETES

5.1 AIMS, RATIONALE AND HYPOTHESIS

In order to fight an infection, the immune system relies on interactions between the invading foreign organism and the innate immune system. This interaction is initially mediated through pattern recognition receptors that include toll-like receptors (TLRs), found on many cell types, of which TLR 3, 7, 8 and 9 are found intracellularly and TLR 1, 2, 4, 5 and 6 are found extracellularly (reviewed by (Akira et al., 2006)). These TLRs signal downstream through an adaptor protein called MyD88, stimulating upregulation of proinflammatory cytokines and costimulation molecules. These TLRS bind specific ligands, known as pathogen-associated molecular patterns, to induce a specific immune response e.g. TLR4 recognises lipopolysaccharides in the Gram-negative bacterial envelope, in conjunction with the co-receptor MD-2, in a species-specific manner which is dictated by differences in TLR4 ligand binding (Shimazu et al., 1999, Hajjar et al., 2002, Ohto et al., 2012). In addition, signalling specificity is mediated by TIRAP, an adaptor molecule, which can impair TLR1, 2, 4 and 6 signalling responses (Horng et al., 2002).

Through TLR signalling, the innate immune response can protect against invading and commensal microbiota, maintaining gut homeostasis (Cario et al., 2004, Fukata et al., 2006, Shang et al., 2008, Mukherji et al., 2013). Interestingly, when these TLRs were deficient, as in knock out mice, homeostasis was disrupted. In *TLR2*$^{-/-}$ mice, bacterial loads and bacteria-associated pathology were increased (Wooten et al., 2002, Echchannaoui et al., 2002), while the proinflammatory responses in diabetic nephropathy (Devaraj et al., 2011c) and liver fibrosis (Ji et al., 2014) were decreased. In addition *TLR2*$^{-/-}$ mice, on the NOD genetic background, were also shown to be protected from the development of diabetes (Kim et al., 2007) and, through TLR2 signalling, tolerance can be established through boosting regulatory T cells and reversing the hyperglycaemia in recent-onset diabetic mice (Burton et al., 2010, Kim et al., 2012). This indicates that while the host became susceptible to infection; autoimmunity, fibrosis and non-

infectious disease-related complications were decreased. Therefore, understanding how all these factors shape the innate immune response is important.

Through TLR signalling, the innate immune response begins and invokes the adaptive immune response through antigen presentation. Interestingly, the adaptive immune response can be dictated by the presence, or lack, of TLR signalling. TLR deficiencies reduce antigen-specific T cell proliferation and activation (Vallois et al., 2007, Gonnella et al., 2008, Zhang et al., 2010, Kim et al., 2012), while signalling through TLRs can boost immunosuppressive cell populations (Burton et al., 2010, Tai et al., 2013). This indicates that TLR signalling can promote autoimmunity, while protecting against infection.

In addition, to the TLR deficient mice, the effects of altering downstream signalling were also investigated e.g. in *MyD88*$^{-/-}$ mice. Following an LCMV infection in the *MyD88*$^{-/-}$ mouse, virus-specific CD8^{+} T cells could not be activated (Zhou et al., 2005), and CD4^{+} T cells could not differentiate into virus-specific T cells (Zhou et al., 2009). Furthermore, *MyD88*$^{-/-}$ NOD mice, were protected from diabetes (Wen et al., 2008), as were C57BL/6 *MyD88*$^{-/-}$ mice that over-expressed islet costimulatory molecules (Alkanani et al., 2014). The NOD MyD88 deficient mice were only protected from the development of diabetes when they were reared in specific pathogen-free mouse facilities, as when the mice were rederived in a germ-free environment, nearly all mice developed diabetes by 30 weeks of age (Wen et al., 2008). This suggested a role for bacteria in shaping the immune response and upon transfer of gut microbiota from protected NOD*MyD88*$^{-/-}$ mice into wildtype NOD mice, insulitis and diabetes were delayed (Peng et al., 2014). This altered disease phenotype corresponded to changes in the gut microbiota, increases in TGF-β and IgA secretion and the number of CD8^{+}CD103^{+} T cells. Altered gut microbiota were also found in TLR-deficient mice (Fukata et al., 2005, Vijay-Kumar et al., 2010). Furthermore, gut microbiota differences were also identified in another spontaneous autoimmune diabetes model, the Bio-Breeding rat, where the rats susceptible to disease had different gut microbiota to those rats protected from disease (Roesch et al., 2009). The gut

microbiota were also shown to be different between individuals with type 1 diabetes/β cell autoimmunity and the gut microbiota from healthy controls (Giongo et al., 2011, de Goffau et al., 2013).

The finding that gut bacteria modify disease susceptibility to autoimmune diabetes promoted the interest in using antibiotics to investigate how that would affect the microbiota and diabetes development. In the NOD mouse model, antibiotics have been shown both to reduce (Hansen et al., 2012) and increase (Tormo-Badia et al., 2014) diabetes incidence depending on the antibiotic(s) used. In addition, the time of administration also appeared to be important in providing this protective or pathogenic response. Furthermore, the altered gut microbiota can be transmitted to the foetus and can impact the development of the gut (Ubeda et al., 2012, Tormo-Badia et al., 2014).

Gut microbiota have also been modified by treatment with bacteria such as *Lactobacillus casei* and other probiotic bacteria corresponding with reduced incidence of diabetes (Matsuzaki et al., 1997, Calcinaro et al., 2005). Furthermore, genetic modification of *Lactobacillus lactis* to secrete IL-10 with human proinsulin or GAD65, two auto-antigens in diabetes, coupled with low-dose α-CD3 treatment reversed diabetes in some NOD mice (Takiishi et al., 2012, Robert et al., 2014). Interestingly, in experimental autoimmune encephalomyelitis (EAE) (Ochoa-Repáraz et al., 2010a, Ochoa-Repáraz et al., 2010b) and intestinal inflammatory disease (Mazmanian et al., 2008), polysaccharide A, a bacterial component, was able to prevent disease. However, in diabetes, no single microbial factor has, as yet, been identified.

Other factors, such as androgen levels, have recently been identified to be altered when the gut microbiota are modified. Normally female NOD mice have a higher incidence of diabetes than male NOD mice; however, when the mice are germ-free, or the males are castrated, the incidence of diabetes is similar (Yurkovetskiy et al., 2013). In addition, faecal transfer from male NOD mice into young female NOD mice was able to protect the recipient mice from diabetes, by inducing changes to the gut microbiota and increasing the testosterone level,

which was associated with decreased islet inflammation (Markle et al., 2013a). This indicates that both the gut microbiota and androgens are capable of shaping the immune response.

While these studies have shown gut microbial differences between mice that were susceptible to disease development and those protected from disease, they focused predominantly on the development of diabetes in polyclonal mice, rats or individuals with a large T cell receptor diversity encompassing diverse antigen specificities. Therefore, work investigating specific antigen-specificities is required to identify any direct or indirect roles the gut microbiota may have on the individual antigen-reactive T cells.

During investigation of diabetes incidence in the single chain TRAV8-1*01TRAJ9 transgenic NOD mice, it was shown 25% of male mice lacking proinsulin 2 developed spontaneous disease, similarly to male G9C8 TCR transgenic mice lacking proinsulin 2 (Terri Thayer, personal communication, manuscript in progress). This observation was made when the mice had prophylactic, intermittent broad-spectrum antibiotics administered for prevention of rectal prolapse. However, it was observed that when the single chain TRAV8-1*01TRAJ9 transgenic NOD mice were not given antibiotics in their drinking water, they were protected from developing diabetes. Therefore, further studies were initiated to formally assess the effect of antibiotic administration on the development of diabetes in single chain TRAV8-1*01 transgenic NOD mice, deficient in proinsulin 2. More specifically, the gut bacteria, the TCR repertoire and the insulin B15-23-reactive T cells were investigated following different antibiotic regimes for any identifiable differences that contributed to this altered diabetes incidence.

Hypothesis:

Antibiotics will alter the gut microbiota, and associated with this, the activation of insulin-reactive $CD8^+$ T cells and consequently affect the incidence of diabetes.

Aims:

1. To investigate the effect of antibiotic administration on the development of autoimmune diabetes in the single chain TRAV8-1*01TRAJ9 transgenic NOD mice deficient in proinsulin 2, and investigate cellular phenotypic and functional changes responsible for any differences.
2. To investigate the TRBV repertoire in single chain TRAV8-1*01TRAJ9 transgenic NOD mice deficient in proinsulin 2 given different antibiotic regimes.
3. To investigate the development of insulin B15-23-reactive $CD8^+$ T cells in these single chain TRAV8-1*01TRAJ9 transgenic NOD mice, deficient in proinsulin 2, following antibiotic administration.
4. To investigate the composition of the gut microbiota in single chain TRAV8-1*01TRAJ9 transgenic NOD mice deficient in proinsulin 2 following antibiotic administration.
5. To study glucose tolerance in single chain TRAV8-1*01TRAJ9 transgenic NOD mice.

5.2 ANTIBIOTIC ADMINISTRATION AFFECTS THE DEVELOPMENT OF SPONTANEOUS DIABETES IN SINGLE CHAIN TRAV8-1*01TRAJ9 TRANSGENIC NOD MICE DEFICIENT IN PROINSULIN 2

Historically, the *A22Cα*$^{-/-}$*PI2*$^{-/-}$ mice had been treated with intermittent antibiotics as a prophylaxis against rectal prolapse, which may be a problem in *TCRCα*$^{-/-}$ mice. As shown in Chapter 3, a proportion of the mice developed autoimmune diabetes. However, on observing a group of mice off antibiotics, it was noted that the diabetes incidence was reduced. Therefore, the studies reported in this chapter were conducted to further examine this phenomenon. In all these experiments outlined, Baytril, a fluoroquinolone containing enrofloxacin as the active ingredient, was added to the drinking water. This is a broad-spectrum antibiotic targeting both Gram-positive and Gram-negative bacteria. It should be noted at the outset that rectal prolapse did not develop in these mice and any changes in diabetes was not related to rectal prolapse.

5.2.1 ANTIBIOTICS ADMINISTERED POST-WEANING AFFECT THE INCIDENCE OF AUTOIMMUNE DIABETES IN SINGLE CHAIN TRAV8-1*01TRAJ9 TRANSGENIC NOD MICE DEFICIENT IN PROINSULIN 2

In the initial experiment 8 female and 19 male mice were observed for the development of autoimmune diabetes. All *A22Cα*$^{-/-}$*PI2*$^{-/-}$ mice received Baytril treatment every other week during pregnancy and up to the age of weaning (3 weeks). These mice were then divided into different treatment groups where they received Baytril (14 males, 8 females) or were not treated with Baytril (5 males). Baytril was administered either intermittently or constantly but as no differences emerged between the two groups, the data were combined. In addition, no spontaneous diabetes was observed in any of the female *A22Cα*$^{-/-}$ *PI2*$^{-/-}$ mice, therefore only the data from male mice are shown. As FIGURE 32 shows, the incidence of diabetes in male *A22Cα*$^{-/-}$*PI2*$^{-/-}$ mice that received Baytril reached 43% (6/14 mice). This was higher than the incidence in those male *A22Cα*$^{-/-}$*PI2*$^{-/-}$ mice which were not treated with Baytril post-weaning (20%, 1/5 mice). Diabetes was observed as early as 36 days (approximately 6 weeks of age) in those male mice that received Baytril constantly compared to 55 days in the

single mouse which developed diabetes without Baytril treatment, post-weaning. While there was a trend towards an increase in diabetes incidence with Baytril administration, the numbers were small and the data were not significantly different.

5.2.2 ANTIBIOTICS ADMINISTERED PRE-PREGNANCY AFFECT THE INCIDENCE OF AUTOIMMUNE DIABETES IN SINGLE CHAIN TRAV8-1*01TRAJ9 TRANSGENIC NOD MICE DEFICIENT IN PROINSULIN 2

Having identified a difference in diabetes incidence in the small cohort of mice treated post-weaning, the question arose as to whether treating these mice earlier i.e. from birth would alter the incidence of diabetes. Therefore, breeder trios (2 females and 1 male) were set up and treated as before with either Baytril constantly in the water, Baytril every other week or no Baytril at all. The pups, up to 3 weeks of age, received the same treatments as their breeder parents. Upon reaching 3 weeks, mice were sexed and divided into cohorts to receive Baytril constantly or not at all (see FIGURE 33). A total cohort of 33 female and 34 male *A22Cα*$^{-/-}$*PI2*$^{-/-}$ mice were observed for diabetes up to 12 weeks. As mentioned previously, any mice that received Baytril from 3 weeks were grouped together as no differences between the groups were observed. FIGURE 34 shows diabetes in male *A22Cα*$^{-/-}$*PI2*$^{-/-}$ mice started from 6 weeks of age, as previously mentioned. However, in the group without Baytril treatment, 1/5 mice (20%) became diabetic at a later time point (10 weeks). The incidence of diabetes reached 43% in those male mice that received Baytril treatment, similarly to the previous study. However, there were no statistically significant differences between the two cohorts. In addition, no diabetes was recorded in any of the female *A22Cα*$^{-/-}$ *PI2*$^{-/-}$ mice.

FIGURE 32: THE EFFECT OF ANTIBIOTIC (BAYTRIL) ADMINISTRATION POST-WEANING ON THE INCIDENCE OF SPONTANEOUS AUTOIMMUNE DIABETES IN SINGLE CHAIN TRAV8-1*01TRAJ9 TRANSGENIC NOD MICE DEFICIENT IN PROINSULIN 2

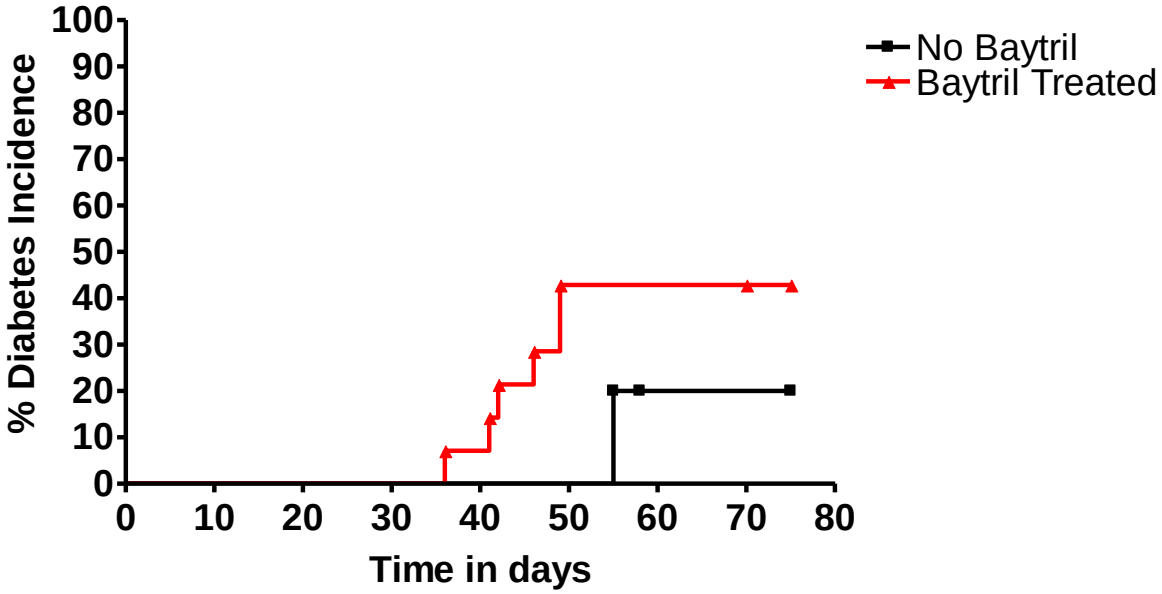

FIGURE 32: Male *A22Cα*$^{-/-}$*PI2*$^{-/-}$ mice were treated with Baytril every other week during pregnancy and weaning (up to 3 weeks of age). After weaning, mice were placed into cohorts to receive Baytril in their water (n=14) or no Baytril (n=5). Mice were observed for 10 weeks with bi-weekly urine tests for glycosuria. If positive, the reading was confirmed the next day by testing blood glucose. Diabetes was diagnosed when blood glucose was above 13.9mmol/L. Data were plotted using GraphPad Prism Version 4 software. Survival curves were compared using a log rank test, where no significant differences were detected between the no Baytril and Baytril treated group (p=0.3222).

FIGURE 33: ANTIBIOTIC TREATMENT GROUPS FOR *A22Cα*$^{-/-}$*PI2*$^{-/-}$ MICE FROM BIRTH

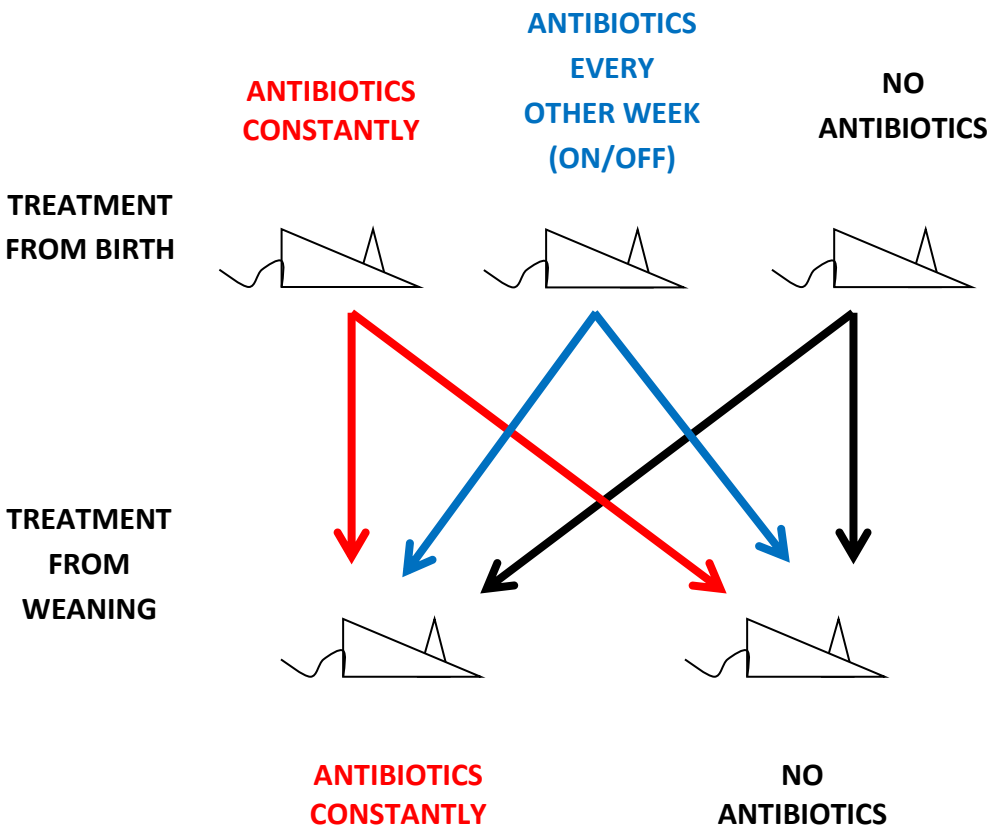

FIGURE 33: Male and Female *A22Cα*$^{-/-}$*PI2*$^{-/-}$ mice (n=34 and 33 respectively) were treated with Baytril constantly, every other week or not at all during pregnancy and weaning (up to 3 weeks of age). After weaning, mice were placed into cohorts to receive Baytril or not at all in their water.

FIGURE 34: THE EFFECT OF ANTIBIOTIC (BAYTRIL) ADMINISTRATION PRE-PREGNANCY ON THE INCIDENCE OF SPONTANEOUS AUTOIMMUNE DIABETES IN SINGLE CHAIN TRAV8-1*01TRAJ9 TRANSGENIC NOD MICE DEFICIENT IN PROINSULIN 2

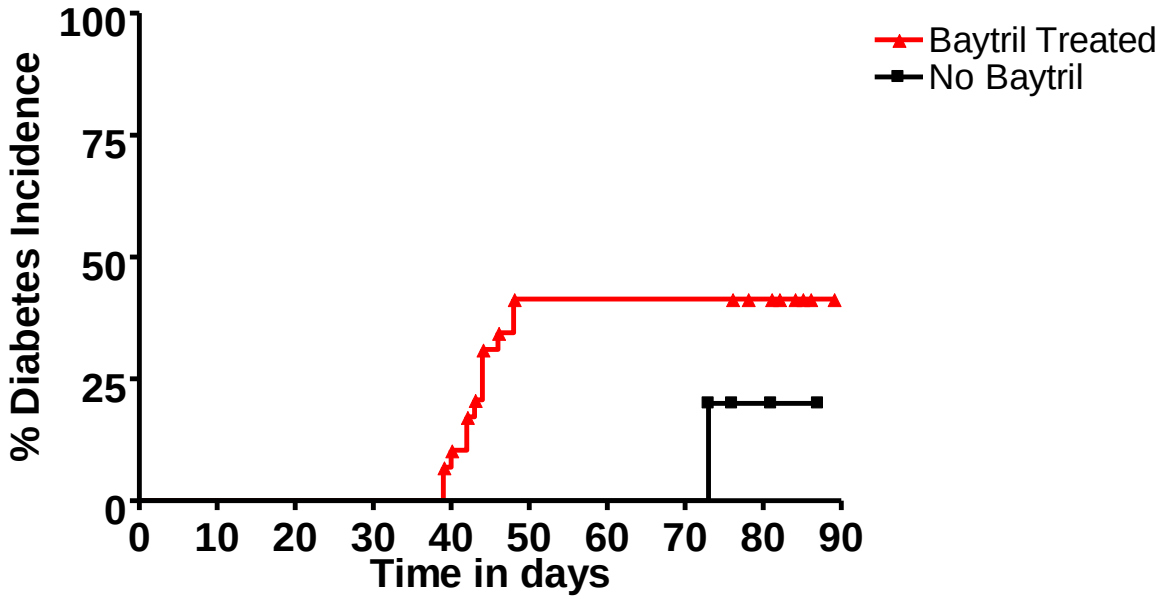

FIGURE 34: Male *A22Cα*$^{-/-}$*PI2*$^{-/-}$ mice were treated with Baytril constantly, every other week or not at all during pregnancy and weaning (up to 3 weeks of age). After weaning, mice were placed into cohorts to receive Baytril constantly (n=29) or not at all in their water (n=5). Mice were observed for 12 weeks with bi-weekly urine tests for glycosuria. If positive, the reading was confirmed the next day by testing blood glucose. Diabetes was diagnosed when blood glucose was above 13.9mmol/L. Data were plotted using GraphPad Prism Version 4 software. Survival curves were compared using a log rank test where no significant differences were detected between the groups (p=0.3284).

5.3 THE CD8+ TCR REPERTOIRES IN SINGLE CHAIN TRAV8-1*01TRAJ9 TRANSGENIC NOD MICE DEFICIENT IN PROINSULIN 2 ARE UNAFFECTED BY THE DIFFERENT ANTIBIOTIC REGIMES

To test whether the difference in incidence of diabetes was due to a specific TCR repertoire expansion or loss, the $CD8^+$ TCR repertoire was investigated in these male and female mice *A22Cα*$^{-/-}$*PI2*$^{-/-}$ mice either at the time they developed diabetes or at the end of the period of observation if no diabetes occurred (10-12 weeks).

5.3.1 ANTIBIOTIC TREATMENT OF SINGLE CHAIN TRAV8-1*01TRAJ9 TRANSGENIC NOD MICE DEFICIENT IN PROINSULIN 2 DOES NOT AFFECT THE NUMBER OF CD4+ OR CD8+ T CELLS

Peyer's patches (PP), mesenteric lymph nodes (MLN) and pancreatic lymph nodes (PLN) were isolated from the *A22Cα*$^{-/-}$*PI2*$^{-/-}$ mice, from which single cell suspensions were stained using antibodies against CD4, CD8 and the TRBV chains (2.9.3.3). Live single $CD4^+$ and $CD8^+$ T cells were gated. FIGURE 35 shows the average T cell numbers stained in each antibody panel from each tissue with an average of 1000-2000 $CD4^+$ T cells in the Peyer's patches compared to 6000-8000 $CD4^+$ T cells within the MLN or PLN. The $CD8^+$ T cell counts were similar to the $CD4^+$ T cells. There were no statistically significant differences between mice on or off Baytril treatment, those mice that became diabetic vs non-diabetic or between males and females and therefore males and female results were combined.

FIGURE 35**:** Peyer's patches, PLNs and MLNs were isolated from single chain TRAV8-1*01TRAJ9 transgenic NOD mice, deficient in proinsulin 2, receiving various antibiotic regimes. Mice were studied either at the time diabetes was diagnosed or at the end of the observation period (12 weeks). Single cell suspensions were stained with a panel of antibodies against CD4 and CD8 and measured on a BD FACS CANTO II. Data were then analysed using Flowjo Version 7.6.5 software where live single $CD4^+$ T cells (**A**) or $CD8^+$ T cells (**B**) were gated. This proportion was then converted to a cell number using the total live cell number. The $CD4^+$ or $CD8^+$ T cell count from each staining panel for each tissue was then used to create an average value. Data were then plotted using GraphPad Version 4 software. The horizontal lines on the dot plot represent the median, while each individual shape represents an individual mouse. There were no statistical differences identified by ANOVA using R software and therefore male and female data were combined. Diabetic data only include male *A22Cα*$^{-/-}$ *PI2*$^{-/-}$ mice as no females became diabetic.

FIGURE 35: T CELL NUMBERS IN SINGLE CHAIN TRAV8-1*01TRAJ9 TRANSGENIC NOD MICE DEFICIENT IN PROINSULIN 2 THAT RECEIVED ANTIBIOTIC TREATMENT OR DID NOT

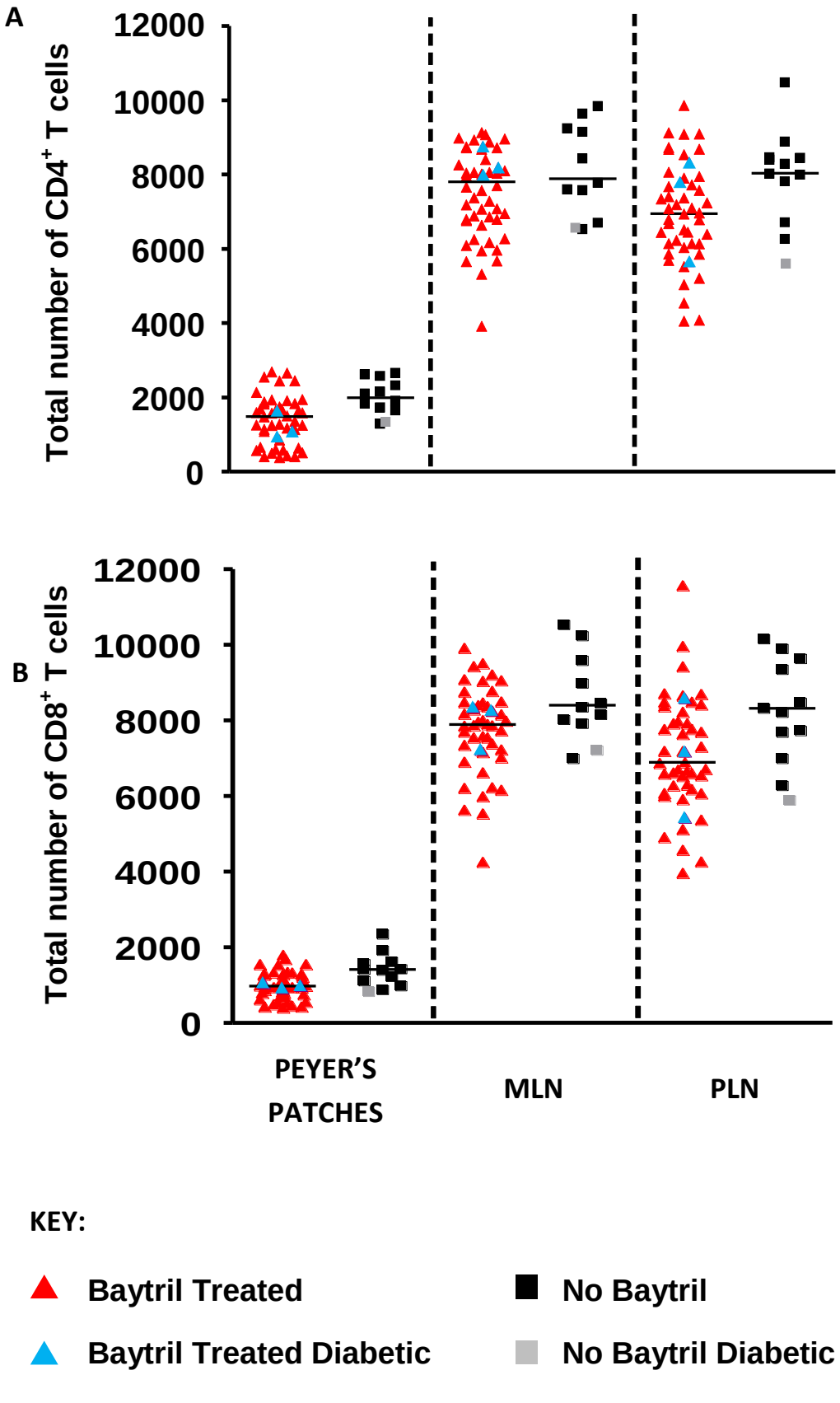

5.3.2 ANTIBIOTIC TREATMENT OF SINGLE CHAIN TRAV8-1*01TRAJ9 TRANSGENIC NOD MICE DEFICIENT IN PROINSULIN 2 DOES NOT AFFECT THE TOTAL CD8αβ+ TCR REPERTOIRE

$CD8^+$ TCR repertoire was investigated by flow cytometry using a modified TRBV repertoire panel used in Chapter 3 (2.9.3.3). TABLE 24 summarises the PLN TRBV repertoire data in cell number per 10,000 $CD8\alpha\beta^+$ T cells, to allow for direct comparison of $CD8^+$ T cells in the Peyer's patches, MLN and PLN. The PLN data is shown, as no differences were seen between the lymph nodes and Peyer's patches and the results are therefore representative also of the MLN and Peyer's patches. This data is presented as those receiving Baytril (regardless of if pre or post-weaning) and those not treated with Baytril, combining both males and females. A full table broken down by treatment group and gender is presented in the appendix. From this data, TRBV13 is the most prevalent followed by TRBV19 then TRBV4. There were no differences between any of the antibiotic treatment groups, between genders or between those diabetic and those non-diabetic. However, the numbers of male diabetic *A22Cα*$^{-/-}$*PI2*$^{-/-}$ mice studied were small (n=1-3).

5.3.3 ANTIBIOTIC TREATMENT OF SINGLE CHAIN TRAV8-1*01TRAJ9 TRANSGENIC NOD MICE, DEFICIENT IN PROINSULIN 2, DOES NOT AFFECT THE PROPORTION OF TOTAL CD8αβ+ MEMORY T CELLS

Although TCR repertoire changes were not identified, we also asked whether there was a difference in memory phenotype of the $CD8\alpha\beta^+$ T cells in these *A22Cα*$^{-/-}$*PI2*$^{-/-}$ mice dependent on antibiotic treatment. The $CD8^+$ T cells were isolated from the Peyer's patches, MLN and PLN and stained with antibodies against CD8α, CD8β, CD44 and CD62L, to enable classification of central memory or effector memory T cells. FIGURE 36 shows $CD44^+CD62L^+$ central memory T cells were increased in the MLN and PLN in comparison to the Peyer's patches; however, this trend was reversed for the $CD44^+CD62L^-$ effector memory T cell populations where there were more present in the Peyer's patches than the lymph nodes. Analysis of the data by ANOVA revealed no statistically significant differences between the treatment groups or gender.

ANTIBIOTIC TREATMENT	TRBV 1	TRBV 2	TRBV 4	TRBV 12	TRBV 13	TRBV 14	TRBV 15	TRBV 16	TRBV 17	TRBV 19	TRBV 24	TRBV 26	TRBV 29	TRBV 31
BAYTRIL TREATED	250	279	1206	347	2867	299	157	321	70	1737	3	212	13	480
NO BAYTRIL	233	274	1212	346	2769	292	171	333	62	1751	3	204	18	478

TABLE 24: PLN CD8αβ^{+} TRBV REPERTOIRE IN SINGLE CHAIN TRAV8-1*01TRAJ9 TRANSGENIC NOD MICE DEFICIENT IN PROINSULIN 2 SHOWN BY ANTIBIOTIC TREATMENT

Data shown refer to the average from all treatment groups whether the mice received Baytril or not. Data is representative of 56 mice receiving Baytril (27 females and 29 males) and 11 mice not treated with Baytril (6 females and 5 males).

FIGURE 36: Peyer's patches, PLNs and MLNs were isolated from single chain TRAV8-1*01 transgenic NOD mice deficient in proinsulin 2 receiving various antibiotic regimes. Mice were studied either at the time diabetes was diagnosed or at the end of the observation period (12 weeks). Single cell suspensions were stained with a panel of antibodies against CD4, CD8α, CD8β, CD44 and CD62L and measured on a BD FACS CANTO II. Data were then analysed using Flowjo Version 7.6.5 software where live single $CD8\alpha\beta^{+}CD44^{+}CD62L^{+}$ or $CD8\alpha\beta^{+}CD44^{+}CD62L^{-}$ T cells were gated. This proportion was then converted to a cell number per 10^{4} $CD8\alpha\beta^{+}$ T cells. Data were then plotted using GraphPad Version 4 software. The horizontal lines on the dot plot represent the median, while each individual shape represents an individual mouse. There were no statistical differences identified by ANOVA using R software and therefore male and female data were combined. Diabetic data only includes male *A22Cα*$^{-/-}$*PI2*$^{-/-}$ mice as no females became diabetic.

FIGURE 36: TOTAL NUMBERS OF CD8αβ$^+$CD44$^+$CD62L$^+$ CENTRAL MEMORY AND CD8αβ$^+$CD44$^+$CD62L$^-$ EFFECTOR T CELLS PRESENT IN THE PEYER'S PATCHES, MESENTERIC LYMPH NODE (MLN) AND PANCREATIC LYMPH NODE (PLN) OF SINGLE CHAIN TRAV8-1*01 TRANSGENIC NOD MICE DEFICIENT IN PROINSULIN 2

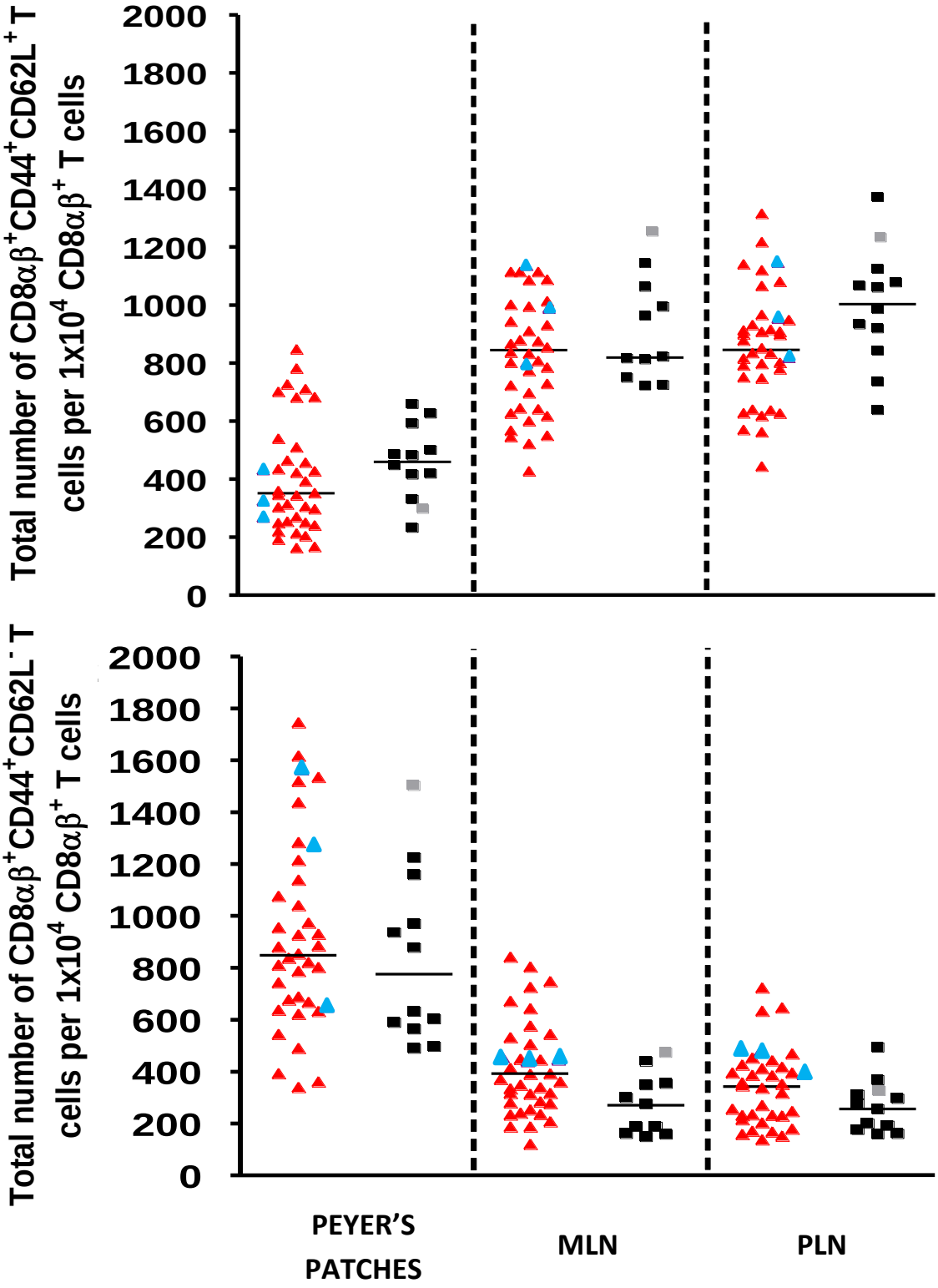

5.4 INSULIN B15-23-REACTIVE CD8+ T CELLS IN SINGLE CHAIN TRAV8-1*01TRAJ9 TRANSGENIC NOD MICE DEFICIENT IN PROINSULIN 2 WERE UNAFFECTED BY DIFFERENT ANTIBIOTIC REGIMES

Having observed no broad $CD8^+$ TCR repertoire changes with different antibiotic treatment regimes, the insulin B15-23 reactive $CD8^+$ T cells were investigated, to establish whether there were any changes in this specific $CD8^+$ T cell population.

5.4.1 FREQUENCY OF INSULIN B15-23-REACTIVE CD8+ T CELLS WAS UNAFFECTED BY ANTIBIOTIC TREATMENT OF SINGLE CHAIN TRAV8-1*01TRAJ9 TRANSGENIC NOD MICE DEFICIENT IN PROINSULIN 2

Using Insulin B15-23 peptide:MHC tetramers, insulin-reactive $CD8^+$ T cells could be identified within the Peyer's patches, the MLN and the PLN from *A22Cα*$^{-/-}$*PI2*$^{-/-}$ mice. FIGURE 37 shows in mice treated without antibiotics, the Peyer's patches had the largest number of insulin B15-23-reactive $CD8^+$ T cells (not significant) and were shown to decrease in the MLN and PLN (not significant). However, in those mice treated with antibiotics, the numbers of insulin B15-23-reactive $CD8^+$ T cells comparing the Peyer's patches and the MLN were more similar, while showing a reduction in the PLN. Furthermore, there was no numerical difference between the insulin B15-23-reactive $CD8^+$ T cells in the diabetic *A22Cα*$^{-/-}$*PI2*$^{-/-}$ mice compared to non-diabetic mice. Although, there was a trend for the number of insulin B15-23-reactive $CD8^+$ T cells to be decreased in the Peyer's patches, while increased in the MLN and PLN when mice were treated with antibiotics compared to those without antibiotics, the numbers are small and the data were not significantly different. In addition, only males were analysed for the insulin B15-23-reactive $CD8^+$ T cells and therefore cannot be compared to the female *A22Cα*$^{-/-}$*PI2*$^{-/-}$ mice.

FIGURE 37: TOTAL NUMBER OF INSULIN B15-23 REACTIVE CD8$^+$ T CELLS PER 10^4 CD8αβ$^+$ T CELLS IN MALE SINGLE CHAIN TRAV8-1*01TRAJ9 TRANSGENIC NOD MICE DEFICIENT IN PROINSULIN 2

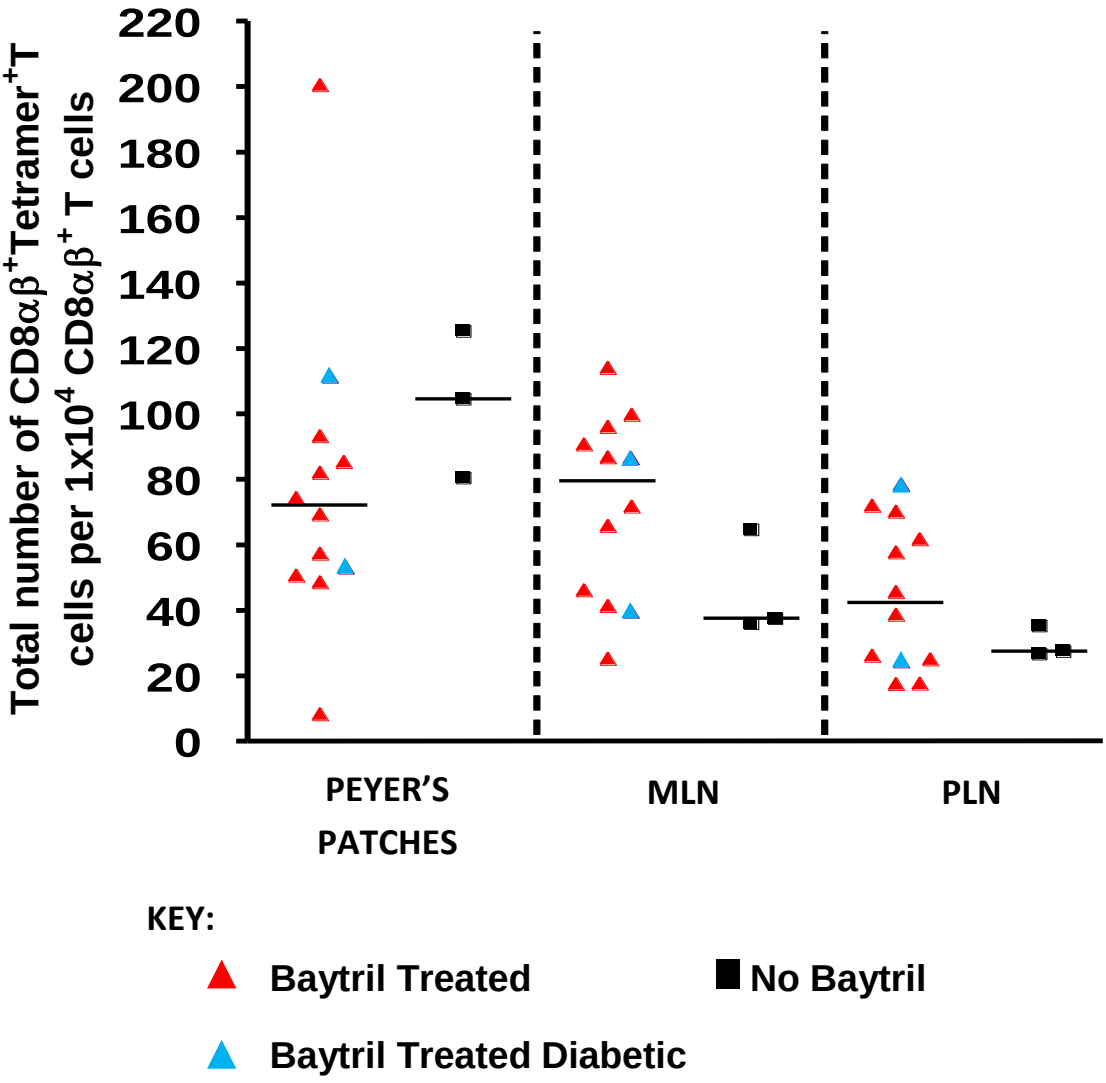

FIGURE 37: Cells were harvested from Peyer's patches, mesenteric lymph nodes (MLN) and pancreatic lymph nodes (PLN) from mice aged 6-12 weeks. These cells were then stained using a multi-colour antibody staining panel (see 2.9.3.3) and measured on a BD FACS CANTO II, to be analysed later using Flowjo Version 7.6.5 software. Background was subtracted from all tissues, using a minimally binding peptide:MHC tetramer. Data were then plotted using GraphPad Version 4 software. Each shape represents an individual mouse (n=3-11). The median is shown by the horizontal line.

5.4.2 ANTIBIOTIC TREATMENT OF SINGLE CHAIN TRAV8-1*01TRAJ9 TRANSGENIC NOD MICE DEFICIENT IN PROINSULIN 2 DOES NOT AFFECT THE NUMBER OF INSULIN B15-23-REACTIVE MEMORY CD8$^+$ T CELLS

Although no statistically significant differences were noted in the number of memory T cells between mice receiving treatment or those without antibiotic treatment, the insulin B15-23-reactive CD8αβ$^+$ T cells were investigated for their memory status as central or effector memory T cells. FIGURE 38 shows that there were similar numbers of central memory and effector memory T cells and that these results were similar between the tissues. The number of effector memory T cells (CD8αβ$^+$CD44$^+$CD62L$^-$) within the Peyer's patches compared to the MLN and PLN, in *A22Cα$^{-/-}$PI2$^{-/-}$* mice not treated with antibiotics, was increased from a median value of 5 per 10,000 cells (in the MLN and PLN) to 27 per 10,000 cells in the Peyer's patches. Interestingly, in those mice treated with antibiotics, the median number of effector memory T cells remained at approximately 5 per 10,000 cells in all tissues. However, the numbers are small and only males were analysed for the insulin B15-23-reactive CD8$^+$ T cells and therefore cannot be compared to female *A22Cα$^{-/-}$PI2$^{-/-}$* mice.

5.5 ANTIBIOTIC ADMINISTRATION ALTERED GUT MICROBIOTA IN SINGLE CHAIN TRAV8-1*01TRAJ9 TRANSGENIC NOD MICE DEFICIENT IN PROINSULIN 2

Administration of antibiotic regimes to *A22Cα$^{-/-}$PI2$^{-/-}$* mice altered the incidence of diabetes observed; however, it was unknown if the gut microbiota played a role in shaping the onset of diabetes. To investigate this, faecal pellets were collected weekly from all mice individually, from weaning to termination; DNA was subsequently extracted and sequenced for known bacteria. This enabled identification of bacterial differences between the treatment groups. This bacterial sequencing was performed by Dr Li Wen and her colleagues at Yale University.

FIGURE 38: Cells were harvested from Peyer's patches, mesenteric lymph nodes (MLN) and pancreatic lymph nodes (PLN) from mice aged 6-12 weeks. These cells were then stained using a multi-colour antibody staining panel (see 2.9.3.3) and measured on a BD FACS CANTO II. Data were then analysed using Flowjo Version 7.6.5 software where live single $CD8\alpha\beta^{+}CD44^{+}CD62L^{+}$ or $CD8\alpha\beta^{+}CD44^{+}CD62L^{-}$ T cells were gated. This proportion was then converted to a cell number per 10^{4} $CD8\alpha\beta^{+}$ T cells. Data were then plotted using GraphPad Version 4 software. The horizontal lines on the dot plot represent the median, while each individual shape represents an individual mouse.

FIGURE 38: TOTAL NUMBERS OF INSULIN B15-23-REACTIVE CD8αβ$^+$CD44$^+$CD62L$^+$ CENTRAL MEMORY T CELLS AND CD8αβ$^+$CD44$^+$CD62L$^-$ EFFECTOR MEMORY T CELLS PRESENT IN THE PEYER'S PATCHES, MESENTERIC LYMPH NODE (MLN) AND PANCREATIC LYMPH NODE (PLN) OF MALE SINGLE CHAIN TRAV8-1*01TRAJ9 TRANSGENIC NOD MICE DEFICIENT IN PROINSULIN 2

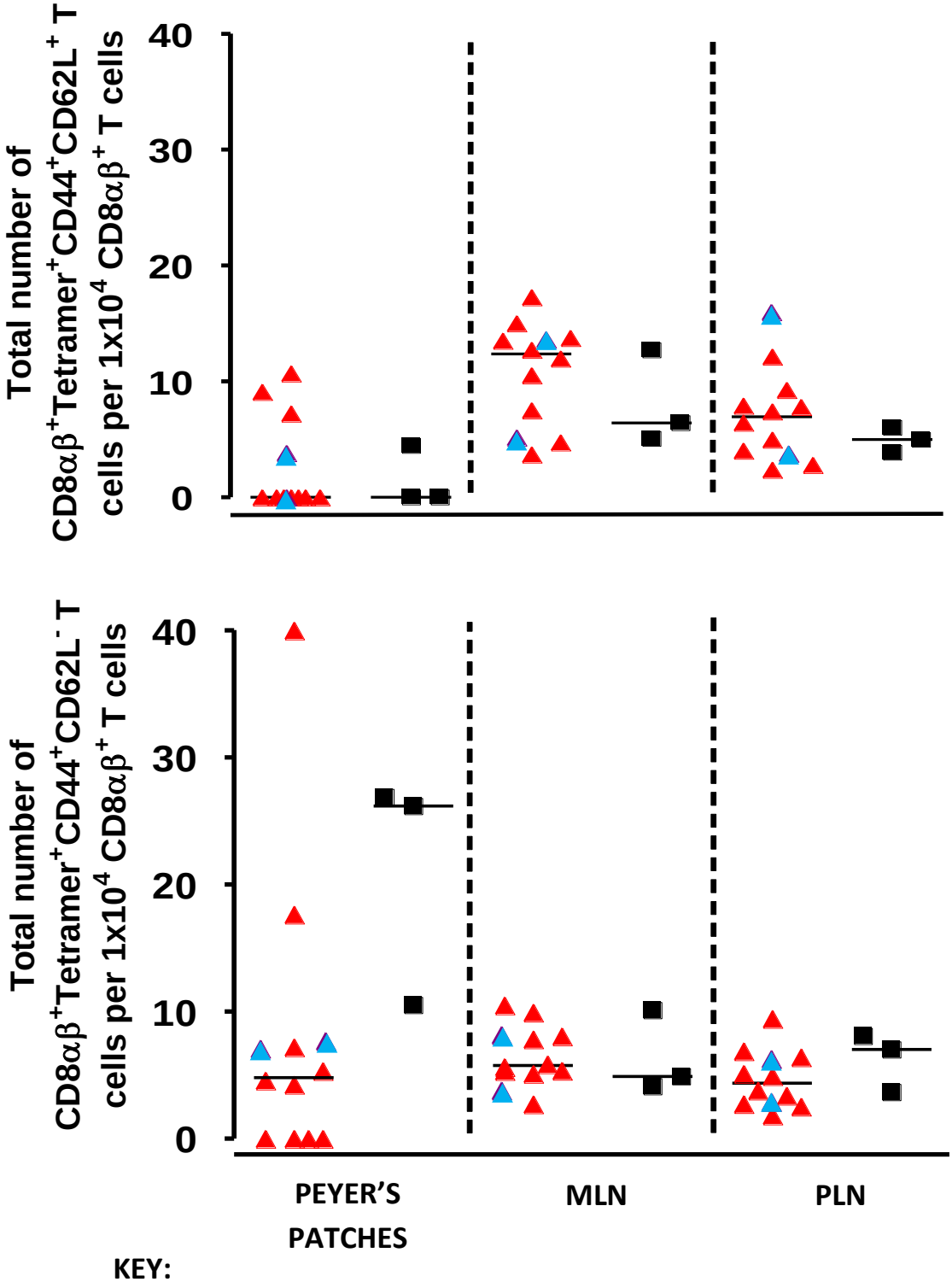

5.5.1 GUT MICROBIOTA IS ALTERED BY ANTIBIOTICS IN SINGLE CHAIN TRAV8-1*01TRAJ9 TRANSGENIC NOD MICE DEFICIENT IN PROINSULIN 2

Faecal pellets from *A22Cα*$^{-/-}$*PI2*$^{-/-}$ mice were sequenced for bacteria present at 3 weeks of age (before the change in antibiotics at weaning) and at 6 weeks of age (at the time spontaneous diabetes was observed). A principal component analysis (PCA) was conducted on the sequenced bacteria to compare the variation between individual mice sequenced as shown in FIGURE 39. This data shows that all mice have similar bacteria present at 3 weeks. However, the mice treated with Baytril from weaning tended to have the most variation between each other. Interestingly, most of the data showed clustering between the different antibiotic treatment groups with a few samples, including some samples from mice that would become diabetic at 6 weeks, separated from the main cluster. By 6 weeks, there were more differences in the gut microbiota between the groups. It can be seen that the mice which did not receive treatment, are found to the left, the Baytril-treated from birth mice cluster in the centre and the Baytril-treated from weaning *A22Cα*$^{-/-}$*PI2*$^{-/-}$ mice are mainly found to the right. The most striking difference is seen in those diabetic male mice, which cluster together. Of these diabetic mice, 4 were treated with antibiotics from weaning and 1 was treated with Baytril from birth. Only 1 diabetic mouse fell outside this cluster. Interestingly, there was a gender difference within the antibiotic treatment cohorts as the males and females tended to cluster separately.

FIGURE 39: Faecal pellets from antibiotic treated *A22Cα$^{-/-}$PI2$^{-/-}$* mice, aged 3 and 6 weeks, were collected and bacterial DNA extracted. DNA was then sequenced and known bacteria were identified through sequence homology. Bacterial variation between mice was identified through a principal component analysis (PCA). Males (n=3-4) and females (n=2-3) treated in the antibiotic regimes – Baytril from birth, Baytril from weaning (3 weeks) and no Baytril are shown. In addition bacterial DNA from faecal pellets from diabetic *A22Cα$^{-/-}$PI2$^{-/-}$* mice were also sequenced (n=2 treated from birth, n=4 treated from weaning). Male mice shown by outlined squares (in blue or orange) were identified to be diabetic at 6 weeks after two consecutive positive glycosuria results and blood glucose over 13.9mmol/L.

FIGURE 39: GUT MICROBIOTA VARIATION BETWEEN SINGLE CHAIN TRAV8-1*01TRAJ9 TRANSGENIC NOD MICE DEFICIENT IN PROINSULIN 2 GIVEN DIFFERENT ANTIBIOTICS REGIMES AT 3 AND 6 WEEKS OF AGE

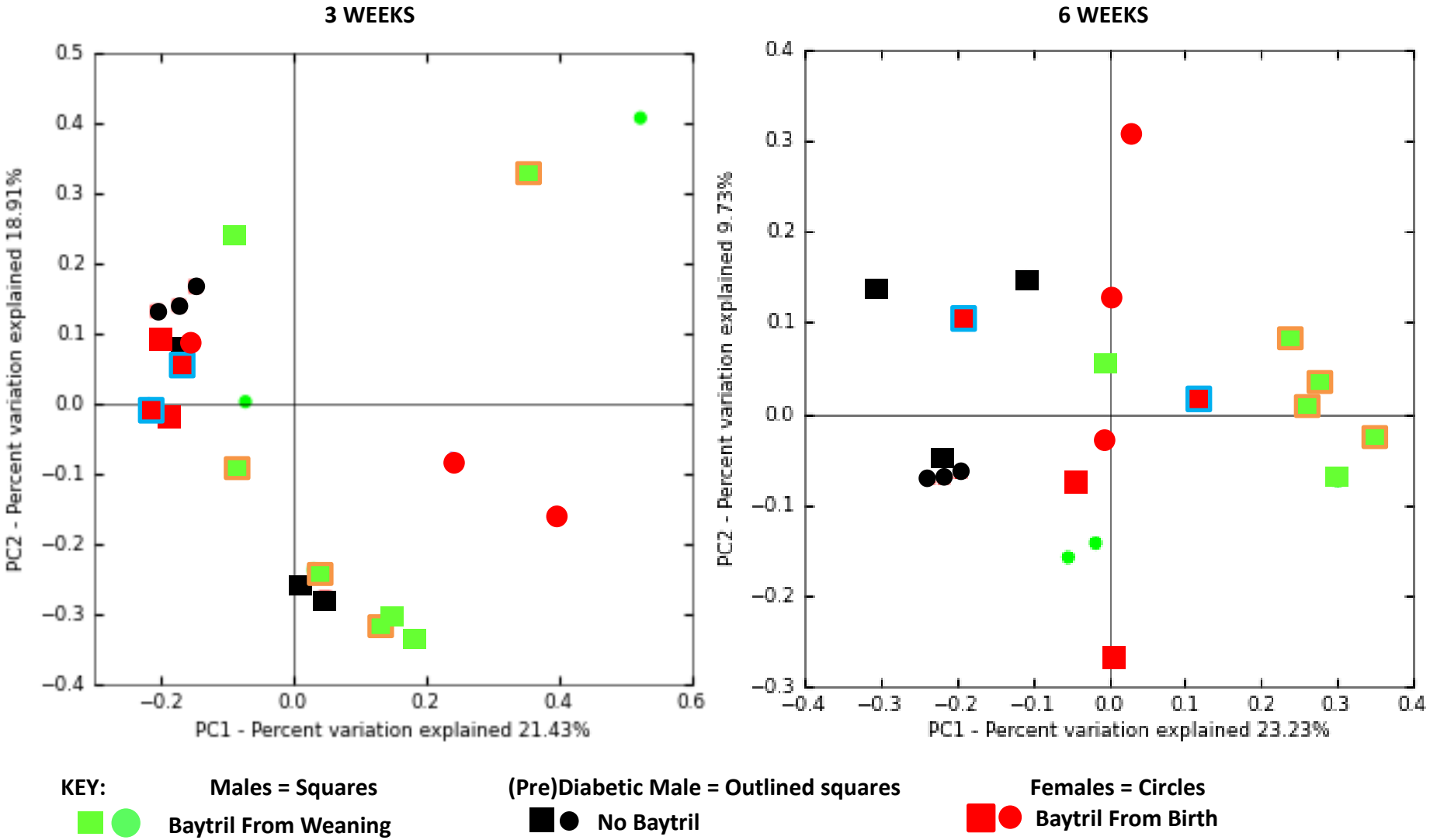

5.5.2 GUT MICROBIOTA DIVERSITY DECREASED WITH AGE IN SINGLE CHAIN TRAV8-1*01TRAJ9 TRANSGENIC NOD MICE, DEFICIENT IN PROINSULIN 2, AND WAS INDEPENDENT OF ANTIBIOTIC TREATMENT

Identification of the total gut microbiota differences between the *A22Cα*$^{-/-}$*PI2*$^{-/-}$ mice receiving different antibiotic treatments revealed greater differences at 6 weeks. However, when the bacteria were subdivided by phylum, there was a considerable decrease in microbial diversity in all mice. FIGURE 40 shows all treatment groups had a predominant Firmicute population at 3 weeks (45-64%), which expands to approximately 90-98% of the entire bacteria sequenced. At 3 weeks, the mice, in all groups, had a greater bacterial diversity, particularly the no antibiotics group and the antibiotic-treated group from weaning. The Baytril treated group from birth predominantly comprised firmicutes and bacteroidetes (making up over 99%) at 3 weeks but by 6 weeks, the firmicutes had expanded and the bacteroidetes populations decreased from 38% to just over 1%. The bacteroidetes, proteobacteria, tenericutes and deferribacteres are all decreased in proportion from 3 to 6 weeks of age. However, the actinobacteria population increased in those mice treated with Baytril from birth and Baytril from weaning from 0.6% and 2.53% to 2.53% and 5.25% respectively. The mice in the antibiotic-treatment from weaning maintained the largest diversity at 6 weeks. This decrease in gut microbial diversity was antibiotic treatment-independent as all groups were similarly affected.

FIGURE 40: Faecal pellets from antibiotic-treated *A22Cα*$^{-/-}$*PI2*$^{-/-}$ mice, aged 3 and 6 weeks, were collected. DNA was then extracted, sequenced and compared to known bacteria testing for sequence homology. Bacteria were then identified and grouped by phylum, with all mice receiving the same treatment grouped together (males and females). Each group comprised 6-8 mice with the proportions in percentages shown in bold on the pie charts.

FIGURE 40: GUT MICROBIOTA DIVERSITY AT THE PHYLUM LEVEL PRESENT IN SINGLE CHAIN TRAV8-1*01TRAJ9 TRANSGENIC NOD MICE DEFICIENT IN PROINSULIN 2 AT 3 AND 6 WEEKS OF AGE

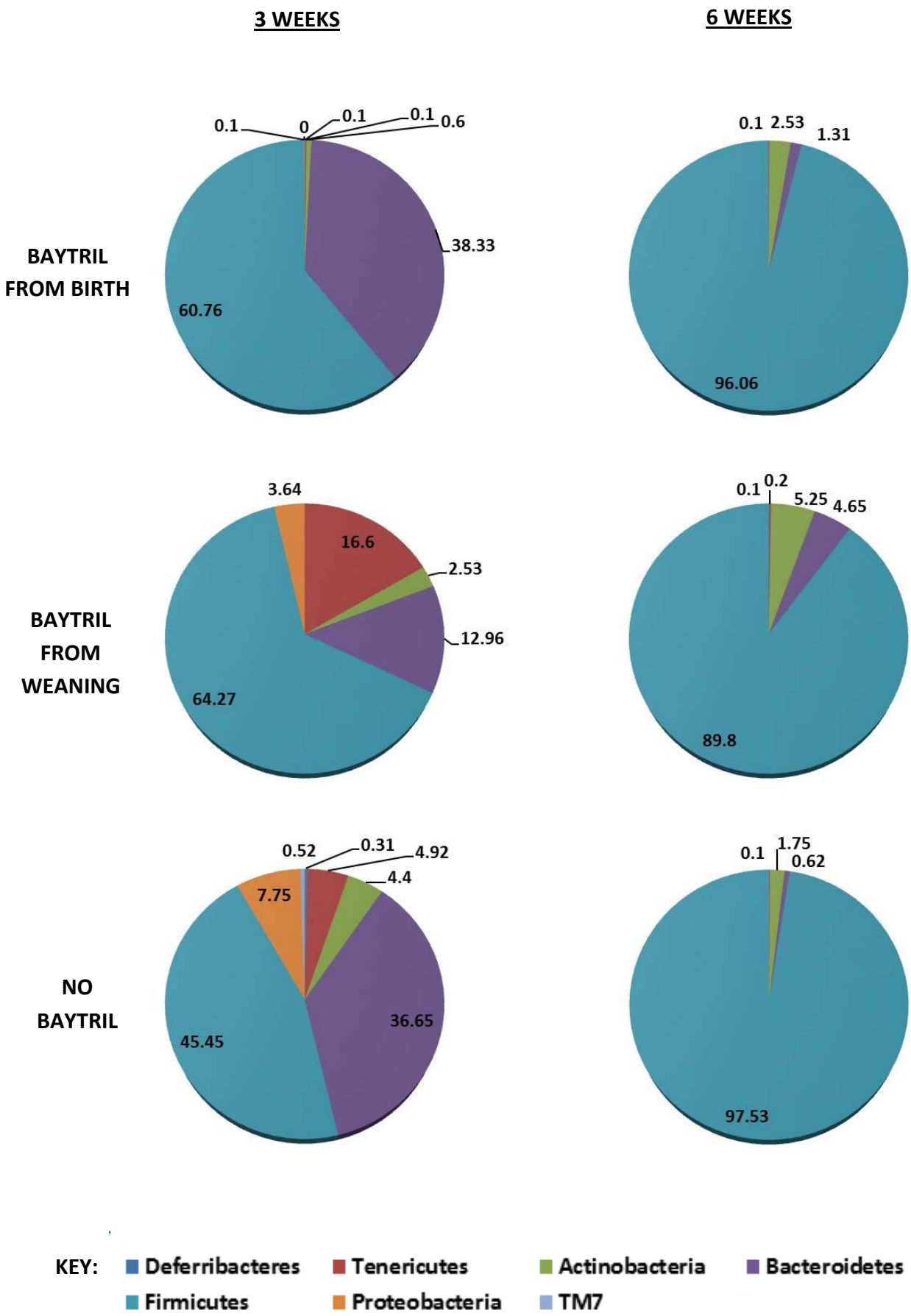

5.6 MALE SINGLE CHAIN TRAV8-1*01TRAJ9 TRANSGENIC NOD MICE DEFICIENT IN PROINSULIN 2 HAD IMPAIRED GLUCOSE TOLERANCE COMPARED TO FEMALE MICE

While investigations into the gut microbiota revealed a dramatic decrease in bacterial diversity, this raised the question as to how this might affect the role microbiota play in metabolism. Therefore, male single chain TRAV8-1*01TRAJ9 transgenic NOD mice were investigated for their ability to respond to a glucose stimulus i.e. through insulin production. Mice were fasted overnight prior to the glucose challenge, with blood glucose levels taken at 0 minutes, then every 15-30 minutes. FIGURE 41 shows that blood glucose was raised within 15 minutes of glucose challenge in all mice. In the male (A) and female (B) NOD mice at 6 weeks of age, blood glucose peaked at 17-18mmol/L at 15 minutes and took less than 60 minutes to fall below the threshold for diabetes (13.9mmol/L). This was similarly seen in the female *A22Cα*$^{-/-}$*PI2*$^{-/-}$ mice at 6 weeks; however, the single female 12 week old *A22Cα*$^{-/-}$*PI2*$^{-/-}$ mouse appeared to have better glucose tolerance than the mice at 6 weeks (B). In contrast to the female *A22Cα*$^{-/-}$*PI2*$^{-/-}$ mice at 6 weeks, the male mice, both at 6 and 12 weeks (A), failed to reduce their blood glucose levels within 90 minutes of a glucose challenge. While the 12-week old male *A22Cα*$^{-/-}$*PI2*$^{-/-}$ mice appeared to have a marginally improved glucose tolerance compared to the 6-week old males, the male mice remained glucose intolerant over the period of this test.

FIGURE 41: 6-12 week old single chain TRAV8-1*01TRAJ9 transgenic NOD mice and polyclonal NOD mice were fasted overnight. A baseline blood glucose reading was taken and then the mice were challenged intra-peritoneally with 1.5g glucose per kg of weight. Blood glucose readings were then taken at 15 minutes, 30 minutes, 60 minutes and 90 minutes post-glucose challenge. Mean data and range were then plotted using GraphPad Prism Version 4 software. Data are representative of 4 independent experiments whereby **A** shows data from the male mice and **B** shows data from the female mice. Data are representive of 9 male and 7 female 6-week old *A22Cα*$^{-/-}$*PI2*$^{-/-}$ mice (M6 and F6 respectively), 1 male and 1 female 12-week old *A22Cα*$^{-/-}$*PI2*$^{-/-}$ mice (M12 and F12 respectively) and 4 male and female 6-week old NOD mice (M6 and F6 respectively).

FIGURE 41: GLUCOSE TOLERANCE TEST RESULTS IN SINGLE CHAIN TRAV8-1*01TRAJ9 TRANSGENIC NOD MICE DEFICIENT IN PROINSULIN 2 AND POLYCLONAL NOD MICE

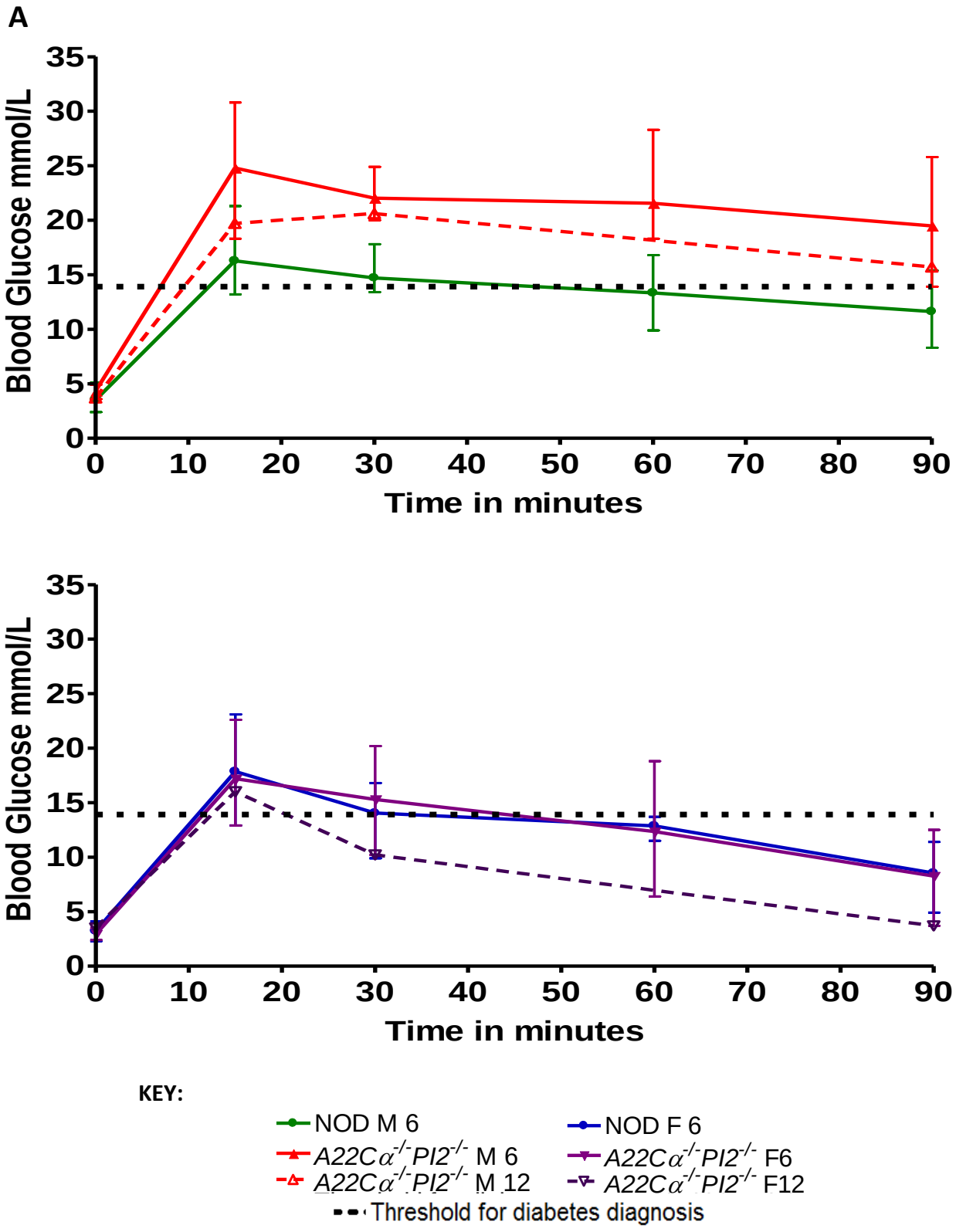

5.7 DISCUSSION

To summarise, more male single chain TRAV8-1*01TRAJ9 transgenic NOD mice deficient in proinsulin 2 developed spontaneous autoimmune diabetes on antibiotic administration, whether treated pre- or post-weaning. However, no female *A22Cα*$^{-/-}$*PI2*$^{-/-}$ mice developed diabetes regardless of antibiotic treatment (consistent with data in Chapter 3). In addition, these male *A22Cα*$^{-/-}$*PI2*$^{-/-}$ mice showed impaired glucose tolerance, reducing blood glucose levels more slowly post-glucose challenge compared with NOD mice, while the female *A22Cα*$^{-/-}$*PI2*$^{-/-}$ mice reduced the blood glucose level more rapidly. Investigation into the gut microbiota revealed greater differences between the antibiotic treatment groups at 6 weeks, with the bacterial species of many of the male diabetic mice clustering together. Upon further investigation at the phylum level, it was noted that all the mice had a greatly reduced bacterial diversity with Firmicutes comprising over approximately 90% of the total bacterial populations, whether they received antibiotics or not. Therefore, bacteria may be important in shaping the insulin B15-23-reactive CD8^{+} T cell response while also affecting glucose metabolism. Further work identifying specific bacterial species will help resolve the role of bacteria in the development of diabetes.

5.7.1 STUDY LIMITATIONS

It is important to note that the numbers in each group are small and therefore a greater number of mice need to be enrolled in the study. In addition, mice were cohoused at 3 weeks even if they had derived from different initial antibiotic treatment groups and therefore it is possible that bacteria were transferred between mice and thus reduced the differences between the mice. However, whether this protected mice or aided diabetes progression is unknown.

While many environmental factors were controlled for e.g. preparing fresh antibiotic-containing water bi-weekly, sterilisation of bottles etc. many could not be controlled for such as the amount of antibiotic-containing water each mouse drank, the food each consumed etc. It should also be mentioned that as illustrated in Chapters 3 and 4, although genetically identical, there was individual

mouse variation in the number of insulin B15-23-reactive $CD8^+$ T cells and therefore this could also not be controlled for.

5.7.2 BAYTRIL AND DIABETES INCIDENCE

Baytril containing enrofloxacin, a fluoroquinolone, is capable of destroying bacteria through inhibiting enzymes involved in bacterial DNA replication. More specifically, it preferentially targets Topoisomerase II (also known as DNA gyrase) in Gram-negative bacteria and Topoisomerase IV in Gram-positive bacteria, stabilising the complexes preventing DNA replication (Hooper, 2000). Through administration of this antibiotic post-weaning, incidence almost doubled from the previously observed 25% in male *A22Cα*$^{-/-}$*PI2*$^{-/-}$ mice (see Chapter 3) to 43% when receiving antibiotics. This suggested that potentially changes to the gut microbiota were affecting the development of autoimmune diabetes. Interestingly, the diabetes was even more accelerated in these studies compared to the incidence reported in Chapter 3 (6 weeks vs 10 weeks).

Only 1 of 5 male mice that did not receive any antibiotics developed diabetes, compared with 6 of 14 mice that were given antibiotics. The diabetes incidence may therefore be affected by the antibiotics circulating in the mouse and also the duration of administration may also play a role in promoting increased diabetogenicity. The antibiotics may also cause preferential expansion of disease-inducing bacteria or a decrease in the disease-preventing bacteria. While these incidence curves were not statistically significantly different, a clear trend was seen.

When the mice were treated in a larger cohort from birth to 3 weeks with different antibiotic regimes and then split into those mice receiving or not receiving Baytril post-weaning (after 3 weeks of age), the incidence was also affected.

The mice from breeders that were treated with antibiotics had a similar age of onset of diabetes (6 weeks) and similar level of diabetes incidence (43%) to that seen when the mice were treated post-weaning. Interestingly, 1/5 mice receiving no antibiotics, developed diabetes but at a delayed time of 10 weeks of age.

During the design of the experiment, breeders and litters from birth were treated with different antibiotic regimes, and when the mice reached 3 weeks, they were divided and placed into other treatment cohorts. At this point, mice were cohoused with other mice that had previously received other treatment regimes and therefore, it is possible that mice were capable of transferring/protecting mice from disease through coprophagic behaviour. Therefore, when designing future experiments, mice will be housed separately to ensure the true incidence, without any other influencing factors, will be observed. It is known environmental factors can influence diabetes including viruses (Atkinson et al., 1994, Drescher et al., 2004), bacteria (Wen et al., 2008, Hansen et al., 2012, Alkanani et al., 2014, Peng et al., 2014, Tormo-Badia et al., 2014), diet (Giulietti et al., 2004, Schmid et al., 2004, Marietta et al., 2013), the pH of drinking water (Sofi et al., 2014) etc. and therefore cohousing mice and transfer of microbiota may explain the diabetes observed in the mouse not treated with antibiotics.

As observed previously, no female *A22Cα*$^{-/-}$*PI2*$^{-/-}$ mice developed diabetes regardless of the antibiotic regime they received. This difference between the gender may have arisen due to the presence of sex hormones whereby in these mice oestrogen or progesterone may protect the females while testosterone may make the males more susceptible in contrast to the roles of these hormones in polyclonal NOD mice (Yurkovetskiy et al., 2013). Yurkovetskiy and colleagues also showed that androgens and gut microbiota are connected and that disease susceptibility can be altered through modifying these factors. In addition, these mice developing diabetes at 6 weeks correlates with the time they begin to sexually mature. Therefore, the gut microbiota may also be interacting with the hormones enabling preferential survival of diabetes causing/preventing bacteria.

Unlike treatment with Vancomycin (Hansen et al., 2012), or with an antibiotic mix during pregnancy (Tormo-Badia et al., 2014), Baytril (containing enrofloxacin) treatment of mice has induced similar increases in incidence when mice were treated either neonatally or post-weaning. In addition, antibiotics administered during pregnancy were shown to increase diabetes incidence. Therefore, it is possible that the gut microbiota in these mice are different and that the

dominant, and potentially protective, *Akkermansia muciniphila* species in the Verrucomicrobia phylum is not found within these TCR restricted *A22Cα*$^{-/-}$*PI2*$^{-/-}$ mice. Species identification would help resolve this question.

5.7.3 BAYTRIL TREATMENT AND TCR REPERTOIRE

To further explore the factors that contributed to the altered diabetes incidence, the TCR repertoire was examined to investigate whether expansion/deletion of a specific T cell population was involved in preventing or causing disease. The Peyer's patches, MLNs and PLNs were isolated and investigated for the TCR repertoire. Interestingly, no differences were observed in the $CD4^+$ or $CD8^+$ T cell number and no differences were seen in the global $CD8\alpha\beta^+$ TCR repertoire between any mice regardless of antibiotic treatment. Even though the TCRα chain is restricted, the T cells can still respond to a variety of antigens and it appears that the antibiotics are not having global effects on the TCR repertoire. However, it did not preclude small changes in antigen-specific populations i.e. bacteria-specific or insulin-specific T cells.

$CD8\alpha\beta^+$ T cells were also investigated for the expression of CD44 and CD62L, identifying subsets of memory T cells. Interestingly, increased numbers of $CD44^+CD62L^+$ central memory T cells but decreased numbers of $CD44^+CD62L^-$ effector memory T cells were found in the MLN and PLN when compared to the Peyer's patches. Given that M cells within the Peyer's patches are constantly sampling the contents of the gut, it is not surprising that there are fewer central and more effector $CD8\alpha\beta^+$ T cells in the Peyer's patches. This increased activation within the Peyer's patches may also stimulate antigen-specific T cells i.e insulin-reactive T cells whether directly or indirectly. It is known that lymphocytes isolated from the gut-associated lymph nodes can transfer diabetes into immunocompromised NOD.scid mice (Jaakkola et al., 2003). Therefore, the insulin B15-23-reactive $CD8^+$ T cells from the Peyer's patches were further investigated.

A similar number of insulin B15-23-reactive $CD8\alpha\beta^+$ T cells were identified in all lymphoid tissues in all male mice regardless of antibiotic treatment. However,

there was a trend to decreasing insulin B15-23-reactive $CD8^+$ T cells from the Peyer's patches to the MLNs to the PLNs in mice not treated with antibiotics. In those treated with antibiotics, the numbers of insulin B15-23-reactive $CD8^+$ T cells were similar between the Peyer's patches and the MLN but reduced in the PLN. It was possible that these auto-reactive $CD8^+$ T cells were trafficking from the Peyer's patches/MLNs upon activation, noted to be important in the early stages of diabetogenic T cell development through a mucosal addressin molecule (Hänninen et al., 1998). However, investigation into the memory subset of these cells revealed similar low numbers of central and effector memory T cells across all tissues. Once again, this suggested that these T cells were being maintained peripherally at low levels and had encountered antigen but were difficult to activate/expand, as seen in Chapter 4. This may be due to a higher activation threshold for these T cells and therefore may only become activated upon increased antigen exposure. In addition, these T cells may be regulated effectively through the presence of regulatory cells. However, few mice have been studied and therefore more data are required to gain better insight into this phenomenon.

It should also be noted that these data were generated from a comparison of mice diabetic at 6 weeks or upon termination at 12 weeks of age and thus have not developed diabetes. Therefore, there may be a greater difference between 6-week old mice that do or do not develop diabetes and these mouse groups should be investigated in the future.

5.7.4 BAYTRIL AND GUT MICROBIOTA

In this study we showed that at 3 weeks of age (up to weaning), the differences in bacteria present in the different antibiotic treated cohorts, as analysed by a principal component analysis, are small. However, by 6 weeks, differences emerged between the treatment groups, with the majority of mice in the different groups clustered together. Given that the antibiotic administered affects both Gram-positive and Gram-negative bacteria it is not surprising that there were differences in the gut microbiota between the groups. Even more interesting was that the diabetic mice tended to fall within the same area

suggesting that these mice had similar bacteria present. Therefore, this shows that the bacteria present within these mice are likely to be important in the development of diabetes. However, whether the bacteria have a direct or indirect role in T cell activation has yet to be identified.

There was more gut bacterial diversity at the phylum level in the mice at 3 weeks. However, as these mice reached 6 weeks they had a significant decrease in diversity with approximately 90% of the bacteria identified to be members of the phylum firmicutes. This effect was found to be antibiotic independent and therefore suggests it is either due to the TCRα chain restriction enforced in these *A22Cα*$^{-/-}$*PI2*$^{-/-}$ mice or due to the lack of proinsulin 2. Both of these factors raise interesting questions as it has been reported that, to maintain health, a diverse TCR repertoire is required and therefore if the repertoire is restricted, control of the bacterial composition may be affected. In addition, gut microbiota are required to maintain health and when the bacterial diversity is greatly reduced it can increase insulitis in germ-free NOD mice (Alam et al., 2011). This may be why the firmicutes increase dramatically as the immune system is less able to control the bacteria. Alternatively, proinsulin 2 may be important for the survival of bacteria from a metabolic point of view. While proinsulin 1 is largely expressed in the periphery, proinsulin 2 is believed to be important in tolerance. However, NOD mice deficient in proinsulin 1 do not develop metabolic or autoimmune diabetes and therefore proinsulin 2 must also be metabolically active. Thus, bacteria may require insulin for signalling and growth or the innate immune system may require insulin signalling to function accordingly.

The phylum firmicutes contains many species, some of which are known to be protective and others which may be more damaging. Within the phylum firmicutes are probiotic bacteria including lactobacillus. Therefore, it is possible that these also expand to prevent T cells from causing diabetes. *Lactobacillus casei*, VSL#3 (containing Lactobacilli) and genetically-modified *Lactobacillus lactis* secreting human proinsulin or GAD65 have all been shown to be important in reducing diabetes incidence and reverting pre-existing diabetes (Matsuzaki et al., 1997, Calcinaro et al., 2005, Takiishi et al., 2012, Robert et al., 2014). However,

identifying causal or protective bacteria would be important in order to devise a more successful therapeutic treatment, minimising the activation of diabetogenic T cells while increasing the regulation of these cells.

Alternatively, if a species of firmicutes were expanding within the gut of these mice due to an inability of the immune system to effectively target these bacteria, it is possible they could be damaging the gut wall and thus making it leakier. This could allow auto-antigens to escape and be presented to T cells and stimulate the immune processes leading to the activation of diabetogenic T cells. However, as yet, we have no data to support this.

As previously mentioned, Vancomycin treatment of NOD mice created a dominant *Akkermansia muciniphila* species in the Verrucomicrobia phylum (Hansen et al., 2012), however, this was not found in these TCR restricted *A22Cα*$^{-/-}$*PI2*$^{-/-}$ mice. As the antibiotics have different mechanisms of action, it may not be surprising to have different dominant species. Therefore, it may be worth in future investigating the role of other antibiotic treatments on the development of insulin B15-23-reactive $CD8^+$ T cells, the gut microbiota and diabetes.

While it has been reported the pH of drinking water can affect the gut microbiota and incidence of autoimmune diabetes (Sofi et al., 2014), it is unlikely to have any effect in our study as all mice received the same water.

5.7.5 IMPAIRED GLUCOSE TOLERANCE IN MALE MICE

Gut bacteria have numerous roles in metabolism. The restricted gut microbiota present in these single chain TRAV8-1*01TRAJ9 transgenic mice may have exerted a metabolic effect. Therefore, we tested the response of these mice to a glucose challenge, requiring the production and secretion of insulin from the pancreas in order to maintain homeostasis.

Using intraperitoneal glucose tolerance tests, it was shown that the male and female polyclonal NOD mice responded well and were capable of reducing their blood glucose within 30 minutes. However, in the single chain TRAV8-1*01TRAJ9 transgenic NOD mice deficient in proinsulin 2, there was a difference in the

metabolic response between males and females, with younger male mice appearing to have reduced functional response. This suggested that it was not the TCR restriction that was causing an impaired glucose response. However, it does suggest that androgens may be important factors and, as seen previously, it may be that the difference in gut microbiota may also be responsible. It has previously been shown in NOD mice that gut bacteria, androgens and the immune system are all important factors in shaping the onset of diabetes. It is not surprising that the *A22Cα*$^{-/-}$*PI2*$^{-/-}$ mice, which may develop diabetes were the ones that had a less efficient response to a glucose challenge. This may be due to a lack of proinsulin 2 in these mice resulting in less insulin being produced; however, the female mice do not have any metabolic defects. Most likely, as these mice develop diabetes, they may already have infiltration in the pancreas and therefore there may be fewer insulin producing cells available. As Chapter 3 showed, there was some infiltration in the *A22Cα*$^{-/-}$*PI2*$^{-/-}$ male mice; however, it was unlike NOD infiltration that is quite robust. In addition, pups born to NOD mice that had been treated in pregnancy, had fewer islets infiltrated compared to NOD litters that had not received any antibiotics (Tormo-Badia et al., 2014). Therefore, it is highly likely that both of these contribute to the male *A22Cα*$^{-/-}$*PI2*$^{-/-}$ mice developing diabetes.

Also, it may be possible that the β cells in the pancreas produce a lower amount of insulin. However, currently, there is no data to suggest this or any factors that may reduce insulin production other than β cell destruction.

Gut microbiota can produce short chain fatty acids to be used by the host as an energy source through the receptor GPR43, which can suppress insulin-mediated fat accumulation (Kimura et al., 2013). However, in this study we have altered the gut microbiota and therefore it is possible that lower amounts of short chain fatty acids are made by the restricted bacteria resulting in greater fat deposition and thus insulin resistance. While the male mice are marginally larger than the females, no studies have been carried out on the fat or fatty acid chains in these mice.

Interestingly, treatment with the antibiotics, ampicillin, neomycin and metronidazole in Swiss mice revealed a decrease in the firmicutes and bacteroidetes phyla resulting in increased insulin signalling and sensitivity (Carvalho et al., 2012). In the *A22Cα*$^{-/-}$*PI2*$^{-/-}$ mice, firmicutes were shown to be dominant, encompassing over 90% of the detectable microbiota; therefore the presence of these bacteria, through contact or secretary mechanisms, may also be making the mice less glucose tolerant. However, for future work, insulin measurements as part of the glucose tolerance tests as well as insulin tolerance tests should be performed, which will provide more information on this phenomenon.

5.7.6 SUMMARY

As discussed in Chapter 5, the administration of antibiotics appears to increase the incidence of diabetes by altering the gut microbiota, but does not affect the TCR repertoire. In addition, it is highly likely that androgens such as testosterone are also involved. However, as of yet, the role of the microbiota and androgens in the activation of the insulin B15-23-reactive CD8^{+} T cells is not fully understood and therefore warrants further investigation.

CHAPTER 6: FINAL DISCUSSION AND FUTURE WORK

6.1 THESIS RESULTS SUMMARY

The aim of this work was to investigate the development of insulin B15-23-reactive $CD8^+$ T cells in different proinsulin-expressing single chain TCRα (TRAV8-1*01TRAJ9) transgenic NOD mice. Initial studies revealed phenotypic differences in the TRBV repertoire, particularly in relation to TRBV19, the same TRBV chain utilised by the insulin B15-23-reactive G9 T cell clone (Wong et al., 1996). Further investigation into the TRBV repertoire of the insulin B15-23-reactive T cells revealed individual clonal expansions, with minimal CDR3 sequence overlap between the different proinsulin-expressing mice. In addition, proinsulin expression did not affect the total proportion of insulin B15-23-reactive T cells.

The role of proinsulin expression in shaping the functional ability of the insulin B15-23-reactive T cells was subsequently assessed using proliferation, cytokine production and cytotoxicity assays. However, due to the low frequency of insulin B15-23-reactive T cells, peptide-specific responses could not be detected in the proinsulin-expressing single chain TCRα (TRAV8-1*01TRAJ9) transgenic NOD mice, above the level of assay sensitivity. Therefore, $TRBV19^+CD8^+$ T cells were expanded *in vitro* and cloned by limiting dilution. Interestingly, the majority of (oligo)clonal T cell lines utilised TRBJ2-3 (the same junctional region found in the G9C8 clone from which the TCRα chain was derived), in conjunction with TRBV19, indicating the importance of this configuration in the TCR pairing for insulin B15-23 recognition. In addition, while a minority of (oligo)clonal lines responded at lower concentrations of insulin B15-23 peptide, most were shown to be of low functional avidity, regardless of proinsulin expression, if they express TRBV19. This was demonstrated in Chapter 4 where the T cell (oligo)clonal T cells responded to antigen, only at high peptide concentrations (1-5µg/ml peptide). The result suggested that the TCR interaction with p:MHC was weak, resulting in low T cell activity, indicating low functional avidity of the p:MHC:TCR interaction. However, while these T cell responses were low, it may not be related to avidity, it could be that these T cells, having been expanded and grown with peptide, may

be more tolerised to the insulin B15-23 peptide, than the directly *ex vivo* isolated insulin B15-23-reactive T cells and therefore these T cells, when assessed, exhibit low functional activity to peptide below 1μg/ml. The different proinsulin-expressing single chain TCRα (TRAV8-1*01TRAJ9) transgenic NOD mice did not, in general develop autoimmune diabetes. However, 25% of male proinsulin 2 deficient mice developed spontaneous autoimmune diabetes. There were a number of possible explanations for this. One possibility was that the insulin-reactive T cells were more functionally active. Another was that higher avidity T cells were present, although there is no current data to support this. A further suggestion could be that due to the expansion of different immunodominant insulin B15-23-reactive $CD8^+$ T cells in each different proinsulin-expressing mouse that some T cells may be able to overcome tolerance easier. Further investigations into the development of autoimmune diabetes in these mice revealed antibiotic-mediated effects on gut microbiota were capable of influencing the development of diabetes, independent of TCR repertoire. In addition, the role of proinsulin 2, while important for thymic and peripheral selection is also important metabolically. This was demonstrated in the single chain TCRα (TRAV8-1*01TRAJ9) transgenic NOD mice deficient in proinsulin 2 in Chapter 5 in relation to the intraperitoneal glucose tolerance tests. This showed that NOD male and female mice, and the female single chain TCRα NOD transgenic mice deficient in proinsulin 2 were able to control their blood glucose sufficiently below the threshold for diabetes within 30-60 minutes. However, in the male single chain TCRα NOD transgenic mice deficient in proinsulin 2, they were not able to reduce their blood glucose, following a glucose bolus, below the threshold for diabetes by 90 minutes, indicating signs of glucose intolerance. This may be due to a lack of insulin secretion and therefore an inability to quickly control the glucose bolus or it may be due to a form of insulin-resistance present in these mice, which results in the insulin not working as effectively on the target tissues and therefore it takes more insulin to be produced to enable the glucose uptake. However, insulin levels in this study were not investigated and therefore the precise reason for these mice having signs of glucose intolerance is unknown.

Thus the work in this thesis has suggested that proinsulin expression alters the functional status of insulin B15-23-reactive $CD8^+$ T cells, independently of TCR repertoire, with individual TCRβ chain clonal expansions identified in each mouse. This data indicates other mechanisms impacting the development of insulin B15-23 auto-reactivity other than antigen expression exist and may include a role for gut microbiota.

6.2 THESIS RESULTS FUTURE WORK

6.2.1 THE ROLE OF PROINSULIN EXPRESSION

Proinsulin is a precursor protein of the metabolically active hormone insulin. NOD mice express two proinsulin proteins called proinsulin 1 and 2, which only vary by 2 amino acids in the B chain and 3 amino acids in the C chain. Proinsulin 2 is believed to be important in inducing tolerance, as NOD mice lacking proinsulin 2 develop robust accelerated diabetes (Thébault-Baumont et al., 2003) and proinsulin 2 expression is capable of reducing and preventing diabetes (French et al., 1997, Faideau et al., 2004, Faideau et al., 2006). On the other hand, proinsulin 1 deficiency prevents the development of diabetes (Moriyama et al., 2003) believed to be mediated by the difference in the location of the expression of the two genes. This study, in agreement with other work, showed proinsulin 2 is predominantly expressed within the thymus with lower levels of proinsulin 1 (Chentoufi and Polychronakos, 2002, Chentoufi et al., 2004, Palumbo et al., 2006); however, some report that proinsulin 1 is not expressed in the thymus (Deltour et al., 1993, Derbinski et al., 2005, Nakayama et al., 2005b). Yet, all agree that both proinsulin 1 and 2 are expressed in the pancreas.

This study is the first antigen-specific study investigating how antigen expression affects the development of Insulin-reactive T cells at both a TCR repertoire and functional level. This study has shown that both proinsulin 1 and 2 are important in shaping TCR repertoire. Native proinsulin expression and proinsulin 2 over-expression induced decreases in the TRBV19 chain usage on a global repertoire basis. In addition, when mice were deficient in either proinsulin 1 or 2, the proportion of $TRBV19^+$ $CD8^+$ T cells was increased. However, while this data shows an importance of proinsulin expression in TCR repertoire composition, only

the proinsulin 2 deficient mice developed diabetes. In this study there appeared to be no functional differences in T cell responses to insulin B15-23 peptide, but only those T cells expressing TRBV19 were evaluated. However, functional investigations in the clonotypic G9 TCRαβ transgenic mouse revealed that when proinsulin 1 and 2 are lacking and the G9 T cells develop in the absence of proinsulin that cells can recognise (due to the mutation in the proinsulin transgene (Nakayama et al., 2005a)), they exhibit the greatest insulin B15-23 proliferative and cytotoxic response, closely followed by proinsulin 2 deficient mice and then the native proinsulin-expressing G9 mice (Terri Thayer, personal communication, manuscript in progress). This data highlights the importance of these models in assessing the development of antigen-specific T cell populations. However, understanding how proinsulin 1 deficiency affects the G9 T cells will need to be investigated.

In this study, utilising single chain TCRα transgenic NOD mice (using the TCRα chain from the G9C8 clone) and in the study involving G9 TCRαβ double transgenic mice, all crossed to various proinsulin-expressing backgrounds, it has been shown proinsulin expression is capable of affecting the development of these T cells and their ability to cause diabetes. By focusing on a single T cell clone, as in the G9C8 transgenic NOD mice, larger functional T cell differences, from the different proinsulin-expressing mice, could be seen in response to peptide; however, in both this study and the G9 transgenic mouse study only mice deficient in proinsulin 2 developed spontaneous diabetes. While the single chain TCRα transgenic NOD mice studies reported here revealed that multiple insulin B15-23-reactive $CD8^+$ TCRβ chains could be used for antigen recognition, functional differences in the insulin-reactive $CD8^+$ T cells could not be detected in this study between the different proinsulin-expressing mice. This may be due to the presence of multiple insulin B15-23-reactive T cells, which due to the various TCRβ chains they express, may recognise antigen differently and therefore respond in a different manner to the single T cell clone in the G9 TCR transgenic mouse work. However, no study to date has investigated the insulin-reactive $CD8^+$ T cell populations in polyclonal mice. Therefore for continued work in this

field, polyclonal NOD mice expressing proinsulin 1 and/or proinsulin 2, and proinsulin 1 and 2 deficient mice, should be investigated for their TCR repertoire, and the presence of other antigen-specific T cells in order to gain insight into how antigen-expression affects insulin-specific $CD8^+$ T cells (both Insulin B15-23 and Insulin A14-20 (Wong et al., 1996, Lamont et al., 2014)) and how this subsequently affects other non-insulin auto-reactive $CD8^+$ T cell populations such as IGRP (Lieberman et al., 2003), which are dependent on insulin autoimmunity (Krishnamurthy et al., 2008), over time. For $CD8^+$ T cells, MHC:tetramers can be used to ask such questions; however, for $CD4^+$ T cells, there are few tetramers available.

In this study, proinsulin-specific effects on TCR repertoire changes were found at a global T cell level. However, how does this expression of proinsulin 1 and 2 affect the repertoire? In relation to TRBV19 expression, a proportional reduction with age in those mice expressing native proinsulin or over-expressing proinsulin 2 would suggest that those $CD8^+$ T cells are likely to have been deleted. This may suggest both proinsulin 1 and 2 have tolerogenic properties - if proinsulin 2 was solely responsible for tolerance, then the $TRBV19^+$ $CD8^+$ T cell proportion in the single chain TCRα transgenic NOD mice deficient in proinsulin 1 would have been reduced to a similar level seen in the native proinsulin-expressing mice. This suggests that both proinsulin 1 and 2 ensure protection from insulin B15-23 autoimmunity and may act either additively or independently from each other. However, proinsulin expression may mediate functional tolerogenic effects and therefore not detected by TCR repertoire. These could include induction of anergy, where the T cell is unresponsive to antigen. Therefore, while we have only seen a small number of TCR repertoire effects, it is possible that other forms of tolerance are operating and therefore the total effect of proinsulin expression on tolerance cannot be assessed in this study. While some studies, including this one, have identified a tolerogenic role for proinsulin 2 (Chentoufi and Polychronakos, 2002, French et al., 1997, Jaeckel et al., 2004, Thébault-Baumont et al., 2003), the role of proinsulin 1 has not been fully established. The only investigation in NOD mice showed that proinsulin 1 deficient mice are protected

from the development of diabetes (Moriyama et al., 2003). Interestingly, on a non-autoimmune background (129/SV), mice deficient in proinsulin 2, showed increased insulin 1 gene transcripts as well as increased beta cell mass to compensate for lower insulin production, indicating the importance of proinsulin 1 in metabolism (Leroux et al., 2001). In addition, in NOD mice, proinsulin 1 and 2 peptide immunisations identified proinsulin 1-reactive T cells cross-reacted with proinsulin 2 epitopes and vice versa, with proinsulin 2 9-23 (B chain) peptide able to induce proliferation in proinsulin 1-reactive NOD T cells and proinsulin 1 9-23 and 49-66 (C chain) peptides able to induce proliferation of proinsulin 2-reactive NOD T cells (Jaeckel et al., 2004). This suggested that these TCRs are selected for by proinsulin 2 and that both proinsulins can facilitate proinsulin-specific populations to be expanded. In addition, work by Halbout and colleagues identified even more proinsulin 1 epitopes in NOD mice following peptide immunisation (Halbout et al., 2002). Therefore further work to assess the relative contributions of both proinsulin 1 and 2 in shaping tolerance and diabetogenicity of insulin B15-23-reactive $CD8^+$ T cells is needed.

In addition to this work investigating the repertoire and antigen-specific populations, further qPCR work would need to be done to study the level of proinsulin 1 and 2 in all the mutated mice, including those deficient in either or both proinsulin genes. This may identify if there is a required threshold for the level of proinsulin expressed in order to mediate tolerogenic effects. Additionally, it may identify a role for proinsulin 1 in shaping the diabetogenic TCR repertoire and may elucidate which antigen-specific populations, if any, are affected by proinsulin 1 expression.

While investigations into genetically modified polyclonal mice that express proinsulin 1 and/or 2 genes would reveal how auto-reactive T cell populations develop, further understanding in this area may be helped by the generation of mice containing proinsulin genes under controlled reporter genes. By switching on or turning off the proinsulin genes, it would enable us to understand how these T cells develop and how they may be manipulated post-development to alter the auto-reactive T cell development.

6.2.2 THE ROLE OF MICROBIOTA IN INSULIN B15-23 AUTOIMMUNITY

Gut microbiota play a role in both health and disease (reviewed by (Sekirov et al., 2010). For maintenance of health, a diverse gut microbiota is beneficial and when the gut microbiota is imbalanced, opportunistic pathogens can cause infections. Through gut microbial interactions with the innate immune system, tolerance and protection can be generated to commensals and potential pathogens. Interestingly, some studies have shown that gut microbiota may be causal or protective in disease and autoimmunity and genetic manipulation of these bacteria may enhance protective responses (Matsuzaki et al., 1997, Calcinaro et al., 2005, Takiishi et al., 2012, Robert et al., 2014). In addition, the gut microbiota can be altered through defects in the innate immune system such as TLRs and their signalling molecules (Echchannaoui et al., 2002, Wooten et al., 2002, Wen et al., 2008, Peng et al., 2014). In addition, there are broad effects on microbiota through treatment with antibiotics (Hansen et al., 2012) and the presence of androgens (Yurkovetskiy et al., 2013, Markle et al., 2013a). Antibiotic effects can be caused both by broad-spectrum agents, whereby both Gram-positive and Gram-negative bacteria are affected or they can more specifically target individual types of bacteria. However the antibiotics work, they reduce the particular bacteria, disrupting the natural homeostasis of commensal bacteria, enabling other bacteria to compete to fill the space. On the other hand, androgens enable the preferential survival and expansion of particular bacteria over others. Therefore, both antibiotic and androgen mediated effects on the microbiota may then disrupt the TLR signalling on the innate immune and subsequently may change their function from pro-tolerogenic to pathogenic or vice versa. In addition, the altered bacteria may produce new molecules, which mimic self-antigens. These may then be presented to antigen-specific T cells, which may cross-react with the self-antigen, leading to the destruction of the bacteria and self-antigen expressing cells, referred to as molecular mimicry. In addition, the bacteria may non-specifically induce a proinflammatory environment leading to bystander activation of the T cells, which, when activated, may promote antigen-specific T cell effects leading to recognition of self-antigen targets.

In the study reported in this thesis, treatment of single chain TCRα transgenic NOD mice deficient in proinsulin 2, with an enrofloxacin-containing antibiotic known as Baytril, was used. This increased the incidence of diabetes in the male proinsulin 2 deficient mice, while not affecting the lack of diabetes in the female mice. Further investigations, revealed the development of diabetes was independent of TCR repertoire and insulin B15-23-reactive T cells but partly dependent on gut microbiota changes by 6 weeks, as diabetic mice had similar gut microbiota in comparison to those non-diabetic. As the principal component analysis data showed in Chapter 5, the majority of diabetic mice at 6 weeks were found to cluster together and therefore have similar gut bacteria to one another. At that point, the results suggested that the gut bacteria were involved in increasing the incidence of diabetes. However, if the diabetic mice were also found to have similar bacteria to the non-diabetic mice then it would have been less likely that the increase in diabetes incidence was caused by bacteria. By sequencing the gut microbiota, significant expansion of the Firmicutes phylum and a marked decrease in gut microbial diversity was seen with age in all the mice. Interestingly, the male proinsulin 2 deficient single TCRα chain transgenic NOD mice were also generally shown to be glucose intolerant. Therefore, gender, metabolism and the microbiota appeared to be interconnected in shaping the development of insulin autoimmunity in an indirect manner.

To further investigate the findings, more single chain TRAV8-1*01TRAJ9 transgenic NOD mice deficient in proinsulin 2 should be studied, increasing the numbers. Additionally, in the experiments shown in this thesis, while some male mice were investigated for the number of insulin B15-23-reactive T cells, female mice were not investigated. Although no difference was noted in the number of insulin B15-23-reactive T cells between the male mice whether they were or were not treated with antibiotics, there may be a functional difference identified when male and female mice are compared. This also links with previous work identifying gender biases in the microbiota caused by the presence of androgens (Yurkovetskiy et al., 2013, Markle et al., 2013a). In the present study both male and female mice had similar gut microbiota composition, with the diabetic mice

exhibiting different microbial composition. In addition, this study looked at restricted TCRα chain transgenic mice, and therefore is not fully comparable to studies investigating the effects in polyclonal mice. Furthermore, as the total number of $CD8^+$ T cells was unaffected by treatment with antibiotics, it suggests other innate immune cells or regulatory cells may be directly affected by antibiotic treatment and therefore other cell populations will need to be investigated.

As mentioned, a proportion of male proinsulin 2 deficient mice developed diabetes; however, it is unknown whether the development of diabetes was mediated by T cells expressing the G9 TCRβ chain or other TCRβ chains. Therefore, investigations into which specific T cell clone(s) are affected by antibiotic administration should be identified to address whether this is an effect on all insulin B15-23-reactive T cells or an effect mediated by a specific-TCR, perhaps recognising a bacterial component due to TCR cross-reactivity. To assess this G9 TCR transgenic mice deficient in proinsulin 2 could be investigated, identifying whether T cells exhibiting a single TCR are similarly influenced by antibiotic administration.

While bacterial sequencing revealed that bacteria from the phylum firmicutes were increased with age and this was the predominant phylum in all mice, irrespective of antibiotic treatment, sequencing at the species level was not carried out. Therefore, further work investigating the species present may help to identify the presence of bacteria with known probiotic activity while also providing information on which bacterial species are expanding or decreasing and whether that is different in those developing diabetes and not. In addition, bacterial transfer studies could also be carried out for direct causal roles in shaping the auto-reactive environment, similar to the work by Peng and colleagues (Peng et al., 2014).

Having shown that some male mice, deficient in proinsulin 2, were glucose intolerant, this phenomenon should also be further investigated. In addition to glucose tolerance, measurements of insulin levels would be important (this had

been attempted but the sensitivity of the assay was insufficient to give conclusive results), as well as insulin tolerance tests. These measurements coupled with an in-depth histology study, would provide information on if insulin production is decreased in the male mice compared to females, and if the lack of proinsulin 2 reduces the number of islets that develop as well as the degree of infiltration in these mice, confirming if these mice have an intrinsic insulin deficiency or some degree of insulin resistance. In addition, bacterial species sequencing may also identify bacteria that affect metabolism and therefore, the level of insulin produced or degree of insulin resistance may be affected by the presence of particular microbiota (Caricilli et al., 2011, Carvalho et al., 2012).

In addition, while this work has focussed on the use of an enrofloxacin containing antibiotic, which has a large impact on both the Gram-positive and Gram-negative bacteria, other antibiotics, such as Vancomycin (Hansen et al., 2012), may be utilised in the future to gain better insight into the collection of microbiota present in the gut. This may also enable larger collections of bacteria to be investigated to see if and how they may alter disease development.

While this work is the first to investigate Insulin B15-23-reactive $CD8^+$ T cells, specifically in relation to the effect of gut microbiota on shaping the auto-reactive environment and diabetes, more work needs to be done to identify if the insulin B15-23-reactive T cells have a direct or indirect role in the onset of diabetes both in these mice and in TCR polyclonal mice.

6.2.3 FINAL SUMMARY

While it was initially hypothesized that proinsulin expression would alter the repertoire of insulin B15-23-reactive $CD8^+$ T cells and their functional ability to respond to insulin peptide, we did not observe any antigen-specific T cell repertoire changes; however, there were functional changes associated with the ability to cause diabetes when proinsulin 2 was deficient. Furthermore, we found different insulin B15-23-reactive $CD8^+$ T cell clonal immunodominance in the different proinsulin-expressing mice, with minimal shared clones, due to different CDR3 sequences, identified between them. This suggests, while proinsulin

expression is important in aiding thymic negative selection and peripheral selection on a global TCR level, that the specific clonal expansion is independent of proinsulin expression. Interestingly, proinsulin 2 over-expression has been able to reduce and prevent diabetes (French et al., 1997, Jaeckel et al., 2004), as seen in this study. However, a minority of mice were still able to develop spontaneous diabetes, albeit at a much later time point (Jaeckel et al., 2004). This suggests that while proinsulin expression may shape tolerance, there are still auto-reactive T cells that escape and become activated. Therefore, in order to develop a therapy targeting these insulin B15-23-reactive $CD8^+$ T cells, other mechanisms influencing clonal selection operate in the periphery and need to be identified. In mice expressing an artificial self-antigen, such as those expressing ovalbumin, T cells can escape central tolerance and only become active when antigen expression is increased. Zehn and Bevan showed this when they expressed ova peptide in Listeria and infected a group of mice (Zehn and Bevan, 2006). While bacterial infection with Listeria alone, without the self-antigen, was unable to cause disease, the infection with ovalbumin-expressing Listeria may have changed the context in which the artificial self-antigen (ovalbumin) was expressed in and thus trigger disease. Therefore, self-antigen expression in an artificial self-antigen system may influence selection but other factors may mediate post-selection development or function. However, it is important to remember that each TCR potentially recognises different antigens, with a different strength of interaction with the p:MHC and therefore what may affect one TCR may not be directly translatable to another. In this study, we showed the sequence of the TCR of the insulin B15-23-reactive T cells were individual to each mouse and therefore, while antigen expression (i.e. proinsulin) may not affect the TCR repertoire selection overall in these mice, it may not be the same for other TCRs. In addition, while it is possible the level of antigen is capable of changing the function of the T cells, only TRBV19 expressing insulin B15-23-reactive T cells were investigated here and proinsulin expression did not appear to affect the function of those. However, how proinsulin expression affects the other insulin B15-23-reactive TRBV expressing T cells remains to be studied. Therefore any future work requires the level of antigen expression on individual TCRs to be

investigated, as each TCR is different, whether functionally or from a TCR repertoire perspective.

While the diabetes incidence in the mice that were deficient in proinsulin 2 was affected by antibiotics, it still remains unknown as to the exact reason for the increase in diabetes incidence. While initial observations were made that antibiotic administration to the breeders during pregnancy, or from birth, did not affect the diabetes incidence, it is possible that there are other immunological changes dependent on when antibiotics are administered (Tormo-Badia et al., 2014). While this study used an enrofloxacin-containing antibiotic, other antibiotics, may have a greater or a lesser impact on the development of autoimmunity in these mice. Therefore, it is important to identify the specific affects the antibiotics have and how that specifically affects antigen-specific populations leading to the onset of or protection from autoimmunity or disease. In this study it was known that diabetes only occurred in male mice from approximately 6 weeks, coinciding with the time the mice reached sexual maturity, therefore, while it still remains untested, it is likely androgens have some effect on the diabetes incidence in this study, as observed by others (Yurkovetskiy et al., 2013, Markle et al., 2013a). While this gut microbiota mediated study has begun investigations into the shaping of insulin B15-23-reactive T cells, there is still much more work to be done. However, if bacterial species can be identified that are capable of mediating protective or activating T cell responses, then targeted specific therapies, through antibiotic administration or probiotic-containing drinks may be developed enabling the beneficial bacteria to boost T cell immunoregulation and thus delay, reduce or prevent diabetes.

Finally, together this data provides an insight into the development of insulin B15-23-reactive T cells, utilising a single TCRα chain, which only when coupled to TRBV19, do we see any TCR repertoire selection effects. However, clonal expansion is individual, and therefore, while antigen expression is important; other mechanisms of control are involved in shaping the insulin B15-23 autoimmunity. Therefore, these mechanisms need to be identified in order to develop therapeutic strategies capable of preventing the onset of insulin B15-23

reactivity. This will not only be beneficial from an animal model perspective but may be similar in human disease, providing key insights into preventing diabetes.

CHAPTER 7: APPENDIX

7.1 APPENDIX TABLES

AGE (WEEKS)	STRAIN NAME	DIFFERENT TO	TISSUE	P VALUE
4-6	***A22Cα$^{-/-}$PI2^{tg}***	*A22Cα$^{-/-}$*	PLN	0.0000004
		A22Cα$^{-/-}$PI1$^{-/-}$	PLN	0.0000001
		A22Cα$^{-/-}$PI2$^{-/-}$	PLN	0.0000009
		A22Cα$^{-/-}$PI1$^{-/-}$PI2$^{-/-}$Y16A^{tg}	PLN	0.0000000
		A22Cα$^{-/-}$	MLN	0.0000000
		A22Cα$^{-/-}$PI1$^{-/-}$	MLN	0.0000000
		A22Cα$^{-/-}$PI2$^{-/-}$	MLN	0.0000001
		A22Cα$^{-/-}$PI1$^{-/-}$PI2$^{-/-}$Y16A^{tg}	MLN	0.0000000
11-16		*A22Cα$^{-/-}$PI1$^{-/-}$*	Thymus	0.0000008
		A22Cα$^{-/-}$PI2$^{-/-}$	Thymus	0.0000000
		A22Cα$^{-/-}$PI1$^{-/-}$PI2$^{-/-}$Y16A^{tg}	Thymus	0.0000000
		A22Cα$^{-/-}$	Spleen	0.0000000
		A22Cα$^{-/-}$PI1$^{-/-}$	Spleen	0.0000000
		A22Cα$^{-/-}$PI2$^{-/-}$	Spleen	0.0000000
		A22Cα$^{-/-}$PI1$^{-/-}$PI2$^{-/-}$Y16A^{tg}	Spleen	0.0000000
		A22Cα$^{-/-}$PI1$^{-/-}$	PLN	0.0000000
		A22Cα$^{-/-}$PI2$^{-/-}$	PLN	0.0000000
		A22Cα$^{-/-}$PI1$^{-/-}$PI2$^{-/-}$Y16A^{tg}	PLN	0.0000000
		A22Cα$^{-/-}$PI1$^{-/-}$	MLN	0.0000000
		A22Cα$^{-/-}$PI2$^{-/-}$	MLN	0.0000000
		A22Cα$^{-/-}$PI1$^{-/-}$PI2$^{-/-}$Y16A^{tg}	MLN	0.0000000

TABLE 25: SIGNIFICANT DIFFERENCES BETWEEN SINGLE CHAIN TRANSGENIC TRAV8-1*01TRAJ9 NOD MICE EXPRESSING TRBV19 IN MICE WITH VARYING LEVELS OF PROINSULIN

ANTIBIOTIC TREATMENT		SEX	TRBV 1	TRBV 2	TRBV 4	TRBV 12	TRBV 13	TRBV 14	TRBV 15	TRBV 16	TRBV 17	TRBV 19	TRBV 24	TRBV 26	TRBV 29	TRBV 31
PRE-WEANING	POST-WEANING															
ON	ON	M	194	236	1214	367	2841	292	160	312	72	1709	1	215	12	480
ON	ON	F	295	267	1289	351	2895	290	98	305	73	1741	6	208	22	514
ON	OFF	M	n/a	268	1232	345	2877	307	153	319	70	1679	1	224	14	458
ON	OFF	F	377	267	1258	328	2932	307	176	297	60	1712	5	185	26	502
ON/OFF	ON	M	230	313	1118	363	2948	331	158	354	59	1738	2	218	7	457
ON/OFF	ON	F	266	313	1223	329	2906	298	166	316	72	1763	4	194	6	496
ON/OFF	OFF	M	197	317	1173	341	2933	288	142	338	71	1792	6	230	6	467
ON/OFF	OFF	F	309	291	1244	325	2858	304	163	308	64	1746	4	210	13	513
OFF	ON	M	287	263	1158	356	2643	292	165	328	71	1776	1	227	8	479
OFF	ON	M	130	258	1078	374	2706	293	172	368	89	1704	1	216	10	445
OFF	ON	F	214	271	1280	338	3001	286	172	290	69	1745	4	205	18	469
OFF	OFF	M	262	252	1199	360	2746	280	165	334	67	1721	3	206	16	483
OFF	OFF	M	193	280	1173	357	2746	304	176	364	58	1802	2	208	14	447
OFF	OFF	F	245	289	1263	321	2815	292	173	300	60	1729	4	199	24	505

TABLE 26: PLN CD8αβ$^+$ TRBV REPERTOIRE IN SINGLE CHAIN TRAV8-1*01 TRANSGENIC NOD MICE DEFICIENT IN PROINSULIN 2 SHOWN BY ANTIBIOTIC TREATMENT AND GENDER

Data were collated from CD8αβ$^+$ TRBV repertoire staining of the PLN (pancreatic lymph nodes) from single chain TRAV8-1*01TRAJ9 NOD transgenic mice deficient in proinsulin 2. Data shown is representative of 4-7 mice per group except the two diabetic groups (in red) which compile data from 1-3 mice. n/a = data unavailable. No differences were found between any of the groups or genders.

7.2 APPENDIX FIGURES

FIGURE 42: THYMOCYTE AND SPLENOCYTE TOTAL CELL COUNTS IN SINGLE CHAIN TRANSGENIC TRAV8-1*01TRAJ9 NOD MICE EXPRESSING VARYING PROINSULIN LEVELS AT 8-10 WEEKS OF AGE

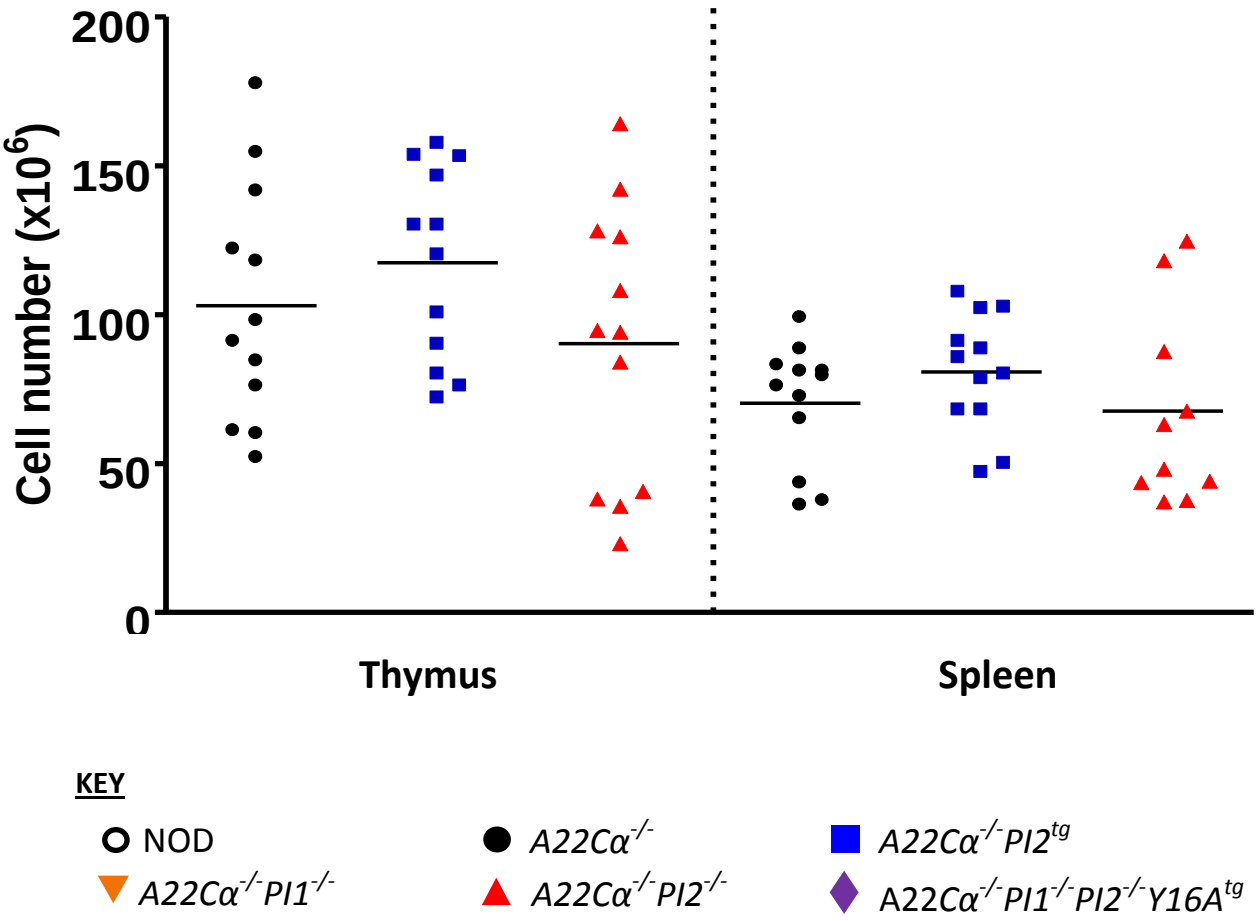

FIGURE 42: Thymocyte and splenocyte cells were harvested and homogenised. The red blood cells were lysed in the splenocyte populations and the splenocytes resuspended in 10mls FACS Buffer for counting. Cell number was determined through exclusion of non-viable cells by Trypan blue using a haemocytometer. Data were analysed by ANOVA using R software. Data shown were not significant at the p=<0.01 level. Each dot represents an individual mouse with the horizontal lines indicating the mean.

FIGURE 43: Lymphoid cells were harvested from thymus, spleen, PLN and MLN of mice aged 4-7 weeks or 11-16 weeks. These cells were stained using a multi-colour antibody staining panel (see 2.9.3.3) and measured on a BD FACS CANTO II to be analysed later using Flowjo Version 7.6.5 software. Data were then plotted using GraphPad Version 4 software. Each shape represents an individual mouse (n=8-13), with unfilled shapes representing those aged 4-7 weeks and filled shapes those aged 11-16 weeks. The median is shown for each data set by a horizontal line with statistically significant differences at p=<0.05 (*) and p=<0.01 (**) between the strains shown following an ANOVA analysis using R software.

FIGURE 43: CD8^{+}TRBV1^{+} T CELL PROPORTIONS IN THE THYMI, SPLEEN, PANCREATIC LYMPH NODE (PLN) AND MESENTERIC LYMPH NODE (MLN) IN SINGLE CHAIN TRANSGENIC TRAV8-1*01TRAJ9 NOD MICE EXPRESSING VARYING PROINSULIN LEVELS

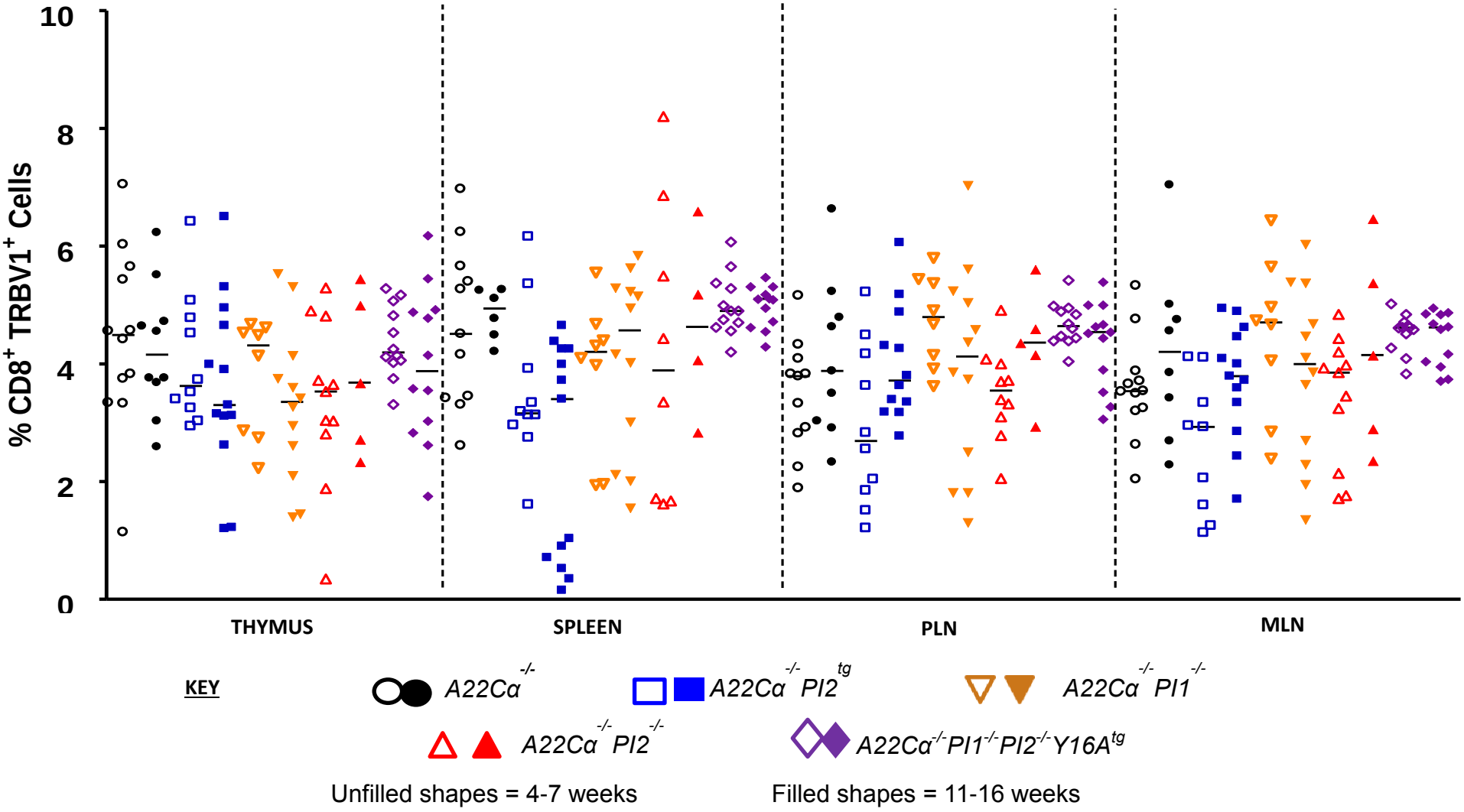

FIGURE 44: Lymphoid cells were harvested from thymus, spleen, PLN and MLN of mice aged 4-7 weeks or 11-16 weeks. These cells were stained using a multi-colour antibody staining panel (see 2.9.3.3) and measured on a BD FACS CANTO II to be analysed later using Flowjo Version 7.6.5 software. Data were then plotted using GraphPad Version 4 software. Each shape represents an individual mouse (n=8-13), with unfilled shapes representing those aged 4-7 weeks and filled shapes those aged 11-16 weeks. The median is shown for each data set by a horizontal line with statistically significant differences at p=<0.05 (*) and p=<0.01 (**) between the strains shown following an ANOVA analysis using R software.

FIGURE 44: CD8^{+}TRBV2^{+} T CELL PROPORTIONS IN THE THYMI, SPLEEN, PANCREATIC LYMPH NODE (PLN) AND MESENTERIC LYMPH NODE (MLN) IN SINGLE CHAIN TRANSGENIC TRAV8-1*01TRAJ9 NOD MICE EXPRESSING VARYING PROINSULIN LEVELS

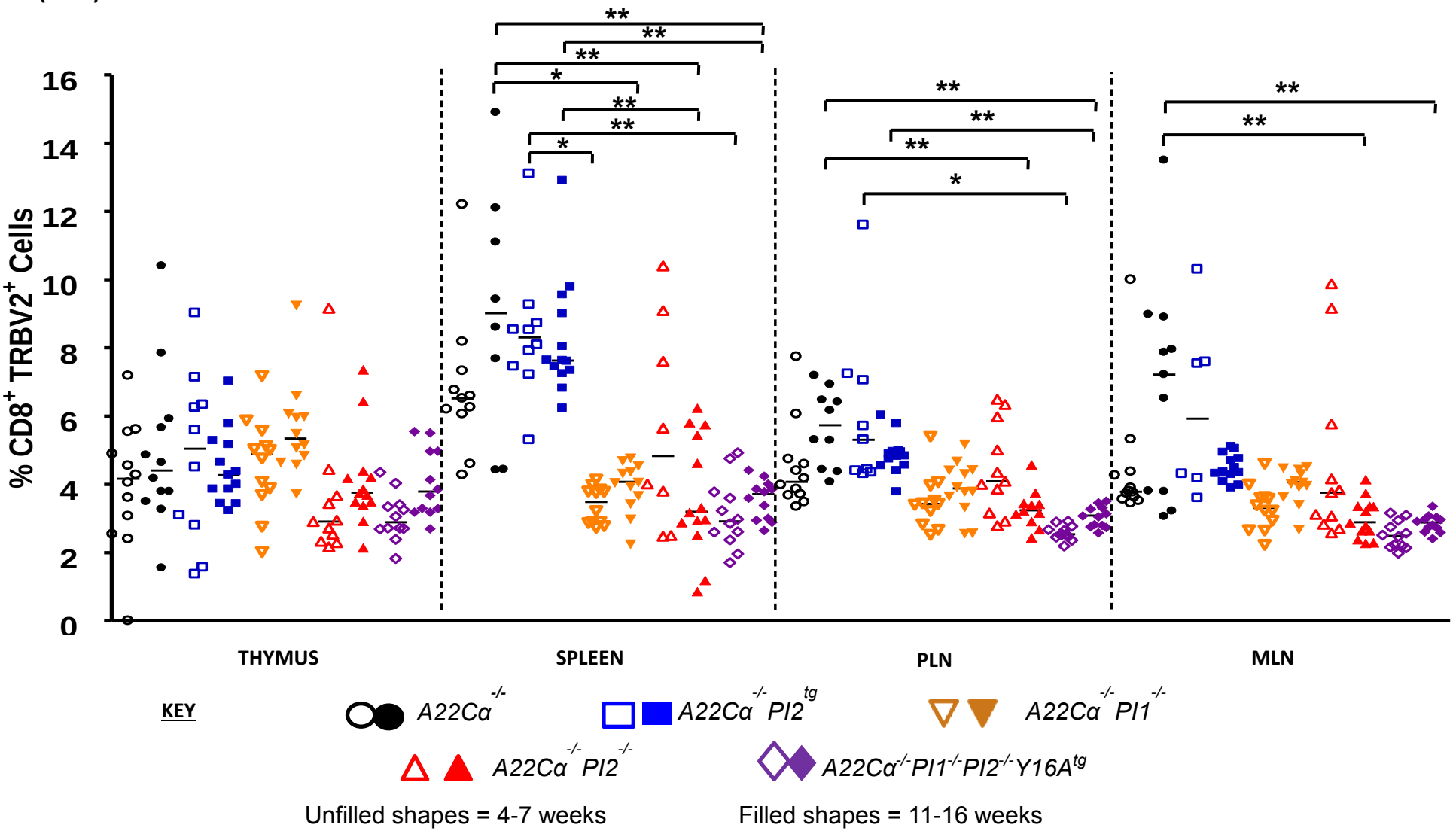

FIGURE 45: Lymphoid cells were harvested from thymus, spleen, PLN and MLN of mice aged 4-7 weeks or 11-16 weeks. These cells were stained using a multi-colour antibody staining panel (see 2.9.3.3) and measured on a BD FACS CANTO II to be analysed later using Flowjo Version 7.6.5 software. Data were then plotted using GraphPad Version 4 software. Each shape represents an individual mouse (n=8-13), with unfilled shapes representing those aged 4-7 weeks and filled shapes those aged 11-16 weeks. The median is shown for each data set by a horizontal line with statistically significant differences at p=<0.05 (*) and p=<0.01 (**) between the strains shown following an ANOVA analysis using R software.

FIGURE 45: CD8^{+}TRBV12^{+} T CELL PROPORTIONS IN THE THYMI, SPLEEN, PANCREATIC LYMPH NODE (PLN) AND MESENTERIC LYMPH NODE (MLN) IN SINGLE CHAIN TRANSGENIC TRAV8-1*01TRAJ9 NOD MICE EXPRESSING VARYING PROINSULIN LEVELS

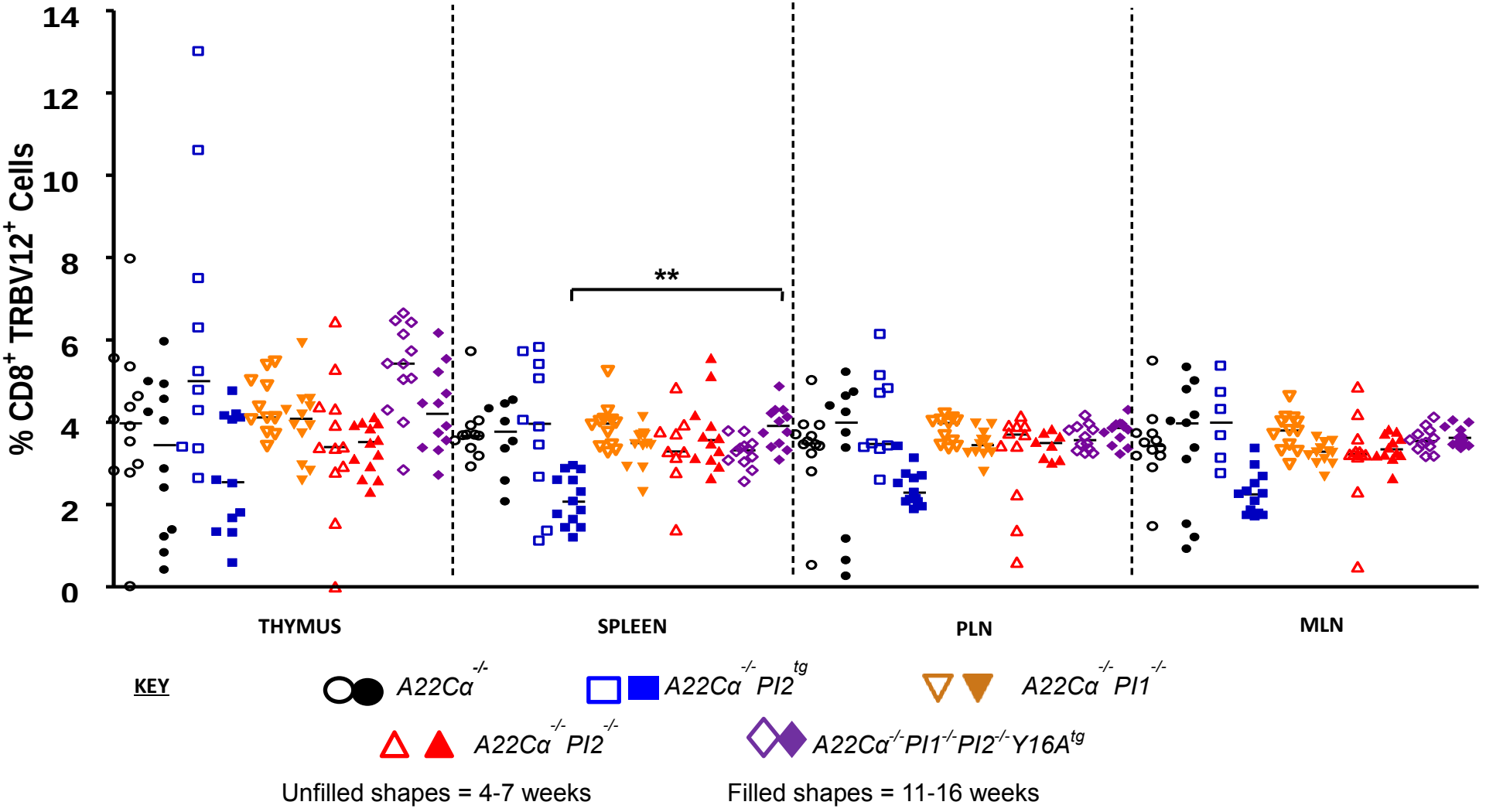

FIGURE 46: Lymphoid cells were harvested from thymus, spleen, PLN and MLN of mice aged 4-7 weeks or 11-16 weeks. These cells were stained using a multi-colour antibody staining panel (see 2.9.3.3) and measured on a BD FACS CANTO II to be analysed later using Flowjo Version 7.6.5 software. Data were then plotted using GraphPad Version 4 software. Each shape represents an individual mouse (n=8-13), with unfilled shapes representing those aged 4-7 weeks and filled shapes those aged 11-16 weeks. The median is shown for each data set by a horizontal line with statistically significant differences at p=<0.05 (*) and p=<0.01 (**) between the strains shown following an ANOVA analysis using R software.

FIGURE 46: CD8^{+}TRBV13^{+} T CELL PROPORTIONS IN THE THYMI, SPLEEN, PANCREATIC LYMPH NODE (PLN) AND MESENTERIC LYMPH NODE (MLN) IN SINGLE CHAIN TRANSGENIC TRAV8-1*01TRAJ9 NOD MICE EXPRESSING VARYING PROINSULIN LEVELS

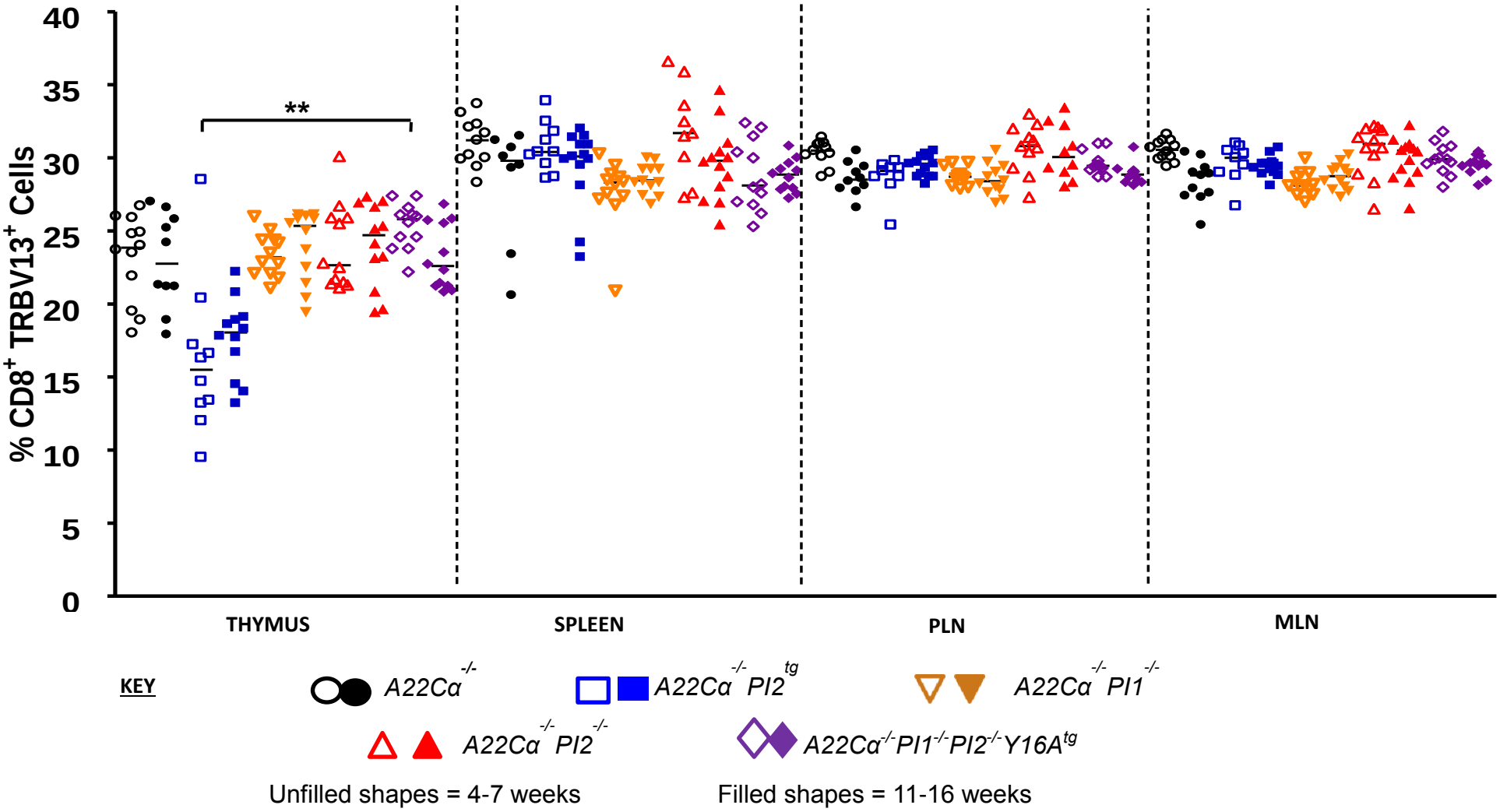

FIGURE 47: Lymphoid cells were harvested from thymus, spleen, PLN and MLN of mice aged 4-7 weeks or 11-16 weeks. These cells were stained using a multi-colour antibody staining panel (see 2.9.3.3) and measured on a BD FACS CANTO II to be analysed later using Flowjo Version 7.6.5 software. Data were then plotted using GraphPad Version 4 software. Each shape represents an individual mouse (n=8-13), with unfilled shapes representing those aged 4-7 weeks and filled shapes those aged 11-16 weeks. The median is shown for each data set by a horizontal line with statistically significant differences at p=<0.05 (*) and p=<0.01 (**) between the strains shown following an ANOVA analysis using R software.

FIGURE 47: CD8^{+}TRBV14^{+} T CELL PROPORTIONS IN THE THYMI, SPLEEN, PANCREATIC LYMPH NODE (PLN) AND MESENTERIC LYMPH NODE (MLN) IN SINGLE CHAIN TRANSGENIC TRAV8-1*01TRAJ9 NOD MICE EXPRESSING VARYING PROINSULIN LEVELS

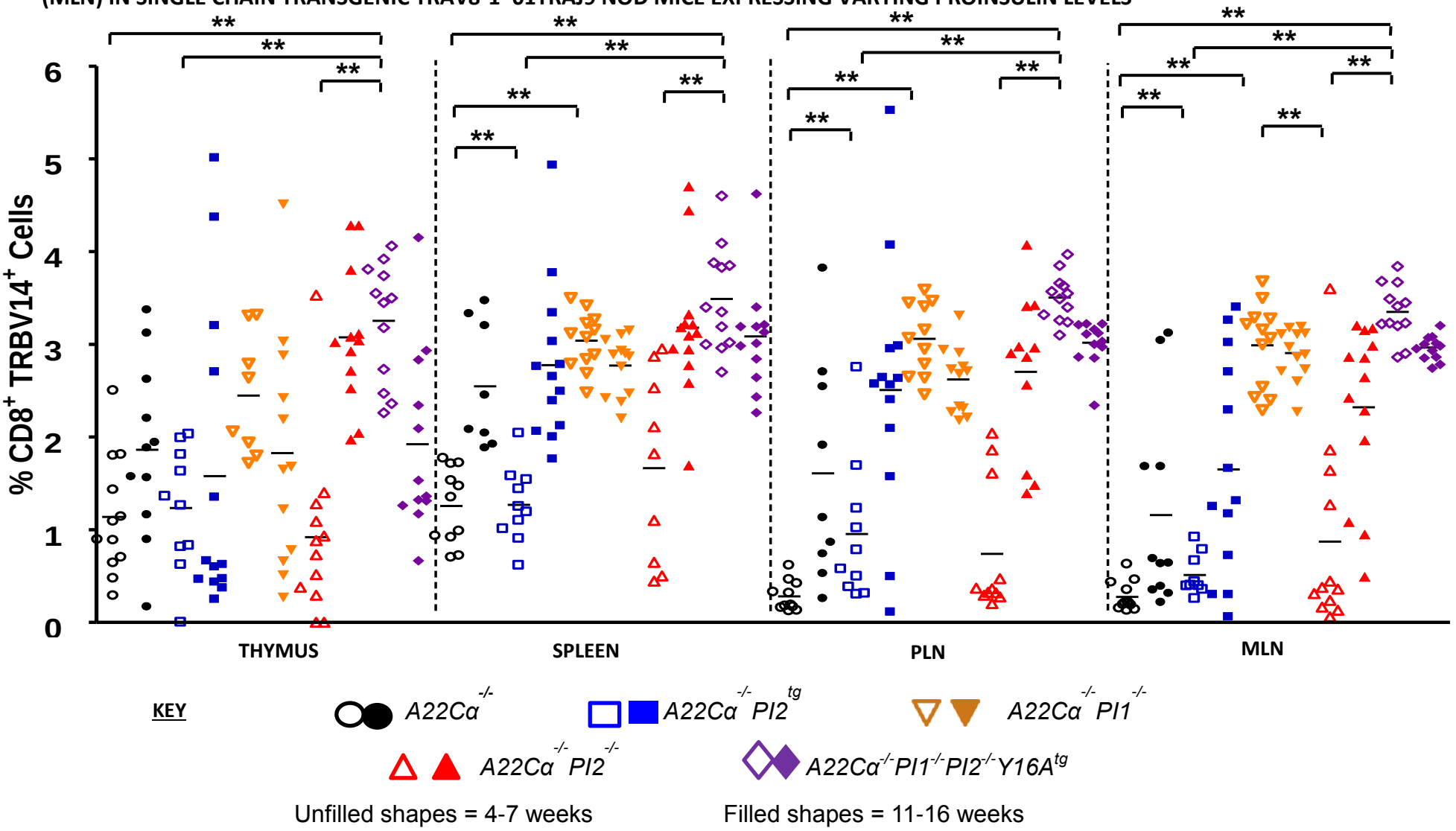

FIGURE 48: Lymphoid cells were harvested from thymus, spleen, PLN and MLN of mice aged 4-7 weeks or 11-16 weeks. These cells were stained using a multi-colour antibody staining panel (see 2.9.3.3) and measured on a BD FACS CANTO II to be analysed later using Flowjo Version 7.6.5 software. Data were then plotted using GraphPad Version 4 software. Each shape represents an individual mouse (n=8-13), with unfilled shapes representing those aged 4-7 weeks and filled shapes those aged 11-16 weeks. The median is shown for each data set by a horizontal line with statistically significant differences at p=<0.05 (*) and p=<0.01 (**) between the strains shown following an ANOVA analysis using R software.

FIGURE 48: CD8^{+}TRBV15^{+} T CELL PROPORTIONS IN THE THYMI, SPLEEN, PANCREATIC LYMPH NODE (PLN) AND MESENTERIC LYMPH NODE (MLN) IN SINGLE CHAIN TRANSGENIC TRAV8-1*01TRAJ9 NOD MICE EXPRESSING VARYING PROINSULIN LEVELS

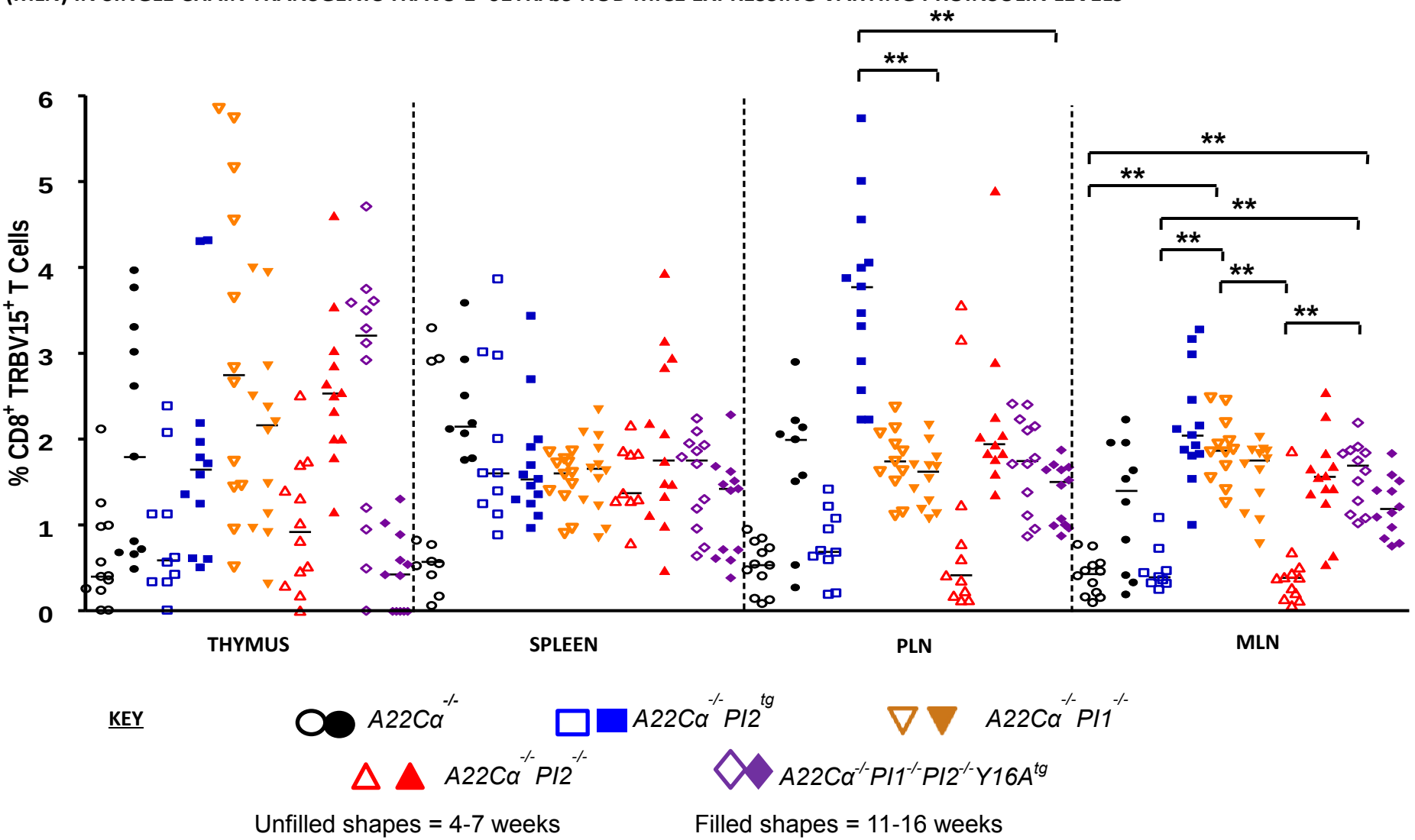

FIGURE 49: Lymphoid cells were harvested from thymus, spleen, PLN and MLN of mice aged 4-7 weeks or 11-16 weeks. These cells were stained using a multi-colour antibody staining panel (see 2.9.3.3) and measured on a BD FACS CANTO II to be analysed later using Flowjo Version 7.6.5 software. Data were then plotted using GraphPad Version 4 software. Each shape represents an individual mouse (n=8-13), with unfilled shapes representing those aged 4-7 weeks and filled shapes those aged 11-16 weeks. The median is shown for each data set by a horizontal line with statistically significant differences at p=<0.05 (*) and p=<0.01 (**) between the strains shown following an ANOVA analysis using R software.

FIGURE 49: CD8^{+}TRBV17^{+} T CELL PROPORTIONS IN THE THYMI, SPLEEN, PANCREATIC LYMPH NODE (PLN) AND MESENTERIC LYMPH NODE (MLN) IN SINGLE CHAIN TRANSGENIC TRAV8-1*01TRAJ9 NOD MICE EXPRESSING VARYING PROINSULIN LEVELS

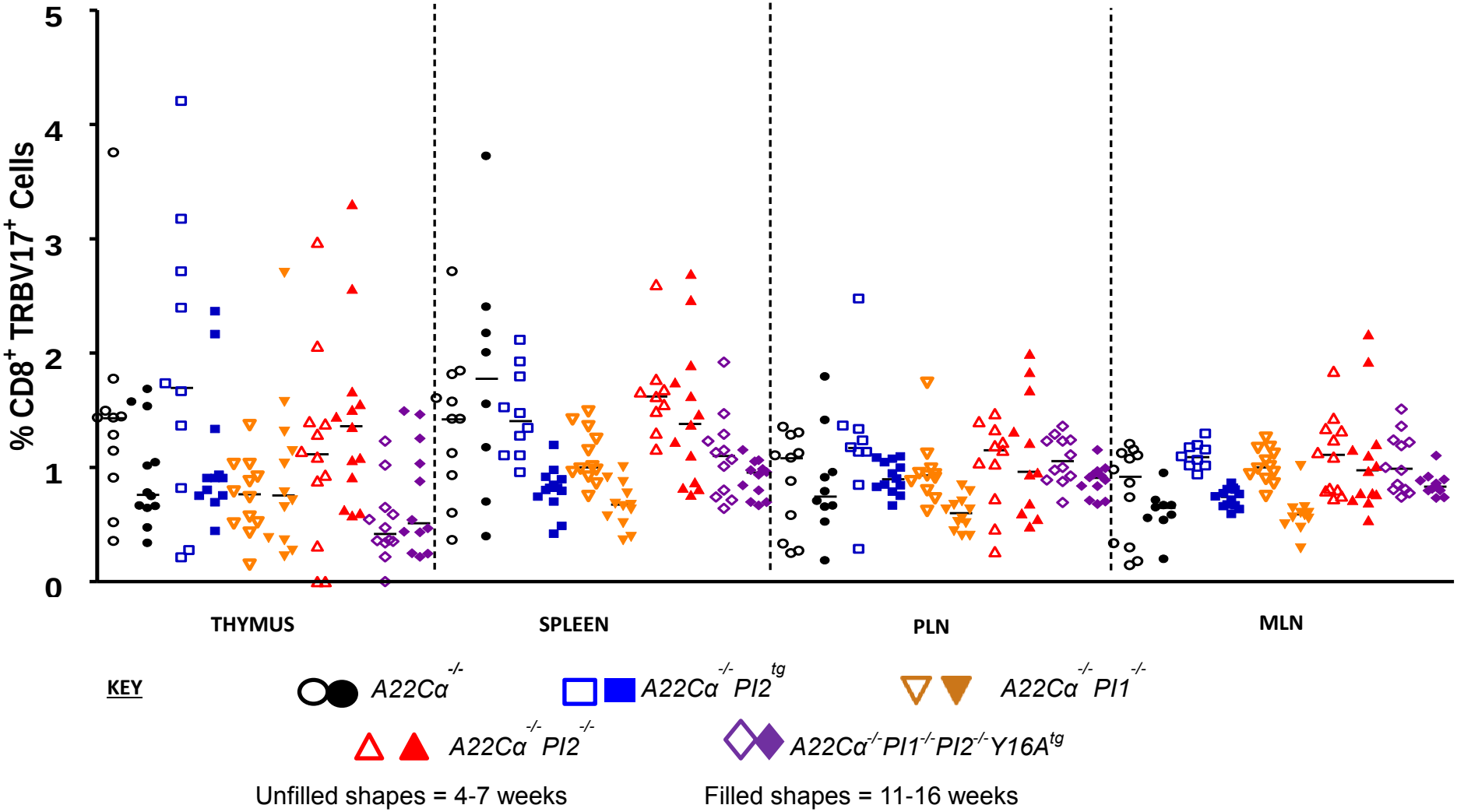

FIGURE 50: Lymphoid cells were harvested from thymus, spleen, PLN and MLN of mice aged 4-7 weeks or 11-16 weeks. These cells were stained using a multi-colour antibody staining panel (see 2.9.3.3) and measured on a BD FACS CANTO II to be analysed later using Flowjo Version 7.6.5 software. Data were then plotted using GraphPad Version 4 software. Each shape represents an individual mouse (n=8-13), with unfilled shapes representing those aged 4-7 weeks and filled shapes those aged 11-16 weeks. The median is shown for each data set by a horizontal line with statistically significant differences at p=<0.05 (*) and p=<0.01 (**) between the strains shown following an ANOVA analysis using R software.

FIGURE 50: CD8$^+$TRBV26$^+$ T CELL PROPORTIONS IN THE THYMI, SPLEEN, PANCREATIC LYMPH NODE (PLN) AND MESENTERIC LYMPH NODE (MLN) IN SINGLE CHAIN TRANSGENIC TRAV8-1*01TRAJ9 NOD MICE EXPRESSING VARYING PROINSULIN LEVELS

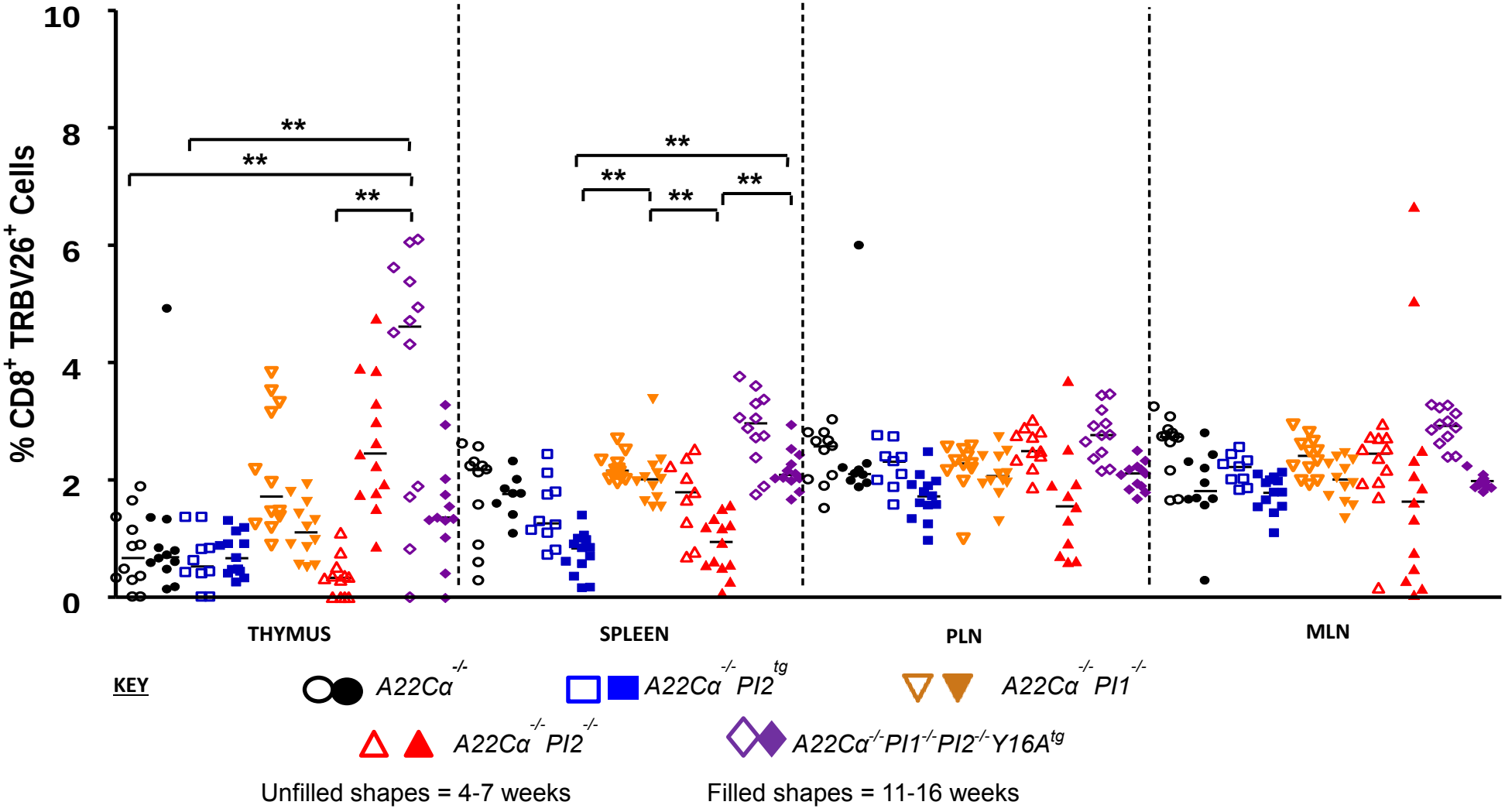

FIGURE 51: Lymphoid cells were harvested from thymus, spleen, PLN and MLN of mice aged 4-7 weeks or 11-16 weeks. These cells were stained using a multi-colour antibody staining panel (see 2.9.3.3) and measured on a BD FACS CANTO II to be analysed later using Flowjo Version 7.6.5 software. Data were then plotted using GraphPad Version 4 software. Each shape represents an individual mouse (n=8-13), with unfilled shapes representing those aged 4-7 weeks and filled shapes those aged 11-16 weeks. The median is shown for each data set by a horizontal line with statistically significant differences at p=<0.05 (*) and p=<0.01 (**) between the strains shown following an ANOVA analysis using R software.

FIGURE 51: CD8^{+}TRBV31^{+} T CELL PROPORTIONS IN THE THYMI, SPLEEN, PANCREATIC LYMPH NODE (PLN) AND MESENTERIC LYMPH NODE (MLN) IN SINGLE CHAIN TRANSGENIC TRAV8-1*01TRAJ9 NOD MICE EXPRESSING VARYING PROINSULIN LEVELS

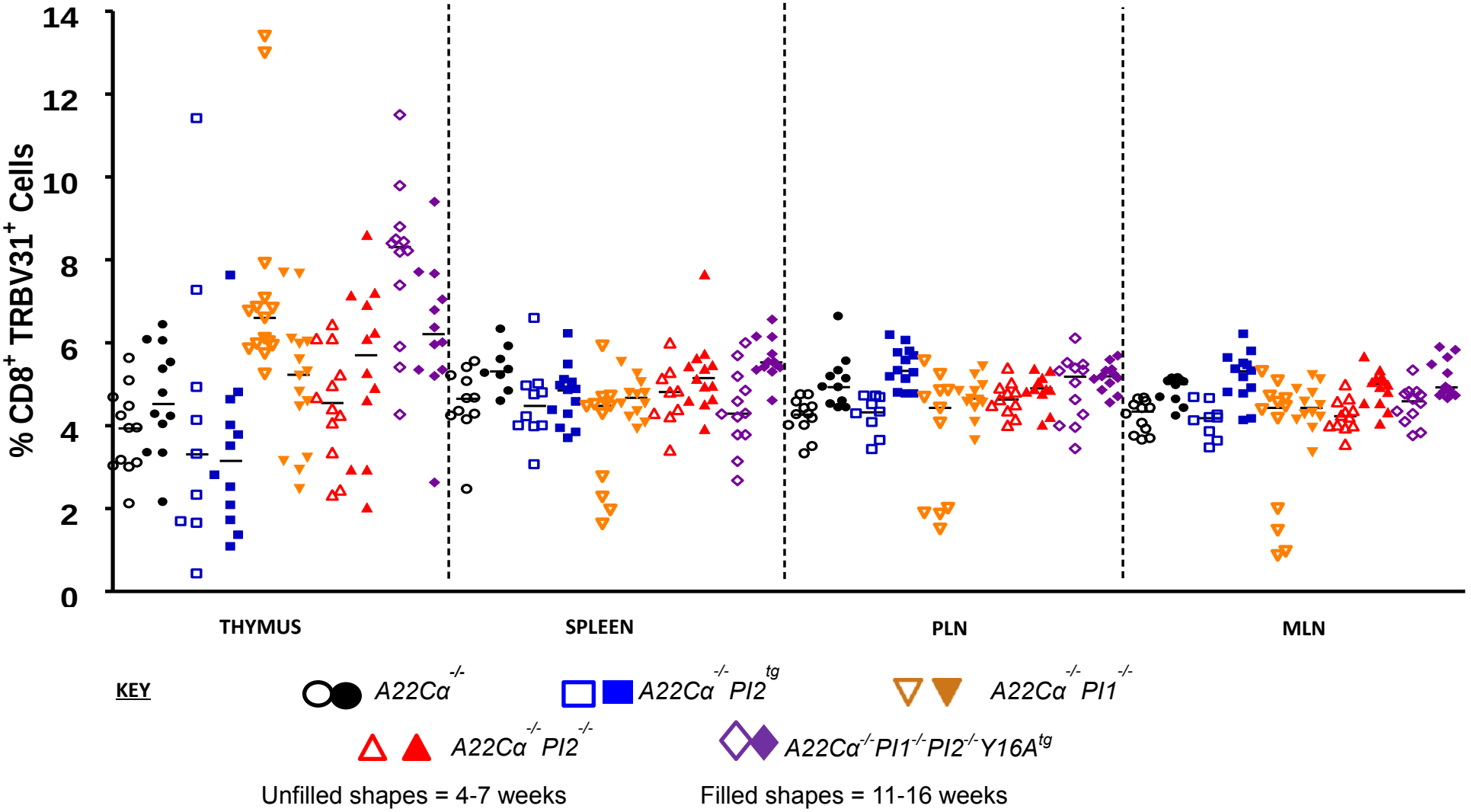

FIGURE 52: THE PREVALENCE OF INSULIN AUTO-ANTIBODIES IN MALE DIABETIC POLYCLONAL NOD MICE, MALE DIABETIC NOD MICE DEFICIENT IN PROINSULIN 2 AND MALE DIABETIC SINGLE CHAIN TRANSGENIC TRAV8-1*01TRAJ9 NOD MICE DEFICIENT IN PROINSULIN 2

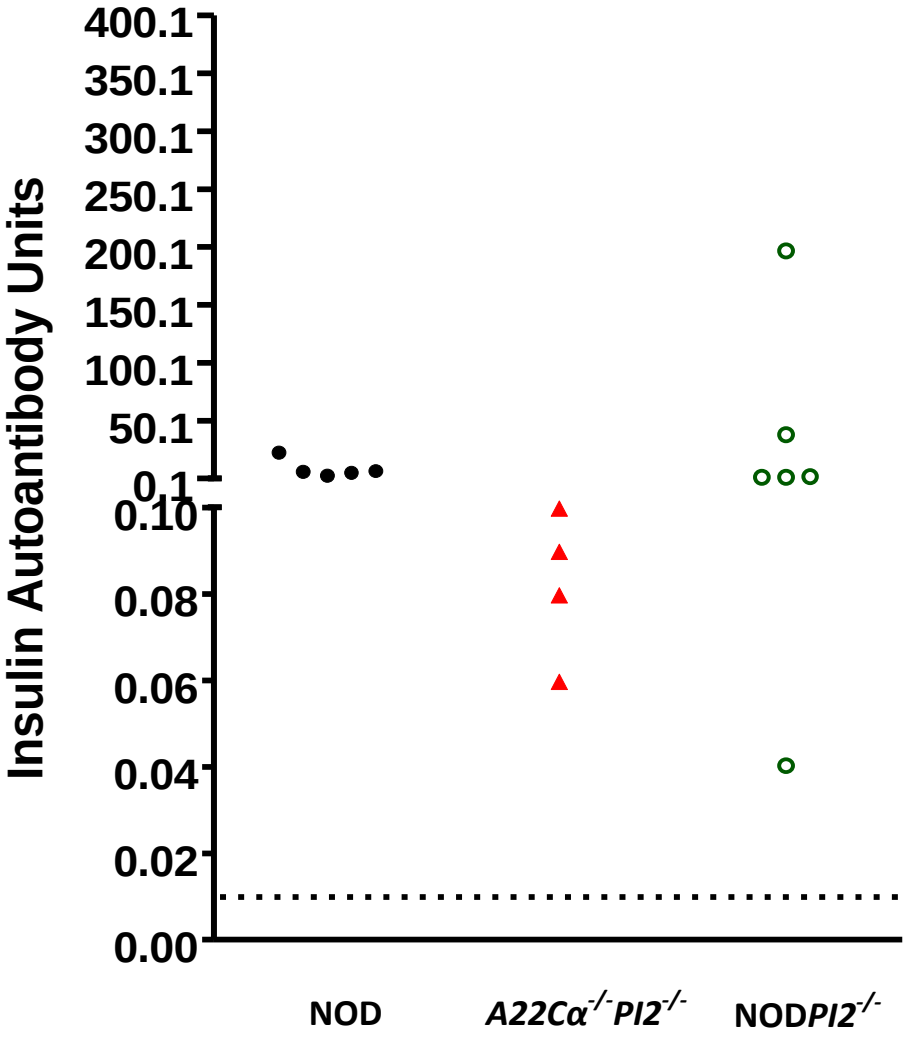

FIGURE 52: Serum was separated from the blood of diabetic male mice. Insulin auto-antibodies were then measured in a competitive insulin radioimmunoassay. Data were then plotted using GraphPad Version 4 software. Each shape represents an individual mouse (n=4-6 per group), with only males shown. Anything over the dotted line (over 0.0103) was deemed positive. Positivity was based on the mean plus 3 standard deviations from antibody measurements of control C57BL/6 mice.

BIBLIOGRAPHY

ABRAHAM, N., MICELI, M. C., PARNES, J. R. & VEILLETTE, A. 1991. Enhancement of T-cell responsiveness by the lymphocyte-specific tyrosine protein kinase p56lck. *Nature,* 350**,** 62-6.

ACHA-ORBEA, H. & MCDEVITT, H. O. 1987. The first external domain of the nonobese diabetic mouse class II I-A beta chain is unique. *Proc Natl Acad Sci U S A,* 84**,** 2435-9.

AHONEN, P., MYLLÄRNIEMI, S., SIPILÄ, I. & PERHEENTUPA, J. 1990. Clinical variation of autoimmune polyendocrinopathy-candidiasis-ectodermal dystrophy (APECED) in a series of 68 patients. *N Engl J Med,* 322**,** 1829-36.

AKERBLOM, H. K., VAARALA, O., HYÖTY, H., ILONEN, J. & KNIP, M. 2002. Environmental factors in the etiology of type 1 diabetes. *Am J Med Genet,* 115**,** 18-29.

AKIRA, S., UEMATSU, S. & TAKEUCHI, O. 2006. Pathogen recognition and innate immunity. *Cell,* 124**,** 783-801.

ALAM, C., BITTOUN, E., BHAGWAT, D., VALKONEN, S., SAARI, A., JAAKKOLA, U., EEROLA, E., HUOVINEN, P. & HÄNNINEN, A. 2011. Effects of a germ-free environment on gut immune regulation and diabetes progression in non-obese diabetic (NOD) mice. *Diabetologia,* 54**,** 1398-406.

ALKANANI, A. K., HARA, N., LIEN, E., IR, D., KOTTER, C. V., ROBERTSON, C. E., WAGNER, B. D., FRANK, D. N. & ZIPRIS, D. 2014. Induction of diabetes in the RIP-B7.1 mouse model is critically dependent on TLR3 and MyD88 pathways and is associated with alterations in the intestinal microbiome. *Diabetes,* 63**,** 619-31.

ALLMAN, D., SAMBANDAM, A., KIM, S., MILLER, J. P., PAGAN, A., WELL, D., MERAZ, A. & BHANDOOLA, A. 2003. Thymopoiesis independent of common lymphoid progenitors. *Nat Immunol,* 4**,** 168-74.

ALY, T. A., IDE, A., JAHROMI, M. M., BARKER, J. M., FERNANDO, M. S., BABU, S. R., YU, L., MIAO, D., ERLICH, H. A., FAIN, P. R., BARRIGA, K. J., NORRIS, J. M., REWERS, M. J. & EISENBARTH, G. S. 2006. Extreme genetic risk for type 1A diabetes. *Proc Natl Acad Sci U S A,* 103**,** 14074-9.

ANDERSON, M. S., VENANZI, E. S., KLEIN, L., CHEN, Z., BERZINS, S. P., TURLEY, S. J., VON BOEHMER, H., BRONSON, R., DIERICH, A., BENOIST, C. & MATHIS, D. 2002. Projection of an immunological self shadow within the thymus by the aire protein. *Science,* 298**,** 1395-401.

APETOH, L., QUINTANA, F. J., POT, C., JOLLER, N., XIAO, S., KUMAR, D., BURNS, E. J., SHERR, D. H., WEINER, H. L. & KUCHROO, V. K. 2010. The aryl hydrocarbon receptor interacts with c-Maf to promote the differentiation of type 1 regulatory T cells induced by IL-27. *Nat Immunol,* 11**,** 854-61.

ARIF, S., TREE, T. I., ASTILL, T. P., TREMBLE, J. M., BISHOP, A. J., DAYAN, C. M., ROEP, B. O. & PEAKMAN, M. 2004. Autoreactive T cell responses show proinflammatory polarization in diabetes but a regulatory phenotype in health. *J Clin Invest,* 113**,** 451-63.

ASHTON-RICKARDT, P. G., BANDEIRA, A., DELANEY, J. R., VAN KAER, L., PIRCHER, H. P., ZINKERNAGEL, R. M. & TONEGAWA, S. 1994. Evidence for a differential avidity model of T cell selection in the thymus. *Cell,* 76**,** 651-63.

ASHTON-RICKARDT, P. G., VAN KAER, L., SCHUMACHER, T. N., PLOEGH, H. L. & TONEGAWA, S. 1993. Peptide contributes to the specificity of positive selection of CD8+ T cells in the thymus. *Cell,* 73**,** 1041-9.

ATKINSON, M. A., BOWMAN, M. A., CAMPBELL, L., DARROW, B. L., KAUFMAN, D. L. & MACLAREN, N. K. 1994. Cellular immunity to a determinant common to glutamate decarboxylase and coxsackie virus in insulin-dependent diabetes. *J Clin Invest,* 94**,** 2125-9.

BACHMANN, M. F., BARNER, M. & KOPF, M. 1999. CD2 sets quantitative thresholds in T cell activation. *J Exp Med,* 190**,** 1383-92.

BAEKKESKOV, S., AANSTOOT, H. J., CHRISTGAU, S., REETZ, A., SOLIMENA, M., CASCALHO, M., FOLLI, F., RICHTER-OLESEN, H., DE CAMILLI, P. & CAMILLI, P. D. 1990. Identification of the 64K autoantigen in insulin-dependent diabetes as the GABA-synthesizing enzyme glutamic acid decarboxylase. *Nature,* 347**,** 151-6.

BARTH, R., COUNCE, S., SMITH, P. & SNELL, G. D. 1956. Strong and weak histocompatibility gene differences in mice and their role in the rejection of homografts of tumors and skin. *Ann Surg,* 144**,** 198-204.

BENACERRAF, B. & MCDEVITT, H. O. 1972. Histocompatibility-linked immune response genes. *Science,* 175**,** 273-9.

BENNETT, S. T., LUCASSEN, A. M., GOUGH, S. C., POWELL, E. E., UNDLIEN, D. E., PRITCHARD, L. E., MERRIMAN, M. E., KAWAGUCHI, Y., DRONSFIELD, M. J. & POCIOT, F. 1995. Susceptibility to human type 1 diabetes at IDDM2 is determined by tandem repeat variation at the insulin gene minisatellite locus. *Nat Genet,* 9**,** 284-92.

BENSELER, V., WARREN, A., VO, M., HOLZ, L. E., TAY, S. S., LE COUTEUR, D. G., BREEN, E., ALLISON, A. C., VAN ROOIJEN, N., MCGUFFOG, C., SCHLITT, H. J., BOWEN, D. G., MCCAUGHAN, G. W. & BERTOLINO, P. 2011. Hepatocyte entry leads to degradation of autoreactive CD8 T cells. *Proc Natl Acad Sci U S A,* 108**,** 16735-40.

BERSCHICK, P., FEHSEL, K., WELTZIEN, H. U. & KOLB, H. 1993. Molecular analysis of the T-cell receptor V beta 5 and V beta 8 repertoire in pancreatic lesions of autoimmune diabetic NOD mice. *J Autoimmun,* 6**,** 405-22.

BESSAOUD, K., BOUDRAA, G., MOLINERO DE ROPOLO, M., DE SEREDAY, M., MARTI, M. L., MOSER, M., LAPERTOSA, S., DAMIANO, M., VERGE, C., HOWARD, N., SCHOBER, E., JORDAN, O., WEETS, I., GORUS, F., COECKELBERGHS, M., ROOMAN, R., VAN GAAL, L., FRANCO, L. J., FERREIRA, S. R. G., LISBOA, H. P. K., KURTZ, L. A., GRAEBIN, R., KUTZKE, L., RODRIGES, C., SAVOVA, R., CHRISTOV, V., IOTOVA, V., TZANEVA, V., PACAUD, D., TOTH, E., TAN, M. H., CARRASCO, E., PEREZ, F., ZE, Y., BO, Y., CHEN, S., FU, L., DENG, L., SHEN, S., TENG, K., WANG, C., JIAN, H., JU, J., YAN, C., DENG, Y., LI, C., ZHANG, Y., LIU, Y., LONG, X., ZHEN, Z., SUN, Z., WANG, B., WONG, G., ORREGO, O. V., ASCHNER, P., DIAZ-DIAZ, O., MATEO DE ACOSTA, O., CINEK, O., VAVRINEC, J., OLSEN, B. S., SVENDSEN, A. J., KREUTZFELDT, J., LUND, E., TULL, E. S., SELMAN-GEARA, A., ALMONTE, A. S., PODAR, T., TUOMILEHTO, J., KARVONEN, M., NOTKOLA, I. L., MOLTCHANOVA, E., TASKINEN, O., LEVY-MARCHAL, C., CZERNICHOW, P., KOCAVA, M., NEU, A., EHEHALT, S., ROSENBAUER, J., GIANI, G., ICKS, A., BARTSOCAS, C., VAZEOU, A., SOLTESZ, G., LARON, Z., GORDON, O., ALBAG, Y., SHAMIS, I., PURRELLO, F., ARPI, M., FICHERA, G., MANCUSO, M., LUCENTI, C., CHIUMELLO, G., BRUNO, G., PAGANO, G., SONGINI, M., CASU, A., MARINARO, A., FRONGIA, P., ZEDDA, M. A., et al. 2006. Incidence and trends of childhood Type 1 diabetes worldwide 1990-1999. *Diabetic Medicine,* 23**,** 857-866.

BLECHSCHMIDT, K., SCHWEIGER, M., WERTZ, K., POULSON, R., CHRISTENSEN, H. M., ROSENTHAL, A., LEHRACH, H. & YASPO, M. L. 1999. The mouse Aire gene: comparative genomic sequencing, gene organization, and expression. *Genome Res,* 9**,** 158-66.

BOITARD, C., BENDELAC, A., RICHARD, M. F., CARNAUD, C. & BACH, J. F. 1988. Prevention of diabetes in nonobese diabetic mice by anti-I-A monoclonal antibodies: transfer of protection by splenic T cells. *Proc Natl Acad Sci U S A,* 85**,** 9719-23.

BONARIUS, H. P., BAAS, F., REMMERSWAAL, E. B., VAN LIER, R. A., TEN BERGE, I. J., TAK, P. P. & DE VRIES, N. 2006. Monitoring the T-cell receptor repertoire at single-clone resolution. *PLoS One,* 1**,** e55.

BONIFACIO, E., LAMPASONA, V., GENOVESE, S., FERRARI, M. & BOSI, E. 1995. Identification of protein tyrosine phosphatase-like IA2 (islet cell antigen 512) as the insulin-dependent diabetes-related 37/40K autoantigen and a target of islet-cell antibodies. *J Immunol,* 155**,** 5419-26.

BOSSELUT, R., FEIGENBAUM, L., SHARROW, S. O. & SINGER, A. 2001. Strength of signaling by CD4 and CD8 coreceptor tails determines the number but not the lineage direction of positively selected thymocytes. *Immunity,* 14**,** 483-94.

BOUMA, G., COPPENS, J. M., MOURITS, S., NIKOLIC, T., SOZZANI, S., DREXHAGE, H. A. & VERSNEL, M. A. 2005. Evidence for an enhanced adhesion of DC to fibronectin and a role of CCL19 and CCL21 in the accumulation of DC around the pre-diabetic islets in NOD mice. *Eur J Immunol,* 35**,** 2386-96.

BOURSALIAN, T. E., GOLOB, J., SOPER, D. M., COOPER, C. J. & FINK, P. J. 2004. Continued maturation of thymic emigrants in the periphery. *Nat Immunol,* 5**,** 418-25.

BOWIE, L., TITE, J. & COOKE, A. 1999. Generation and maintenance of autoantigen-specific CD8(+) T cell clones isolated from NOD mice. *J Immunol Methods,* 228**,** 87-95.

BOYD, R. L., TUCEK, C. L., GODFREY, D. I., IZON, D. J., WILSON, T. J., DAVIDSON, N. J., BEAN, A. G., LADYMAN, H. M., RITTER, M. A. & HUGO, P. 1993. The thymic microenvironment. *Immunol Today,* 14**,** 445-59.

BRITANOVA, O. V., PUTINTSEVA, E. V., SHUGAY, M., MERZLYAK, E. M., TURCHANINOVA, M. A., STAROVEROV, D. B., BOLOTIN, D. A., LUKYANOV, S., BOGDANOVA, E. A., MAMEDOV, I. Z., LEBEDEV, Y. B. & CHUDAKOV, D. M. 2014. Age-related decrease in TCR repertoire diversity measured with deep and normalized sequence profiling. *J Immunol,* 192**,** 2689-98.

BUBECK WARDENBURG, J., FU, C., JACKMAN, J. K., FLOTOW, H., WILKINSON, S. E., WILLIAMS, D. H., JOHNSON, R., KONG, G., CHAN, A. C. & FINDELL, P. R. 1996. Phosphorylation of SLP-76 by the ZAP-70 protein-tyrosine kinase is required for T-cell receptor function. *J Biol Chem,* 271**,** 19641-4.

BULEK, A. M., COLE, D. K., SKOWERA, A., DOLTON, G., GRAS, S., MADURA, F., FULLER, A., MILES, J. J., GOSTICK, E., PRICE, D. A., DRIJFHOUT, J. W., KNIGHT, R. R., HUANG, G. C., LISSIN, N., MOLLOY, P. E., WOOLDRIDGE, L., JAKOBSEN, B. K., ROSSJOHN, J., PEAKMAN, M., RIZKALLAH, P. J. & SEWELL, A. K. 2012. Structural basis for the killing of human beta cells by CD8(+) T cells in type 1 diabetes. *Nat Immunol*.

BURTON, A. R., VINCENT, E., ARNOLD, P. Y., LENNON, G. P., SMELTZER, M., LI, C. S., HASKINS, K., HUTTON, J., TISCH, R. M., SERCARZ, E. E., SANTAMARIA, P., WORKMAN, C. J. & VIGNALI, D. A. 2008. On the pathogenicity of autoantigen-specific T-cell receptors. *Diabetes,* 57**,** 1321-30.

BURTON, O. T., GIBBS, S., MILLER, N., JONES, F. M., WEN, L., DUNNE, D. W., COOKE, A. & ZACCONE, P. 2010. Importance of TLR2 in the direct response of T lymphocytes to Schistosoma mansoni antigens. *Eur J Immunol,* 40**,** 2221-9.

BYTH, K. F., CONROY, L. A., HOWLETT, S., SMITH, A. J., MAY, J., ALEXANDER, D. R. & HOLMES, N. 1996. CD45-null transgenic mice reveal a positive regulatory role for CD45 in early thymocyte development, in the selection of CD4+CD8+ thymocytes, and B cell maturation. *J Exp Med,* 183**,** 1707-18.

CABANIOLS, J. P., FAZILLEAU, N., CASROUGE, A., KOURILSKY, P. & KANELLOPOULOS, J. M. 2001. Most alpha/beta T cell receptor diversity is due to terminal deoxynucleotidyl transferase. *J Exp Med,* 194**,** 1385-90.

CALCINARO, F., DIONISI, S., MARINARO, M., CANDELORO, P., BONATO, V., MARZOTTI, S., CORNELI, R. B., FERRETTI, E., GULINO, A., GRASSO, F., DE SIMONE, C., DI MARIO, U., FALORNI, A., BOIRIVANT, M. & DOTTA, F. 2005. Oral probiotic administration induces interleukin-10 production and prevents spontaneous autoimmune diabetes in the non-obese diabetic mouse. *Diabetologia,* 48**,** 1565-75.

CANDÉIAS, S., KATZ, J., BENOIST, C., MATHIS, D. & HASKINS, K. 1991a. Islet-specific T-cell clones from nonobese diabetic mice express heterogeneous T-cell receptors. *Proc Natl Acad Sci U S A,* 88**,** 6167-70.

CANDÉIAS, S., KATZ, J., BENOIST, C., MATHIS, D. & HASKINS, K. 1991b. Islet-specific T-cell clones from nonobese diabetic mice express heterogeneous T-cell receptors. *Proc Natl Acad Sci U S A,* 88**,** 6167-70.

CARBONE, F. R. & BEVAN, M. J. 1990. Class I-restricted processing and presentation of exogenous cell-associated antigen in vivo. *J Exp Med,* 171**,** 377-87.

CARICILLI, A. M., PICARDI, P. K., DE ABREU, L. L., UENO, M., PRADA, P. O., ROPELLE, E. R., HIRABARA, S. M., CASTOLDI, Â., VIEIRA, P., CAMARA, N. O., CURI, R., CARVALHEIRA, J. B. & SAAD, M. J. 2011. Gut microbiota is a key modulator of insulin resistance in TLR 2 knockout mice. *PLoS Biol,* 9**,** e1001212.

CARIO, E., GERKEN, G. & PODOLSKY, D. K. 2004. Toll-like receptor 2 enhances ZO-1-associated intestinal epithelial barrier integrity via protein kinase C. *Gastroenterology,* 127**,** 224-38.

CARVALHO, B. M., GUADAGNINI, D., TSUKUMO, D. M., SCHENKA, A. A., LATUF-FILHO, P., VASSALLO, J., DIAS, J. C., KUBOTA, L. T., CARVALHEIRA, J. B. & SAAD, M. J. 2012. Modulation of gut microbiota by antibiotics improves insulin signalling in high-fat fed mice. *Diabetologia,* 55**,** 2823-34.

CASTEELS, K. M., GYSEMANS, C. A., WAER, M., BOUILLON, R., LAUREYS, J. M., DEPOVERE, J. & MATHIEU, C. 1998. Sex difference in resistance to dexamethasone-induced apoptosis in NOD mice: treatment with 1,25(OH)2D3 restores defect. *Diabetes,* 47**,** 1033-7.

CHAKRABARTI, R. & KUMAR, S. 2000. Diacylglycerol mediates the T-cell receptor-driven Ca(2+) influx in T cells by a novel mechanism independent of protein kinase C activation. *J Cell Biochem,* 78**,** 222-30.

CHAMBERLAIN, G., WÅLLBERG, M., RAINBOW, D., HUNTER, K., WICKER, L. S. & GREEN, E. A. 2006. A 20-Mb region of chromosome 4 controls TNF-alpha-mediated CD8+ T cell aggression toward beta cells in type 1 diabetes. *J Immunol,* 177**,** 5105-14.

CHAN, A. C., IRVING, B. A., FRASER, J. D. & WEISS, A. 1991. The zeta chain is associated with a tyrosine kinase and upon T-cell antigen receptor stimulation associates with ZAP-70, a 70-kDa tyrosine phosphoprotein. *Proc Natl Acad Sci U S A,* 88**,** 9166-70.

CHANG, T. T., JABS, C., SOBEL, R. A., KUCHROO, V. K. & SHARPE, A. H. 1999. Studies in B7-deficient mice reveal a critical role for B7 costimulation in both induction and effector phases of experimental autoimmune encephalomyelitis. *J Exp Med,* 190**,** 733-40.

CHAO, C. C., SYTWU, H. K., CHEN, E. L., TOMA, J. & MCDEVITT, H. O. 1999. The role of MHC class II molecules in susceptibility to type I diabetes: identification of peptide epitopes and characterization of the T cell repertoire. *Proc Natl Acad Sci U S A,* 96**,** 9299-304.

CHARLTON, B. & MANDEL, T. E. 1989. Recurrence of insulitis in the NOD mouse after early prolonged anti-CD4 monoclonal antibody treatment. *Autoimmunity,* 4**,** 1-7.

CHATENOUD, L., THERVET, E., PRIMO, J. & BACH, J. F. 1992. [Remission of established disease in diabetic NOD mice induced by anti-CD3 monoclonal antibody]. *C R Acad Sci III,* 315**,** 225-8.

CHENTOUFI, A. A., PALUMBO, M. & POLYCHRONAKOS, C. 2004. Proinsulin expression by Hassall's corpuscles in the mouse thymus. *Diabetes,* 53**,** 354-9.

CHENTOUFI, A. A. & POLYCHRONAKOS, C. 2002. Insulin expression levels in the thymus modulate insulin-specific autoreactive T-cell tolerance: the mechanism by which the IDDM2 locus may predispose to diabetes. *Diabetes,* 51**,** 1383-90.

CHIKUMA, S., IMBODEN, J. B. & BLUESTONE, J. A. 2003. Negative regulation of T cell receptor-lipid raft interaction by cytotoxic T lymphocyte-associated antigen 4. *J Exp Med,* 197**,** 129-35.

CHRISTIANSON, S. W., SHULTZ, L. D. & LEITER, E. H. 1993. Adoptive transfer of diabetes into immunodeficient NOD-scid/scid mice. Relative contributions of CD4+ and CD8+ T-cells from diabetic versus prediabetic NOD.NON-Thy-1a donors. *Diabetes,* 42**,** 44-55.

CLEMENT, M., LADELL, K., EKERUCHE-MAKINDE, J., MILES, J. J., EDWARDS, E. S., DOLTON, G., WILLIAMS, T., SCHAUENBURG, A. J., COLE, D. K., LAUDER, S. N., GALLIMORE, A. M., GODKIN, A. J., BURROWS, S. R., PRICE, D. A., SEWELL, A. K. & WOOLDRIDGE, L. 2011. Anti-CD8 antibodies can trigger CD8+ T cell effector function in the absence of TCR engagement and improve peptide-MHCI tetramer staining. *J Immunol,* 187**,** 654-63.

COCHET, M., PANNETIER, C., REGNAULT, A., DARCHE, S., LECLERC, C. & KOURILSKY, P. 1992. Molecular detection and in vivo analysis of the specific T cell response to a protein antigen. *Eur J Immunol,* 22**,** 2639-47.

CONCANNON, P., RICH, S. S. & NEPOM, G. T. 2009. Genetics of type 1A diabetes. *N Engl J Med,* 360**,** 1646-54.

COOKE, A., TONKS, P., JONES, F. M., O'SHEA, H., HUTCHINGS, P., FULFORD, A. J. & DUNNE, D. W. 1999. Infection with Schistosoma mansoni prevents insulin dependent diabetes mellitus in non-obese diabetic mice. *Parasite Immunol,* 21**,** 169-76.

COPPIETERS, K. T., DOTTA, F., AMIRIAN, N., CAMPBELL, P. D., KAY, T. W., ATKINSON, M. A., ROEP, B. O. & VON HERRATH, M. G. 2012. Demonstration of islet-autoreactive CD8 T cells in insulitic lesions from recent onset and long-term type 1 diabetes patients. *J Exp Med,* 209**,** 51-60.

CORTHAY, A. 2009. How do regulatory T cells work? *Scand J Immunol,* 70**,** 326-36.

COSE, S. C., KELLY, J. M. & CARBONE, F. R. 1995. Characterization of diverse primary herpes simplex virus type 1 gB-specific cytotoxic T-cell response showing a preferential V beta bias. *J Virol,* 69**,** 5849-52.

DANI, A., CHAUDHRY, A., MUKHERJEE, P., RAJAGOPAL, D., BHATIA, S., GEORGE, A., BAL, V., RATH, S. & MAYOR, S. 2004. The pathway for MHCII-mediated presentation of endogenous proteins involves peptide transport to the endo-lysosomal compartment. *J Cell Sci,* 117**,** 4219-30.

DANIEL, D. & WEGMANN, D. R. 1996. Protection of nonobese diabetic mice from diabetes by intranasal or subcutaneous administration of insulin peptide B-(9-23). *Proc Natl Acad Sci U S A,* 93**,** 956-60.

DANSKA, J. S., LIVINGSTONE, A. M., PARAGAS, V., ISHIHARA, T. & FATHMAN, C. G. 1990. The presumptive CDR3 regions of both T cell receptor alpha and beta chains determine T cell specificity for myoglobin peptides. *J Exp Med,* 172**,** 27-33.

DAVIDSON, H. W., RHODES, C. J. & HUTTON, J. C. 1988. Intraorganellar calcium and pH control proinsulin cleavage in the pancreatic beta cell via two distinct site-specific endopeptidases. *Nature,* 333**,** 93-6.

DAVIES, T. F., MARTIN, A., CONCEPCION, E. S., GRAVES, P., COHEN, L. & BEN-NUN, A. 1991. Evidence of limited variability of antigen receptors on intrathyroidal T cells in autoimmune thyroid disease. *N Engl J Med,* 325**,** 238-44.

DAVIES, T. F., MARTIN, A., CONCEPCION, E. S., GRAVES, P., LAHAT, N., COHEN, W. L. & BEN-NUN, A. 1992. Evidence for selective accumulation of intrathyroidal T lymphocytes in human autoimmune thyroid disease based on T cell receptor V gene usage. *J Clin Invest,* 89**,** 157-62.

DE AIZPURUA, H. J., FRENCH, M. B., CHOSICH, N. & HARRISON, L. C. 1994. Natural history of humoral immunity to glutamic acid decarboxylase in non-obese diabetic (NOD) mice. *J Autoimmun,* 7**,** 643-53.

DE GOFFAU, M. C., LUOPAJÄRVI, K., KNIP, M., ILONEN, J., RUOHTULA, T., HÄRKÖNEN, T., ORIVUORI, L., HAKALA, S., WELLING, G. W., HARMSEN, H. J. & VAARALA, O. 2013. Fecal microbiota composition differs between children with β-cell autoimmunity and those without. *Diabetes,* 62**,** 1238-44.

DEGEN, E., COHEN-DOYLE, M. F. & WILLIAMS, D. B. 1992. Efficient dissociation of the p88 chaperone from major histocompatibility complex class I molecules requires both beta 2-microglobulin and peptide. *J Exp Med,* 175**,** 1653-61.

DELTOUR, L., LEDUQUE, P., BLUME, N., MADSEN, O., DUBOIS, P., JAMI, J. & BUCCHINI, D. 1993. Differential expression of the two nonallelic proinsulin genes in the developing mouse embryo. *Proc Natl Acad Sci U S A,* 90**,** 527-31.

DERBINSKI, J., GÄBLER, J., BRORS, B., TIERLING, S., JONNAKUTY, S., HERGENHAHN, M., PELTONEN, L., WALTER, J. & KYEWSKI, B. 2005. Promiscuous gene expression in thymic epithelial cells is regulated at multiple levels. *J Exp Med,* 202**,** 33-45.

DERBINSKI, J., SCHULTE, A., KYEWSKI, B. & KLEIN, L. 2001. Promiscuous gene expression in medullary thymic epithelial cells mirrors the peripheral self. *Nat Immunol,* 2**,** 1032-9.

DESILVA, M. G., JUN, H. S., YOON, J. W., NOTKINS, A. L. & LAN, M. S. 1996. Autoantibodies to IA-2 not detected in NOD mice or BB rats. *Diabetologia,* 39**,** 1237-8.

DEVARAJ, S., JIALAL, I., YUN, J. M. & BREMER, A. 2011a. Demonstration of increased toll-like receptor 2 and toll-like receptor 4 expression in monocytes of type 1 diabetes mellitus patients with microvascular complications. *Metabolism,* 60**,** 256-9.

DEVARAJ, S., TOBIAS, P. & JIALAL, I. 2011b. Knockout of toll-like receptor-4 attenuates the pro-inflammatory state of diabetes. *Cytokine,* 55**,** 441-5.

DEVARAJ, S., TOBIAS, P., KASINATH, B. S., RAMSAMOOJ, R., AFIFY, A. & JIALAL, I. 2011c. Knockout of toll-like receptor-2 attenuates both the proinflammatory state of diabetes and incipient diabetic nephropathy. *Arterioscler Thromb Vasc Biol,* 31**,** 1796-804.

DIANA, J., SIMONI, Y., FURIO, L., BEAUDOIN, L., AGERBERTH, B., BARRAT, F. & LEHUEN, A. 2013. Crosstalk between neutrophils, B-1a cells and plasmacytoid dendritic cells initiates autoimmune diabetes. *Nat Med,* 19**,** 65-73.

DILLON, S. R., JAMESON, S. C. & FINK, P. J. 1994. V beta 5+ T cell receptors skew toward OVA+H-2Kb recognition. *J Immunol,* 152**,** 1790-801.

DILORENZO, T. P., GRASER, R. T., ONO, T., CHRISTIANSON, G. J., CHAPMAN, H. D., ROOPENIAN, D. C., NATHENSON, S. G. & SERREZE, D. V. 1998. Major histocompatibility complex class I-restricted T cells are required for all but the end stages of diabetes development in nonobese diabetic mice and use a prevalent T cell receptor alpha chain gene rearrangement. *Proc Natl Acad Sci U S A,* 95**,** 12538-43.

DONG, C., JUEDES, A. E., TEMANN, U. A., SHRESTA, S., ALLISON, J. P., RUDDLE, N. H. & FLAVELL, R. A. 2001. ICOS co-stimulatory receptor is essential for T-cell activation and function. *Nature,* 409**,** 97-101.

DORNAN, S., SEBESTYEN, Z., GAMBLE, J., NAGY, P., BODNAR, A., ALLDRIDGE, L., DOE, S., HOLMES, N., GOFF, L. K., BEVERLEY, P., SZOLLOSI, J. & ALEXANDER, D. R. 2002. Differential association of CD45 isoforms with CD4 and CD8 regulates the actions of specific pools of p56lck tyrosine kinase in T cell antigen receptor signal transduction. *J Biol Chem,* 277**,** 1912-8.

DOUEK, D. C. & ALTMANN, D. M. 2000. T-cell apoptosis and differential human leucocyte antigen class II expression in human thymus. *Immunology,* 99**,** 249-56.

DOUEK, D. C., MCFARLAND, R. D., KEISER, P. H., GAGE, E. A., MASSEY, J. M., HAYNES, B. F., POLIS, M. A., HAASE, A. T., FEINBERG, M. B., SULLIVAN, J. L., JAMIESON, B. D., ZACK, J. A., PICKER, L. J. & KOUP, R. A. 1998. Changes in thymic function with age and during the treatment of HIV infection. *Nature,* 396**,** 690-5.

DOYLE, H. A. & MAMULA, M. J. 2012. Autoantigenesis: the evolution of protein modifications in autoimmune disease. *Curr Opin Immunol,* 24**,** 112-8.

DRESCHER, K. M., KONO, K., BOPEGAMAGE, S., CARSON, S. D. & TRACY, S. 2004. Coxsackievirus B3 infection and type 1 diabetes development in NOD mice: insulitis determines susceptibility of pancreatic islets to virus infection. *Virology,* 329**,** 381-94.

DUNN, K. W. & MAXFIELD, F. R. 1992. Delivery of ligands from sorting endosomes to late endosomes occurs by maturation of sorting endosomes. *J Cell Biol,* 117**,** 301-10.

DUNN, K. W., MCGRAW, T. E. & MAXFIELD, F. R. 1989. Iterative fractionation of recycling receptors from lysosomally destined ligands in an early sorting endosome. *J Cell Biol,* 109**,** 3303-14.

DUNNE, J. L., OVERBERGH, L., PURCELL, A. W. & MATHIEU, C. 2012. Posttranslational modifications of proteins in type 1 diabetes: the next step in finding the cure? *Diabetes,* 61**,** 1907-14.

ECHCHANNAOUI, H., FREI, K., SCHNELL, C., LEIB, S. L., ZIMMERLI, W. & LANDMANN, R. 2002. Toll-like receptor 2-deficient mice are highly susceptible to Streptococcus pneumoniae meningitis because of reduced bacterial clearing and enhanced inflammation. *J Infect Dis,* 186**,** 798-806.

EDOUARD, P., THIVOLET, C., BEDOSSA, P., OLIVI, M., LEGRAND, B., BENDELAC, A., BACH, J. F. & CARNAUD, C. 1993. Evidence for a preferential V beta usage by the T cells which adoptively transfer diabetes in NOD mice. *Eur J Immunol,* 23**,** 727-33.

EHEHALT, S., DIETZ, K., WILLASCH, A. M., NEU, A. & BADEN-WUERTTEMBERG DAIBET, I. 2010. Epidemiological Perspectives on Type 1 Diabetes in Childhood and Adolescence in Germany - 20 years of the Baden-Wurttemberg Diabetes Incidence Registry (DIARY). *Diabetes Care,* 33**,** 338-340.

EHRENSTEIN, M. R., EVANS, J. G., SINGH, A., MOORE, S., WARNES, G., ISENBERG, D. A. & MAURI, C. 2004. Compromised function of regulatory T cells in rheumatoid arthritis and reversal by anti-TNFalpha therapy. *J Exp Med,* 200**,** 277-85.

EJRNAES, M., VIDEBAEK, N., CHRISTEN, U., COOKE, A., MICHELSEN, B. K. & VON HERRATH, M. 2005. Different diabetogenic potential of autoaggressive CD8+ clones associated with IFN-gamma-inducible protein 10 (CXC chemokine ligand 10) production but not cytokine expression, cytolytic activity, or homing characteristics. *J Immunol,* 174**,** 2746-55.

EL ANDALOUSSI, A., GRAVES, S., MENG, F., MANDAL, M., MASHAYEKHI, M. & AIFANTIS, I. 2006. Hedgehog signaling controls thymocyte progenitor homeostasis and differentiation in the thymus. *Nat Immunol,* 7**,** 418-26.

EMERSON, R. O., SHERWOOD, A. M., RIEDER, M. J., GUENTHOER, J., WILLIAMSON, D. W., CARLSON, C. S., DRESCHER, C. W., TEWARI, M., BIELAS, J. H. & ROBINS, H. S. 2013. High-throughput sequencing of T-cell receptors reveals a homogeneous

repertoire of tumour-infiltrating lymphocytes in ovarian cancer. *J Pathol,* 231**,** 433-40.

ENDL, J., OTTO, H., JUNG, G., DREISBUSCH, B., DONIE, F., STAHL, P., ELBRACHT, R., SCHMITZ, G., MEINL, E., HUMMEL, M., ZIEGLER, A. G., WANK, R. & SCHENDEL, D. J. 1997. Identification of naturally processed T cell epitopes from glutamic acid decarboxylase presented in the context of HLA-DR alleles by T lymphocytes of recent onset IDDM patients. *J Clin Invest,* 99**,** 2405-15.

ENOUZ, S., CARRIÉ, L., MERKLER, D., BEVAN, M. J. & ZEHN, D. 2012. Autoreactive T cells bypass negative selection and respond to self-antigen stimulation during infection. *J Exp Med,* 209**,** 1769-79.

ERLICH, H., VALDES, A. M., NOBLE, J., CARLSON, J. A., VARNEY, M., CONCANNON, P., MYCHALECKYJ, J. C., TODD, J. A., BONELLA, P., FEAR, A. L., LAVANT, E., LOUEY, A., MOONSAMY, P. & CONSORTIUM, T. D. G. 2008. HLA DR-DQ haplotypes and genotypes and type 1 diabetes risk: analysis of the type 1 diabetes genetics consortium families. *Diabetes,* 57**,** 1084-92.

EVERTSEN, J., ALEMZADEH, R. & WANG, X. 2009. Increasing Incidence of Pediatric Type 1 Diabetes Mellitus in Southeastern Wisconsin: Relationship with Body Weight at Diagnosis. *Plos One,* 4.

FAIDEAU, B., BRIAND, J. P., LOTTON, C., TARDIVEL, I., HALBOUT, P., JAMI, J., ELLIOTT, J. F., KRIEF, P., MULLER, S., BOITARD, C. & CAREL, J. C. 2004. Expression of preproinsulin-2 gene shapes the immune response to preproinsulin in normal mice. *J Immunol,* 172**,** 25-33.

FAIDEAU, B., LOTTON, C., LUCAS, B., TARDIVEL, I., ELLIOTT, J. F., BOITARD, C. & CAREL, J. C. 2006. Tolerance to proinsulin-2 is due to radioresistant thymic cells. *J Immunol,* 177**,** 53-60.

FAIRCHILD, S., KNIGHT, A. M., DYSON, P. J. & TOMONARI, K. 1991. Co-segregation of a gene encoding a deletion ligand for Tcrb-V3+ T cells with Mtv-3. *Immunogenetics,* 34**,** 227-30.

FANNING, S. L., ZILBERBERG, J., STEIN, J., VAZZANA, K., BERGER, S. A., KORNGOLD, R. & FRIEDMAN, T. M. 2013. Unraveling graft-versus-host disease and graft-versus-leukemia responses using TCR Vβ spectratype analysis in a murine bone marrow transplantation model. *J Immunol,* 190**,** 447-57.

FERREIRA, C., SINGH, Y., FURMANSKI, A. L., WONG, F. S., GARDEN, O. A. & DYSON, J. 2009. Non-obese diabetic mice select a low-diversity repertoire of natural regulatory T cells. *Proc Natl Acad Sci U S A,* 106**,** 8320-5.

FIFE, B. T., GULERIA, I., GUBBELS BUPP, M., EAGAR, T. N., TANG, Q., BOUR-JORDAN, H., YAGITA, H., AZUMA, M., SAYEGH, M. H. & BLUESTONE, J. A. 2006. Insulin-induced remission in new-onset NOD mice is maintained by the PD-1-PD-L1 pathway. *J Exp Med,* 203**,** 2737-47.

FIFE, B. T., PAUKEN, K. E., EAGAR, T. N., OBU, T., WU, J., TANG, Q., AZUMA, M., KRUMMEL, M. F. & BLUESTONE, J. A. 2009. Interactions between PD-1 and PD-L1 promote tolerance by blocking the TCR-induced stop signal. *Nat Immunol,* 10**,** 1185-92.

FISCHER, D. C., OPALKA, B., HOFFMANN, A., MAYR, W. & HAUBECK, H. D. 1996. Limited heterogeneity of rearranged T cell receptor V alpha and V beta transcripts in synovial fluid T cells in early stages of rheumatoid arthritis. *Arthritis Rheum,* 39**,** 454-62.

FISCHER, K. D., ZMULDZINAS, A., GARDNER, S., BARBACID, M., BERNSTEIN, A. & GUIDOS, C. 1995. Defective T-cell receptor signalling and positive selection of Vav-deficient CD4+ CD8+ thymocytes. *Nature,* 374**,** 474-7.

FLETCHER, A. L., LUKACS-KORNEK, V., REYNOSO, E. D., PINNER, S. E., BELLEMARE-PELLETIER, A., CURRY, M. S., COLLIER, A. R., BOYD, R. L. & TURLEY, S. J. 2010. Lymph node fibroblastic reticular cells directly present peripheral tissue antigen under steady-state and inflammatory conditions. *J Exp Med,* 207**,** 689-97.

FOULIS, A. K. 1993. The pathology of islets in diabetes. *Eye (Lond),* 7 (Pt 2)**,** 197-201.

FOULIS, A. K., LIDDLE, C. N., FARQUHARSON, M. A., RICHMOND, J. A. & WEIR, R. S. 1986. The histopathology of the pancreas in type 1 (insulin-dependent) diabetes mellitus: a 25-year review of deaths in patients under 20 years of age in the United Kingdom. *Diabetologia,* 29**,** 267-74.

FOUSTERI, G., JASINSKI, J., DAVE, A., NAKAYAMA, M., PAGNI, P., LAMBOLEZ, F., JUNTTI, T., SARIKONDA, G., CHENG, Y., CROFT, M., CHEROUTRE, H., EISENBARTH, G. & VON HERRATH, M. 2012. Following the fate of one insulin-reactive CD4 T cell: conversion into Teffs and Tregs in the periphery controls diabetes in NOD mice. *Diabetes,* 61**,** 1169-79.

FOX, H. S. 1992. Androgen treatment prevents diabetes in nonobese diabetic mice. *J Exp Med,* 175**,** 1409-12.

FRENCH, M. B., ALLISON, J., CRAM, D. S., THOMAS, H. E., DEMPSEY-COLLIER, M., SILVA, A., GEORGIOU, H. M., KAY, T. W., HARRISON, L. C. & LEW, A. M. 1997. Transgenic expression of mouse proinsulin II prevents diabetes in nonobese diabetic mice. *Diabetes,* 46**,** 34-9.

FUKATA, M., CHEN, A., KLEPPER, A., KRISHNAREDDY, S., VAMADEVAN, A. S., THOMAS, L. S., XU, R., INOUE, H., ARDITI, M., DANNENBERG, A. J. & ABREU, M. T. 2006. Cox-2 is regulated by Toll-like receptor-4 (TLR4) signaling: Role in proliferation and apoptosis in the intestine. *Gastroenterology,* 131**,** 862-77.

FUKATA, M., MICHELSEN, K. S., ERI, R., THOMAS, L. S., HU, B., LUKASEK, K., NAST, C. C., LECHAGO, J., XU, R., NAIKI, Y., SOLIMAN, A., ARDITI, M. & ABREU, M. T. 2005. Toll-like receptor-4 is required for intestinal response to epithelial injury and limiting bacterial translocation in a murine model of acute colitis. *Am J Physiol Gastrointest Liver Physiol,* 288**,** G1055-65.

GALLEY, K. A. & DANSKA, J. S. 1995. Peri-islet infiltrates of young non-obese diabetic mice display restricted TCR beta-chain diversity. *J Immunol,* 154**,** 2969-82.

GANZ, T. 2003. The role of antimicrobial peptides in innate immunity. *Integr Comp Biol,* 43**,** 300-4.

GARCIA, K. C., DEGANO, M., PEASE, L. R., HUANG, M., PETERSON, P. A., TEYTON, L. & WILSON, I. A. 1998. Structural basis of plasticity in T cell receptor recognition of a self peptide-MHC antigen. *Science,* 279**,** 1166-72.

GAUDREAU, M. C., HEYD, F., BASTIEN, R., WILHELM, B. & MÖRÖY, T. 2012. Alternative splicing controlled by heterogeneous nuclear ribonucleoprotein L regulates development, proliferation, and migration of thymic pre-T cells. *J Immunol,* 188**,** 5377-88.

GEIJTENBEEK, T. B., TORENSMA, R., VAN VLIET, S. J., VAN DUIJNHOVEN, G. C., ADEMA, G. J., VAN KOOYK, Y. & FIGDOR, C. G. 2000. Identification of DC-SIGN, a novel dendritic cell-specific ICAM-3 receptor that supports primary immune responses. *Cell,* 100**,** 575-85.

GENOLET, R., STEVENSON, B. J., FARINELLI, L., OSTERÅS, M. & LUESCHER, I. F. 2012. Highly diverse TCRα chain repertoire of pre-immune $CD8^+$ T cells reveals new insights in gene recombination. *EMBO J,* 31**,** 1666-78.

GEPTS, W. 1965. Pathologic anatomy of the pancreas in juvenile diabetes mellitus. *Diabetes,* 14**,** 619-33.

GERMAIN, R. N. 1994. MHC-dependent antigen processing and peptide presentation: providing ligands for T lymphocyte activation. *Cell,* 76**,** 287-99.

GEROLD, K. D., ZHENG, P., RAINBOW, D. B., ZERNECKE, A., WICKER, L. S. & KISSLER, S. 2011. The soluble CTLA-4 splice variant protects from type 1 diabetes and potentiates regulatory T-cell function. *Diabetes,* 60**,** 1955-63.

GILLESPIE, K. M., BAIN, S. C., BARNETT, A. H., BINGLEY, P. J., CHRISTIE, M. R., GILL, G. V. & GALE, E. A. M. 2004. The rising incidence of childhood type 1 diabetes and reduced contribution of high-risk HLA haplotypes. *Lancet,* 364**,** 1699-1700.

GIONGO, A., GANO, K. A., CRABB, D. B., MUKHERJEE, N., NOVELO, L. L., CASELLA, G., DREW, J. C., ILONEN, J., KNIP, M., HYÖTY, H., VEIJOLA, R., SIMELL, T., SIMELL, O., NEU, J., WASSERFALL, C. H., SCHATZ, D., ATKINSON, M. A. & TRIPLETT, E. W. 2011. Toward defining the autoimmune microbiome for type 1 diabetes. *ISME J,* 5**,** 82-91.

GIRVIN, A. M., DAL CANTO, M. C., RHEE, L., SALOMON, B., SHARPE, A., BLUESTONE, J. A. & MILLER, S. D. 2000. A critical role for B7/CD28 costimulation in experimental autoimmune encephalomyelitis: a comparative study using costimulatory molecule-deficient mice and monoclonal antibody blockade. *J Immunol,* 164**,** 136-43.

GIULIETTI, A., GYSEMANS, C., STOFFELS, K., VAN ETTEN, E., DECALLONNE, B., OVERBERGH, L., BOUILLON, R. & MATHIEU, C. 2004. Vitamin D deficiency in early life accelerates Type 1 diabetes in non-obese diabetic mice. *Diabetologia,* 47**,** 451-462.

GODFREY, D. I., KENNEDY, J., MOMBAERTS, P., TONEGAWA, S. & ZLOTNIK, A. 1994. Onset of TCR-beta gene rearrangement and role of TCR-beta expression during CD3-CD4-CD8- thymocyte differentiation. *J Immunol,* 152**,** 4783-92.

GODFREY, D. I., KENNEDY, J., SUDA, T. & ZLOTNIK, A. 1993. A developmental pathway involving four phenotypically and functionally distinct subsets of CD3-CD4-CD8-triple-negative adult mouse thymocytes defined by CD44 and CD25 expression. *J Immunol,* 150**,** 4244-52.

GOLDRATH, A. W. & BEVAN, M. J. 1999. Selecting and maintaining a diverse T-cell repertoire. *Nature,* 402**,** 255-62.

GONNELLA, P. A., WALDNER, H., DEL NIDO, P. J. & MCGOWAN, F. X. 2008. Inhibition of experimental autoimmune myocarditis: peripheral deletion of TcR Vbeta 8.1, 8.2+ CD4+ T cells in TLR-4 deficient mice. *J Autoimmun,* 31**,** 180-7.

GRANJA, C., LIN, L. L., YUNIS, E. J., RELIAS, V. & DASGUPTA, J. D. 1991. PLC gamma 1, a possible mediator of T cell receptor function. *J Biol Chem,* 266**,** 16277-80.

GRAS, S., SAULQUIN, X., REISER, J. B., DEBEAUPUIS, E., ECHASSERIEAU, K., KISSENPFENNIG, A., LEGOUX, F., CHOUQUET, A., LE GORREC, M., MACHILLOT, P., NEVEU, B., THIELENS, N., MALISSEN, B., BONNEVILLE, M. & HOUSSET, D. 2009. Structural bases for the affinity-driven selection of a public TCR against a dominant human cytomegalovirus epitope. *J Immunol,* 183**,** 430-7.

GROUP, T. S. 2008. The Environmental Determinants of Diabetes in the Young (TEDDY) Study. *Ann N Y Acad Sci,* 1150**,** 1-13.

HAJJAR, A. M., ERNST, R. K., TSAI, J. H., WILSON, C. B. & MILLER, S. I. 2002. Human Toll-like receptor 4 recognizes host-specific LPS modifications. *Nat Immunol,* 3**,** 354-9.

HALAPI, E., YAMAMOTO, Y., JUHLIN, C., JEDDI-TEHRANI, M., GRUNEWALD, J., ANDERSSON, R., HISING, C., MASUCCI, G., MELLSTEDT, H. & KIESSLING, R. 1993. Restricted T cell receptor V-beta and J-beta usage in T cells from interleukin-2-cultured lymphocytes of ovarian and renal carcinomas. *Cancer Immunol Immunother,* 36**,** 191-7.

HALBOUT, P., BRIAND, J. P., BÉCOURT, C., MULLER, S. & BOITARD, C. 2002. T cell response to preproinsulin I and II in the nonobese diabetic mouse. *J Immunol,* 169**,** 2436-43.

HAMILTON-WILLIAMS, E. E., CHEUNG, J., RAINBOW, D. B., HUNTER, K. M., WICKER, L. S. & SHERMAN, L. A. 2012. Cellular mechanisms of restored β-cell tolerance mediated by protective alleles of Idd3 and Idd5. *Diabetes,* 61**,** 166-74.

HAMILTON-WILLIAMS, E. E., WONG, S. B., MARTINEZ, X., RAINBOW, D. B., HUNTER, K. M., WICKER, L. S. & SHERMAN, L. A. 2010. Idd9.2 and Idd9.3 protective alleles function in CD4+ T-cells and nonlymphoid cells to prevent expansion of pathogenic islet-specific CD8+ T-cells. *Diabetes,* 59**,** 1478-86.

HAN, B., SERRA, P., YAMANOUCHI, J., AMRANI, A., ELLIOTT, J. F., DICKIE, P., DILORENZO, T. P. & SANTAMARIA, P. 2005. Developmental control of CD8 T cell-avidity maturation in autoimmune diabetes. *J Clin Invest,* 115**,** 1879-87.

HAN, H., TANIGAKI, K., YAMAMOTO, N., KURODA, K., YOSHIMOTO, M., NAKAHATA, T., IKUTA, K. & HONJO, T. 2002. Inducible gene knockout of transcription factor recombination signal binding protein-J reveals its essential role in T versus B lineage decision. *Int Immunol,* 14**,** 637-45.

HANSEN, C. H., KRYCH, L., NIELSEN, D. S., VOGENSEN, F. K., HANSEN, L. H., SØRENSEN, S. J., BUSCHARD, K. & HANSEN, A. K. 2012. Early life treatment with vancomycin propagates Akkermansia muciniphila and reduces diabetes incidence in the NOD mouse. *Diabetologia,* 55**,** 2285-94.

HARJUTSALO, V., SJÖBERG, L. & TUOMILEHTO, J. 2008a. Time trends in the incidence of type 1 diabetes in Finnish children: a cohort study. *Lancet,* 371**,** 1777-82.

HARJUTSALO, V., SJÖBERG, L. & TUOMILEHTO, J. 2008b. Time trends in the incidence of type 1 diabetes in Finnish children: a cohort study. *Lancet,* 371**,** 1777-82.

HASHIMOTO, K., SOHN, S. J., LEVIN, S. D., TADA, T., PERLMUTTER, R. M. & NAKAYAMA, T. 1996. Requirement for p56lck tyrosine kinase activation in T cell receptor-mediated thymic selection. *J Exp Med,* 184**,** 931-43.

HATTORI, M., BUSE, J. B., JACKSON, R. A., GLIMCHER, L., DORF, M. E., MINAMI, M., MAKINO, S., MORIWAKI, K., KUZUYA, H. & IMURA, H. 1986. The NOD mouse: recessive diabetogenic gene in the major histocompatibility complex. *Science,* 231**,** 733-5.

HAWIGER, D., INABA, K., DORSETT, Y., GUO, M., MAHNKE, K., RIVERA, M., RAVETCH, J. V., STEINMAN, R. M. & NUSSENZWEIG, M. C. 2001. Dendritic cells induce peripheral T cell unresponsiveness under steady state conditions in vivo. *J Exp Med,* 194**,** 769-79.

HAWKINS, T., GALA, R. R. & DUNBAR, J. C. 1993. The effect of neonatal sex hormone manipulation on the incidence of diabetes in nonobese diabetic mice. *Proc Soc Exp Biol Med,* 202**,** 201-5.

HAYAKAWA, M., YOKONO, K., NAGATA, M., HATAMORI, N., OGAWA, W., MIKI, A., MIZOGUTI, H. & BABA, S. 1991. Morphological analysis of selective destruction of pancreatic beta-cells by cytotoxic T lymphocytes in NOD mice. *Diabetes,* 40**,** 1210-7.

HAYASHI, Y., HAMANO, H., HANEJI, N., ISHIMARU, N. & YANAGI, K. 1995. Biased T cell receptor V beta gene usage during specific stages of the development of autoimmune sialadenitis in the MRL/lpr mouse model of Sjögren's syndrome. *Arthritis Rheum,* 38**,** 1077-84.

HE, X., DAVE, V. P., ZHANG, Y., HUA, X., NICOLAS, E., XU, W., ROE, B. A. & KAPPES, D. J. 2005. The zinc finger transcription factor Th-POK regulates CD4 versus CD8 T-cell lineage commitment. *Nature,* 433**,** 826-33.

HE, X. L., RADU, C., SIDNEY, J., SETTE, A., WARD, E. S. & GARCIA, K. C. 2002. Structural snapshot of aberrant antigen presentation linked to autoimmunity: the immunodominant epitope of MBP complexed with I-Au. *Immunity,* 17**,** 83-94.

HEINO, M., PETERSON, P., SILLANPÄÄ, N., GUÉRIN, S., WU, L., ANDERSON, G., SCOTT, H. S., ANTONARAKIS, S. E., KUDOH, J., SHIMIZU, N., JENKINSON, E. J., NAQUET, P. & KROHN, K. J. 2000. RNA and protein expression of the murine autoimmune regulator gene (Aire) in normal, RelB-deficient and in NOD mouse. *Eur J Immunol,* 30**,** 1884-93.

HENINGER, A. K., MONTI, P., WILHELM, C., SCHWAIGER, P., KUEHN, D., ZIEGLER, A. G. & BONIFACIO, E. 2013. Activation of islet autoreactive naïve T cells in infants is influenced by homeostatic mechanisms and antigen-presenting capacity. *Diabetes,* 62**,** 2059-66.

HINDLEY, J. P., FERREIRA, C., JONES, E., LAUDER, S. N., LADELL, K., WYNN, K. K., BETTS, G. J., SINGH, Y., PRICE, D. A., GODKIN, A. J., DYSON, J. & GALLIMORE, A. 2011. Analysis of the T-cell receptor repertoires of tumor-infiltrating conventional and regulatory T cells reveals no evidence for conversion in carcinogen-induced tumors. *Cancer Res,* 71**,** 736-46.

HJERN, A. & SÖDERSTRÖM, U. 2008. Parental country of birth is a major determinant of childhood type 1 diabetes in Sweden. *Pediatr Diabetes,* 9**,** 35-9.

HOGQUIST, K. A., JAMESON, S. C., HEATH, W. R., HOWARD, J. L., BEVAN, M. J. & CARBONE, F. R. 1994. T cell receptor antagonist peptides induce positive selection. *Cell,* 76**,** 17-27.

HONEYMAN, M. C., STONE, N. L., FALK, B. A., NEPOM, G. & HARRISON, L. C. 2010. Evidence for molecular mimicry between human T cell epitopes in rotavirus and pancreatic islet autoantigens. *J Immunol,* 184**,** 2204-10.

HOOPER, D. C. 2000. Mechanisms of action and resistance of older and newer fluoroquinolones. *Clin Infect Dis,* 31 Suppl 2**,** S24-8.

HORCHER, M., SOUABNI, A. & BUSSLINGER, M. 2001. Pax5/BSAP maintains the identity of B cells in late B lymphopoiesis. *Immunity,* 14**,** 779-90.

HORNG, T., BARTON, G. M., FLAVELL, R. A. & MEDZHITOV, R. 2002. The adaptor molecule TIRAP provides signalling specificity for Toll-like receptors. *Nature,* 420**,** 329-33.

HORWITZ, D. A., ZHENG, S. G. & GRAY, J. D. 2003. The role of the combination of IL-2 and TGF-beta or IL-10 in the generation and function of CD4+ CD25+ and CD8+ regulatory T cell subsets. *J Leukoc Biol,* 74**,** 471-8.

HUGHES, M. M., YASSAI, M., SEDY, J. R., WEHRLY, T. D., HUANG, C. Y., KANAGAWA, O., GORSKI, J. & SLECKMAN, B. P. 2003. T cell receptor CDR3 loop length repertoire is determined primarily by features of the V(D)J recombination reaction. *Eur J Immunol,* 33**,** 1568-75.

HUMPHREYS-BEHER, M. G., BRINKLEY, L., PURUSHOTHAM, K. R., WANG, P. L., NAKAGAWA, Y., DUSEK, D., KERR, M., CHEGINI, N. & CHAN, E. K. 1993. Characterization of antinuclear autoantibodies present in the serum from nonobese diabetic (NOD) mice. *Clin Immunol Immunopathol,* 68**,** 350-6.

HUNTER, K., RAINBOW, D., PLAGNOL, V., TODD, J. A., PETERSON, L. B. & WICKER, L. S. 2007. Interactions between Idd5.1/Ctla4 and other type 1 diabetes genes. *J Immunol,* 179**,** 8341-9.

HURTADO, J. C., KIM, S. H., POLLOK, K. E., LEE, Z. H. & KWON, B. S. 1995. Potential role of 4-1BB in T cell activation. Comparison with the costimulatory molecule CD28. *J Immunol,* 155**,** 3360-7.

HYTTINEN, V., KAPRIO, J., KINNUNEN, L., KOSKENVUO, M. & TUOMILEHTO, J. 2003. Genetic liability of type 1 diabetes and the onset age among 22,650 young Finnish twin pairs: a nationwide follow-up study. *Diabetes,* 52**,** 1052-5.

HÄNNINEN, A., JAAKKOLA, I. & JALKANEN, S. 1998. Mucosal addressin is required for the development of diabetes in nonobese diabetic mice. *J Immunol,* 160**,** 6018-25.

HÜNIG, T., TIEFENTHALER, G., MEYER ZUM BÜSCHENFELDE, K. H. & MEUER, S. C. 1987. Alternative pathway activation of T cells by binding of CD2 to its cell-surface ligand. *Nature,* 326**,** 298-301.

JAAKKOLA, I., JALKANEN, S. & HÄNNINEN, A. 2003. Diabetogenic T cells are primed both in pancreatic and gut-associated lymph nodes in NOD mice. *Eur J Immunol,* 33**,** 3255-64.

JAECKEL, E., LIPES, M. A. & VON BOEHMER, H. 2004. Recessive tolerance to preproinsulin 2 reduces but does not abolish type 1 diabetes. *Nat Immunol,* 5**,** 1028-35.

JANAS, M. L., GROVES, P., KIENZLE, N. & KELSO, A. 2005. IL-2 regulates perforin and granzyme gene expression in CD8+ T cells independently of its effects on survival and proliferation. *J Immunol,* 175**,** 8003-10.

JANSEN, A., HOMO-DELARCHE, F., HOOIJKAAS, H., LEENEN, P. J., DARDENNE, M. & DREXHAGE, H. A. 1994. Immunohistochemical characterization of monocytes-macrophages and dendritic cells involved in the initiation of the insulitis and beta-cell destruction in NOD mice. *Diabetes,* 43**,** 667-75.

JARCHUM, I., NICHOL, L., TRUCCO, M., SANTAMARIA, P. & DILORENZO, T. P. 2008. Identification of novel IGRP epitopes targeted in type 1 diabetes patients. *Clin Immunol,* 127**,** 359-65.

JI, L., XUE, R., TANG, W., WU, W., HU, T., LIU, X., PENG, X., GU, J., CHEN, S. & ZHANG, S. 2014. Toll like receptor 2 knock-out attenuates carbon tetrachloride (CCl4)-induced liver fibrosis by downregulating MAPK and NF-κB signaling pathways. *FEBS Lett,* 588**,** 2095-100.

JOHN, B. & CRISPE, I. N. 2004. Passive and active mechanisms trap activated CD8+ T cells in the liver. *J Immunol,* 172**,** 5222-9.

JUNE, C. H., FLETCHER, M. C., LEDBETTER, J. A., SCHIEVEN, G. L., SIEGEL, J. N., PHILLIPS, A. F. & SAMELSON, L. E. 1990. Inhibition of tyrosine phosphorylation prevents T-cell receptor-mediated signal transduction. *Proc Natl Acad Sci U S A,* 87**,** 7722-6.

KATZ, J. D., WANG, B., HASKINS, K., BENOIST, C. & MATHIS, D. 1993. Following a diabetogenic T cell from genesis through pathogenesis. *Cell,* 74**,** 1089-100.

KAUFMAN, D. L., CLARE-SALZLER, M., TIAN, J., FORSTHUBER, T., TING, G. S., ROBINSON, P., ATKINSON, M. A., SERCARZ, E. E., TOBIN, A. J. & LEHMANN, P. V. 1993. Spontaneous loss of T-cell tolerance to glutamic acid decarboxylase in murine insulin-dependent diabetes. *Nature,* 366**,** 69-72.

KIM, D. H., LEE, J. C., LEE, M. K., KIM, K. W. & LEE, M. S. 2012. Treatment of autoimmune diabetes in NOD mice by Toll-like receptor 2 tolerance in conjunction with dipeptidyl peptidase 4 inhibition. *Diabetologia,* 55**,** 3308-17.

KIM, H. J., VERBINNEN, B., TANG, X., LU, L. & CANTOR, H. 2010. Inhibition of follicular T-helper cells by CD8(+) regulatory T cells is essential for self tolerance. *Nature,* 467**,** 328-32.

KIM, H. S., HAN, M. S., CHUNG, K. W., KIM, S., KIM, E., KIM, M. J., JANG, E., LEE, H. A., YOUN, J., AKIRA, S. & LEE, M. S. 2007. Toll-like receptor 2 senses beta-cell death and contributes to the initiation of autoimmune diabetes. *Immunity,* 27**,** 321-33.

KIMURA, I., OZAWA, K., INOUE, D., IMAMURA, T., KIMURA, K., MAEDA, T., TERASAWA, K., KASHIHARA, D., HIRANO, K., TANI, T., TAKAHASHI, T., MIYAUCHI, S., SHIOI, G., INOUE, H. & TSUJIMOTO, G. 2013. The gut microbiota suppresses insulin-mediated fat accumulation via the short-chain fatty acid receptor GPR43. *Nat Commun,* 4**,** 1829.

KISHIMOTO, H. & SPRENT, J. 2000. The thymus and negative selection. *Immunol Res,* 21**,** 315-23.

KISHIMOTO, H. & SPRENT, J. 2001. A defect in central tolerance in NOD mice. *Nat Immunol,* 2**,** 1025-31.

KLAUSNER, R. D., O'SHEA, J. J., LUONG, H., ROSS, P., BLUESTONE, J. A. & SAMELSON, L. E. 1987. T cell receptor tyrosine phosphorylation. Variable coupling for different activating ligands. *J Biol Chem,* 262**,** 12654-9.

KLEIN, L., KLUGMANN, M., NAVE, K. A., TUOHY, V. K. & KYEWSKI, B. 2000. Shaping of the autoreactive T-cell repertoire by a splice variant of self protein expressed in thymic epithelial cells. *Nat Med,* 6**,** 56-61.

KNIP, M. & SIMELL, O. 2012. Environmental triggers of type 1 diabetes. *Cold Spring Harb Perspect Med,* 2**,** a007690.

KOBAYASHI, E., MIZUKOSHI, E., KISHI, H., OZAWA, T., HAMANA, H., NAGAI, T., NAKAGAWA, H., JIN, A., KANEKO, S. & MURAGUCHI, A. 2013. A new cloning and expression system yields and validates TCRs from blood lymphocytes of patients with cancer within 10 days. *Nat Med,* 19**,** 1542-6.

KOBAYASHI, M., JASINSKI, J., LIU, E., LI, M., MIAO, D., ZHANG, L., YU, L., NAKAYAMA, M. & EISENBARTH, G. S. 2008. Conserved T cell receptor alpha-chain induces insulin autoantibodies. *Proc Natl Acad Sci U S A,* 105**,** 10090-4.

KONDO, M., WEISSMAN, I. L. & AKASHI, K. 1997. Identification of clonogenic common lymphoid progenitors in mouse bone marrow. *Cell,* 91**,** 661-72.

KONING, D., COSTA, A. I., HOOF, I., MILES, J. J., NANLOHY, N. M., LADELL, K., MATTHEWS, K. K., VENTURI, V., SCHELLENS, I. M., BORGHANS, J. A., KESMIR, C., PRICE, D. A. & VAN BAARLE, D. 2013. CD8+ TCR repertoire formation is guided primarily by the peptide component of the antigenic complex. *J Immunol,* 190**,** 931-9.

KONING, F., LEW, A. M., MALOY, W. L., VALAS, R. & COLIGAN, J. E. 1988. The biosynthesis and assembly of T cell receptor alpha- and beta-chains with the CD3 complex. *J Immunol,* 140**,** 3126-34.

KONT, V., LAAN, M., KISAND, K., MERITS, A., SCOTT, H. S. & PETERSON, P. 2008. Modulation of Aire regulates the expression of tissue-restricted antigens. *Mol Immunol,* 45**,** 25-33.

KOUSKOFF, V., SIGNORELLI, K., BENOIST, C. & MATHIS, D. 1995. Cassette vectors directing expression of T cell receptor genes in transgenic mice. *J Immunol Methods,* 180**,** 273-80.

KRISHNAMURTHY, B., MARIANA, L., GELLERT, S. A., COLMAN, P. G., HARRISON, L. C., LEW, A. M., SANTAMARIA, P., THOMAS, H. E. & KAY, T. W. 2008. Autoimmunity to both proinsulin and IGRP is required for diabetes in nonobese diabetic 8.3 TCR transgenic mice. *J Immunol,* 180**,** 4458-64.

KRUTZIK, S. R., TAN, B., LI, H., OCHOA, M. T., LIU, P. T., SHARFSTEIN, S. E., GRAEBER, T. G., SIELING, P. A., LIU, Y. J., REA, T. H., BLOOM, B. R. & MODLIN, R. L. 2005. TLR activation triggers the rapid differentiation of monocytes into macrophages and dendritic cells. *Nat Med,* 11**,** 653-60.

KURTS, C., KOSAKA, H., CARBONE, F. R., MILLER, J. F. & HEATH, W. R. 1997. Class I-restricted cross-presentation of exogenous self-antigens leads to deletion of autoreactive CD8(+) T cells. *J Exp Med,* 186**,** 239-45.

LAMONT, D., MUKHERJEE, G., KUMAR, P. R., SAMANTA, D., MCPHEE, C. G., KAY, T. W., ALMO, S. C., DILORENZO, T. P. & SERREZE, D. V. 2014. Compensatory mechanisms allow undersized anchor-deficient class I MHC ligands to mediate pathogenic autoreactive T cell responses. *J Immunol,* 193**,** 2135-46.

LAUVAU, G., VIJH, S., KONG, P., HORNG, T., KERKSIEK, K., SERBINA, N., TUMA, R. A. & PAMER, E. G. 2001. Priming of memory but not effector CD8 T cells by a killed bacterial vaccine. *Science,* 294**,** 1735-9.

LEE, H. M., BAUTISTA, J. L., SCOTT-BROWNE, J., MOHAN, J. F. & HSIEH, C. S. 2012a. A broad range of self-reactivity drives thymic regulatory T cell selection to limit responses to self. *Immunity,* 37**,** 475-86.

LEE, J. S., SCANDIUZZI, L., RAY, A., WEI, J., HOFMEYER, K. A., ABADI, Y. M., LOKE, P., LIN, J., YUAN, J., SERREZE, D. V., ALLISON, J. P. & ZANG, X. 2012b. B7x in the periphery abrogates pancreas-specific damage mediated by self-reactive CD8 T cells. *J Immunol,* 189**,** 4165-74.

LEE, J. W., EPARDAUD, M., SUN, J., BECKER, J. E., CHENG, A. C., YONEKURA, A. R., HEATH, J. K. & TURLEY, S. J. 2007. Peripheral antigen display by lymph node stroma promotes T cell tolerance to intestinal self. *Nat Immunol,* 8**,** 181-90.

LEE, K. C., OUWEHAND, I., GIANNINI, A. L., THOMAS, N. S., DIBB, N. J. & BIJLMAKERS, M. J. 2010. Lck is a key target of imatinib and dasatinib in T-cell activation. *Leukemia,* 24**,** 896-900.

LEE, K. U., AMANO, K. & YOON, J. W. 1988. Evidence for initial involvement of macrophage in development of insulitis in NOD mice. *Diabetes,* 37**,** 989-91.

LEE, Y. H., ISHIDA, Y., RIFA'I, M., SHI, Z., ISOBE, K. & SUZUKI, H. 2008. Essential role of CD8+CD122+ regulatory T cells in the recovery from experimental autoimmune encephalomyelitis. *J Immunol,* 180**,** 825-32.

LEE-MACARY, A. E., ROSS, E. L., DAVIES, D., LAYLOR, R., HONEYCHURCH, J., GLENNIE, M. J., SNARY, D. & WILKINSON, R. W. 2001. Development of a novel flow cytometric cell-mediated cytotoxicity assay using the fluorophores PKH-26 and TO-PRO-3 iodide. *J Immunol Methods,* 252**,** 83-92.

LEITENBERG, D., NOVAK, T. J., FARBER, D., SMITH, B. R. & BOTTOMLY, K. 1996. The extracellular domain of CD45 controls association with the CD4-T cell receptor complex and the response to antigen-specific stimulation. *J Exp Med,* 183**,** 249-59.

LEROUX, L., DESBOIS, P., LAMOTTE, L., DUVILLIÉ, B., CORDONNIER, N., JACKEROTT, M., JAMI, J., BUCCHINI, D. & JOSHI, R. L. 2001. Compensatory responses in mice carrying a null mutation for Ins1 or Ins2. *Diabetes,* 50 Suppl 1**,** S150-3.

LIEBERMAN, S. M., EVANS, A. M., HAN, B., TAKAKI, T., VINNITSKAYA, Y., CALDWELL, J. A., SERREZE, D. V., SHABANOWITZ, J., HUNT, D. F., NATHENSON, S. G., SANTAMARIA, P. & DILORENZO, T. P. 2003. Identification of the beta cell antigen targeted by a prevalent population of pathogenic CD8+ T cells in autoimmune diabetes. *Proc Natl Acad Sci U S A,* 100**,** 8384-8.

LIEBERMAN, S. M., TAKAKI, T., HAN, B., SANTAMARIA, P., SERREZE, D. V. & DILORENZO, T. P. 2004. Individual nonobese diabetic mice exhibit unique patterns of CD8+ T cell reactivity to three islet antigens, including the newly identified widely expressed dystrophia myotonica kinase. *J Immunol,* 173**,** 6727-34.

LISTON, A., GRAY, D. H., LESAGE, S., FLETCHER, A. L., WILSON, J., WEBSTER, K. E., SCOTT, H. S., BOYD, R. L., PELTONEN, L. & GOODNOW, C. C. 2004. Gene dosage--limiting role of Aire in thymic expression, clonal deletion, and organ-specific autoimmunity. *J Exp Med,* 200**,** 1015-26.

LISTON, A., LESAGE, S., WILSON, J., PELTONEN, L. & GOODNOW, C. C. 2003. Aire regulates negative selection of organ-specific T cells. *Nat Immunol,* 4**,** 350-4.

LIU, Z., CORT, L., EBERWINE, R., HERRMANN, T., LEIF, J. H., GREINER, D. L., YAHALOM, B., BLANKENHORN, E. P. & MORDES, J. P. 2012. Prevention of type 1 diabetes in the rat with an allele-specific anti-T-cell receptor antibody: Vβ13 as a therapeutic target and biomarker. *Diabetes,* 61**,** 1160-8.

LIVÁK, F., TOURIGNY, M., SCHATZ, D. G. & PETRIE, H. T. 1999. Characterization of TCR gene rearrangements during adult murine T cell development. *J Immunol,* 162**,** 2575-80.

LU, J., LI, Q., XIE, H., CHEN, Z. J., BOROVITSKAYA, A. E., MACLAREN, N. K., NOTKINS, A. L. & LAN, M. S. 1996. Identification of a second transmembrane protein tyrosine

phosphatase, IA-2beta, as an autoantigen in insulin-dependent diabetes mellitus: precursor of the 37-kDa tryptic fragment. *Proc Natl Acad Sci U S A,* 93**,** 2307-11.

LU, L., KIM, H. J., WERNECK, M. B. & CANTOR, H. 2008. Regulation of CD8+ regulatory T cells: Interruption of the NKG2A-Qa-1 interaction allows robust suppressive activity and resolution of autoimmune disease. *Proc Natl Acad Sci U S A,* 105**,** 19420-5.

LUC, S., LUIS, T. C., BOUKARABILA, H., MACAULAY, I. C., BUZA-VIDAS, N., BOURIEZ-JONES, T., LUTTEROPP, M., WOLL, P. S., LOUGHRAN, S. J., MEAD, A. J., HULTQUIST, A., BROWN, J., MIZUKAMI, T., MATSUOKA, S., FERRY, H., ANDERSON, K., DUARTE, S., ATKINSON, D., SONEJI, S., DOMANSKI, A., FARLEY, A., SANJUAN-PLA, A., CARELLA, C., PATIENT, R., DE BRUIJN, M., ENVER, T., NERLOV, C., BLACKBURN, C., GODIN, I. & JACOBSEN, S. E. 2012. The earliest thymic T cell progenitors sustain B cell and myeloid lineage potential. *Nat Immunol,* 13**,** 412-9.

LUCIANI, F., SANDERS, M. T., OVEISSI, S., PANG, K. C. & CHEN, W. 2013. Increasing viral dose causes a reversal in CD8+ T cell immunodominance during primary influenza infection due to differences in antigen presentation, T cell avidity, and precursor numbers. *J Immunol,* 190**,** 36-47.

LUCKHEERAM, R. V., ZHOU, R., VERMA, A. D. & XIA, B. 2012. $CD4^+$T cells: differentiation and functions. *Clin Dev Immunol,* 2012**,** 925135.

LUKACS-KORNEK, V., MALHOTRA, D., FLETCHER, A. L., ACTON, S. E., ELPEK, K. G., TAYALIA, P., COLLIER, A. R. & TURLEY, S. J. 2011. Regulated release of nitric oxide by nonhematopoietic stroma controls expansion of the activated T cell pool in lymph nodes. *Nat Immunol,* 12**,** 1096-104.

LUND, T., O'REILLY, L., HUTCHINGS, P., KANAGAWA, O., SIMPSON, E., GRAVELY, R., CHANDLER, P., DYSON, J., PICARD, J. K. & EDWARDS, A. 1990. Prevention of insulin-dependent diabetes mellitus in non-obese diabetic mice by transgenes encoding modified I-A beta-chain or normal I-E alpha-chain. *Nature,* 345**,** 727-9.

MA, Y., PANNICKE, U., SCHWARZ, K. & LIEBER, M. R. 2002. Hairpin opening and overhang processing by an Artemis/DNA-dependent protein kinase complex in nonhomologous end joining and V(D)J recombination. *Cell,* 108**,** 781-94.

MAEDA, T., MERGHOUB, T., HOBBS, R. M., DONG, L., MAEDA, M., ZAKRZEWSKI, J., VAN DEN BRINK, M. R., ZELENT, A., SHIGEMATSU, H., AKASHI, K., TERUYA-FELDSTEIN, J., CATTORETTI, G. & PANDOLFI, P. P. 2007. Regulation of B versus T lymphoid lineage fate decision by the proto-oncogene LRF. *Science,* 316**,** 860-6.

MAKINO, S., KUNIMOTO, K., MURAOKA, Y. & KATAGIRI, K. 1981. Effect of castration on the appearance of diabetes in NOD mouse. *Jikken Dobutsu,* 30**,** 137-40.

MAKINO, S., KUNIMOTO, K., MURAOKA, Y., MIZUSHIMA, Y., KATAGIRI, K. & TOCHINO, Y. 1980. Breeding of a non-obese, diabetic strain of mice. *Jikken Dobutsu,* 29**,** 1-13.

MANNERING, S. I., HARRISON, L. C., WILLIAMSON, N. A., MORRIS, J. S., THEARLE, D. J., JENSEN, K. P., KAY, T. W., ROSSJOHN, J., FALK, B. A., NEPOM, G. T. & PURCELL, A. W. 2005. The insulin A-chain epitope recognized by human T cells is posttranslationally modified. *J Exp Med,* 202**,** 1191-7.

MANOLIOS, N., KEMP, O. & LI, Z. G. 1994. The T cell antigen receptor alpha and beta chains interact via distinct regions with CD3 chains. *Eur J Immunol,* 24**,** 84-92.

MANUEL, M., TREDAN, O., BACHELOT, T., CLAPISSON, G., COURTIER, A., PARMENTIER, G., RABEONY, T., GRIVES, A., PEREZ, S., MOURET, J. F., PEROL, D., CHABAUD, S., RAY-COQUARD, I., LABIDI-GALY, I., HEUDEL, P., PIERGA, J. Y., CAUX, C., BLAY, J. Y., PASQUAL, N. & MÉNÉTRIER-CAUX, C. 2012. Lymphopenia combined with low TCR diversity (divpenia) predicts poor overall survival in metastatic breast cancer patients. *Oncoimmunology,* 1**,** 432-440.

MARIETTA, E. V., GOMEZ, A. M., YEOMAN, C., TILAHUN, A. Y., CLARK, C. R., LUCKEY, D. H., MURRAY, J. A., WHITE, B. A., KUDVA, Y. C. & RAJAGOPALAN, G. 2013. Low incidence of spontaneous type 1 diabetes in non-obese diabetic mice raised on gluten-free diets is associated with changes in the intestinal microbiome. *PLoS One,* 8**,** e78687.

MARKLE, J. G., FRANK, D. N., MORTIN-TOTH, S., ROBERTSON, C. E., FEAZEL, L. M., ROLLE-KAMPCZYK, U., VON BERGEN, M., MCCOY, K. D., MACPHERSON, A. J. & DANSKA, J. S. 2013a. Sex differences in the gut microbiome drive hormone-dependent regulation of autoimmunity. *Science,* 339**,** 1084-8.

MARKLE, J. G., MORTIN-TOTH, S., WONG, A. S., GENG, L., HAYDAY, A. & DANSKA, J. S. 2013b. γδ T Cells Are Essential Effectors of Type 1 Diabetes in the Nonobese Diabetic Mouse Model. *J Immunol*.

MARLIN, S. D. & SPRINGER, T. A. 1987. Purified intercellular adhesion molecule-1 (ICAM-1) is a ligand for lymphocyte function-associated antigen 1 (LFA-1). *Cell,* 51**,** 813-9.

MARTIN-PAGOLA, A., PILEGGI, A., ZAHR, E., VENDRAME, F., DAMARIS MOLANO, R., SNOWHITE, I., RICORDI, C., EISENBARTH, G. S., NAKAYAMA, M. & PUGLIESE, A. 2009. Insulin2 gene (Ins2) transcription by NOD bone marrow-derived cells does not influence autoimmune diabetes development in NOD-Ins2 knockout mice. *Scand J Immunol,* 70**,** 439-46.

MARTINEZ, X., KREUWEL, H. T., REDMOND, W. L., TRENNEY, R., HUNTER, K., ROSEN, H., SARVETNICK, N., WICKER, L. S. & SHERMAN, L. A. 2005. CD8+ T cell tolerance in nonobese diabetic mice is restored by insulin-dependent diabetes resistance alleles. *J Immunol,* 175**,** 1677-85.

MARTINUZZI, E., NOVELLI, G., SCOTTO, M., BLANCOU, P., BACH, J. M., CHAILLOUS, L., BRUNO, G., CHATENOUD, L., VAN ENDERT, P. & MALLONE, R. 2008. The frequency and immunodominance of islet-specific CD8+ T-cell responses change after type 1 diabetes diagnosis and treatment. *Diabetes,* 57**,** 1312-20.

MATHOULIN, M. P., XERRI, L., JACQUEMIER, J., ADELAIDE, J., PARC, P. & HASSOUN, J. 1993. Unrestricted T-cell receptor V-region gene repertoire in tumor-infiltrating lymphocytes from human breast carcinomas. *Cancer,* 72**,** 506-10.

MATSUMOTO, M., YAGI, H., KUNIMOTO, K., KAWAGUCHI, J., MAKINO, S. & HARADA, M. 1993. Transfer of autoimmune diabetes from diabetic NOD mice to NOD athymic nude mice: the roles of T cell subsets in the pathogenesis. *Cell Immunol,* 148**,** 189-97.

MATSUZAKI, T., NAGATA, Y., KADO, S., UCHIDA, K., KATO, I., HASHIMOTO, S. & YOKOKURA, T. 1997. Prevention of onset in an insulin-dependent diabetes mellitus model, NOD mice, by oral feeding of Lactobacillus casei. *APMIS,* 105**,** 643-9.

MAURANO, F., MAZZARELLA, G., LUONGO, D., STEFANILE, R., D'ARIENZO, R., ROSSI, M., AURICCHIO, S. & TRONCONE, R. 2005. Small intestinal enteropathy in non-obese diabetic mice fed a diet containing wheat. *Diabetologia,* 48**,** 931-7.

MAYNARD, J., PETERSSON, K., WILSON, D. H., ADAMS, E. J., BLONDELLE, S. E., BOULANGER, M. J., WILSON, D. B. & GARCIA, K. C. 2005. Structure of an autoimmune T cell receptor complexed with class II peptide-MHC: insights into MHC bias and antigen specificity. *Immunity,* 22**,** 81-92.

MAZMANIAN, S. K., ROUND, J. L. & KASPER, D. L. 2008. A microbial symbiosis factor prevents intestinal inflammatory disease. *Nature,* 453**,** 620-5.

MCBLANE, J. F., VAN GENT, D. C., RAMSDEN, D. A., ROMEO, C., CUOMO, C. A., GELLERT, M. & OETTINGER, M. A. 1995. Cleavage at a V(D)J recombination signal requires only RAG1 and RAG2 proteins and occurs in two steps. *Cell,* 83**,** 387-95.

MCGEACHY, M. J., STEPHENS, L. A. & ANDERTON, S. M. 2005. Natural recovery and protection from autoimmune encephalomyelitis: contribution of CD4+CD25+ regulatory cells within the central nervous system. *J Immunol,* 175**,** 3025-32.

MCNEILL, L., SALMOND, R. J., COOPER, J. C., CARRET, C. K., CASSADY-CAIN, R. L., ROCHE-MOLINA, M., TANDON, P., HOLMES, N. & ALEXANDER, D. R. 2007. The differential regulation of Lck kinase phosphorylation sites by CD45 is critical for T cell receptor signaling responses. *Immunity,* 27**,** 425-37.

MEDZHITOV, R., PRESTON-HURLBURT, P. & JANEWAY, C. A. 1997. A human homologue of the Drosophila Toll protein signals activation of adaptive immunity. *Nature,* 388**,** 394-7.

MESSAOUDI, I., GUEVARA PATIÑO, J. A., DYALL, R., LEMAOULT, J. & NIKOLICH-ZUGICH, J. 2002. Direct link between mhc polymorphism, T cell avidity, and diversity in immune defense. *Science,* 298**,** 1797-800.

MICHEL, C., BOITARD, C. & BACH, J. F. 1989. Insulin autoantibodies in non-obese diabetic (NOD) mice. *Clin Exp Immunol,* 75**,** 457-60.

MILES, J. J., DOUEK, D. C. & PRICE, D. A. 2011. Bias in the αβ T-cell repertoire: implications for disease pathogenesis and vaccination. *Immunol Cell Biol,* 89**,** 375-87.

MINAMI, Y., SAMELSON, L. E. & KLAUSNER, R. D. 1987a. Internalization and cycling of the T cell antigen receptor. Role of protein kinase C. *J Biol Chem,* 262**,** 13342-7.

MINAMI, Y., WEISSMAN, A. M., SAMELSON, L. E. & KLAUSNER, R. D. 1987b. Building a multichain receptor: synthesis, degradation, and assembly of the T-cell antigen receptor. *Proc Natl Acad Sci U S A,* 84**,** 2688-92.

MIYAZAKI, A., HANAFUSA, T., YAMADA, K., MIYAGAWA, J., FUJINO-KURIHARA, H., NAKAJIMA, H., NONAKA, K. & TARUI, S. 1985. Predominance of T lymphocytes in pancreatic islets and spleen of pre-diabetic non-obese diabetic (NOD) mice: a longitudinal study. *Clin Exp Immunol,* 60**,** 622-30.

MOHAN, J. F., LEVISETTI, M. G., CALDERON, B., HERZOG, J. W., PETZOLD, S. J. & UNANUE, E. R. 2010. Unique autoreactive T cells recognize insulin peptides generated within the islets of Langerhans in autoimmune diabetes. *Nat Immunol,* 11**,** 350-4.

MOHAN, J. F., PETZOLD, S. J. & UNANUE, E. R. 2011. Register shifting of an insulin peptide-MHC complex allows diabetogenic T cells to escape thymic deletion. *J Exp Med,* 208**,** 2375-83.

MOMBAERTS, P., CLARKE, A. R., RUDNICKI, M. A., IACOMINI, J., ITOHARA, S., LAFAILLE, J. J., WANG, L., ICHIKAWA, Y., JAENISCH, R. & HOOPER, M. L. 1992a. Mutations in T-cell antigen receptor genes alpha and beta block thymocyte development at different stages. *Nature,* 360**,** 225-31.

MOMBAERTS, P., IACOMINI, J., JOHNSON, R. S., HERRUP, K., TONEGAWA, S. & PAPAIOANNOU, V. E. 1992b. RAG-1-deficient mice have no mature B and T lymphocytes. *Cell,* 68**,** 869-77.

MONROE, R. J., SEIDL, K. J., GAERTNER, F., HAN, S., CHEN, F., SEKIGUCHI, J., WANG, J., FERRINI, R., DAVIDSON, L., KELSOE, G. & ALT, F. W. 1999. RAG2:GFP knockin mice reveal novel aspects of RAG2 expression in primary and peripheral lymphoid tissues. *Immunity,* 11**,** 201-12.

MONTANE, J., BISCHOFF, L., SOUKHATCHEVA, G., DAI, D. L., HARDENBERG, G., LEVINGS, M. K., ORBAN, P. C., KIEFFER, T. J., TAN, R. & VERCHERE, C. B. 2011. Prevention of murine autoimmune diabetes by CCL22-mediated Treg recruitment to the pancreatic islets. *J Clin Invest,* 121**,** 3024-8.

MOORE, M. W., CARBONE, F. R. & BEVAN, M. J. 1988. Introduction of soluble protein into the class I pathway of antigen processing and presentation. *Cell,* 54**,** 777-85.

MOR, F. & COHEN, I. R. 2013. Beta-lactam antibiotics modulate T-cell functions and gene expression via covalent binding to cellular albumin. *Proc Natl Acad Sci U S A,* 110**,** 2981-6.

MORIYAMA, H., ABIRU, N., PARONEN, J., SIKORA, K., LIU, E., MIAO, D., DEVENDRA, D., BEILKE, J., GIANANI, R., GILL, R. G. & EISENBARTH, G. S. 2003. Evidence for a primary islet autoantigen (preproinsulin 1) for insulitis and diabetes in the nonobese diabetic mouse. *Proc Natl Acad Sci U S A,* 100**,** 10376-81.

MUKHERJI, A., KOBIITA, A., YE, T. & CHAMBON, P. 2013. Homeostasis in intestinal epithelium is orchestrated by the circadian clock and microbiota cues transduced by TLRs. *Cell,* 153**,** 812-27.

MURATA, S., SASAKI, K., KISHIMOTO, T., NIWA, S., HAYASHI, H., TAKAHAMA, Y. & TANAKA, K. 2007. Regulation of CD8+ T cell development by thymus-specific proteasomes. *Science,* 316**,** 1349-53.

MUSTELIN, T., COGGESHALL, K. M., ISAKOV, N. & ALTMAN, A. 1990. T cell antigen receptor-mediated activation of phospholipase C requires tyrosine phosphorylation. *Science,* 247**,** 1584-7.

MYERS, L., JOEDICKE, J. J., CARMODY, A. B., MESSER, R. J., KASSIOTIS, G., DUDLEY, J. P., DITTMER, U. & HASENKRUG, K. J. 2013. IL-2-Independent and TNF-α-Dependent Expansion of Vβ5+ Natural Regulatory T Cells during Retrovirus Infection. *J Immunol*.

NAGAMINE, K., PETERSON, P., SCOTT, H. S., KUDOH, J., MINOSHIMA, S., HEINO, M., KROHN, K. J., LALIOTI, M. D., MULLIS, P. E., ANTONARAKIS, S. E., KAWASAKI, K., ASAKAWA, S., ITO, F. & SHIMIZU, N. 1997. Positional cloning of the APECED gene. *Nat Genet,* 17**,** 393-8.

NAGATA, M., SANTAMARIA, P., KAWAMURA, T., UTSUGI, T. & YOON, J. W. 1994a. Evidence for the role of CD8+ cytotoxic T cells in the destruction of pancreatic beta-cells in nonobese diabetic mice. *J Immunol,* 152**,** 2042-50.

NAGATA, M., SANTAMARIA, P., KAWAMURA, T., UTSUGI, T. & YOON, J. W. 1994b. Evidence for the role of CD8+ cytotoxic T cells in the destruction of pancreatic beta-cells in nonobese diabetic mice. *J Immunol,* 152**,** 2042-50.

NAGATA, M., YOKONO, K., HAYAKAWA, M., KAWASE, Y., HATAMORI, N., OGAWA, W., YONEZAWA, K., SHII, K. & BABA, S. 1989. Destruction of pancreatic islet cells by cytotoxic T lymphocytes in nonobese diabetic mice. *J Immunol,* 143**,** 1155-62.

NAKAYAMA, M., ABIRU, N., MORIYAMA, H., BABAYA, N., LIU, E., MIAO, D., YU, L., WEGMANN, D. R., HUTTON, J. C., ELLIOTT, J. F. & EISENBARTH, G. S. 2005a. Prime role for an insulin epitope in the development of type 1 diabetes in NOD mice. *Nature,* 435**,** 220-3.

NAKAYAMA, M., BABAYA, N., MIAO, D., SIKORA, K., ELLIOTT, J. F. & EISENBARTH, G. S. 2005b. Thymic expression of mutated B16:A preproinsulin messenger RNA does not reverse acceleration of NOD diabetes associated with insulin 2 (thymic expressed insulin) knockout. *J Autoimmun,* 25**,** 193-8.

NAKAYAMA, M., CASTOE, T., SOSINOWSKI, T., HE, X., JOHNSON, K., HASKINS, K., VIGNALI, D. A., GAPIN, L., POLLOCK, D. & EISENBARTH, G. S. 2012. Germline TRAV5D-4 T-cell receptor sequence targets a primary insulin peptide of NOD mice. *Diabetes,* 61**,** 857-65.

NAKHOODA, A. F., LIKE, A. A., CHAPPEL, C. I., MURRAY, F. T. & MARLISS, E. B. 1977. The spontaneously diabetic Wistar rat. Metabolic and morphologic studies. *Diabetes,* 26**,** 100-12.

NAYAK, D. K., CALDERON, B., VOMUND, A. N. & UNANUE, E. R. 2014. In NOD mice ZnT8 reactive T cells are weakly pathogenic but can participate in diabetes under inflammatory conditions. *Diabetes*.

NAYLOR, K., LI, G., VALLEJO, A. N., LEE, W. W., KOETZ, K., BRYL, E., WITKOWSKI, J., FULBRIGHT, J., WEYAND, C. M. & GORONZY, J. J. 2005. The influence of age on T cell generation and TCR diversity. *J Immunol,* 174**,** 7446-52.

NEERMAN-ARBEZ, M., CIRULLI, V. & HALBAN, P. A. 1994. Levels of the conversion endoproteases PC1 (PC3) and PC2 distinguish between insulin-producing pancreatic islet beta cells and non-beta cells. *Biochem J,* 300 (Pt 1)**,** 57-61.

NEGISHI, I., MOTOYAMA, N., NAKAYAMA, K., SENJU, S., HATAKEYAMA, S., ZHANG, Q., CHAN, A. C. & LOH, D. Y. 1995. Essential role for ZAP-70 in both positive and negative selection of thymocytes. *Nature,* 376**,** 435-8.

NEJENTSEV, S., HOWSON, J. M., WALKER, N. M., SZESZKO, J., FIELD, S. F., STEVENS, H. E., REYNOLDS, P., HARDY, M., KING, E., MASTERS, J., HULME, J., MAIER, L. M., SMYTH, D., BAILEY, R., COOPER, J. D., RIBAS, G., CAMPBELL, R. D., CLAYTON, D. G., TODD, J. A. & CONSORTIUM, W. T. C. C. 2007. Localization of type 1 diabetes susceptibility to the MHC class I genes HLA-B and HLA-A. *Nature,* 450**,** 887-92.

NEPOM, G. T., LIPPOLIS, J. D., WHITE, F. M., MASEWICZ, S., MARTO, J. A., HERMAN, A., LUCKEY, C. J., FALK, B., SHABANOWITZ, J., HUNT, D. F., ENGELHARD, V. H. & NEPOM, B. S. 2001. Identification and modulation of a naturally processed T cell epitope from the diabetes-associated autoantigen human glutamic acid decarboxylase 65 (hGAD65). *Proc Natl Acad Sci U S A,* 98**,** 1763-8.

NGUYEN, T. H., ROWNTREE, L. C., PELLICCI, D. G., BIRD, N. L., HANDEL, A., KJER-NIELSEN, L., KEDZIERSKA, K., KOTSIMBOS, T. C. & MIFSUD, N. A. 2014. Recognition of Distinct Cross-Reactive Virus-Specific CD8+ T Cells Reveals a Unique TCR Signature in a Clinical Setting. *J Immunol,* 192**,** 5039-49.

NISHIMOTO, H., KIKUTANI, H., YAMAMURA, K. & KISHIMOTO, T. 1987. Prevention of autoimmune insulitis by expression of I-E molecules in NOD mice. *Nature,* 328**,** 432-4.

NITTA, T., MURATA, S., SASAKI, K., FUJII, H., RIPEN, A. M., ISHIMARU, N., KOYASU, S., TANAKA, K. & TAKAHAMA, Y. 2010. Thymoproteasome shapes immunocompetent repertoire of CD8+ T cells. *Immunity,* 32**,** 29-40.

O'BRIEN, B. A., GENG, X., ORTEU, C. H., HUANG, Y., GHOREISHI, M., ZHANG, Y., BUSH, J. A., LI, G., FINEGOOD, D. T. & DUTZ, J. P. 2006. A deficiency in the in vivo clearance of apoptotic cells is a feature of the NOD mouse. *J Autoimmun,* 26**,** 104-15.

O'SHEA, H., YOUSAF, N., ALTMANN, D., FEHERVARI, Z., TONKS, P., HETHERINGTON, C., HARACH, S., BLAND, C., COOKE, A. & LUND, T. 2006. Effect of X- and Y-box deletions on the development of diabetes in H-2Ealpha-chain transgenic nonobese diabetic mice. *Scand J Immunol,* 63**,** 17-25.

OCHOA-REPÁRAZ, J., MIELCARZ, D. W., DITRIO, L. E., BURROUGHS, A. R., BEGUM-HAQUE, S., DASGUPTA, S., KASPER, D. L. & KASPER, L. H. 2010a. Central nervous system demyelinating disease protection by the human commensal Bacteroides fragilis depends on polysaccharide A expression. *J Immunol,* 185**,** 4101-8.

OCHOA-REPÁRAZ, J., MIELCARZ, D. W., WANG, Y., BEGUM-HAQUE, S., DASGUPTA, S., KASPER, D. L. & KASPER, L. H. 2010b. A polysaccharide from the human commensal Bacteroides fragilis protects against CNS demyelinating disease. *Mucosal Immunol,* 3**,** 487-95.

OETTINGER, M. A., SCHATZ, D. G., GORKA, C. & BALTIMORE, D. 1990. RAG-1 and RAG-2, adjacent genes that synergistically activate V(D)J recombination. *Science,* 248**,** 1517-23.

OH, S., AITKEN, M., SIMONS, D. M., BASEHOAR, A., GARCIA, V., KROPF, E. & CATON, A. J. 2012. Requirement for diverse TCR specificities determines regulatory T cell activity in a mouse model of autoimmune arthritis. *J Immunol,* 188**,** 4171-80.

OHASHI, P. S., OEHEN, S., BUERKI, K., PIRCHER, H., OHASHI, C. T., ODERMATT, B., MALISSEN, B., ZINKERNAGEL, R. M. & HENGARTNER, H. 1991. Ablation of "tolerance" and induction of diabetes by virus infection in viral antigen transgenic mice. *Cell,* 65**,** 305-17.

OHTO, U., FUKASE, K., MIYAKE, K. & SHIMIZU, T. 2012. Structural basis of species-specific endotoxin sensing by innate immune receptor TLR4/MD-2. *Proc Natl Acad Sci U S A,* 109**,** 7421-6.

OKAJIMA, M., WADA, T., NISHIDA, M., YOKOYAMA, T., NAKAYAMA, Y., HASHIDA, Y., SHIBATA, F., TONE, Y., ISHIZAKI, A., SHIMIZU, M., SAITO, T., OHTA, K., TOMA, T. & YACHIE, A. 2009. Analysis of T cell receptor Vbeta diversity in peripheral CD4 and CD8 T lymphocytes in patients with autoimmune thyroid diseases. *Clin Exp Immunol,* 155**,** 166-72.

OKUNO, Y., MURAKOSHI, A., NEGITA, M., AKANE, K., KOJIMA, S. & SUZUKI, H. 2013. CD8+ CD122+ regulatory T cells contain clonally expanded cells with identical CDR3 sequences of the T-cell receptor β-chain. *Immunology,* 139**,** 309-17.

OLDSTONE, M. B., NERENBERG, M., SOUTHERN, P., PRICE, J. & LEWICKI, H. 1991. Virus infection triggers insulin-dependent diabetes mellitus in a transgenic model: role of anti-self (virus) immune response. *Cell,* 65**,** 319-31.

OLIVE, C., GATENBY, P. A. & SERJEANTSON, S. W. 1991. Analysis of T cell receptor V alpha and V beta gene usage in synovia of patients with rheumatoid arthritis. *Immunol Cell Biol,* 69 (Pt 5)**,** 349-54.

OSMAN, G. E., TODA, M., KANAGAWA, O. & HOOD, L. E. 1993. Characterization of the T cell receptor repertoire causing collagen arthritis in mice. *J Exp Med,* 177**,** 387-95.

PALMER, J. P., ASPLIN, C. M., CLEMONS, P., LYEN, K., TATPATI, O., RAGHU, P. K. & PAQUETTE, T. L. 1983. Insulin antibodies in insulin-dependent diabetics before insulin treatment. *Science,* 222**,** 1337-9.

PALUMBO, M. O., LEVI, D., CHENTOUFI, A. A. & POLYCHRONAKOS, C. 2006. Isolation and characterization of proinsulin-producing medullary thymic epithelial cell clones. *Diabetes,* 55**,** 2595-601.

PANAGIOTOPOULOS, C., QIN, H., TAN, R. & VERCHERE, C. B. 2003. Identification of a beta-cell-specific HLA class I restricted epitope in type 1 diabetes. *Diabetes,* 52**,** 2647-51.

PANINA-BORDIGNON, P., LANG, R., VAN ENDERT, P. M., BENAZZI, E., FELIX, A. M., PASTORE, R. M., SPINAS, G. A. & SINIGAGLIA, F. 1995. Cytotoxic T cells specific for glutamic acid decarboxylase in autoimmune diabetes. *J Exp Med,* 181**,** 1923-7.

PANTALEO, G., OLIVE, D., POGGI, A., KOZUMBO, W. J., MORETTA, L. & MORETTA, A. 1987. Transmembrane signalling via the T11-dependent pathway of human T cell activation. Evidence for the involvement of 1,2-diacylglycerol and inositol phosphates. *Eur J Immunol,* 17**,** 55-60.

PARISH, N. M., ACHA-ORBEA, H., SIMPSON, E., QIN, S. X., LUND, T. & COOKE, A. 1993. A comparative study of T-cell receptor V beta usage in non-obese diabetic (NOD) and I-E transgenic NOD mice. *Immunology,* 78**,** 606-10.

PARK, Y., PARK, S., YOO, E., KIM, D. & SHIN, H. 2004. Association of the polymorphism for Toll-like receptor 2 with type 1 diabetes susceptibility. *Ann N Y Acad Sci,* 1037**,** 170-4.

PARONEN, J., MORIYAMA, H., ABIRU, N., SIKORA, K., MELANITOU, E., BABU, S., BAO, F., LIU, E., MIAO, D. & EISENBARTH, G. S. 2003. Establishing insulin 1 and insulin 2 knockout congenic strains on NOD genetic background. *Ann N Y Acad Sci,* 1005**,** 205-10.

PATRA, A. K., DREWES, T., ENGELMANN, S., CHUVPILO, S., KISHI, H., HÜNIG, T., SERFLING, E. & BOMMHARDT, U. H. 2006. PKB rescues calcineurin/NFAT-induced arrest of Rag expression and pre-T cell differentiation. *J Immunol,* 177**,** 4567-76.

PEARSE, G. 2006. Normal structure, function and histology of the thymus. *Toxicol Pathol,* 34**,** 504-14.

PENG, J., NARASIMHAN, S., MARCHESI, J. R., BENSON, A., WONG, F. S. & WEN, L. 2014. Long term effect of gut microbiota transfer on diabetes development. *J Autoimmun*.

PEOPLES, G. E., DAVEY, M. P., GOEDEGEBUURE, P. S., SCHOOF, D. D. & EBERLEIN, T. J. 1993. T cell receptor V beta 2 and V beta 6 mediate tumor-specific cytotoxicity by tumor-infiltrating lymphocytes in ovarian cancer. *J Immunol,* 151**,** 5472-80.

PETRICH DE MARQUESINI, L. G., MOUSTAKAS, A. K., THOMAS, I. J., WEN, L., PAPADOPOULOS, G. K. & WONG, F. S. 2008. Functional inhibition related to structure of a highly potent insulin-specific CD8 T cell clone using altered peptide ligands. *Eur J Immunol,* 38**,** 240-9.

PETRIE, H. T., LIVAK, F., SCHATZ, D. G., STRASSER, A., CRISPE, I. N. & SHORTMAN, K. 1993. Multiple rearrangements in T cell receptor alpha chain genes maximize the production of useful thymocytes. *J Exp Med,* 178**,** 615-22.

PETRIE, H. T., SCOLLAY, R. & SHORTMAN, K. 1992. Commitment to the T cell receptor-alpha beta or -gamma delta lineages can occur just prior to the onset of CD4 and CD8 expression among immature thymocytes. *Eur J Immunol,* 22**,** 2185-8.

PFISTER, G., WEISKOPF, D., LAZUARDI, L., KOVAIOU, R. D., CIOCA, D. P., KELLER, M., LORBEG, B., PARSON, W. & GRUBECK-LOEBENSTEIN, B. 2006. Naive T cells in the elderly: are they still there? *Ann N Y Acad Sci,* 1067**,** 152-7.

PHILPOTT, K. L., VINEY, J. L., KAY, G., RASTAN, S., GARDINER, E. M., CHAE, S., HAYDAY, A. C. & OWEN, M. J. 1992. Lymphoid development in mice congenitally lacking T cell receptor alpha beta-expressing cells. *Science,* 256**,** 1448-52.

POLYCHRONAKOS, C. & LI, Q. 2011. Understanding type 1 diabetes through genetics: advances and prospects. *Nat Rev Genet,* 12**,** 781-92.

PONTESILLI, O., CAROTENUTO, P., GAZDA, L. S., PRATT, P. F. & PROWSE, S. J. 1987. Circulating lymphocyte populations and autoantibodies in non-obese diabetic (NOD) mice: a longitudinal study. *Clin Exp Immunol,* 70**,** 84-93.

POZZILLI, P., SIGNORE, A., WILLIAMS, A. J. & BEALES, P. E. 1993. NOD mouse colonies around the world--recent facts and figures. *Immunol Today,* 14**,** 193-6.

PRICE, D. A., BRENCHLEY, J. M., RUFF, L. E., BETTS, M. R., HILL, B. J., ROEDERER, M., KOUP, R. A., MIGUELES, S. A., GOSTICK, E., WOOLDRIDGE, L., SEWELL, A. K., CONNORS, M. & DOUEK, D. C. 2005. Avidity for antigen shapes clonal dominance in CD8+ T cell populations specific for persistent DNA viruses. *J Exp Med,* 202**,** 1349-61.

PROCHNICKA-CHALUFOUR, A., CASANOVA, J. L., AVRAMEAS, S., CLAVERIE, J. M. & KOURILSKY, P. 1991. Biased amino acid distributions in regions of the T cell receptors and MHC molecules potentially involved in their association. *Int Immunol,* 3**,** 853-64.

PUGLIESE, A., ZELLER, M., FERNANDEZ, A., ZALCBERG, L. J., BARTLETT, R. J., RICORDI, C., PIETROPAOLO, M., EISENBARTH, G. S., BENNETT, S. T. & PATEL, D. D. 1997. The insulin gene is transcribed in the human thymus and transcription levels correlated with allelic variation at the INS VNTR-IDDM2 susceptibility locus for type 1 diabetes. *Nat Genet,* 15**,** 293-7.

PURBHOO, M. A., BOULTER, J. M., PRICE, D. A., VUIDEPOT, A. L., HOURIGAN, C. S., DUNBAR, P. R., OLSON, K., DAWSON, S. J., PHILLIPS, R. E., JAKOBSEN, B. K., BELL, J. I. & SEWELL, A. K. 2001. The human CD8 coreceptor effects cytotoxic T cell

activation and antigen sensitivity primarily by mediating complete phosphorylation of the T cell receptor zeta chain. *J Biol Chem,* 276**,** 32786-92.

QUINN, A., MCINERNEY, B., REICH, E. P., KIM, O., JENSEN, K. P. & SERCARZ, E. E. 2001a. Regulatory and effector CD4 T cells in nonobese diabetic mice recognize overlapping determinants on glutamic acid decarboxylase and use distinct V beta genes. *J Immunol,* 166**,** 2982-91.

QUINN, A., MCINERNEY, M. F. & SERCARZ, E. E. 2001b. MHC class I-restricted determinants on the glutamic acid decarboxylase 65 molecule induce spontaneous CTL activity. *J Immunol,* 167**,** 1748-57.

RADTKE, F., WILSON, A., STARK, G., BAUER, M., VAN MEERWIJK, J., MACDONALD, H. R. & AGUET, M. 1999. Deficient T cell fate specification in mice with an induced inactivation of Notch1. *Immunity,* 10**,** 547-58.

RAJASAGI, M., VITACOLONNA, M., BENJAK, B., MARHABA, R. & ZÖLLER, M. 2009. CD44 promotes progenitor homing into the thymus and T cell maturation. *J Leukoc Biol,* 85**,** 251-61.

RELLAND, L. M., WILLIAMS, J. B., RELLAND, G. N., HARIBHAI, D., ZIEGELBAUER, J., YASSAI, M., GORSKI, J. & WILLIAMS, C. B. 2012. The TCR repertoires of regulatory and conventional T cells specific for the same foreign antigen are distinct. *J Immunol,* 189**,** 3566-74.

RIFA'I, M., KAWAMOTO, Y., NAKASHIMA, I. & SUZUKI, H. 2004. Essential roles of CD8+CD122+ regulatory T cells in the maintenance of T cell homeostasis. *J Exp Med,* 200**,** 1123-34.

RINCÓN, M. & FLAVELL, R. A. 1994. AP-1 transcriptional activity requires both T-cell receptor-mediated and co-stimulatory signals in primary T lymphocytes. *EMBO J,* 13**,** 4370-81.

ROBERT, S., GYSEMANS, C., TAKIISHI, T., KORF, H., SPAGNUOLO, I., SEBASTIANI, G., VAN HUYNEGEM, K., STEIDLER, L., CALUWAERTS, S., DEMETTER, P., WASSERFALL, C. H., ATKINSON, M. A., DOTTA, F., ROTTIERS, P., VAN BELLE, T. L. & MATHIEU, C. 2014. Oral Delivery of Glutamic Acid Decarboxylase (GAD)-65 and IL10 by Lactococcus lactis Reverses Diabetes in Recent-Onset NOD Mice. *Diabetes,* 63**,** 2876-87.

ROBINS, H. S., CAMPREGHER, P. V., SRIVASTAVA, S. K., WACHER, A., TURTLE, C. J., KAHSAI, O., RIDDELL, S. R., WARREN, E. H. & CARLSON, C. S. 2009. Comprehensive assessment of T-cell receptor beta-chain diversity in alphabeta T cells. *Blood,* 114**,** 4099-107.

ROBLES, D. T., EISENBARTH, G. S., DAILEY, N. J., PETERSON, L. B. & WICKER, L. S. 2003. Insulin autoantibodies are associated with islet inflammation but not always related to diabetes progression in NOD congenic mice. *Diabetes,* 52**,** 882-6.

ROCK, E. P., SIBBALD, P. R., DAVIS, M. M. & CHIEN, Y. H. 1994. CDR3 length in antigen-specific immune receptors. *J Exp Med,* 179**,** 323-8.

ROESCH, L. F., LORCA, G. L., CASELLA, G., GIONGO, A., NARANJO, A., PIONZIO, A. M., LI, N., MAI, V., WASSERFALL, C. H., SCHATZ, D., ATKINSON, M. A., NEU, J. & TRIPLETT, E. W. 2009. Culture-independent identification of gut bacteria correlated with the onset of diabetes in a rat model. *ISME J,* 3**,** 536-48.

ROMAGNOLI, P. A., PREMENKO-LANIER, M. F., LORIA, G. D. & ALTMAN, J. D. 2013. CD8 T cell memory recall is enhanced by novel direct interactions with CD4 T cells enabled by MHC class II transferred from APCs. *PLoS One,* 8**,** e56999.

ROOSE, J. P., DIEHN, M., TOMLINSON, M. G., LIN, J., ALIZADEH, A. A., BOTSTEIN, D., BROWN, P. O. & WEISS, A. 2003. T cell receptor-independent basal signaling via Erk and Abl kinases suppresses RAG gene expression. *PLoS Biol,* 1**,** E53.

ROOT-BERNSTEIN, R. 2009. Autoreactive T-cell receptor (Vbeta/D/Jbeta) sequences in diabetes are homologous to insulin, glucagon, the insulin receptor, and the glucagon receptor. *J Mol Recognit,* 22**,** 177-87.

RUBTSOVA, K., SCOTT-BROWNE, J. P., CRAWFORD, F., DAI, S., MARRACK, P. & KAPPLER, J. W. 2009. Many different Vbeta CDR3s can reveal the inherent MHC reactivity of germline-encoded TCR V regions. *Proc Natl Acad Sci U S A,* 106**,** 7951-6.

RUDD, B. D., VENTURI, V., DAVENPORT, M. P. & NIKOLICH-ZUGICH, J. 2011. Evolution of the antigen-specific CD8+ TCR repertoire across the life span: evidence for clonal homogenization of the old TCR repertoire. *J Immunol,* 186**,** 2056-64.

RUDD, C. E., TREVILLYAN, J. M., DASGUPTA, J. D., WONG, L. L. & SCHLOSSMAN, S. F. 1988. The CD4 receptor is complexed in detergent lysates to a protein-tyrosine kinase (pp58) from human T lymphocytes. *Proc Natl Acad Sci U S A,* 85**,** 5190-4.

SAD, S., MARCOTTE, R. & MOSMANN, T. R. 1995. Cytokine-induced differentiation of precursor mouse CD8+ T cells into cytotoxic CD8+ T cells secreting Th1 or Th2 cytokines. *Immunity,* 2**,** 271-9.

SAINT-RUF, C., UNGEWISS, K., GROETTRUP, M., BRUNO, L., FEHLING, H. J. & VON BOEHMER, H. 1994. Analysis and expression of a cloned pre-T cell receptor gene. *Science,* 266**,** 1208-12.

SAINZ-PEREZ, A., LIM, A., LEMERCIER, B. & LECLERC, C. 2012. The T-cell receptor repertoire of tumor-infiltrating regulatory T lymphocytes is skewed toward public sequences. *Cancer Res,* 72**,** 3557-69.

SAITO, T., WEISS, A., GUNTER, K. C., SHEVACH, E. M. & GERMAIN, R. N. 1987. Cell surface T3 expression requires the presence of both alpha- and beta-chains of the T cell receptor. *J Immunol,* 139**,** 625-8.

SAKAGUCHI, S., SAKAGUCHI, N., ASANO, M., ITOH, M. & TODA, M. 1995. Immunologic self-tolerance maintained by activated T cells expressing IL-2 receptor alpha-chains (CD25). Breakdown of a single mechanism of self-tolerance causes various autoimmune diseases. *J Immunol,* 155**,** 1151-64.

SALLUSTO, F., LENIG, D., FÖRSTER, R., LIPP, M. & LANZAVECCHIA, A. 1999. Two subsets of memory T lymphocytes with distinct homing potentials and effector functions. *Nature,* 401**,** 708-12.

SAMBANDAM, A., MAILLARD, I., ZEDIAK, V. P., XU, L., GERSTEIN, R. M., ASTER, J. C., PEAR, W. S. & BHANDOOLA, A. 2005. Notch signaling controls the generation and differentiation of early T lineage progenitors. *Nat Immunol,* 6**,** 663-70.

SAMELSON, L. E., PHILLIPS, A. F., LUONG, E. T. & KLAUSNER, R. D. 1990. Association of the fyn protein-tyrosine kinase with the T-cell antigen receptor. *Proc Natl Acad Sci U S A,* 87**,** 4358-62.

SANCHO, J., CHATILA, T., WONG, R. C., HALL, C., BLUMBERG, R., ALARCON, B., GEHA, R. S. & TERHORST, C. 1989. T-cell antigen receptor (TCR)-alpha/beta heterodimer formation is a prerequisite for association of CD3-zeta 2 into functionally competent TCR.CD3 complexes. *J Biol Chem,* 264**,** 20760-9.

SATO, A. K., STURNIOLO, T., SINIGAGLIA, F. & STERN, L. J. 1999. Substitution of aspartic acid at beta57 with alanine alters MHC class II peptide binding activity but not protein stability: HLA-DQ (alpha1*0201, beta1*0302) and (alpha1*0201, beta1*0303). *Hum Immunol,* 60**,** 1227-36.

SAVINO, W., BOITARD, C., BACH, J. F. & DARDENNE, M. 1991. Studies on the thymus in nonobese diabetic mouse. I. Changes in the microenvironmental compartments. *Lab Invest,* 64**,** 405-17.

SAVINO, W., CARNAUD, C., LUAN, J. J., BACH, J. F. & DARDENNE, M. 1993. Characterization of the extracellular matrix-containing giant perivascular spaces in the NOD mouse thymus. *Diabetes,* 42**,** 134-40.

SCHATZ, D. G., OETTINGER, M. A. & BALTIMORE, D. 1989. The V(D)J recombination activating gene, RAG-1. *Cell,* 59**,** 1035-48.

SCHATZ, D. G., OETTINGER, M. A. & SCHLISSEL, M. S. 1992. V(D)J recombination: molecular biology and regulation. *Annu Rev Immunol,* 10**,** 359-83.

SCHLOOT, N. C., WILLEMEN, S., DUINKERKEN, G., DE VRIES, R. R. & ROEP, B. O. 1998. Cloned T cells from a recent onset IDDM patient reactive with insulin B-chain. *J Autoimmun,* 11**,** 169-75.

SCHMID, S., KOCZWARA, K., SCHWINGHAMMER, S., LAMPASONA, V., ZIEGLER, A. G. & BONIFACIO, E. 2004. Delayed exposure to wheat and barley proteins reduces diabetes incidence in non-obese diabetic mice. *Clin Immunol,* 111**,** 108-18.

SCHMIDT, D., VERDAGUER, J., AVERILL, N. & SANTAMARIA, P. 1997. A mechanism for the major histocompatibility complex-linked resistance to autoimmunity. *J Exp Med,* 186**,** 1059-75.

SCHMITT, T. M., CIOFANI, M., PETRIE, H. T. & ZÚÑIGA-PFLÜCKER, J. C. 2004. Maintenance of T cell specification and differentiation requires recurrent notch receptor-ligand interactions. *J Exp Med,* 200**,** 469-79.

SCHWARZ, B. A. & BHANDOOLA, A. 2004. Circulating hematopoietic progenitors with T lineage potential. *Nat Immunol,* 5**,** 953-60.

SCIMONE, M. L., AIFANTIS, I., APOSTOLOU, I., VON BOEHMER, H. & VON ANDRIAN, U. H. 2006. A multistep adhesion cascade for lymphoid progenitor cell homing to the thymus. *Proc Natl Acad Sci U S A,* 103**,** 7006-11.

SCOTT, C. A., PETERSON, P. A., TEYTON, L. & WILSON, I. A. 1998. Crystal structures of two I-Ad-peptide complexes reveal that high affinity can be achieved without large anchor residues. *Immunity,* 8**,** 319-29.

SEBZDA, E., WALLACE, V. A., MAYER, J., YEUNG, R. S., MAK, T. W. & OHASHI, P. S. 1994. Positive and negative thymocyte selection induced by different concentrations of a single peptide. *Science,* 263**,** 1615-8.

SEKIROV, I., RUSSELL, S. L., ANTUNES, L. C. & FINLAY, B. B. 2010. Gut microbiota in health and disease. *Physiol Rev,* 90**,** 859-904.

SEMANA, G., GAUSLING, R., JACKSON, R. A. & HAFLER, D. A. 1999. T cell autoreactivity to proinsulin epitopes in diabetic patients and healthy subjects. *J Autoimmun,* 12**,** 259-67.

SEN, R. & BALTIMORE, D. 1986. Inducibility of kappa immunoglobulin enhancer-binding protein Nf-kappa B by a posttranslational mechanism. *Cell,* 47**,** 921-8.

SERREZE, D. V., CHAPMAN, H. D., VARNUM, D. S., HANSON, M. S., REIFSNYDER, P. C., RICHARD, S. D., FLEMING, S. A., LEITER, E. H. & SHULTZ, L. D. 1996. B lymphocytes are essential for the initiation of T cell-mediated autoimmune diabetes: analysis of a new "speed congenic" stock of NOD.Ig mu null mice. *J Exp Med,* 184**,** 2049-53.

SERREZE, D. V., FLEMING, S. A., CHAPMAN, H. D., RICHARD, S. D., LEITER, E. H. & TISCH, R. M. 1998. B lymphocytes are critical antigen-presenting cells for the initiation of T cell-mediated autoimmune diabetes in nonobese diabetic mice. *J Immunol,* 161**,** 3912-8.

SERREZE, D. V., LEITER, E. H., CHRISTIANSON, G. J., GREINER, D. & ROOPENIAN, D. C. 1994. Major histocompatibility complex class I-deficient NOD-B2mnull mice are diabetes and insulitis resistant. *Diabetes,* 43**,** 505-9.

SHANG, L., FUKATA, M., THIRUNARAYANAN, N., MARTIN, A. P., ARNABOLDI, P., MAUSSANG, D., BERIN, C., UNKELESS, J. C., MAYER, L., ABREU, M. T. & LIRA, S. A. 2008. Toll-like receptor signaling in small intestinal epithelium promotes B-cell recruitment and IgA production in lamina propria. *Gastroenterology,* 135**,** 529-38.

SHAW, J. P., UTZ, P. J., DURAND, D. B., TOOLE, J. J., EMMEL, E. A. & CRABTREE, G. R. 1988. Identification of a putative regulator of early T cell activation genes. *Science,* 241**,** 202-5.

SHERWOOD, A. M., EMERSON, R. O., SCHERER, D., HABERMANN, N., BUCK, K., STAFFA, J., DESMARAIS, C., HALAMA, N., JAEGER, D., SCHIRMACHER, P., HERPEL, E., KLOOR, M., ULRICH, A., SCHNEIDER, M., ULRICH, C. M. & ROBINS, H. 2013. Tumor-infiltrating lymphocytes in colorectal tumors display a diversity of T cell receptor sequences that differ from the T cells in adjacent mucosal tissue. *Cancer Immunol Immunother,* 62**,** 1453-61.

SHIBUYA, H. & TANIGUCHI, T. 1989. Identification of multiple cis-elements and trans-acting factors involved in the induced expression of human IL-2 gene. *Nucleic Acids Res,* 17**,** 9173-84.

SHIMAZU, R., AKASHI, S., OGATA, H., NAGAI, Y., FUKUDOME, K., MIYAKE, K. & KIMOTO, M. 1999. MD-2, a molecule that confers lipopolysaccharide responsiveness on Toll-like receptor 4. *J Exp Med,* 189**,** 1777-82.

SHINKAI, Y., RATHBUN, G., LAM, K. P., OLTZ, E. M., STEWART, V., MENDELSOHN, M., CHARRON, J., DATTA, M., YOUNG, F. & STALL, A. M. 1992. RAG-2-deficient mice lack mature lymphocytes owing to inability to initiate V(D)J rearrangement. *Cell,* 68**,** 855-67.

SHIZURU, J. A., TAYLOR-EDWARDS, C., LIVINGSTONE, A. & FATHMAN, C. G. 1991. Genetic dissection of T cell receptor V beta gene requirements for spontaneous murine diabetes. *J Exp Med,* 174**,** 633-8.

SIMONE, E., DANIEL, D., SCHLOOT, N., GOTTLIEB, P., BABU, S., KAWASAKI, E., WEGMANN, D. & EISENBARTH, G. S. 1997. T cell receptor restriction of diabetogenic autoimmune NOD T cells. *Proc Natl Acad Sci U S A,* 94**,** 2518-21.

SIOUD, M., KJELDSEN-KRAGH, J., SULEYMAN, S., VINJE, O., NATVIG, J. B. & FØRRE, O. 1992. Limited heterogeneity of T cell receptor variable region gene usage in juvenile rheumatoid arthritis synovial T cells. *Eur J Immunol,* 22**,** 2413-8.

SMITH, C., GRAS, S., BRENNAN, R. M., BIRD, N. L., VALKENBURG, S. A., TWIST, K. A., BURROWS, J. M., MILES, J. J., CHAMBERS, D., BELL, S., CAMPBELL, S., KEDZIERSKA, K., BURROWS, S. R., ROSSJOHN, J. & KHANNA, R. 2014. Molecular imprint of exposure to naturally occurring genetic variants of human cytomegalovirus on the T cell repertoire. *Sci Rep,* 4**,** 3993.

SOFI, M. H., GUDI, R., KARUMUTHIL-MELETHIL, S., PEREZ, N., JOHNSON, B. M. & VASU, C. 2014. pH of drinking water influences the composition of gut microbiome and type 1 diabetes incidence. *Diabetes,* 63**,** 632-44.

SOUABNI, A., COBALEDA, C., SCHEBESTA, M. & BUSSLINGER, M. 2002. Pax5 promotes B lymphopoiesis and blocks T cell development by repressing Notch1. *Immunity,* 17**,** 781-93.

STADINSKI, B. D., DELONG, T., REISDORPH, N., REISDORPH, R., POWELL, R. L., ARMSTRONG, M., PIGANELLI, J. D., BARBOUR, G., BRADLEY, B., CRAWFORD, F., MARRACK, P., MAHATA, S. K., KAPPLER, J. W. & HASKINS, K. 2010a. Chromogranin A is an autoantigen in type 1 diabetes. *Nat Immunol,* 11**,** 225-31.

STADINSKI, B. D., ZHANG, L., CRAWFORD, F., MARRACK, P., EISENBARTH, G. S. & KAPPLER, J. W. 2010b. Diabetogenic T cells recognize insulin bound to IA(g7) in an unexpected, weakly binding register. *Proceedings of the National Academy of Sciences of the United States of America,* 107**,** 10978-10983.

STANDIFER, N. E., OUYANG, Q., PANAGIOTOPOULOS, C., VERCHERE, C. B., TAN, R., GREENBAUM, C. J., PIHOKER, C. & NEPOM, G. T. 2006. Identification of Novel HLA-A*0201-restricted epitopes in recent-onset type 1 diabetic subjects and antibody-positive relatives. *Diabetes,* 55**,** 3061-7.

STAUNTON, D. E., DUSTIN, M. L. & SPRINGER, T. A. 1989. Functional cloning of ICAM-2, a cell adhesion ligand for LFA-1 homologous to ICAM-1. *Nature,* 339**,** 61-4.

STIER, S., CHENG, T., DOMBKOWSKI, D., CARLESSO, N. & SCADDEN, D. T. 2002. Notch1 activation increases hematopoietic stem cell self-renewal in vivo and favors lymphoid over myeloid lineage outcome. *Blood,* 99**,** 2369-78.

STRAUS, D. B. & WEISS, A. 1993. The CD3 chains of the T cell antigen receptor associate with the ZAP-70 tyrosine kinase and are tyrosine phosphorylated after receptor stimulation. *J Exp Med,* 178**,** 1523-30.

STUMPF, M., ZHOU, X. & BLUESTONE, J. A. 2013. The B7-independent isoform of CTLA-4 functions to regulate autoimmune diabetes. *J Immunol,* 190**,** 961-9.

SUN, X., FUJIWARA, M., SHI, Y., KUSE, N., GATANAGA, H., APPAY, V., GAO, G. F., OKA, S. & TAKIGUCHI, M. 2014. Superimposed Epitopes Restricted by the Same HLA Molecule Drive Distinct HIV-Specific CD8+ T Cell Repertoires. *J Immunol,* 193**,** 77-84.

SURH, C. D. & SPRENT, J. 1994. T-cell apoptosis detected in situ during positive and negative selection in the thymus. *Nature,* 372**,** 100-3.

SUSSMAN, J. J., BONIFACINO, J. S., LIPPINCOTT-SCHWARTZ, J., WEISSMAN, A. M., SAITO, T., KLAUSNER, R. D. & ASHWELL, J. D. 1988. Failure to synthesize the T cell CD3-zeta chain: structure and function of a partial T cell receptor complex. *Cell,* 52**,** 85-95.

TAI, N., WONG, F. S. & WEN, L. 2013. TLR9 deficiency promotes CD73 expression in T cells and diabetes protection in nonobese diabetic mice. *J Immunol,* 191**,** 2926-37.

TAKAHASHI, M., ISHIMARU, N., YANAGI, K., HANEJI, N., SAITO, I. & HAYASHI, Y. 1997. High incidence of autoimmune dacryoadenitis in male non-obese diabetic (NOD) mice depending on sex steroid. *Clin Exp Immunol,* 109**,** 555-61.

TAKI, T., NAGATA, M., OGAWA, W., HATAMORI, N., HAYAKAWA, M., HARI, J., SHII, K., BABA, S. & YOKONO, K. 1991. Prevention of cyclophosphamide-induced and spontaneous diabetes in NOD/Shi/Kbe mice by anti-MHC class I Kd monoclonal antibody. *Diabetes,* 40**,** 1203-9.

TAKIISHI, T., KORF, H., VAN BELLE, T. L., ROBERT, S., GRIECO, F. A., CALUWAERTS, S., GALLERI, L., SPAGNUOLO, I., STEIDLER, L., VAN HUYNEGEM, K., DEMETTER, P., WASSERFALL, C., ATKINSON, M. A., DOTTA, F., ROTTIERS, P., GYSEMANS, C. & MATHIEU, C. 2012. Reversal of autoimmune diabetes by restoration of antigen-specific tolerance using genetically modified Lactococcus lactis in mice. *J Clin Invest,* 122**,** 1717-25.

TANG, Q., HENRIKSEN, K. J., BI, M., FINGER, E. B., SZOT, G., YE, J., MASTELLER, E. L., MCDEVITT, H., BONYHADI, M. & BLUESTONE, J. A. 2004. In vitro-expanded antigen-specific regulatory T cells suppress autoimmune diabetes. *J Exp Med,* 199**,** 1455-65.

TARBELL, K. V., LEE, M., RANHEIM, E., CHAO, C. C., SANNA, M., KIM, S. K., DICKIE, P., TEYTON, L., DAVIS, M. & MCDEVITT, H. 2002. CD4(+) T cells from glutamic acid decarboxylase (GAD)65-specific T cell receptor transgenic mice are not diabetogenic and can delay diabetes transfer. *J Exp Med,* 196**,** 481-92.

TESTI, R., PHILLIPS, J. H. & LANIER, L. L. 1989. T cell activation via Leu-23 (CD69). *J Immunol,* 143**,** 1123-8.

THÉBAULT-BAUMONT, K., DUBOIS-LAFORGUE, D., KRIEF, P., BRIAND, J. P., HALBOUT, P., VALLON-GEOFFROY, K., MORIN, J., LALOUX, V., LEHUEN, A., CAREL, J. C., JAMI, J., MULLER, S. & BOITARD, C. 2003. Acceleration of type 1 diabetes mellitus in proinsulin 2-deficient NOD mice. *J Clin Invest,* 111**,** 851-7.

TIMSIT, J., DEBRAY-SACHS, M., BOITARD, C. & BACH, J. F. 1988. Cell-mediated immunity to pancreatic islet cells in the non-obese diabetic (NOD) mouse: in vitro characterization and time course study. *Clin Exp Immunol,* 73**,** 260-4.

TORMO-BADIA, N., HÅKANSSON, A., VASUDEVAN, K., MOLIN, G., AHRNÉ, S. & CILIO, C. M. 2014. Antibiotic treatment of pregnant non-obese diabetic (NOD) mice leads to altered gut microbiota and intestinal immunological changes in the offspring. *Scand J Immunol*.

TRAPANI, J. A. & SMYTH, M. J. 2002. Functional significance of the perforin/granzyme cell death pathway. *Nat Rev Immunol,* 2**,** 735-47.

TROP, S., CHARRON, J., ARGUIN, C., LESAGE, S. & HUGO, P. 2000. Thymic selection generates T cells expressing self-reactive TCRs in the absence of CD45. *J Immunol,* 165**,** 3073-9.

TRUNEH, A., ALBERT, F., GOLSTEIN, P. & SCHMITT-VERHULST, A. M. 1985. Early steps of lymphocyte activation bypassed by synergy between calcium ionophores and phorbol ester. *Nature,* 313**,** 318-20.

TSAI, S., SERRA, P., CLEMENTE-CASARES, X., SLATTERY, R. M. & SANTAMARIA, P. 2013a. Dendritic Cell-Dependent In Vivo Generation of Autoregulatory T Cells by Antidiabetogenic MHC Class II. *J Immunol,* 191**,** 70-82.

TSAI, S., SERRA, P., CLEMENTE-CASARES, X., YAMANOUCHI, J., THIESSEN, S., SLATTERY, R. M., ELLIOTT, J. F. & SANTAMARIA, P. 2013b. Antidiabetogenic MHC class II promotes the differentiation of MHC-promiscuous autoreactive T cells into FOXP3+ regulatory T cells. *Proc Natl Acad Sci U S A,* 110**,** 3471-6.

TSUDA, K., TODA, M., KIM, G., SAITOH, K., YOSHIMURA, S., YOSHIDA, T., TAKI, W., WAGA, S. & KURIBAYASHI, K. 2000. Survival-promoting activity of IL-7 on IL-2-dependent cytotoxic T lymphocyte clones: resultant induction of G1 arrest. *J Immunol Methods,* 236**,** 37-51.

TUSSIWAND, R., ENGDAHL, C., GEHRE, N., BOSCO, N., CEREDIG, R. & ROLINK, A. G. 2011. The preTCR-dependent DN3 to DP transition requires Notch signaling, is improved by CXCL12 signaling and is inhibited by IL-7 signaling. *Eur J Immunol,* 41**,** 3371-80.

UBEDA, C., LIPUMA, L., GOBOURNE, A., VIALE, A., LEINER, I., EQUINDA, M., KHANIN, R. & PAMER, E. G. 2012. Familial transmission rather than defective innate immunity shapes the distinct intestinal microbiota of TLR-deficient mice. *J Exp Med,* 209**,** 1445-56.

URBAN, J. L., KUMAR, V., KONO, D. H., GOMEZ, C., HORVATH, S. J., CLAYTON, J., ANDO, D. G., SERCARZ, E. E. & HOOD, L. 1988. Restricted use of T cell receptor V genes in murine autoimmune encephalomyelitis raises possibilities for antibody therapy. *Cell,* 54**,** 577-92.

VAARALA, O., ATKINSON, M. A. & NEU, J. 2008. The "perfect storm" for type 1 diabetes: the complex interplay between intestinal microbiota, gut permeability, and mucosal immunity. *Diabetes,* 57**,** 2555-62.

VAFIADIS, P., BENNETT, S. T., TODD, J. A., NADEAU, J., GRABS, R., GOODYER, C. G., WICKRAMASINGHE, S., COLLE, E. & POLYCHRONAKOS, C. 1997. Insulin expression in human thymus is modulated by INS VNTR alleles at the IDDM2 locus. *Nat Genet,* 15**,** 289-92.

VALLOIS, D., GRIMM, C. H., AVNER, P., BOITARD, C. & ROGNER, U. C. 2007. The type 1 diabetes locus Idd6 controls TLR1 expression. *J Immunol,* 179**,** 3896-903.

VAN GENT, D. C., RAMSDEN, D. A. & GELLERT, M. 1996. The RAG1 and RAG2 proteins establish the 12/23 rule in V(D)J recombination. *Cell,* 85**,** 107-13.

VAN OERS, N. S., KILLEEN, N. & WEISS, A. 1996. Lck regulates the tyrosine phosphorylation of the T cell receptor subunits and ZAP-70 in murine thymocytes. *J Exp Med,* 183**,** 1053-62.

VEILLETTE, A., BOOKMAN, M. A., HORAK, E. M. & BOLEN, J. B. 1988. The CD4 and CD8 T cell surface antigens are associated with the internal membrane tyrosine-protein kinase p56lck. *Cell,* 55**,** 301-8.

VELLOSO, L. A., EIZIRIK, D. L., KARLSSON, F. A. & KÄMPE, O. 1994. Absence of autoantibodies against glutamate decarboxylase (GAD) in the non-obese diabetic (NOD) mouse and low expression of the enzyme in mouse islets. *Clin Exp Immunol,* 96**,** 129-37.

VELTHUIS, J. H., UNGER, W. W., ABREU, J. R., DUINKERKEN, G., FRANKEN, K., PEAKMAN, M., BAKKER, A. H., REKER-HADRUP, S., KEYMEULEN, B., DRIJFHOUT, J. W., SCHUMACHER, T. N. & ROEP, B. O. 2010. Simultaneous detection of circulating autoreactive CD8+ T-cells specific for different islet cell-associated epitopes using combinatorial MHC multimers. *Diabetes,* 59**,** 1721-30.

VERDAGUER, J., SCHMIDT, D., AMRANI, A., ANDERSON, B., AVERILL, N. & SANTAMARIA, P. 1997. Spontaneous autoimmune diabetes in monoclonal T cell nonobese diabetic mice. *J Exp Med,* 186**,** 1663-76.

VERDAGUER, J., YOON, J. W., ANDERSON, B., AVERILL, N., UTSUGI, T., PARK, B. J. & SANTAMARIA, P. 1996. Acceleration of spontaneous diabetes in TCR-beta-transgenic nonobese diabetic mice by beta-cell cytotoxic CD8+ T cells expressing identical endogenous TCR-alpha chains. *J Immunol,* 157**,** 4726-35.

VIDEBAEK, N., HARACH, S., PHILLIPS, J., HUTCHINGS, P., OZEGBE, P., MICHELSEN, B. K. & COOKE, A. 2003. An islet-homing NOD CD8+ cytotoxic T cell clone recognizes GAD65 and causes insulitis. *J Autoimmun,* 20**,** 97-109.

VIJAY-KUMAR, M., AITKEN, J. D., CARVALHO, F. A., CULLENDER, T. C., MWANGI, S., SRINIVASAN, S., SITARAMAN, S. V., KNIGHT, R., LEY, R. E. & GEWIRTZ, A. T. 2010. Metabolic syndrome and altered gut microbiota in mice lacking Toll-like receptor 5. *Science,* 328**,** 228-31.

VIJAYAKRISHNAN, L., SLAVIK, J. M., ILLÉS, Z., GREENWALD, R. J., RAINBOW, D., GREVE, B., PETERSON, L. B., HAFLER, D. A., FREEMAN, G. J., SHARPE, A. H., WICKER, L. S. & KUCHROO, V. K. 2004. An autoimmune disease-associated CTLA-4 splice variant lacking the B7 binding domain signals negatively in T cells. *Immunity,* 20**,** 563-75.

VIRET, C., LAMARE, C., GUIRAUD, M., FAZILLEAU, N., BOUR, A., MALISSEN, B., CARRIER, A. & GUERDER, S. 2011a. Thymus-specific serine protease contributes to the diversification of the functional endogenous CD4 T cell receptor repertoire. *J Exp Med,* 208**,** 3-11.

VIRET, C., LEUNG-THEUNG-LONG, S., SERRE, L., LAMARE, C., VIGNALI, D. A., MALISSEN, B., CARRIER, A. & GUERDER, S. 2011b. Thymus-specific serine protease controls autoreactive CD4 T cell development and autoimmune diabetes in mice. *J Clin Invest,* 121**,** 1810-21.

VON HERRATH, M. G., DOCKTER, J. & OLDSTONE, M. B. 1994. How virus induces a rapid or slow onset insulin-dependent diabetes mellitus in a transgenic model. *Immunity,* 1**,** 231-42.

VONG, A. M., DANESHJOU, N., NORORI, P. Y., SHENG, H., BRACIAK, T. A., SERCARZ, E. E. & GABAGLIA, C. R. 2011. Spectratyping analysis of the islet-reactive T cell repertoire in diabetic NOD Igμ(null) mice after polyclonal B cell reconstitution. *J Transl Med,* 9**,** 101.

WALUNAS, T. L., LENSCHOW, D. J., BAKKER, C. Y., LINSLEY, P. S., FREEMAN, G. J., GREEN, J. M., THOMPSON, C. B. & BLUESTONE, J. A. 1994. CTLA-4 can function as a negative regulator of T cell activation. *Immunity,* 1**,** 405-13.

WANG, B., GONZALEZ, A., BENOIST, C. & MATHIS, D. 1996. The role of CD8+ T cells in the initiation of insulin-dependent diabetes mellitus. *Eur J Immunol,* 26**,** 1762-9.

WANG, D., ZHENG, M., LEI, L., JI, J., YAO, Y., QIU, Y., MA, L., LOU, J., OUYANG, C., ZHANG, X., HE, Y., CHI, J., WANG, L., KUANG, Y., WANG, J., CAO, X. & LU, L. 2012a. Tespa1 is involved in late thymocyte development through the regulation of TCR-mediated signaling. *Nat Immunol,* 13**,** 560-8.

WANG, F., HUANG, C. Y. & KANAGAWA, O. 1998. Rapid deletion of rearranged T cell antigen receptor (TCR) Valpha-Jalpha segment by secondary rearrangement in the thymus: role of continuous rearrangement of TCR alpha chain gene and positive selection in the T cell repertoire formation. *Proc Natl Acad Sci U S A,* 95**,** 11834-9.

WANG, J., TSAI, S., HAN, B., TAILOR, P. & SANTAMARIA, P. 2012b. Autoantigen recognition is required for recruitment of IGRP(206-214)-autoreactive CD8+ T cells but is dispensable for tolerance. *J Immunol,* 189**,** 2975-84.

WEGMANN, D. R., GILL, R. G., NORBURY-GLASER, M., SCHLOOT, N. & DANIEL, D. 1994. Analysis of the spontaneous T cell response to insulin in NOD mice. *J Autoimmun,* 7**,** 833-43.

WEIDMANN, E., WHITESIDE, T. L., GIORDA, R., HERBERMAN, R. B. & TRUCCO, M. 1992. The T-cell receptor V beta gene usage in tumor-infiltrating lymphocytes and blood of patients with hepatocellular carcinoma. *Cancer Res,* 52**,** 5913-20.

WEINSTEIN, J. A., JIANG, N., WHITE, R. A., FISHER, D. S. & QUAKE, S. R. 2009. High-throughput sequencing of the zebrafish antibody repertoire. *Science,* 324**,** 807-10.

WEN, L., LEY, R. E., VOLCHKOV, P. Y., STRANGES, P. B., AVANESYAN, L., STONEBRAKER, A. C., HU, C., WONG, F. S., SZOT, G. L., BLUESTONE, J. A., GORDON, J. I. & CHERVONSKY, A. V. 2008. Innate immunity and intestinal microbiota in the development of Type 1 diabetes. *Nature,* 455**,** 1109-13.

WENZLAU, J. M., MOUA, O., LIU, Y., EISENBARTH, G. S., HUTTON, J. C. & DAVIDSON, H. W. 2008a. Identification of a major humoral epitope in Slc30A8 (ZnT8). *Ann N Y Acad Sci,* 1150**,** 252-5.

WENZLAU, J. M., MOUA, O., SARKAR, S. A., YU, L., REWERS, M., EISENBARTH, G. S., DAVIDSON, H. W. & HUTTON, J. C. 2008b. SlC30A8 is a major target of humoral autoimmunity in type 1 diabetes and a predictive marker in prediabetes. *Ann N Y Acad Sci,* 1150**,** 256-9.

WETTSTEIN, P., STRAUSBAUCH, M., THERNEAU, T. & BORSON, N. 2008. The application of real-time PCR to the analysis of T cell repertoires. *Nucleic Acids Res,* 36**,** e140.

WICKER, L. S., LEITER, E. H., TODD, J. A., RENJILIAN, R. J., PETERSON, E., FISCHER, P. A., PODOLIN, P. L., ZIJLSTRA, M., JAENISCH, R. & PETERSON, L. B. 1994a. Beta 2-microglobulin-deficient NOD mice do not develop insulitis or diabetes. *Diabetes,* 43**,** 500-4.

WICKER, L. S., TODD, J. A., PRINS, J. B., PODOLIN, P. L., RENJILIAN, R. J. & PETERSON, L. B. 1994b. Resistance alleles at two non-major histocompatibility complex-linked insulin-dependent diabetes loci on chromosome 3, Idd3 and Idd10, protect nonobese diabetic mice from diabetes. *J Exp Med,* 180**,** 1705-13.

WILLCOX, A., RICHARDSON, S. J., BONE, A. J., FOULIS, A. K. & MORGAN, N. G. 2009. Analysis of islet inflammation in human type 1 diabetes. *Clin Exp Immunol,* 155**,** 173-81.

WILSON, A., HELD, W. & MACDONALD, H. R. 1994. Two waves of recombinase gene expression in developing thymocytes. *J Exp Med,* 179**,** 1355-60.

WONG, F. S., HU, C., ZHANG, L., DU, W., ALEXOPOULOU, L., FLAVELL, R. A. & WEN, L. 2008. The role of Toll-like receptors 3 and 9 in the development of autoimmune diabetes in NOD mice. *Ann N Y Acad Sci,* 1150**,** 146-8.

WONG, F. S., KARTTUNEN, J., DUMONT, C., WEN, L., VISINTIN, I., PILIP, I. M., SHASTRI, N., PAMER, E. G. & JANEWAY, C. A. 1999. Identification of an MHC class I-restricted autoantigen in type 1 diabetes by screening an organ-specific cDNA library. *Nat Med,* 5**,** 1026-31.

WONG, F. S., MOUSTAKAS, A. K., WEN, L., PAPADOPOULOS, G. K. & JANEWAY, C. A. 2002. Analysis of structure and function relationships of an autoantigenic peptide of insulin bound to H-2K(d) that stimulates CD8 T cells in insulin-dependent diabetes mellitus. *Proc Natl Acad Sci U S A,* 99**,** 5551-6.

WONG, F. S., SIEW, L. K., SCOTT, G., THOMAS, I. J., CHAPMAN, S., VIRET, C. & WEN, L. 2009. Activation of insulin-reactive CD8 T-cells for development of autoimmune diabetes. *Diabetes,* 58**,** 1156-64.

WONG, F. S., VISINTIN, I., WEN, L., FLAVELL, R. A. & JANEWAY, C. A. 1996. CD8 T cell clones from young nonobese diabetic (NOD) islets can transfer rapid onset of diabetes in NOD mice in the absence of CD4 cells. *J Exp Med,* 183**,** 67-76.

WONG, F. S., VISINTIN, I., WEN, L., GRANATA, J., FLAVELL, R. & JANEWAY, C. A. 1998. The role of lymphocyte subsets in accelerated diabetes in nonobese diabetic-rat insulin promoter-B7-1 (NOD-RIP-B7-1) mice. *J Exp Med,* 187**,** 1985-93.

WONG, J., MATHIS, D. & BENOIST, C. 2007a. TCR-based lineage tracing: no evidence for conversion of conventional into regulatory T cells in response to a natural self-antigen in pancreatic islets. *J Exp Med,* 204**,** 2039-45.

WONG, J., OBST, R., CORREIA-NEVES, M., LOSYEV, G., MATHIS, D. & BENOIST, C. 2007b. Adaptation of TCR repertoires to self-peptides in regulatory and nonregulatory CD4+ T cells. *J Immunol,* 178**,** 7032-41.

WOOLDRIDGE, L., CLEMENT, M., LISSINA, A., EDWARDS, E. S., LADELL, K., EKERUCHE, J., HEWITT, R. E., LAUGEL, B., GOSTICK, E., COLE, D. K., DEBETS, R., BERREVOETS, C., MILES, J. J., BURROWS, S. R., PRICE, D. A. & SEWELL, A. K. 2010a. MHC class I molecules with Superenhanced CD8 binding properties bypass the requirement for cognate TCR recognition and nonspecifically activate CTLs. *J Immunol,* 184**,** 3357-66.

WOOLDRIDGE, L., EKERUCHE-MAKINDE, J., VAN DEN BERG, H. A., SKOWERA, A., MILES, J. J., TAN, M. P., DOLTON, G., CLEMENT, M., LLEWELLYN-LACEY, S., PRICE, D. A., PEAKMAN, M. & SEWELL, A. K. 2012. A single autoimmune T cell receptor recognizes more than a million different peptides. *J Biol Chem,* 287**,** 1168-77.

WOOLDRIDGE, L., LAUGEL, B., EKERUCHE, J., CLEMENT, M., VAN DEN BERG, H. A., PRICE, D. A. & SEWELL, A. K. 2010b. CD8 controls T cell cross-reactivity. *J Immunol,* 185**,** 4625-32.

WOOTEN, R. M., MA, Y., YODER, R. A., BROWN, J. P., WEIS, J. H., ZACHARY, J. F., KIRSCHNING, C. J. & WEIS, J. J. 2002. Toll-like receptor 2 is required for innate, but not acquired, host defense to Borrelia burgdorferi. *J Immunol,* 168**,** 348-55.

YABLONSKI, D., KADLECEK, T. & WEISS, A. 2001. Identification of a phospholipase C-gamma1 (PLC-gamma1) SH3 domain-binding site in SLP-76 required for T-cell receptor-mediated activation of PLC-gamma1 and NFAT. *Mol Cell Biol,* 21**,** 4208-18.

YACHI, P. P., AMPUDIA, J., ZAL, T. & GASCOIGNE, N. R. 2006. Altered peptide ligands induce delayed CD8-T cell receptor interaction--a role for CD8 in distinguishing antigen quality. *Immunity,* 25**,** 203-11.

YAGER, E. J., AHMED, M., LANZER, K., RANDALL, T. D., WOODLAND, D. L. & BLACKMAN, M. A. 2008. Age-associated decline in T cell repertoire diversity leads to holes in the repertoire and impaired immunity to influenza virus. *J Exp Med,* 205**,** 711-23.

YAGI, H., MATSUMOTO, M., KUNIMOTO, K., KAWAGUCHI, J., MAKINO, S. & HARADA, M. 1992. Analysis of the roles of CD4+ and CD8+ T cells in autoimmune diabetes of NOD mice using transfer to NOD athymic nude mice. *Eur J Immunol,* 22**,** 2387-93.

YANG, J., DANKE, N. A., BERGER, D., REICHSTETTER, S., REIJONEN, H., GREENBAUM, C., PIHOKER, C., JAMES, E. A. & KWOK, W. W. 2006. Islet-specific glucose-6-phosphatase catalytic subunit-related protein-reactive CD4+ T cells in human subjects. *J Immunol,* 176**,** 2781-9.

YANG, M., CHARLTON, B. & GAUTAM, A. M. 1997. Development of insulitis and diabetes in B cell-deficient NOD mice. *J Autoimmun,* 10**,** 257-60.

YASSAI, M. B., NAUMOV, Y. N., NAUMOVA, E. N. & GORSKI, J. 2009. A clonotype nomenclature for T cell receptors. *Immunogenetics,* 61**,** 493-502.

YASUDA, Y., KANEKO, A., NISHIJIMA, I., MIYATAKE, S. & ARAI, K. 2002. Interleukin-7 inhibits pre-T-cell differentiation induced by the pre-T-cell receptor signal and the effect is mimicked by hGM-CSF in hGM-CSF receptor transgenic mice. *Immunology,* 106**,** 212-21.

YASUTOMO, K., DOYLE, C., MIELE, L., FUCHS, C. & GERMAIN, R. N. 2000. The duration of antigen receptor signalling determines CD4+ versus CD8+ T-cell lineage fate. *Nature,* 404**,** 506-10.

YIN, Y., LI, Y., KERZIC, M. C., MARTIN, R. & MARIUZZA, R. A. 2011. Structure of a TCR with high affinity for self-antigen reveals basis for escape from negative selection. *EMBO J,* 30**,** 1137-48.

YIP, L., SU, L., SHENG, D., CHANG, P., ATKINSON, M., CZESAK, M., ALBERT, P. R., COLLIER, A. R., TURLEY, S. J., FATHMAN, C. G. & CREUSOT, R. J. 2009. Deaf1 isoforms control the expression of genes encoding peripheral tissue antigens in the pancreatic lymph nodes during type 1 diabetes. *Nat Immunol,* 10**,** 1026-33.

YONEDA, R., YOKONO, K., NAGATA, M., TOMINAGA, Y., MORIYAMA, H., TSUKAMOTO, K., MIKI, M., OKAMOTO, N., YASUDA, H., AMANO, K. & KASUGA, M. 1997. CD8 cytotoxic T-cell clone rapidly transfers autoimmune diabetes in very young NOD and MHC class I-compatible scid mice. *Diabetologia,* 40**,** 1044-52.

YURKOVETSKIY, L., BURROWS, M., KHAN, A. A., GRAHAM, L., VOLCHKOV, P., BECKER, L., ANTONOPOULOS, D., UMESAKI, Y. & CHERVONSKY, A. V. 2013. Gender bias in autoimmunity is influenced by microbiota. *Immunity,* 39**,** 400-12.

ZACCONE, P., BURTON, O., MILLER, N., JONES, F. M., DUNNE, D. W. & COOKE, A. 2009. Schistosoma mansoni egg antigens induce Treg that participate in diabetes prevention in NOD mice. *Eur J Immunol,* 39**,** 1098-107.

ZACCONE, P., BURTON, O. T., GIBBS, S. E., MILLER, N., JONES, F. M., SCHRAMM, G., HAAS, H., DOENHOFF, M. J., DUNNE, D. W. & COOKE, A. 2011. The S. mansoni glycoprotein ω-1 induces Foxp3 expression in NOD mouse $CD4^+$ T cells. *Eur J Immunol,* 41**,** 2709-18.

ZACCONE, P., RAINE, T., SIDOBRE, S., KRONENBERG, M., MASTROENI, P. & COOKE, A. 2004. Salmonella typhimurium infection halts development of type 1 diabetes in NOD mice. *Eur J Immunol,* 34**,** 3246-56.

ZALLER, D. M., OSMAN, G., KANAGAWA, O. & HOOD, L. 1990. Prevention and treatment of murine experimental allergic encephalomyelitis with T cell receptor V beta-specific antibodies. *J Exp Med,* 171**,** 1943-55.

ZANKER, D., WAITHMAN, J., YEWDELL, J. W. & CHEN, W. 2013. Mixed Proteasomes Function To Increase Viral Peptide Diversity and Broaden Antiviral CD8+ T Cell Responses. *J Immunol,* 191**,** 52-9.

ZEHN, D. & BEVAN, M. J. 2006. T cells with low avidity for a tissue-restricted antigen routinely evade central and peripheral tolerance and cause autoimmunity. *Immunity,* 25**,** 261-70.

ZEHN, D., LEE, S. Y. & BEVAN, M. J. 2009. Complete but curtailed T-cell response to very low-affinity antigen. *Nature,* 458**,** 211-4.

ZEKZER, D., WONG, F. S., WEN, L., ALTIERI, M., GURLO, T., VON GRAFENSTEIN, H. & SHERWIN, R. S. 1997. Inhibition of diabetes by an insulin-reactive CD4 T-cell clone in the nonobese diabetic mouse. *Diabetes,* 46**,** 1124-32.

ZHANG, J., ZHANG, M., WANG, Y., SHI, B., ZHU, B. & SI, L. 2006. Infiltrating T-lymphocyte receptor Vbeta gene family utilization in autoimmune thyroid disease. *J Int Med Res,* 34**,** 585-95.

ZHANG, L., JASINSKI, J. M., KOBAYASHI, M., DAVENPORT, B., JOHNSON, K., DAVIDSON, H., NAKAYAMA, M., HASKINS, K. & EISENBARTH, G. S. 2009. Analysis of T cell receptor beta chains that combine with dominant conserved TRAV5D-4*04 anti-insulin B:9-23 alpha chains. *J Autoimmun,* 33**,** 42-9.

ZHANG, W., SLOAN-LANCASTER, J., KITCHEN, J., TRIBLE, R. P. & SAMELSON, L. E. 1998. LAT: the ZAP-70 tyrosine kinase substrate that links T cell receptor to cellular activation. *Cell,* 92**,** 83-92.

ZHANG, Y., LEE, A. S., SHAMELI, A., GENG, X., FINEGOOD, D., SANTAMARIA, P. & DUTZ, J. P. 2010. TLR9 blockade inhibits activation of diabetogenic CD8+ T cells and delays autoimmune diabetes. *J Immunol,* 184**,** 5645-53.

ZHONG, X. P., HAINEY, E. A., OLENCHOCK, B. A., JORDAN, M. S., MALTZMAN, J. S., NICHOLS, K. E., SHEN, H. & KORETZKY, G. A. 2003. Enhanced T cell responses due to diacylglycerol kinase zeta deficiency. *Nat Immunol,* 4**,** 882-90.

ZHOU, S., KURT-JONES, E. A., CERNY, A. M., CHAN, M., BRONSON, R. T. & FINBERG, R. W. 2009. MyD88 intrinsically regulates CD4 T-cell responses. *J Virol,* 83**,** 1625-34.

ZHOU, S., KURT-JONES, E. A., MANDELL, L., CERNY, A., CHAN, M., GOLENBOCK, D. T. & FINBERG, R. W. 2005. MyD88 is critical for the development of innate and adaptive immunity during acute lymphocytic choriomeningitis virus infection. *Eur J Immunol,* 35**,** 822-30.

ZIEGLER, A. G., REWERS, M., SIMELL, O., SIMELL, T., LEMPAINEN, J., STECK, A., WINKLER, C., ILONEN, J., VEIJOLA, R., KNIP, M., BONIFACIO, E. & EISENBARTH, G. S. 2013. Seroconversion to multiple islet autoantibodies and risk of progression to diabetes in children. *JAMA,* 309**,** 2473-9.

ZIEGLER, A. G., VARDI, P., RICKER, A. T., HATTORI, M., SOELDNER, J. S. & EISENBARTH, G. S. 1989. Radioassay determination of insulin autoantibodies in NOD mice. Correlation with increased risk of progression to overt diabetes. *Diabetes,* 38**,** 358-63.

ZOU, L., MENDEZ, F., MARTIN-OROZCO, N. & PETERSON, E. J. 2008. Defective positive selection results in T cell lymphopenia and increased autoimmune diabetes in ADAP-deficient BDC2.5-C57BL/6 mice. *Eur J Immunol,* 38**,** 986-94.

ZUKLYS, S., BALCIUNAITE, G., AGARWAL, A., FASLER-KAN, E., PALMER, E. & HOLLÄNDER, G. A. 2000. Normal thymic architecture and negative selection are associated with Aire expression, the gene defective in the autoimmune-polyendocrinopathy-candidiasis-ectodermal dystrophy (APECED). *J Immunol,* 165**,** 1976-83.

ÉNÉE, É., KRATZER, R., ARNOUX, J. B., BARILLEAU, E., HAMEL, Y., MARCHI, C., BELTRAND, J., MICHAUD, B., CHATENOUD, L., ROBERT, J. J. & VAN ENDERT, P. 2012. ZnT8 is a major CD8+ T cell-recognized autoantigen in pediatric type 1 diabetes. *Diabetes,* 61**,** 1779-84.